

# Calculable methods for many-body scattering

R. F. Barrett

*Department of Physics, The University of Western Australia, Nedlands, W.A., 6009, Australia*

B. A. Robson\*

*Research School of Physical Sciences, The Australian National University, Canberra, A.C.T. 2600, Australia  
and Sektion Physik, Universität München, 8046 Garching, West Germany*

W. Tobocman

*Physics Department, Case Western Reserve University, University Circle, Cleveland, Ohio 44106*

The review consists of two major parts. In the first part, several calculable  $R$ -matrix and related theories are described and discussed. These include the Kapur-Peierls, Wigner-Eisenbud, calculable standard  $R$ -matrix, extended  $R$ -matrix, finite-element, natural boundary condition, and variational methods. The various approaches are critically compared using four selected applications: (i) exactly soluble model using two coupled square-well potentials, (ii) elastic scattering of neutrons from  $^{12}\text{C}$ , (iii) elastic scattering of electrons from He atoms, and (iv)  $\alpha$ - $\alpha$  elastic scattering. In the second part, the Baer, Kouri, Levin, and Tobocman many-body scattering theory is reviewed. The principal results of the theory are derived, and a survey of calculations applying the theory is presented. The derivation is carried out in the context of the  $R$ -matrix method wherein the many-body scattering is treated *ab initio* as a steady-state process. This has the advantage that the channel states form a complete orthogonal set. These same channel states are used to provide explicit representations of the partition Green's-function operators.

## CONTENTS

I. Introduction	156	VI. Variational Methods	176
II. Many-Body Scattering Problem	158	A. Hulthén-Kohn variational methods for the $K$ matrix	176
A. Formalism	158	B. Kohn variational method for the $\tilde{U}$ matrix	179
B. Alternative asymptotic boundary conditions	159	C. Hulthén-Kohn variational method for the $R$ matrix	180
1. Scattering boundary conditions	159	D. Schwinger variational methods for the $T$ matrix	181
2. Standing-wave boundary conditions (open channels)	159	VII. Calculable Methods for Composite Particle Scattering	181
3. Eigenchannel boundary conditions (open channels)	160	A. Resonating group and generator coordinate methods	182
4. Reactance matrix (or $K$ -matrix) boundary conditions (open channels)	160	B. Solution of Hill-Wheeler equation in whole configuration space	184
5. Transformation between different asymptotic boundary conditions	160	1. Direct solution (method of de Takacsy)	184
III. $R$ -Matrix Scattering Formalism	161	2. Variational method	185
A. Some concepts and definitions	161	C. Solution of Hill-Wheeler equation in interaction region only	185
B. $R$ -matrix formulations of collision matrix	162	1. Microscopic $R$ -matrix method	185
C. Insertion of optical potential	163	2. Variational methods	187
D. $X$ -matrix formalism	164	D. Natural boundary condition method	187
IV. Calculable $R$ -Matrix and Related Methods	165	VIII. Practical Application of $R$ -Matrix and Related Theories	188
A. Kapur-Peierls theory	165	A. Coupled square wells	188
B. Wigner-Eisenbud theory	166	1. Wigner-Eisenbud $R$ -matrix theory	189
C. Standard calculable $R$ -matrix method	167	2. Kapur-Peierls theory	190
D. Buttle correction	168	3. Standard calculable $R$ -matrix method	191
E. Finite-element method	169	4. Extended $R$ -matrix method	191
F. Extended (or generalized) $R$ -matrix method	169	5. Natural boundary condition methods	197
V. Natural Boundary Condition Methods	170	B. Neutron elastic scattering from $^{12}\text{C}$	197
A. Natural boundary condition parameters	170	1. Multilevel $R$ -matrix fit	198
B. Eigenchannel method	171	2. Standard calculable $R$ -matrix method	199
C. Barrett-Delsanto method	172	3. Extended $R$ -matrix method	200
1. Energy correction to the BD method	173	4. Natural boundary condition methods	204
2. Perturbation treatment for the BD method	175	C. Low-energy electron-helium scattering	206
D. Iterated $R$ -matrix method	175	1. Experimental measurements	206
		2. $R$ -matrix method	207
		3. Natural boundary condition methods	208
		4. Variational calculations	210
		D. $\alpha$ - $\alpha$ elastic scattering	212
		1. Direct solution of Hill-Wheeler equation	212
		2. Variational techniques	214
		3. Microscopic $R$ -matrix method	215
		4. Natural boundary condition method	216

\*Permanent address: Research School of Physical Sciences, The Australian National University, Canberra, A.C.T., 2600, Australia.

5. Discussion	217
E. Conclusion	217
IX. Calculable Transition Operator Formalism	218
X. BKL T Equations	220
A. The BKL T reaction matrix operator equations	220
B. The BKL T and LS wave-function equations	222
C. Alternative many-body scattering theories	223
XI. Variational Principles for Transition Amplitude	223
A. Variational functional based on LS equations [Eq. (10.32)]	223
B. Variational functional based on Hahn-Kouri-Levin equations [Eq. (10.25)]	224
XII. Exchange Symmetry	225
A. BKL T equations including exchange symmetry	225
B. Single-clustering approximation	226
XIII. Few-Cluster and Restricted Basis Models	228
XIV. Breakup Reaction Channels	230
A. $T$ -matrix including breakup channels explicitly	230
B. Coupled LS equations for $T$ -matrix operators	231
XV. Spurious Solutions	232
XVI. Review of BKL T Calculations	233
Acknowledgments	235
Appendix A: Justification for Neglecting Surface Terms in the Resolvent Relations and Projection Factors in the LS Equations for the Reaction Matrix Operator	235
Appendix B: Post-Prior Equivalence and the Lippmann Identity	236
Appendix C: Unitariness Constraints on the BKL T Formalism	240
References	240

## I. INTRODUCTION

The narrow resonances observed in nuclear reaction cross sections led to the "compound nucleus" picture (Bohr, 1936) in which the available kinetic energy is assumed to be shared among many nucleons and the sharp resonances considered to correspond to very complicated compound states of the colliding systems. Consequently the early reaction theories (Kapur and Peierls, 1938; Wigner, 1946a, 1946b; Wigner and Eisenbud, 1947) were of a formal nature and did not attempt to describe the resonances in terms of nuclear structure models. Indeed, it was considered advantageous that resonances could be simply parametrized and cataloged without such models. However, following the successful description of low-lying nuclear energy levels in terms of the shell model (Mayer, 1949; Haxel, Jensen, and Suess, 1949) attempts were made (Lane, 1960; Barker, 1961) to relate resonance parameters to shell model (bound-state) calculations. A more unified approach involving projection operators to specify both open and closed channels and emphasizing the dynamical origin of the resonances was proposed by Feshbach (1958, 1962). Subsequently, this approach was followed by the development of a wide variety of reaction formalisms (see, for example, Robson, 1975) which permit the calculation of scattering and reaction cross sections from a model Hamiltonian. Some of these—e.g., the standard  $R$ -matrix method (Lane and Robson, 1966)—have been widely used not only in nuclear physics but also in atomic and molecular physics (Burke and Robb, 1975). It should be mentioned, however, that the resonating-

group method of Wheeler (1937a, 1937b) has been employed since the early 1940's (Buckingham and Massey, 1941) for fairly sophisticated calculations of few-body scattering problems. This quite general approach (see Sec. VIII) gives rise to a set of coupled integrodifferential equations. Unfortunately, these equations become more unwieldy as the number of particles increases, especially if the exchange effects arising from the Pauli exclusion principle need to be taken into account. It is for this reason that considerable attention has been given in recent years to developing alternative techniques.

In this review article we consider primarily two types of calculable theories. In the first part (Secs. II–VIII) we deal with those techniques which employ the division of configuration space into internal and external regions, as in  $R$ -matrix theory. These methods are more suitable (Takeuchi and Moldauer, 1970) for the inclusion of exchange effects than either the Feshbach and related (MacDonald, 1964a, 1964b, 1964c; Bloch and Gillet, 1965; Weidenmüller, 1966; Weidenmüller and Dietrich, 1966) approaches or the coupled-channels method (Tamura, 1965) associated with various collective nuclear models. In the second part (Secs. IX–XVI), a calculable transition operator formalism which is based upon the  $R$ -matrix approach is described.

In Sec. II, the many-body scattering problem is stated and various useful forms of asymptotic boundary conditions are discussed. Section III gives a description of the  $R$ -matrix method which determines the scattering wave function from the Schrödinger equation and the boundary condition constraints. This description is carried out using the elegant operator method of Bloch (Bloch, 1957; Lane and Robson, 1966) and two alternative system Green's-function operators. Modifications of these  $R$ -matrix formalisms to include an optical-model Hamiltonian to represent background scattering and to give the  $X$ -matrix description (Garside and Tobocman, 1969) are also discussed.

The calculable standard  $R$ -matrix (SRM) method (Haglund and Robson, 1965; Lane and Robson, 1966) is introduced in Sec. IV following brief reviews of the earlier related theories of Kapur and Peierls (1938) and Wigner and Eisenbud (1947). The SRM method involves the separation of the Hamiltonian into two components: a part  $H_0$  defining the basis states when certain homogeneous boundary conditions are applied at the internal boundary (channel radius) of the channel region, and a residual interaction. Unfortunately, the SRM method suffers from slow convergence of the basis set expansion arising from the discontinuity of the derivative of the scattering wave function at the boundary. Various techniques for overcoming this problem are discussed: the correction of Buttle (1967) in Sec. IV.D; the finite-element method (Nordholm and Bacskey, 1978) in Sec. IV.E; the extended  $R$ -matrix method (Tobocman and Nagarajan, 1965; Garside and Tobocman, 1968, 1969; Lane and Robson, 1969a; 1969b), which was primarily developed in an attempt to extend shell model and related techniques into the continuum, in Sec. IV.F; several natural boundary condition

methods; the eigenchannel method (Danos and Greiner, 1966; Barrett *et al.*, 1973); the method of Barrett and Del-santo (1974); and the iterative  $R$ -matrix method (Ahmad, Barrett, and Robson, 1976a, 1976b), in Sec. V, and variational techniques in Sec. VI.

In Sec. VII the scattering of composite particles is considered in more detail. Several approaches in which the generator coordinate method (Hill and Wheeler, 1953; Griffin and Wheeler, 1957) is combined with one or another of the calculable reaction theories are discussed.

Section VIII, which forms the final section of the first part, gives a fairly detailed discussion of four selected examples in which several different calculable methods have been applied to the same scattering problem. A critical comparison is made of the alternative approaches.

In the second part of this review article we discuss a calculable transition operator formalism for many-body scattering. The  $R$ -matrix type of formalisms discussed in the first part of this article ultimately require the solution of the Schrödinger equation by the inversion of  $E-H$  subject to appropriate asymptotic boundary condition constraints. In contrast to this, transition operator formalisms seek to determine the many-body collision matrix by solving the integral equations for the transition operators. In this approach the asymptotic boundary condition constraints enter through the driving terms and partition Green's-function operators employed in the integral equations.

As is well known there are several obstacles in the way of doing this for the Lippmann-Schwinger (LS) (Lippmann and Schwinger, 1950) integral equations for the transition operators. It was noted by Foldy and Tobocman (1957) that these integral equations may fail to embody a complete specification of the asymptotic boundary conditions of the scattering process. Secondly, as observed by Faddeev (1960), the LS equations do not have connected kernels. Since this property is necessary for compactness and since compactness is sufficient for the Fredholm alternative, one does not expect that these equations are susceptible to solution by standard methods. Finally, the LS equations involve the partition Green's-function operators  $\bar{G}_\alpha, \bar{G}_\beta, \dots$ , which will be defined below. These are complex many-body operators which must fulfill complicated asymptotic boundary conditions. Thus the difficulty in constructing an adequate representation for the partition Green's-function operators is a third obstacle for a transition operator formalism.

These difficulties were overcome for the three-body problem by Faddeev (1960). In this treatment, the transition operator is written as the sum of three auxiliary operators which are the solutions of three coupled integral equations. These equations become connected-kernel equations after a single iteration. By using three simultaneous equations one can fully specify the asymptotic boundary conditions for the three-body system. The partition Green's-function operators are replaced by free-particle propagators in a transformation which replaces the two-body interaction potentials by two-body transition operators. Lovelace (1964) later derived a similar set of

three coupled integral equations for the transition operators themselves, thus avoiding the introduction of auxiliary operators.

The Faddeev-Lovelace approach was generalized to the more-than-three-body case by Yakubovskii (1967), Alt, Grassberger, and Sandhas (1967), Sloane (1972), Bencze (1973), Redish (1974), Karlson and Zeiger (1975), and Vanzani (1976). Again free-body propagators replace partition Green's-function operators. However, in place of the two-body transition operators needed in the three-body case, the  $N$ -body problem requires a family of two-, three-,  $\dots$ , and  $(N-1)$ -body transition operators to be determined via the solution of a hierarchy of equations.

In Secs. IX and X, an alternative transition operator treatment of the many-body scattering problem is given. In contrast to the Faddeev-Lovelace approach, the original LS equations are retained as the dynamical equations to be solved. It is shown that for an  $N$ -body system it is possible to specify a set of  $\mathcal{N}(N)$  coupled LS equations which fully incorporate the  $N$ -body asymptotic boundary conditions and which after  $\mathcal{N}(N)-1$  iterations become a set of  $\mathcal{N}(N)$  uncoupled, connected-kernel integral equations for the transition operators. The quantity  $\mathcal{N}(N)$  is the number of distinct two-cluster partitions that can be formed from the given  $N$ -particle system. In place of the fewer-than- $N$ -body transition operators required by the Faddeev-Lovelace method, this approach requires as input all the subsystem bound and scattering state wave functions. The set of  $\mathcal{N}(N)$  coupled LS equations chosen are known as the Baer, Kouri, Levin, and Tobocman (BKLT) equations.

To derive the dynamical equations for many-body scattering we adopt the  $R$ -matrix theory approach rather than the more conventional wave packet method. This method has two distinctive aspects which are advantageous. First, the system is confined to a finite volume in configuration space for the process of deriving the equations of motion. The limit of infinite volume is then taken as the very last step. This allows one to formulate the scattering problem in terms of orthogonal, normalizable channel states. Second, the dynamical development is formulated as a steady-state flow rather than as the collision of wave packets. This permits one to avoid the preliminary step of using time-dependent scattering theory in the derivation of the time-independent equations of motion.

The  $R$ -matrix formalism is used to derive the LS equations. This method introduces the asymptotic boundary constraints in a very explicit and well-defined way. In this manner it is possible to formulate the LS equations employing a calculable representation of the partition Green's-function operators in place of the conventional ones. As a consequence of this and of the fact that one has connected-kernel equations, we call the resulting transition operator formalism calculable. Some variational functionals for the many-body transition amplitude are given in Sec. XI, and the extension of the BKLT formalism to include exchange symmetry is discussed in Sec. XII.

Of course, the fact remains that the complexity of the BKLT equations increases with the number of degrees of freedom and that this in turn depends on the number of particles. Thus a full dynamical calculation is presently feasible only for few-body systems. Nevertheless, we believe that the calculable transition operator many-body formalism will prove useful because its simple structure and calculable form should provide a sound basis for introducing approximate treatments for the many-body problem. This is illustrated in Sec. XIII, where it is shown how the BKLT formalism can serve as the basis of a few-cluster model or a restricted basis model analysis of the many-body problem. The ease and directness with which this may be done is one of the attractive features of this formalism.

The explicit inclusion of breakup channels in the calculable transition operator formalism is discussed in Sec. XIV, and the question of spurious solutions of the BKLT equations is considered in Sec. XV. Finally, Sec. XVI gives a short review of the various calculational tests and applications of the BKLT formalism which have been made so far.

## II. MANY-BODY SCATTERING PROBLEM

### A. Formalism

The nonrelativistic quantum-mechanical dynamical problem for an  $N$ -body system consists of the solution of the Schrödinger equation subject to certain asymptotic boundary conditions. The Schrödinger equation has the form

$$(H - E)\Psi_k = 0, \quad (2.1)$$

where

$$H = T + \mathcal{V}, \quad (2.2)$$

$$T = - \sum_{i=1}^N \frac{\hbar^2}{2M_i} \nabla_{\mathbf{R}_i}^2 + \frac{\hbar^2}{2M} \nabla_{\mathbf{R}}^2, \quad (2.3)$$

is the kinetic energy and  $\mathcal{V}$  is the potential energy. In the kinetic energy term,  $M_i$  is the mass of the  $i$ th particle and  $\mathbf{R}_i$  is its position, while  $M$  is the total mass and  $\mathbf{R}$  is the position of the cm. The potential energy  $\mathcal{V}$  will consist of a sum of functions of the relative displacements of the particles, and many-body potentials may be included as well as two-body potentials. All the terms of  $\mathcal{V}$  which involve the particles  $i$  and  $j$  will be required to decrease at least as rapidly as  $(|\mathbf{R}_i - \mathbf{R}_j|)^{-1}$  in the region of configuration space where the separation of particles  $i$  and  $j$  is large.

The asymptotic boundary conditions are formulated in terms of the concepts of partition and channel. A partition of the system is the division of the  $N$  particles into  $n$  groups or clusters. For this purpose all particles are regarded as distinguishable, and the consequences of exchange symmetry will be introduced only at a later stage of the analysis (see Secs. VII.C, XII). For the most part we shall require only two-cluster partitions, which will be identified by lower case Greek letters. Associated with

each partition  $\alpha$  is an infinite set of channels  $c, c', c'', \dots$ , each corresponding to a possible product state of the internal motion states of the two clusters of partition  $\alpha$ .

Let  $h_\alpha^{(1)}$  and  $h_\alpha^{(2)}$  be the Hamiltonians for the internal degrees of freedom of the two clusters of partition  $\alpha$ . The channel states  $\chi_{ac}$  are defined to be the eigenstates of  $h_\alpha^{(1)} + h_\alpha^{(2)}$ , i.e.,

$$(h_\alpha^{(1)} + h_\alpha^{(2)} - \varepsilon_{ac})\chi_{ac} = 0. \quad (2.4)$$

Let  $\mathbf{r}_\alpha$  be the relative displacement of the centers of mass of the two clusters for partition  $\alpha$ . The region of configuration space where  $r_\alpha$  is large relative to the internal coordinates of each cluster is called the partition  $\alpha$  asymptotic region. In this region of configuration space, the scattering state wave function  $\Psi_k$  may be expanded in terms of the partition  $\alpha$  channel states

$$\Psi_k = \sum_{c \in \alpha} \chi_{ac} u_{ac}^{(k)}(\mathbf{r}_\alpha) \quad (\text{large } r_\alpha), \quad (2.5)$$

where the expansion coefficients, the channel relative motion wave functions, necessarily are solutions of

$$\left[ -\frac{\hbar^2}{2m_c} \nabla_{r_\alpha}^2 + \frac{Z_\alpha^{(1)} Z_\alpha^{(2)} e^2}{r_\alpha} - E_{ac} \right] u_{ac}^{(k)}(\mathbf{r}_\alpha) = 0 \quad (2.6)$$

where

$$E_{ac} = E - \varepsilon_{ac}. \quad (2.7)$$

Here  $m_c$  is the reduced mass of the two partition  $\alpha$  clusters in channel  $c$ , and  $Z_\alpha^{(1)}e$  and  $Z_\alpha^{(2)}e$  are their electric charges. The index  $k$  serves as a reminder that the Hilbert space of the multichannel scattering system at any energy is  $m$ -fold degenerate, where  $m$  is the number of open channels. To describe the system completely, it is therefore necessary to determine a set of  $m$  wave functions  $\Psi_1, \Psi_2, \dots, \Psi_m$ .

The asymptotic boundary conditions for the scattering wave function  $\Psi_k$  may now be stated in terms of the channel relative motion wave functions. It is required that for large values of  $r_\alpha$  the latter must have the form

$$u_{ac}^{(k)}(\mathbf{r}_\alpha) = Y_{l_c}^{\mu_c}(\hat{r}_\alpha) [\zeta_{ac}^{(-)}(r_\alpha) \delta_{ck} - \zeta_{ac}^{(+)}(r_\alpha) U_{ck}] \quad (\text{large } r_\alpha), \quad (2.8)$$

where  $Y_{l_c}^{\mu_c}$  is the spherical harmonic and for open channels  $\zeta_{ac}^{(+)}$  ( $\zeta_{ac}^{(-)}$ ) is the unit current outgoing (incoming) radial Coulomb wave function, given by

$$\begin{aligned} \zeta_{ac}^{(\pm)}(r_\alpha) &= \left[ \frac{m_c}{\hbar k_c} \right]^{1/2} i e^{\mp i \sigma_c} [G_{l_c}(k_c r_\alpha) \pm i F_{l_c}(k_c r_\alpha)] r_\alpha^{-1} \\ &\sim \left[ \frac{m_c}{\hbar k_c} \right]^{1/2} \frac{i}{r_\alpha} \\ &\times \exp(\pm i \{ k_c r_\alpha - \eta_c \ln 2k_c r_\alpha - \frac{1}{2} l_c \pi \}). \end{aligned} \quad (2.9)$$

For closed channels ( $E_{ac} < 0$ ) we assume

$$\zeta_{ac}^{(+)}(r_\alpha) \sim \frac{1}{r_\alpha} \exp(-k_c r_\alpha - \eta_c \ln 2k_c r_\alpha). \quad (2.10)$$

Here

$$k_c = (2m_c |E_{ac}| / \hbar^2)^{1/2}, \quad (2.11)$$

$$\eta_c = Z_\alpha^{(1)} Z_\alpha^{(2)} e^2 m_c / (\hbar^2 k_c), \quad (2.12)$$

$$\sigma_c = \arg \Gamma(l_c + 1 + i\eta_c), \quad (2.13)$$

and  $U$  is the collision (or scattering) matrix. It is evident that  $\Psi_k$  represents the scattering state which has unit flux incident in channel  $k$  and purely outgoing flux in all other channels. These states will be denoted by  $\Psi_k^{(+)}$ . We have implicitly assumed above that the index  $c$  includes within it the quantum numbers  $l_c$  and  $\mu_c$ .

It will be convenient to make our notation a little more compact by redefining the channel state so that it includes the spherical harmonic. In addition, the spherical harmonic is coupled to the spins of the two clusters to form an angular momentum eigenstate. Henceforth by channel state we shall mean the quantity

$$|c\rangle = (\chi_{ac} \times Y_{l_c})_{j_c}^{\mu_c} \equiv [(\chi_{ac, j_c^{(1)}}^{(1)} \times \chi_{ac, j_c^{(2)}}^{(2)}) \times Y_{l_c}]_{j_c}^{\bar{\mu}_c}. \quad (2.14)$$

The convention of Bloch (1957) has been used in which  $| \ )$  denotes functions of all coordinates except  $r_\alpha$ . Then Eqs. (2.5), (2.6), and (2.8) become

$$\Psi_k^{(+)} = \sum_{c \in \alpha} |c\rangle w_{ac}^{(k)}(r_\alpha) \quad (r_\alpha \text{ large}), \quad (2.15)$$

$$\left[ -\frac{\hbar^2}{2m_c} \left( \frac{1}{r_\alpha} \frac{d^2}{dr_\alpha^2} r_\alpha - \frac{l_c(l_c+1)}{r_\alpha^2} \right) + \frac{Z_\alpha^{(1)} Z_\alpha^{(2)} e^2}{r_\alpha} - E_{ac} \right] w_{ac}^{(k)}(r_\alpha) = 0, \quad (2.16)$$

and

$$w_{ac}^{(k)}(r_\alpha) = \zeta_{ac}^{(-)}(r_\alpha) \delta_{ck} - \zeta_{ac}^{(+)}(r_\alpha) U_{ck} \quad (2.17)$$

is the channel radial wave function.

The partition  $\alpha$  asymptotic states  $|c\rangle w_{ac}^{(k)}$  are eigenstates of the partition Hamiltonian  $H_\alpha$ :

$$(H_\alpha - E) |c\rangle w_{ac}^{(k)} = 0, \quad (2.18)$$

where

$$H_\alpha = h_\alpha^{(1)} + h_\alpha^{(2)} - \frac{\hbar^2}{2m_c} \nabla_{r_\alpha}^2 + \frac{Z_\alpha^{(1)} Z_\alpha^{(2)} e^2}{r_\alpha}. \quad (2.19)$$

The partition  $\alpha$  residual interaction

$$V_\alpha = H - H_\alpha \quad (2.20)$$

vanishes in the partition  $\alpha$  asymptotic region.

The above equations show how the solution of the many-body Schrödinger equation is characterized by the collision matrix  $U$  when scattering boundary condition constraints are imposed. The objective of any reaction calculation is the determination of the matrix elements  $U_{ck}$ . Once the collision matrix is known, the calculation

of the various reaction cross sections is straightforward (see, for instance, Preston, 1962).

## B. Alternative asymptotic boundary conditions

Although Eqs. (2.14), (2.15), and (2.17) define the physical scattering boundary conditions, it is often very convenient to use alternative asymptotic boundary conditions. Such equivalent mathematical formulations of the many-body scattering problem are simply linear transformations of the equations which incorporate the physical asymptotic boundary conditions. This means that the  $U$ -matrix elements can be obtained by linear transformations of related quantities in the alternative formulation.

In the partition  $\alpha$  asymptotic region, the general solution of the radial wave equation [Eq. (2.16)] has the form

$$x_{ac}^{(k)}(r_\alpha) \equiv (c | \Psi_k \rangle = \zeta_{ac}^{(-)}(r_\alpha) A_{ck} - \zeta_{ac}^{(+)}(r_\alpha) B_{ck}, \quad (2.21)$$

where  $A_{ck}$  and  $B_{ck}$  are complex coefficients and the collision matrix is given by

$$U_{ck} = \sum_{k'} B_{ck'} (A^{-1})_{k'k}. \quad (2.22)$$

Several different sets of asymptotic boundary conditions have been used widely in the literature and we shall discuss each in turn.

### 1. Scattering boundary conditions

As indicated earlier, in this case each of the wave functions  $\Psi_k^{(+)}$  ( $k = 1, 2, \dots, m$ ) is required to represent a system with unit incoming flux in channel  $k$  and only outgoing flux in all other channels. This implies

$$A_{ck} = \delta_{ck} \quad (2.23)$$

and

$$B_{ck} = U_{ck}, \quad (2.24)$$

so that  $x_{ac}^{(k)}(r_\alpha) \equiv w_{ac}^{(k)}(r_\alpha)$  is given by Eq. (2.17).

In the following it will be convenient to distinguish between open ( $\bar{c}$ ) and closed ( $\bar{c}$ ) channels. Thus we write for large  $r_\alpha$

$$| \Psi_k^{(+)} \rangle = \sum_{\bar{c}} | \bar{c} \rangle [\zeta_{a\bar{c}}^{(-)}(r_\alpha) \delta_{\bar{c}k} - \zeta_{a\bar{c}}^{(+)}(r_\alpha) U_{\bar{c}k}] - \sum_{\bar{c}} | \bar{c} \rangle \zeta_{a\bar{c}}^{(+)}(r_\alpha) U_{\bar{c}k}. \quad (2.25)$$

### 2. Standing-wave boundary conditions (open channels)

The imposition of standing-wave boundary conditions requires that the amplitudes of ingoing and outgoing waves be equal in each *open* reaction channel but that there be a phase shift between them. These requirements may be written

$$|A_{\bar{c}k}| = |B_{\bar{c}k}| = v_{\bar{c}k}, \quad (2.26)$$

$$A_{\bar{c}k} = v_{\bar{c}k} e^{-i\delta_{\bar{c}k}}, \quad (2.27a)$$

and

$$B_{\bar{c}k} = v_{\bar{c}k} e^{+i\delta_{\bar{c}k}}, \quad (2.27b)$$

where  $v_{\bar{c}k}$  and  $\delta_{\bar{c}k}$  are real. Thus for large  $r_\alpha$

$$|\Psi_k\rangle = \sum_{\bar{c}} |\bar{c}\rangle v_{\bar{c}k} [\zeta_{\alpha\bar{c}}^{(-)}(r_\alpha) e^{-i\delta_{\bar{c}k}} - \zeta_{\alpha\bar{c}}^{(+)}(r_\alpha) e^{+i\delta_{\bar{c}k}}] - \sum_{\bar{c}} |\bar{c}\rangle \zeta_{\alpha\bar{c}}^{(+)}(r_\alpha) U_{\bar{c}k}. \quad (2.28)$$

The restrictions of Eqs. (2.26) and (2.27), combined with the requirement that the  $|\Psi_k\rangle$  be degenerate eigenfunctions of the Hamiltonian in the internal region, are insufficient to specify completely the set of functions  $|\Psi_k\rangle$ , and an infinity of such sets of standing waves is possible.

### 3. Eigenchannel boundary conditions (open channels)

The eigenchannel boundary conditions require that there exist a set of standing waves with a common phase shift in each open reaction channel in the external region. In other words, the requirements of Eqs. (2.26) and (2.27) are satisfied with the additional restriction that

$$\delta_{1k} = \delta_{2k} = \dots = \delta_{mk} = \delta_k. \quad (2.29)$$

This extra condition restricts the infinity of allowed sets of  $|\Psi_k\rangle$  which existed in the previous section to just one set. In this case

$$A_{\bar{c}k} = v_{\bar{c}k} e^{-i\delta_k}, \quad (2.30)$$

$$B_{\bar{c}k} = v_{\bar{c}k} e^{+i\delta_k}, \quad (2.31)$$

and for large  $r_\alpha$

$$|\Psi_k\rangle = \sum_{\bar{c}} |\bar{c}\rangle v_{\bar{c}k} [\zeta_{\alpha\bar{c}}^{(-)}(r_\alpha) e^{-i\delta_k} - \zeta_{\alpha\bar{c}}^{(+)}(r_\alpha) e^{+i\delta_k}] - \sum_{\bar{c}} |\bar{c}\rangle \zeta_{\alpha\bar{c}}^{(+)}(r_\alpha) U_{\bar{c}k}. \quad (2.32)$$

### 4. Reactance matrix (or $K$ -matrix) boundary conditions (open channels)

The eigenchannel boundary conditions generate one specific set of standing waves out of the infinite number of possible sets that can be constructed in the various open reaction channels. Another important set of standing waves can be generated by the imposition of reactance matrix (or  $K$ -matrix) boundary conditions in the external region.

In this case, for large  $r_\alpha$

$$(\bar{c}|\Psi_k\rangle) = \left[ \frac{m_{\bar{c}}}{\hbar k_{\bar{c}}} \right]^{1/2} [F_{l_{\bar{c}}}(k_{\bar{c}} r_\alpha) \delta_{\bar{c}k} + G_{l_{\bar{c}}}(k_{\bar{c}} r_\alpha) K_{\bar{c}k}] r_\alpha^{-1}, \quad (2.33)$$

where  $K_{\bar{c}k}$  are the elements of the real reactance matrix. Thus here,

$$A_{\bar{c}k} = \frac{1}{2} (\delta_{\bar{c}k} - iK_{\bar{c}k}) e^{-i\sigma_{\bar{c}}}, \quad (2.34)$$

$$B_{\bar{c}k} = \frac{1}{2} (\delta_{\bar{c}k} + iK_{\bar{c}k}) e^{+i\sigma_{\bar{c}}}, \quad (2.35)$$

and

$$|A_{\bar{c}k}| = |B_{\bar{c}k}|. \quad (2.36)$$

If  $\mathbb{1}$ ,  $A$ ,  $B$ ,  $K$ , and  $\Sigma$  are the matrices with elements  $\delta_{\bar{c}k}$ ,  $A_{\bar{c}k}$ ,  $B_{\bar{c}k}$ ,  $K_{\bar{c}k}$ , and  $e^{i\sigma_{\bar{c}}}$ , respectively, then the collision matrix for the subspace of open channels

$$\begin{aligned} \tilde{U} &= BA^{-1} \\ &= \Sigma(\mathbb{1} + iK)(\mathbb{1} - iK)^{-1}\Sigma \\ &= \Sigma(\mathbb{1} - iK)^{-1}(\mathbb{1} + iK)\Sigma. \end{aligned} \quad (2.37)$$

The tilde over  $\tilde{U}$  serves to indicate that only the subspace of open channels is included.

### 5. Transformation between different asymptotic boundary conditions

In the internal region, each of the wave functions  $|\Psi_k\rangle$  is a degenerate eigenfunction of the Hamiltonian of the system. Any linear combination of the  $|\Psi_k\rangle$  will also be a degenerate eigenfunction of the same Hamiltonian. In the external region, this means that a linear combination can be taken of the wave functions  $|\Psi_k^1\rangle$  corresponding to one set of asymptotic boundary conditions to transform to the wave functions  $|\Psi_k^2\rangle$  corresponding to another set.

For example, let  $x_{\alpha\bar{c}}^{(k)}(r_\alpha)$  represent the radial wave functions in channel  $\bar{c}$  belonging to partition  $\alpha$  obtained with standing-wave boundary conditions as discussed in Sec. II.B.2 and let  $w_{\alpha\bar{c}}^{(k)}(r_\alpha)$  represent the corresponding wave functions for the scattering boundary conditions of Sec. II.B.1. Then for large  $r_\alpha$ , we can write

$$w_{\alpha\bar{c}}^{(k)}(r_\alpha) = \sum_{k'} x_{\alpha\bar{c}}^{(k')}(r_\alpha) (A^{-1})_{k'k}, \quad (2.38)$$

where  $A$  is the transformation matrix with elements  $A_{kk'} = v_{kk'} e^{-i\delta_{kk'}}$ . In this notation

$$x_{\alpha\bar{c}}^{(k')}(r_\alpha) = \zeta_{\alpha\bar{c}}^{(-)}(r_\alpha) A_{\bar{c}k'} - \zeta_{\alpha\bar{c}}^{(+)}(r_\alpha) A_{\bar{c}k'}^* \quad (\text{large } r_\alpha), \quad (2.39)$$

so that

$$w_{\alpha\bar{c}}^{(k)}(r_\alpha) = \zeta_{\alpha\bar{c}}^{(-)}(r_\alpha) \delta_{k\bar{c}} - \zeta_{\alpha\bar{c}}^{(+)}(r_\alpha) \sum_{k'} A_{\bar{c}k'}^* (A^{-1})_{k'k} \quad (\text{large } r_\alpha). \quad (2.40)$$

Comparing Eqs. (2.40) and (2.17), we can see that

$$\tilde{U} = A^* A^{-1}. \quad (2.41)$$

Using this relationship and the symmetry of the  $\tilde{U}$  matrix, we can readily see that the matrix product  $A^\dagger A$ , where  $\dagger$  denotes the Hermitian conjugate, is *real*. From a

knowledge of the amplitudes  $v_{\bar{c}k}$  and the phase shifts  $\delta_{\bar{c}k}$  obtained for a particular set of standing-wave boundary conditions, Eq. (2.41) enables the collision matrix and hence the various reaction cross sections to be determined.

In the special case of eigenchannel boundary conditions,

$$A_{\bar{c}k} = v_{\bar{c}k} e^{-i\delta_k}, \quad (2.42)$$

or

$$A = v e^{-i\Delta}, \quad (2.43)$$

where  $v$  and  $\Delta$  are matrices whose elements are  $v_{\bar{c}k}$  and  $\delta_k \delta_{\bar{c}k}$ , respectively. In this case the collision matrix is given [Eq. (2.41)] by

$$\tilde{U} = v e^{2i\Delta} v^{-1}. \quad (2.44)$$

The columns of the matrix  $v$  contain the eigenchannel vectors, and the diagonal elements of the matrix  $\Delta$  are known as the eigenphases.

In this section we have discussed the channel region of configuration space where the short-range polarizing interactions are negligible and the asymptotic forms of the wave functions of the ingoing and outgoing clusters are known. The complete specification of the wave functions throughout configuration space requires a solution of the dynamical equations for the system in the internal region where the short-range interactions are important. There is a variety of methods to achieve this aim. Some of these methods will be discussed in detail in the following sections.

### III. *R*-MATRIX SCATTERING FORMALISM

#### A. Some concepts and definitions

At this point we shall use the *R*-matrix formalism (Lane and Thomas, 1958; Breit, 1959) approach to refine our discussion of the asymptotic boundary condition constraints on the scattering wave function. The discussion given in Sec. II lacks precision, because it is not clear what criterion is to be used to specify when the partition radial coordinate  $r_\alpha$  is to be regarded as large compared to the internal coordinates of either cluster. In addition, the channel states  $|c\rangle$  belonging to one partition are not independent of the channel states belonging to any other partition. Thus it is not clear that the boundary condition constraints imposed in the asymptotic region of one partition are necessarily independent of those imposed in another such region.

The *R*-matrix method avoids these difficulties. The procedure is to introduce a finite volume of the  $3N-3$ -dimensional configuration space of the  $N$ -body system. This volume is centered on the point corresponding to all  $N$  particles being at the same position. The  $3N-4$ -dimensional hypersurface enclosing this volume is called the channel entrance surface, and the interior is called the interaction or inside region. The asymptotic boundary conditions constraining the scattering wave function are

then specified in terms of a complete, orthogonal set of surface harmonics defined on the channel entrance surface.

The channel entrance surface harmonics are defined in the following way. The channel entrance surface is taken to be a  $3N-4$ -dimensional polyhedron, which has a face defined by  $r_\alpha = a_\alpha$  for each two-cluster partition  $\alpha$ . This face is called the partition  $\alpha$  channel entrance, and the constant  $a_\alpha$  is the partition  $\alpha$  channel radius. On each channel entrance a complete, orthogonal set of states is defined. The channel radii will be taken to be sufficiently large that these states can be taken to be the channel states  $|c\rangle$  defined by Eqs. (2.4) and (2.14). However, Eq. (2.4) will be supplemented by the requirement that the states  $|c\rangle$  fulfill real homogeneous boundary conditions on the outer boundary of channel entrance  $\alpha$ . This outer boundary is the intersection of channel entrance  $\alpha$  with its neighboring channel entrances.

We can see that this scheme has several desirable consequences. First, by allowing all the channel radii simultaneously to become sufficiently large, we can cause all the channel entrances to become asymptotic in the sense that the non-Coulomb part of the residual interaction  $V_\alpha$  will be negligible in the vicinity of channel entrance  $\alpha$ . The geometrical constraints are such that as all the  $a_\alpha$ 's increase simultaneously, the difference between  $a_\alpha$  and the maximum value possible on channel entrance  $\alpha$  for any of the internal relative coordinates of the two partition  $\alpha$  clusters becomes arbitrarily large. Thus the concept of asymptotic region has been endowed with precision.

Another desirable consequence is that the spectrum of channel states  $|c\rangle$  becomes purely discrete and the channel state wave functions are all normalizable. There is no overlap between channel state wave functions belonging to different partitions. Thus the channel state wave functions form a complete, orthogonal set of harmonics for the channel entrance surface.

The one undesirable consequence of confining the channel states to the interiors of their respective channel entrances is that they can no longer be regarded as representing physical asymptotic states of motion. If only two-body channels are open, all the channel states are bound states and the use of finite channel entrances has a negligible effect. However, in the case where three-body channels are open, the channel states approach the physical asymptotic states of motion only in the limit that all channel radii simultaneously become infinitely large.

An alternative formulation of multibody breakup channels, which has been outlined by Robson (1975) for a schematic three-body model, does not possess the above undesirable feature, but requires the use of nonorthogonal channel wave functions. This formalism has not yet been employed in any practical application.

To employ the *R*-matrix formalism at energies above the breakup threshold would probably require larger channel radii than are really practical. Thus for such cases a transition matrix formalism like the one discussed in Sec. IX is likely to be more useful.

### B. $R$ -matrix formulations of collision matrix

Having made our specification of the asymptotic boundary condition constraints unambiguous, we next derive two relationships, each of which determines the scattering wave function from the Schrödinger equation and the boundary condition constraints.

Consider the quantity

$$\langle \Theta | \Delta | \Psi_k \rangle = \langle \Theta | H - H^\dagger | \Psi_k \rangle, \quad (3.1)$$

where  $\Theta$  is a function which is regular within the interaction region but otherwise is arbitrary. The integrations denoted by angular brackets are confined to the interaction region. This will be tacitly assumed for all such matrix elements unless explicitly stated otherwise. Assuming the interaction potentials to be real multiplicative operators allows us to write

$$\langle \Theta | \Delta | \Psi_k \rangle = \langle \Theta | T - T^\dagger | \Psi_k \rangle. \quad (3.2)$$

By a simple change of scale, the kinetic energy operator  $T$  can be transformed into a  $3N - 3$ -dimensional Laplacian (Breit, 1940, 1959). Then Green's theorem can be used to transform the volume integral into a surface integral over the channel entrance surface. The result can be written very concisely, using the fact that the channel states  $|c\rangle$  are a set of surface harmonics for the channel entrance surface. We have

$$\langle \Theta | H - H^\dagger | \Psi_k \rangle = \langle \Theta | \mathcal{L}^\dagger(b_c^*) - \mathcal{L}(b_c) | \Psi_k \rangle, \quad (3.3)$$

where  $\mathcal{L}(b_c)$  is the boundary condition operator (Bloch, 1957)

$$\mathcal{L}(b_c) = \sum_{\alpha} \sum_{c \in \alpha} |c\rangle \frac{\hbar^2}{2m_c a_\alpha} \delta(r_\alpha - a_\alpha) \left[ \frac{\partial}{\partial r_\alpha} r_\alpha - b_c \right] \langle c|, \quad (3.4)$$

with arbitrary constants  $b_c$ , which in general may be complex.

Since  $\Theta$  is arbitrary and since  $\Psi_k$  is a solution of the Schrödinger equation, Eq. (3.3) can be written

$$(E - H^\dagger)\Psi_k = \{\mathcal{L}^\dagger(b_c^*) - \mathcal{L}(b_c)\}\Psi_k = \Delta\Psi_k. \quad (3.5)$$

Operating on both sides of this equation with the system Green's-function operator  $G$ , which is defined to be the left inverse of  $(E - H^\dagger)$ , or, equivalently, the right inverse of  $(E - H)$ , i.e.,

$$G(E - H^\dagger) = (E - H)G = 1, \quad (3.6)$$

we obtain

$$\Psi_k = G\{\mathcal{L}^\dagger(b_c^*) - \mathcal{L}(b_c)\}\Psi_k = G\Delta\Psi_k. \quad (3.7)$$

This result is the Green's-function relationship for the scattering wave function, which expresses the value of  $\Psi_k$  at any point in the inside region in terms of its value and normal derivative at the channel entrance surface.

An alternative form of Eq. (3.7) was originally given by

Bloch (Bloch, 1957; Lane and Robson, 1966), who added  $\mathcal{L}(b_c)\Psi_k$  to both sides of the Schrödinger equation:

$$\{H + \mathcal{L}(b_c) - E\}\Psi_k = \mathcal{L}(b_c)\Psi_k. \quad (3.8)$$

Operating on both sides of this equation with the system Green's-function operator  $G^L$ , which is the left inverse of  $\{H + \mathcal{L}(b_c) - E\}$  or the right inverse of  $\{H^\dagger + \mathcal{L}^\dagger(b_c^*) - E\}$ , i.e.,

$$G^L\{H + \mathcal{L}(b_c) - E\} = \{H^\dagger + \mathcal{L}^\dagger(b_c^*) - E\}G^L = 1, \quad (3.9)$$

yields

$$\Psi_k = G^L \mathcal{L}(b_c) \Psi_k. \quad (3.10)$$

If the parameters  $b_c$  are real (from here on this will be assumed unless explicitly stated otherwise), there is no need to distinguish between left and right inverses for  $\{H + \mathcal{L}(b_c) - E\}$ , since Eq. (3.3) implies

$$H + \mathcal{L}(b_c) = H^\dagger + \mathcal{L}^\dagger(b_c). \quad (3.11)$$

The distinction between  $G$  and  $-G^L$  is that the surface term in Eq. (3.9) constrains  $G^L$  to fulfill a particular boundary condition on the channel entrance surface, while there is no such constraint for  $G$  contained in Eq. (3.6). Indeed, Eq. (3.9) is equivalent to the two equations:

$$(E - H)(-G^L) = 1 \quad (3.12)$$

and

$$\mathcal{L}(b_c)G^L = 0. \quad (3.13)$$

If the constraint of Eq. (3.13) is imposed on the operator  $G$  and the parameters  $b_c$  are real, Eq. (3.7) becomes identical in form to Eq. (3.10). The system Green's-function operators play a central role in the  $R$ -matrix formalism. They embody the dynamics of the system, and Eq. (3.7) or (3.10) serves to join the dynamics to the boundary condition constraints. The task of solving the Schrödinger equation has now been replaced by the task of constructing a system Green's-function operator.

Suppose we had succeeded in constructing  $G^L$ . How would we use it to calculate  $\Psi_k$ ? We cannot simply make direct use of Eq. (3.10), because from Eqs. (2.14), (2.15), and (2.17) we see that the asymptotic behavior of  $\Psi_k$  is parametrized in terms of the collision matrix  $U$ , which remains to be determined from the dynamical equations. Well, Eq. (3.10) expresses the dynamics, since  $G^L$  has been constructed. So we use Eq. (3.10) first to calculate  $U$  by matching at the channel entrance surface and then substitute  $U$  back into Eq. (3.10) to obtain  $\Psi_k$ .

Projecting both sides of Eq. (3.10) onto the channel state  $\langle c|$  and matching the internal [Eq. (3.10)] and external [Eq. (2.15)] solutions for  $\Psi_k \equiv \Psi_k^{(+)}$  at  $r_\alpha = a_\alpha$  gives the set of coupled equations



$$\begin{aligned} & \zeta_{\alpha c}^{(-)}(a_\alpha) \delta_{ck} - \zeta_{\alpha c}^{(+)}(a_\alpha) U_{ck} \\ &= \sum_{\beta} \sum_{c' \in \beta} R_{cc'}^L(a_\alpha, a_\beta) \left[ \frac{\partial}{\partial a_\beta} a_\beta - b_{c'} \right] \\ & \quad \times [\zeta_{\beta c'}^{(-)}(a_\beta) \delta_{c'k} - \zeta_{\beta c'}^{(+)}(a_\beta) U_{c'k}], \end{aligned} \quad (3.14)$$

where the  $R$  matrix  $R^L(a_\alpha, a_\beta)$  has elements

$$\begin{aligned} R_{cc'}^L(a_\alpha, a_\beta) &= \frac{\hbar^2 a_\beta}{2m_{c'}} \sum_{jj'} (c, a_\alpha | \phi_j \rangle \langle G^L \rangle_{jj'} \langle \tilde{\phi}_{j'} | c', a_\beta \rangle \\ &\equiv \frac{\hbar^2 a_\beta}{2m_{c'}} (c, a_\alpha | G^L | c', a_\beta \rangle, \end{aligned} \quad (3.15)$$

and the quantities  $(c, a_\alpha | \phi_j \rangle$  are radial functions at  $r_\alpha = a_\alpha$  corresponding to some complete set of basis states  $|\phi_j \rangle$ , which are regular at the origin and in general are nonorthogonal over the internal region. The notation  $(c, a_\alpha | \phi_j \rangle$  denotes integration over all coordinates except  $r_\alpha$ , which is set equal to  $a_\alpha$ , i.e.,

$$(c, a_\alpha | \phi_j \rangle \equiv (c | \phi_j \rangle_{r_\alpha = a_\alpha}. \quad (3.16)$$

The elements  $(G^L)_{jj'}$  belong to a matrix whose inverse has elements  $\langle \tilde{\phi}_j | H + \mathcal{L}(b_c) - E | \phi_{j'} \rangle$ , where the tilde denotes that the radial part of the wave function is to be complex conjugated. It should be noted that for nonorthogonal basis states

$$\langle \tilde{\phi}_j | \phi_{j'} \rangle = O_{jj'} \neq \delta_{jj'} \quad (3.17)$$

and

$$\langle \tilde{\phi}_j | \{H + \mathcal{L}(b_c) - E\}^{-1} | \phi_{j'} \rangle \equiv \langle \tilde{\phi}_j | G^L | \phi_{j'} \rangle \neq (G^L)_{jj'}. \quad (3.18)$$

When we define

$$\begin{aligned} Z_{cc'}^{(\pm)L} &= \delta_{cc'} \zeta_{\beta c'}^{(\pm)}(a_\beta) \\ & \quad - R_{cc'}^L(a_\alpha, a_\beta) \left[ \frac{\partial}{\partial a_\beta} a_\beta - b_{c'} \right] \zeta_{\beta c'}^{(\pm)}(a_\beta), \end{aligned} \quad (3.19)$$

the collision matrix for the subspace of open channels is given by

$$\tilde{U} = [Z^{(+L)}]^{-1} Z^{(-L)}. \quad (3.20)$$

If the same procedure is carried out for Eq. (3.7), one obtains the set of coupled equations

$$\begin{aligned} & \zeta_{\alpha c}^{(-)}(a_\alpha) \delta_{ck} - \zeta_{\alpha c}^{(+)}(a_\alpha) U_{ck} \\ &= \sum_{\beta} \sum_{c' \in \beta} R_{cc'}(a_\alpha, a_\beta) \left[ \left[ \frac{\partial}{\partial a_\beta} \right] a_\beta - \frac{\partial}{\partial a_\beta} a_\beta \right] \\ & \quad \times [\zeta_{\beta c'}^{(-)}(a_\beta) \delta_{c'k} - \zeta_{\beta c'}^{(+)}(a_\beta) U_{c'k}], \end{aligned} \quad (3.21)$$

where the  $R$  matrix  $R(a_\alpha, a_\beta)$  has elements

$$\begin{aligned} R_{cc'}(a_\alpha, a_\beta) &= \frac{\hbar^2 a_\beta}{2m_{c'}} \sum_{jj'} (c, a_\alpha | \phi_j \rangle \langle G \rangle_{jj'} \langle \tilde{\phi}_{j'} | c', a_\beta \rangle \\ &\equiv \frac{\hbar^2 a_\beta}{2m_{c'}} (c, a_\alpha | G | c', a_\beta \rangle, \end{aligned} \quad (3.22)$$

and the arrow indicates operation to the left. The corresponding  $Z$  matrices are

$$\begin{aligned} Z_{cc'}^{(\pm)} &= \delta_{cc'} \zeta_{\beta c'}^{(\pm)}(a_\beta) - R_{cc'}(a_\alpha, a_\beta) \\ & \quad \times \left[ \left[ \frac{\partial}{\partial a_\beta} \right] a_\beta - \frac{\partial}{\partial a_\beta} a_\beta \right] \zeta_{\beta c'}^{(\pm)}(a_\beta), \end{aligned} \quad (3.23)$$

and the collision matrix is given by a relation analogous to Eq. (3.20).

It should be noted that Eq. (3.6) does not determine  $G$  uniquely. Its asymptotic behavior can be varied by adding regular solutions of the corresponding homogeneous equations. However, these variations in asymptotic behavior have no effect on Eqs. (3.21)–(3.23) and Eq. (3.7), which determine the scattering wave function from the Schrödinger equation and the boundary condition constraints.

## C. Insertion of optical potential

Both of the  $R$ -matrix formalisms discussed above may be modified by the insertion of an optical-model Hamiltonian  $\bar{H}_\alpha$  to represent the background scattering for partition  $\alpha$ . These insertions are based on the resolvent relations for the Green's-function operators:

$$G^L = \{H + \mathcal{L}(b_c) - E\}^{-1} = \bar{G}_\alpha^L - \bar{G}_\alpha^L \bar{V}_\alpha G^L \quad (3.24)$$

or

$$G = (E - H^\dagger)^{-1} = \bar{G}_\alpha + \bar{G}_\alpha (\bar{V}_\alpha + \Delta) G = \bar{G}_\alpha + \bar{G}_\alpha \bar{W}_\alpha G, \quad (3.25)$$

where the optical-model Green's-function operators  $\bar{G}_\alpha^L$  and  $\bar{G}_\alpha$  are given by

$$\bar{G}_\alpha^L \{ \bar{H}_\alpha + \mathcal{L}(b_c) - E \} = 1 \quad (3.26)$$

and

$$\bar{G}_\alpha (E - \bar{H}_\alpha^\dagger) = 1, \quad (3.27)$$

and

$$\bar{V}_\alpha = H - \bar{H}_\alpha = (H - \bar{H}_\alpha)^\dagger \quad (3.28)$$

is the residual interaction. We require that  $\bar{H}_\alpha$  does not produce any nonelastic scattering. Then for partition  $\alpha$

$$\bar{H}_\alpha = H_\alpha + U_\alpha(r_\alpha), \quad (3.29)$$

where  $H_\alpha$  is given by Eq. (2.19) and  $U_\alpha$  is a real optical-model potential. Thus the residual interaction  $\bar{V}_\alpha$  is given by

$$\bar{V}_\alpha = V_\alpha - U_\alpha, \quad (3.30)$$

which vanishes in the partition  $\alpha$  asymptotic region.

The Hamiltonian  $\bar{H}_\alpha$  has regular scattering eigenstates  $|\tilde{c}\rangle \bar{u}_{\alpha\tilde{c}}$  such that

$$(\bar{H}_\alpha - E)|\tilde{c}\rangle \bar{u}_{\alpha\tilde{c}}(r_\alpha) = 0, \quad (3.31)$$

and for large  $r_\alpha$

$$\bar{u}_{\alpha\tilde{c}}(r_\alpha) \sim \left[ \frac{m_{\tilde{c}}}{\hbar k_{\tilde{c}}} \right]^{1/2} r_\alpha^{-1} \sin(\theta_{\tilde{c}} + \bar{\delta}_{\tilde{c}}), \quad (3.32)$$

where

$$\theta_{\tilde{c}} = k_{\tilde{c}} r_\alpha - \eta_{\tilde{c}} \ln 2k_{\tilde{c}} r_\alpha - \frac{1}{2} l_{\tilde{c}} \pi \quad (3.33)$$

and  $\bar{\delta}_{\tilde{c}}$  is the phase shift due to  $U_\alpha$  and the Coulomb interaction. Corresponding to each such regular solution, there is an irregular solution  $|\tilde{c}\rangle \bar{v}_{\alpha\tilde{c}}$  such that

$$(\bar{H}_\alpha - E)|\tilde{c}\rangle \bar{v}_{\alpha\tilde{c}}(r_\alpha) = 0, \quad (3.34)$$

and for large  $r_\alpha$

$$\bar{v}_{\alpha\tilde{c}}(r_\alpha) \sim \left[ \frac{m_{\tilde{c}}}{\hbar k_{\tilde{c}}} \right]^{1/2} r_\alpha^{-1} \cos(\theta_{\tilde{c}} + \bar{\delta}_{\tilde{c}}) - s_{\tilde{c}} \bar{u}_{\alpha\tilde{c}}. \quad (3.35)$$

Here the parameters  $s_{\tilde{c}}$  are arbitrary and the phase shifts  $\bar{\delta}_{\tilde{c}}$  are real.

Provided the  $s_{\tilde{c}}$  are appropriately chosen, both the matrices  $(-\bar{R}_\alpha^L)$  and  $\bar{R}_\alpha$  corresponding to  $(-\bar{G}_\alpha^L)$  and  $\bar{G}_\alpha$ , respectively, may be represented by

$$\begin{aligned} \bar{R}_{\tilde{c}\tilde{c}'}(a_\alpha, a_\beta) &\equiv \left[ \frac{\hbar^2 a_\beta}{2m_{\tilde{c}'}} \right] (\tilde{c}, a_\alpha | \bar{G}_\alpha | \tilde{c}', a_\beta) \\ &= - \left[ \frac{\hbar a_\beta}{m_{\tilde{c}'}} \right] \bar{u}_{\alpha\tilde{c}}(a_\alpha) \bar{v}_{\beta\tilde{c}'}(a_\beta) \delta_{\tilde{c}\tilde{c}'}. \end{aligned} \quad (3.36)$$

For the representation of  $(-\bar{R}_\alpha^L)$ , the  $s_{\tilde{c}}$  must be chosen so that

$$\mathcal{L}(b_{\tilde{c}'}) |\tilde{c}'\rangle \bar{v}_{\beta\tilde{c}'}(r_\beta) = 0, \quad (3.37)$$

so that  $\mathcal{L}(b_{\tilde{c}}) \bar{G}_\alpha^L = 0$ .

Substitution of Eqs. (3.24) and (3.36) into Eq. (3.19) and using Eq. (3.37) gives the  $Z^L$  matrices modified by the inclusion of an optical-model Hamiltonian:

$$\begin{aligned} Z_{\tilde{c}\tilde{c}'}^{(\pm)L} &= \bar{v}_{\alpha\tilde{c}}(a_\alpha) \left[ i e^{\mp i \bar{\delta}_{\tilde{c}}} \delta_{\tilde{c}\tilde{c}'} + \left[ \frac{\hbar a_\alpha}{m_{\tilde{c}}} \right] \langle \bar{u}_{\alpha\tilde{c}} | \bar{V}_\alpha G^L | \tilde{c}', a_\beta \rangle \right. \\ &\quad \left. \times \left[ \frac{\partial}{\partial a_\beta} a_\beta - b_{\tilde{c}'} \right] \zeta_{\beta\tilde{c}'}^{(\pm)}(a_\beta) \right], \end{aligned} \quad (3.38)$$

where

$$|\bar{u}_{\alpha\tilde{c}}\rangle = |\tilde{c}\rangle \bar{u}_{\alpha\tilde{c}}(r_\alpha). \quad (3.39)$$

Similarly, substitution of Eqs. (3.25) and (3.36) into Eq. (3.23) yields the corresponding modified  $Z$  matrices:

$$\begin{aligned} Z_{\tilde{c}\tilde{c}'}^{(\pm)} &= \bar{v}_{\alpha\tilde{c}}(a_\alpha) \left\{ i e^{\mp i \bar{\delta}_{\tilde{c}}} \delta_{\tilde{c}\tilde{c}'} + \left[ \frac{\hbar a_\alpha}{m_{\tilde{c}}} \right] \langle \bar{u}_{\alpha\tilde{c}} | \bar{W}_\alpha G | \tilde{c}', a_\beta \rangle \right. \\ &\quad \left. \times \left[ \left[ \frac{\partial}{\partial a_\beta} \right] a_\beta - \frac{\partial}{\partial a_\beta} a_\beta \right] \zeta_{\beta\tilde{c}'}^{(\pm)}(a_\beta) \right\}. \end{aligned} \quad (3.40)$$

#### D. X-matrix formalism

Both of the  $R$ -matrix formalisms of Sec. III.B may be transformed by the following substitutions for the Green's-function operators:

$$G^L = \bar{G}_\alpha^L - \bar{G}_\alpha^L \bar{V}_\alpha \bar{G}_\beta^L + \bar{G}_\alpha^L \bar{V}_\alpha G^L \bar{V}_\beta \bar{G}_\beta^L = \bar{G}_\alpha^L + \bar{G}_\alpha^L \hat{X}_{\alpha\beta}^L \bar{G}_\beta^L, \quad (3.41)$$

$$\bar{G} = \bar{G}_\alpha + \bar{G}_\alpha \bar{W}_\alpha \bar{G}_\beta + \bar{G}_\alpha \bar{W}_\alpha G \bar{W}_\beta \bar{G}_\beta = \bar{G}_\alpha + \bar{G}_\alpha \hat{X}_{\alpha\beta} \bar{G}_\beta, \quad (3.42)$$

where

$$\hat{X}_{\alpha\beta}^L = -\bar{V}_\alpha + \bar{V}_\alpha G^L \bar{V}_\beta \quad (3.43)$$

and

$$\hat{X}_{\alpha\beta} = \bar{W}_\alpha + \bar{W}_\alpha G \bar{W}_\beta \quad (3.44)$$

are the *reaction* matrix operators. Equations (3.41) and (3.42) result from iterating the resolvent relations, Eqs. (3.24) and (3.25). For details see Sec. IX.

Substitution of Eqs. (3.41) and (3.36) into Eq. (3.19) gives, using Eq. (3.37), the  $X$ -matrix form of the  $Z^L$  matrices,

$$Z_{\tilde{c}\tilde{c}'}^{(\pm)L} = i \bar{v}_{\alpha\tilde{c}}(a_\alpha) [\delta_{\tilde{c}\tilde{c}'} - (s_{\tilde{c}'} \pm i) X_{\tilde{c}\tilde{c}'}^L] e^{\mp i \bar{\delta}_{\tilde{c}'}} \quad (3.45)$$

where

$$X_{\tilde{c}\tilde{c}'}^L = -2\hbar^{-1} \langle \bar{u}_{\alpha\tilde{c}} | \hat{X}_{\alpha\beta}^L | \bar{u}_{\beta\tilde{c}'} \rangle. \quad (3.46)$$

Similarly, substitution of Eqs. (3.42) and (3.36) into Eq. (3.23) yields

$$Z_{\tilde{c}\tilde{c}'}^{(\pm)} = i \bar{v}_{\alpha\tilde{c}}(a_\alpha) [\delta_{\tilde{c}\tilde{c}'} - (s_{\tilde{c}'} \pm i) X_{\tilde{c}\tilde{c}'}] e^{\mp i \bar{\delta}_{\tilde{c}'}} \quad (3.47)$$

where

$$X_{\tilde{c}\tilde{c}'} = -2\hbar^{-1} \langle \bar{u}_{\alpha\tilde{c}} | \hat{X}_{\alpha\beta} | \bar{u}_{\beta\tilde{c}'} \rangle. \quad (3.48)$$

The collision matrix  $\tilde{U}$  is given by

$$\tilde{U} = d(1 - Y_s^+)^{-1} (1 - Y_s^-) d, \quad (3.49)$$

where

$$(s^\pm)_{\tilde{c}\tilde{c}'} = (s_{\tilde{c}'} \pm i) \delta_{\tilde{c}\tilde{c}'}, \quad (3.50)$$

$$d_{\tilde{c}\tilde{c}'} = e^{i \bar{\delta}_{\tilde{c}}} \delta_{\tilde{c}\tilde{c}'}, \quad (3.51)$$

and  $Y$  is  $X^L$  or  $X$ , respectively.

The  $X$ -matrix formalism leads to the "volume" form of the collision matrix in the sense that the channel radii appear only *implicitly* in the expression [Eq. (3.49)], serving

to define the volume of configuration space for the matrix elements and the boundary at which the boundary condition parameters are defined. It is expected that such a form should be less sensitive to the values of the channel radii than the corresponding "surface" forms of Sec. III.B. The  $X$ -matrix formalism also permits the use of an optical potential to describe the background, and a judicious choice of such a potential should give results which are much less sensitive to the truncation of the basis used to construct the system Green's-function operators.

If all the parameters  $s_{\bar{c}}$  are chosen equal to  $-i$  and  $U_{\alpha}=0$ , the  $Y$  matrix becomes equal to minus the conventional  $T$  matrix (see also Secs. VI.D and IX). The theory of Brown and de Dominicis (1958) discussed in Sec. IV.A falls into this category. For  $s_{\bar{c}}=0$  (all  $\bar{c}$ ), the  $Y$  matrix is closely related to the  $K$  matrix of Sec. II.B.4. Note that, for this case, Eq. (3.49) reduces to Eq. (2.37) for  $U_{\alpha}=0$ . Calculations based on the  $X$ -matrix formalism will be discussed in Sec. VIII. Further discussion of the closely related  $T$ -matrix formalism and the more general  $X$ -matrix formalism is given in Sec. IX.

#### IV. CALCULABLE $R$ -MATRIX AND RELATED METHODS

As we have seen in Sec. III, the collision matrix may be obtained within the  $R$ -matrix formalism once a Green's-function operator has been constructed for the system. In general, it is not practicable to use eigenfunctions of the total Hamiltonian as basis states for representing such a Green's-function operator; a "calculable"  $R$ -matrix method usually employs eigenstates of some simpler Hamiltonian to generate the required basis states. However, since the original  $R$ -matrix reaction theory (Wigner 1946a, 1946b; Wigner and Eisenbud, 1947) has been extensively used in the analysis of data to obtain empirical information on the energies and partial widths of nuclear resonances, we shall first give a brief review of both this method and the closely related earlier theory of Kapur and Peierls (1938) before discussing such calculable  $R$ -matrix methods.

##### A. Kapur-Peierls theory

We start from Eq. (3.14), which when multiplied by the factor  $(\hbar^2 a_{\alpha}/2m_c)^{1/2}$ , allows a more symmetrical  $R$  matrix,  $\tilde{R}_{cc'}$ , to be defined. We have

$$\begin{aligned} y_{ac}^{(k)}(a_{\alpha}) &= \left[ \frac{\hbar^2 a_{\alpha}}{2m_c} \right]^{1/2} (c, a_{\alpha} | \Psi_k) \\ &= \sum_{\beta} \sum_{c' \in \beta} \tilde{R}_{cc'}^L(a_{\alpha}, a_{\beta}) \\ &\quad \times \left[ a_{\beta}^{1/2} \frac{\partial}{\partial a_{\beta}} a_{\beta}^{1/2} - b_{c'} \right] y_{\beta c'}^{(k)}(a_{\beta}), \end{aligned} \quad (4.1)$$

where

$$\tilde{R}_{cc'}^L(a_{\alpha}, a_{\beta}) = \sum_{jj'} \gamma_{jc}(G^L)_{jj'} \gamma_{j'c'}, \quad (4.2)$$

$$\gamma_{jc} = \left[ \frac{\hbar^2 a_{\alpha}}{2m_c} \right]^{1/2} (c, a_{\alpha} | \phi_j) \quad (4.3)$$

is called the *reduced width amplitude* and where the surface integrals are evaluated at the boundary of the internal and external regions. The functions  $\phi_j$  are members of a complete orthogonal basis set.

In the theory of Kapur and Peierls, the parameters  $b_{\bar{c}}$  corresponding to open channels are chosen such that

$$\begin{aligned} b_{\bar{c}} &= \frac{\partial}{\partial a_{\alpha}} [a_{\alpha} \xi_{\alpha \bar{c}}^{(+)}(a_{\alpha})] / \xi_{\alpha \bar{c}}^{(+)}(a_{\alpha}) \\ &= S_{\bar{c}}(k_{\bar{c}} a_{\alpha}) + iP_{\bar{c}}(k_{\bar{c}} a_{\alpha}), \end{aligned} \quad (4.4)$$

where

$$P_{\bar{c}}(k_{\bar{c}} a_{\alpha}) = (k_{\bar{c}} a_{\alpha}) [G_{l_{\bar{c}}}^2(k_{\bar{c}} a_{\alpha}) + F_{l_{\bar{c}}}^2(k_{\bar{c}} a_{\alpha})]^{-1} \quad (4.5)$$

and

$$\begin{aligned} S_{\bar{c}}(k_{\bar{c}} a_{\alpha}) &= \left[ G_{l_{\bar{c}}}(k_{\bar{c}} a_{\alpha}) \frac{\partial}{\partial a_{\alpha}} G_{l_{\bar{c}}}(k_{\bar{c}} a_{\alpha}) \right. \\ &\quad \left. + F_{l_{\bar{c}}}(k_{\bar{c}} a_{\alpha}) \frac{\partial}{\partial a_{\alpha}} F_{l_{\bar{c}}}(k_{\bar{c}} a_{\alpha}) \right] P_{\bar{c}}(k_{\bar{c}} a_{\alpha}) k_{\bar{c}}^{-1} \end{aligned} \quad (4.6)$$

are known as the *penetration* and *shift* factors, respectively. Thus defining

$$\begin{aligned} I_{\alpha \bar{c}}(k_{\bar{c}} a_{\alpha}) &= e^{+i\sigma_{\bar{c}}} [G_{l_{\bar{c}}}(k_{\bar{c}} a_{\alpha}) - iF_{l_{\bar{c}}}(k_{\bar{c}} a_{\alpha})] \\ &= O_{\alpha \bar{c}}^*(k_{\bar{c}} a_{\alpha}), \end{aligned} \quad (4.7)$$

we have for open channels, assuming  $\Psi_k$  satisfies scattering boundary conditions,

$$\begin{aligned} \left[ a_{\beta}^{1/2} \frac{\partial}{\partial a_{\beta}} a_{\beta}^{1/2} - b_{\bar{c}'} \right] y_{\beta \bar{c}'}^{(k)}(a_{\beta}) &= i \left[ \frac{\hbar a_{\beta}}{2k_{\bar{c}'}} \right]^{1/2} O_{\beta \bar{c}'}^{-1}(k_{\bar{c}'}, a_{\beta}) \delta_{k\bar{c}'} \left[ O_{\beta \bar{c}'}(k_{\bar{c}'}, a_{\beta}) \frac{\partial}{\partial a_{\beta}} I_{\beta \bar{c}'}(k_{\bar{c}'}, a_{\beta}) - I_{\beta \bar{c}'}(k_{\bar{c}'}, a_{\beta}) \frac{\partial}{\partial a_{\beta}} O_{\beta \bar{c}'}(k_{\bar{c}'}, a_{\beta}) \right] \\ &= i \left[ \frac{\hbar a_{\beta}}{2k_{\bar{c}'}} \right]^{1/2} (-2ik_{\bar{c}'}) O_{\beta \bar{c}'}^{-1}(k_{\bar{c}'}, a_{\beta}) \delta_{k\bar{c}'}. \end{aligned} \quad (4.8)$$

For closed channels

$$\left[ a_{\beta}^{1/2} \frac{\partial}{\partial a_{\beta}} a_{\beta}^{1/2} - b_{\bar{c}} \right] y_{\beta \bar{c}}^{(k)}(a_{\beta}) = 0. \quad (4.9)$$

Thus Eq. (4.1) becomes

$$\begin{aligned} & \left[ \frac{\hbar}{2k_c a_{\alpha}} \right]^{1/2} (I_{ac} \delta_{ck} - O_{ac} U_{ck}) \\ &= \sum_{\beta} \sum_{\bar{c}' \in \beta} \tilde{R}_{\bar{c}'\bar{c}}^L \left[ \frac{\hbar}{2k_{\bar{c}'} a_{\beta}} \right]^{1/2} (-2ik_{\bar{c}'} a_{\beta}) O_{\beta \bar{c}'}^{-1} \delta_{\bar{c}'k} \end{aligned} \quad (4.10)$$

and

$$U_{ck} = \left[ \frac{I_{ac}}{O_{ac}} \right] \delta_{ck} + i \frac{(2k_c a_{\alpha})^{1/2} (2k_k a_{\beta})^{1/2}}{O_{ac} O_{\beta k}} \tilde{R}_{ck}^L. \quad (4.11)$$

Defining

$$\left[ \frac{I_{a\bar{c}}}{O_{a\bar{c}}} \right]^{1/2} = e^{i\sigma_{\bar{c}}} \left[ \frac{(G_{l_{\bar{c}}} - iF_{l_{\bar{c}}})}{(G_{l_{\bar{c}}} + iF_{l_{\bar{c}}})} \right]^{1/2} = e^{i(\sigma_{\bar{c}} - \phi_{\bar{c}})} = e^{i\Omega_{\bar{c}}}, \quad (4.12)$$

where

$$\phi_{\bar{c}} = \tan^{-1}(F_{l_{\bar{c}}}/G_{l_{\bar{c}}}) \quad (4.13)$$

is known as the *hard-sphere phase shift* (since it is the phase shift produced by an infinitely repulsive sphere of radius  $a_{\alpha}$ ), Eq. (4.11) may be written for open channels

$$\begin{aligned} U_{\bar{c}k} = e^{i(\Omega_{\bar{c}} + \Omega_k)} & \left[ \delta_{\bar{c}k} + i \left[ \frac{2k_{\bar{c}} a_{\alpha}}{I_{a\bar{c}} O_{a\bar{c}}} \right]^{1/2} \right. \\ & \left. \times \tilde{R}_{\bar{c}k}^L \left[ \frac{2k_k a_{\beta}}{I_{\beta k} O_{\beta k}} \right]^{1/2} \right]. \end{aligned} \quad (4.14)$$

Now

$$P_{\bar{c}} = (k_{\bar{c}} a_{\alpha}) / (I_{a\bar{c}} O_{a\bar{c}}), \quad (4.15)$$

and defining the *partial width amplitude*

$$\Gamma_{j\bar{c}}^{1/2} = (2P_{\bar{c}})^{1/2} \gamma_{j\bar{c}}, \quad (4.16)$$

then

$$U_{\bar{c}k} = e^{i(\Omega_{\bar{c}} + \Omega_k)} \left[ \delta_{\bar{c}k} + i \sum_{jj'} \Gamma_{j\bar{c}}^{1/2} (G^L)_{jj'} \Gamma_{j'k}^{1/2} \right]. \quad (4.17)$$

In the Kapur-Peierls theory, the basis states  $|\phi_j\rangle$  are assumed to be normalized regular eigenstates of the total Hamiltonian, i.e.,

$$H |\phi_j\rangle = \mathcal{E}_j |\phi_j\rangle \quad (4.18)$$

and to obey the boundary conditions

$$\mathcal{L}(b_c) |\phi_j\rangle = 0, \quad (4.19)$$

where the parameters  $b_c$  are defined by Eqs. (4.4) and (4.9). In this case, the eigenenergies  $\mathcal{E}_j$  are in general complex. For this orthogonal representation, the Green's-function operator  $G^L$  is given by

$$\begin{aligned} (G^L)_{jj'} &= \langle \tilde{\phi}_j | \{H + \mathcal{L}(b_c) - E\}^{-1} | \phi_{j'} \rangle \\ &= (\mathcal{E}_j - E)^{-1} \delta_{jj'}, \end{aligned} \quad (4.20)$$

where  $\tilde{\phi}_j$  is the state  $\phi_j$  with complex conjugated radial part. Thus

$$U_{\bar{c}k} = e^{i(\Omega_{\bar{c}} + \Omega_k)} \left[ \delta_{\bar{c}k} + i \sum_j \Gamma_{jk}^{1/2} (\mathcal{E}_j - E)^{-1} \Gamma_{j\bar{c}}^{1/2} \right]. \quad (4.21)$$

If  $E \approx \mathcal{E}_j$ , one can make a one-level approximation to the  $\tilde{U}$  matrix,

$$U_{\bar{c}k} \approx e^{i(\Omega_{\bar{c}} + \Omega_k)} [\delta_{\bar{c}k} + i \Gamma_{jk}^{1/2} (\mathcal{E}_j - E)^{-1} \Gamma_{j\bar{c}}^{1/2}]. \quad (4.22)$$

Lejeune and Nagarajan (1970, 1971) have applied the Kapur-Peierls formalism to a soluble model of weakly coupled square-well potentials. These studies will be discussed in Sec. VIII.

The theory of Brown and de Dominicis (1958) uses the same basis states [i.e., eigenstates of  $H + \mathcal{L}(b_c)$ ] and boundary condition parameters  $b_{\bar{c}}$  [Eq. (4.4)] as the Kapur-Peierls theory but is based upon Eq. (3.45) of the  $X$ -matrix formalism, with  $s_{\bar{c}} = -i$ , i.e., the  $T$ -matrix form.

Both the Kapur-Peierls and Brown-de Dominicis theories have two major shortcomings from a practical point of view. These arise because energy-dependent and complex boundary condition parameters are employed. Such parameters lead to (i) energy-dependent and complex eigenenergies  $\mathcal{E}_j$  and reduced widths  $\gamma_{j\bar{c}}^2$  and (ii) a non-unitary collision matrix for a truncated basis set. The original  $R$ -matrix formalism of Wigner and Eisenbud (1947) was developed to overcome both these deficiencies of the Kapur-Peierls dispersion theory.

## B. Wigner-Eisenbud theory

In the Wigner-Eisenbud theory, the normalized orthogonal and regular (at the origin) basis states satisfy Eq. (4.18) but obey the boundary conditions

$$\mathcal{L}(B_c) |\phi_j\rangle = 0, \quad (4.23)$$

where the parameters  $B_c$  are *real* arbitrary numbers. In this case

$$\begin{aligned} (G^{L^{-1}})_{jj'} &= \langle \phi_j | H + \mathcal{L}(b_c) - E | \phi_{j'} \rangle \\ &= (\mathcal{E}_j - E) \delta_{jj'} + \sum_c \gamma_{jc} \gamma_{j'c} (B_c - b_c). \end{aligned} \quad (4.24)$$

For closed channels, we can choose for convenience

$$B_{\bar{c}} = b_{\bar{c}}, \quad (4.25)$$

so that Eq. (4.24) can be written

$$(G^{L^{-1}})_{jj'} = (\mathcal{E}_j - E)\delta_{jj'} + \sum_{\bar{c}} \gamma_{j\bar{c}} \gamma_{j'\bar{c}} (B_{\bar{c}} - S_{\bar{c}} - iP_{\bar{c}}), \quad (4.26)$$

where the penetration factor  $P_{\bar{c}}$  and shift factor  $S_{\bar{c}}$  are given by Eqs. (4.5) and (4.6), respectively. Thus the collision matrix is rather more complicated than the corresponding expression in the Kapur-Peierls formalism [Eq. (4.21)], being given by Eqs. (4.1) and (4.26). However, since the parameters  $B_{\bar{c}}$  are real, both the eigenenergies  $\mathcal{E}_j$  and the reduced widths  $\gamma_{j\bar{c}}^2$  are also real (and energy independent). Moreover, it can be shown (Wigner and Eisenbud, 1947; Lane and Thomas, 1958) that the corresponding  $\tilde{U}$  matrix is unitary and symmetric even for a truncated basis set, i.e.,

$$U_{ck} = U_{kc} = (U^{-1})_{\bar{c}k}^*. \quad (4.27)$$

This form of the  $R$ -matrix theory has been reviewed in detail by Lane and Thomas (1958).

The one-level approximation, as in the Kapur-Peierls theory [Eq. (4.22)], leads to the Breit-Wigner formula for the scattering cross sections. The retention of additional levels corresponds to the various multilevel formulas which are used to describe cross sections which deviate appreciably from the simple Breit-Wigner shape. In the Wigner-Eisenbud theory, these formulas are considerably simpler to employ than the analogous formulas of the Kapur-Peierls theory, since the parameters  $\mathcal{E}_j$  and  $\gamma_{j\bar{c}}^2$  are both real and energy independent. Thus the Wigner-Eisenbud formalism has been used extensively to parametrize resonance data to obtain empirical information on the energies and partial widths of the various nuclear levels.

The values obtained for the energies and widths will depend on the choice of the real boundary condition parameters  $B_{\bar{c}}$ . Vogt (1962) has studied the accuracy of the one-level  $R$ -matrix formula for the simple case of  $s$ -wave neutron potential scattering. He concluded that in this case, the one-level approximation is most accurate when  $B_{\bar{c}}$  is chosen so that

$$B_{\bar{c}} = S_{\bar{c}}. \quad (4.28)$$

It should be noted that the collision matrix is given only by Eq. (4.17) for  $b_{\bar{c}} = S_{\bar{c}} + iP_{\bar{c}}$ ; any arbitrary choice (e.g.,  $b_{\bar{c}} = 0$ ) will lead to the same results (Mori, 1972), but the expression for the  $\tilde{U}$  matrix is more complicated [Eq. (3.20)]. We have, writing Eq. (3.19) in matrix form,

$$Z^{(\pm)L} = \{ \mathbb{1} - R^L L^{(\pm)} \} \zeta^{(\pm)}, \quad (4.29)$$

where  $L^{(\pm)}$  and  $\zeta^{(\pm)}$  are matrices with elements

$$L_{\bar{c}\bar{c}'}^{(\pm)} = (S_{\bar{c}} \pm iP_{\bar{c}} - b_{\bar{c}'}) \delta_{\bar{c}\bar{c}'}, \quad (4.30)$$

and

$$\zeta_{\bar{c}\bar{c}'}^{(\pm)} = \zeta_{\beta\bar{c}'}^{(\pm)} (a_{\beta}) \delta_{\bar{c}\bar{c}'}, \quad (4.31)$$

respectively. Using Eqs. (3.20) and (4.29), we can write the collision matrix  $\tilde{U}$  in the form

$$\begin{aligned} \tilde{U} &= [\zeta^{(+)}]^{-1} \{ \mathbb{1} - R^L L^{(+)} \}^{-1} \{ \mathbb{1} - R^L L^{(-)} \} \zeta^{(-)} \\ &= \Omega P^{1/2} \{ \mathbb{1} - \tilde{R}^L L^{(+)} \}^{-1} \{ \mathbb{1} - \tilde{R}^L L^{(-)} \} P^{-1/2} \Omega, \end{aligned} \quad (4.32)$$

where  $\Omega$  and  $P^{1/2}$  are matrices with elements  $e^{i\Omega_{\bar{c}\bar{c}'}} \delta_{\bar{c}\bar{c}'}$  and  $P_{\bar{c}\bar{c}'}^{1/2} \delta_{\bar{c}\bar{c}'}$ , respectively.

For the special choice  $b_{\bar{c}} = B_{\bar{c}}$ , Eq. (4.32) becomes the standard form given by Eq. (1.5) of Sec. VII.1 in the paper by Lane and Thomas (1958), with

$$\tilde{R}_{\bar{c}\bar{c}'}^L(a_{\alpha}, a_{\beta}) = \sum_j \gamma_{j\bar{c}} (\mathcal{E}_j - E)^{-1} \gamma_{j\bar{c}'}. \quad (4.33)$$

For  $b_{\bar{c}} = S_{\bar{c}} + iP_{\bar{c}}$ ,  $L^{(+)}$  becomes the null matrix and Eq. (4.32) reduces to Eq. (4.17). The latter equation corresponds to the standard level matrix formula for the collision matrix  $\tilde{U}$ , given by Eq. (1.14) of Sec. IX.1 in the paper by Lane and Thomas (1958), when their  $R^0$  matrix vanishes.

### C. Standard calculable $R$ -matrix method

Although the Wigner-Eisenbud  $R$ -matrix formalism represents a valuable framework for the analysis and description of experimental data, it has become clear in the last decade that the  $R$ -matrix approach is also useful for the calculation of reaction cross sections starting from an assumed underlying model Hamiltonian for the system. In this section, we shall discuss the  $R$ -matrix method from this point of view.

In the Wigner-Eisenbud theory, the basis states are taken to be eigenfunctions of the total Hamiltonian  $H$ , and the resonance energies  $\mathcal{E}_j$  and partial widths  $\Gamma_{j\bar{c}}$  are fitted to the experimental data. For an *ab initio* calculation employing a model Hamiltonian, it is generally necessary to generate the basis states  $|\phi_j\rangle$  as the eigenfunctions of some simpler Hamiltonian  $H_0$ , for which the Schrödinger equation is readily soluble, i.e.,

$$H_0 |\phi_j\rangle = \mathcal{E}_j |\phi_j\rangle, \quad (4.34)$$

where

$$H_0 = H - V \quad (4.35)$$

and  $V$  is a residual interaction. The basis states are assumed to satisfy the boundary conditions of Eqs. (4.23) and (4.25), so that

$$\begin{aligned} (G^{L^{-1}})_{jj'} &= (\mathcal{E}_j - E)\delta_{jj'} + \langle \phi_j | V | \phi_{j'} \rangle \\ &+ \sum_{\bar{c}} \gamma_{j\bar{c}} \gamma_{j'\bar{c}} (B_{\bar{c}} - S_{\bar{c}} - iP_{\bar{c}}), \end{aligned} \quad (4.36)$$

and the matrix  $\tilde{R}^L$  can be obtained by means of Eqs. (4.2) and (4.3). The calculation of the collision matrix using Eq. (4.17) is then straightforward. We call the above formalism the standard (calculable)  $R$ -matrix (SRM) method.

As previously indicated, the choice of the basis states  $|\phi_j\rangle$  is dependent upon the way in which the total Hamiltonian  $H$  is split into the two components,  $H_0$  and  $V$ ,

and also upon the boundary conditions satisfied by these states at the channel radii  $a_\alpha$ . Although in principle any complete set of basis states will allow the computation of the collision matrix using the procedure outlined above, in practice a judicious choice of the states  $|\phi_j\rangle$  will enable the number of terms which must be retained in the expansions in Eq. (4.2) to be minimized. A reduction in the numerical computational effort is thereby achieved.

The division of the Hamiltonian  $H$  into the components  $H_0$  and  $V$  is often governed by the nature of the scattering problem to be solved. In any case, a selection which ensures that the residual interaction  $V$  is as small as possible ensures optimum convergence of the series in Eq. (4.2). The second problem, the choice of the optimum set of boundary conditions to be satisfied by the basis states at the channel radii, forms the subject of Sec. V.

Haglund and Robson (1965) first applied the SRM method to the simple case of two weakly coupled square-well potentials, and later Buttle (1967) considered the more realistic case of nucleon scattering from  $^{12}\text{C}$  in a particle-plus-rotator picture. These calculations showed that the SRM method is a practical approach for the solution of coupled-channels problems. However, the method has one major flaw. Since the basis states are assumed to satisfy fixed boundary conditions at the channel radii [Eq. (4.23)], the scattering wave function which is expanded in terms of such basis states will have the same boundary conditions. This means that in general the scattering wave function which has been constructed will have a *discontinuity* of slope at the channel radii. This discontinuity gives rise to slow convergence of the basis set expansion for the scattering wave function

$$|\Psi_k\rangle = \sum_j a_j^{(k)} |\phi_j\rangle, \quad (4.37)$$

where the  $a_j^{(k)}$  are appropriate coefficients.

One method of improving the results obtained using the SRM method is the "Buttle correction," which is discussed in the next section. Another approach is to employ basis states which are complete over a larger region of configuration space than the internal region. This extended (or generalized)  $R$ -matrix (ERM) method will be considered in Sec. IV.F. Other techniques are the finite-element method (Nordholm and Bacskay, 1978) (see Sec. IV.E), the natural boundary condition (NBC) methods (see Sec. V), and variational methods (see Sec. VI).

#### D. Buttle correction

In any calculation of the scattering cross sections for an assumed Hamiltonian, it is possible to investigate the effect on the scattering cross sections of "switching-off" the residual interaction, i.e., of arbitrarily setting the term  $V$  in Eq. (4.36) equal to zero. If the unperturbed Hamiltonian  $H_0$  is single particle in nature, the scattering problem reduces to simple potential scattering, which is readily soluble exactly. However, it is still possible (although unnecessary) to use the  $R$ -matrix formulation for the solution of the potential scattering problem. In general, a

truncation error arises because of the retention of only a finite number of basis states in the expansion of Eq. (4.2) for the  $\tilde{R}^L$  matrix, and as a consequence, even in this simple case, the  $R$ -matrix method yields a result which differs from the correct solution.

Buttle (1967) has given a procedure to obtain a corrected  $R$ -matrix,  $\tilde{R}^B$ , in which the truncation error described above has been completely eliminated when the residual interaction is zero. It is expected that the same procedure will also reduce the truncation error in the more general case when the residual interaction is finite, since the coupling  $\langle\phi_j|V|\phi_{j'}\rangle$  between distant levels ( $j' \neq j$ ), which oscillate rapidly with the radial coordinate, is likely to be weak. We shall now describe the "Buttle correction" to the SRM method in some detail.

In the following, a convention is adopted where a left superscript zero added to a quantity indicates that this quantity is calculated when the residual interaction  $V$  has been set equal to zero. For instance, with this convention, we have from Eqs. (4.36) and (4.2)

$$({}^0G^{L-1})_{jj'} = (\mathcal{E}_j - E)\delta_{jj'} + \sum_{\bar{c}} \gamma_{j\bar{c}} \gamma_{j'\bar{c}} (B_{\bar{c}} - S_{\bar{c}} - iP_{\bar{c}}), \quad (4.38)$$

so that

$${}^0\tilde{R}_{cc'}^L = \sum_{jj'} \gamma_{jc} ({}^0G^L)_{jj'} \gamma_{j'c'} \delta_{cc'}. \quad (4.39)$$

The term  $\delta_{cc'}$  in Eq. (4.39) arises, since, for  $H_0$  single particle in nature, there is no channel-coupling present.

The equation analogous to Eq. (3.10), which defines the scattering wave function when  $V=0$ , can be written

$$|{}^0\Psi_k\rangle = {}^0G^L \mathcal{L}(b_c) |{}^0\Psi_k\rangle. \quad (4.40)$$

Then, corresponding to Eq. (4.1), we have

$$\begin{aligned} {}^0y_{ac}^{(k)}(a_\alpha) &= \left[ \frac{\hbar^2 a_\alpha}{2m_c} \right]^{1/2} (c | {}^0\Psi_k \rangle \\ &= \sum_{\beta} \sum_{c' \in \beta} {}^0\tilde{R}_{cc'}^L(a_\alpha, a_\beta) \\ &\quad \times \left[ a_\beta^{1/2} \frac{\partial}{\partial a_\beta} a_\beta^{1/2} - b_{c'} \right] {}^0y_{\beta c'}^{(k)}(a_\beta) \\ &= {}^0\tilde{R}_{cc}^L \left[ a_\alpha^{1/2} \frac{\partial}{\partial a_\alpha} a_\alpha^{1/2} - b_c \right] {}^0y_{ac}^{(k)}(a_\alpha). \end{aligned} \quad (4.41)$$

In Eq. (4.41), application has been made of the fact that  ${}^0\Psi_k$  has components in only one channel and that the matrix  ${}^0\tilde{R}^L$  is diagonal in channel space. Thus

$${}^0\tilde{R}_{cc'}^L = \left[ \frac{a_\alpha^{1/2}}{{}^0y_{ac}^{(k)}(a_\alpha)} \frac{\partial}{\partial a_\alpha} [a_\alpha^{1/2} {}^0y_{ac}^{(k)}(a_\alpha)] - b_c \right]^{-1} \delta_{cc'}, \quad (4.42)$$

which is readily calculable from the known eigenfunctions of the single-particle Hamiltonian  $H_0$ .

Equations (4.39) and (4.42) thus represent two alternative expressions for the matrix elements  ${}^0\tilde{R}_{cc'}^L$ . If the representation of  ${}^0G^L$  in Eq. (4.39) is truncated at  $j=n$ , the error  $(\Delta R)$  involved in the truncation is given by

$$(\Delta R)_{cc'} = \left[ \left[ \frac{a_\alpha^{1/2}}{{}^0y_{ac}^{(k)}(a_\alpha)} \frac{\partial}{\partial a_\alpha} [a_\alpha^{1/2} {}^0y_{ac}^{(k)}(a_\alpha)] - b_c \right]^{-1} - \sum_{j,j'=1}^n \gamma_{jc} ({}^0G^L)_{jj'} \gamma_{j'c} \right] \delta_{cc'}, \quad (4.43)$$

where  ${}^0G^L$  is the inverse of the matrix given by Eq. (4.38). Thus the Buttle-corrected  $R$ -matrix (BCRM),  $\tilde{R}^B$ , has elements

$$\tilde{R}_{cc'}^B = \sum_{j,j'=1}^n \gamma_{jc} (G^L)_{jj'} \gamma_{j'c} + (\Delta R)_{cc'}. \quad (4.44)$$

The Buttle correction  $(\Delta R)$  vanishes in the limit as  $n \rightarrow \infty$ . For finite values of  $n$ , it is anticipated that  $\tilde{R}^B$  will lead to more accurate results for the collision matrix than the uncorrected corresponding  $R$  matrix,  $\tilde{R}^L$ . In the case where the residual interaction  $V$  becomes vanishingly small, the BCRM leads to the exact result for the  $U$  matrix.

The Buttle correction also vanishes if the basis states satisfy the same (natural) boundary conditions at the channel radii as the scattering wave function, i.e.,

$$\mathcal{L}(b_c | \phi_j) = \mathcal{L}(b_c | \Psi_k) = 0. \quad (4.45)$$

For such boundary condition parameters, the matrix  ${}^0\tilde{R}^L$  given by Eq. (4.42) becomes singular. This implies [Eq. (4.39)] that the matrix  ${}^0G^L$  is also singular for natural boundary conditions. Indeed,  ${}^0G^L$  has matrix elements

$$({}^0G^L)_{jj'} = (\mathcal{E}_j - E)^{-1} \delta_{jj'} \quad (4.46)$$

with one of the eigenvalues  $\mathcal{E}_i$  equal to  $E$ . In this case

$$\begin{aligned} {}^0\tilde{R}_{cc'}^L &= \sum_{jj'} \gamma_{jc} ({}^0G^L)_{jj'} \gamma_{j'c} \delta_{cc'} \\ &= \sum_j \gamma_{jc} (\mathcal{E}_j - E)^{-1} \gamma_{j'c} \delta_{cc'}. \end{aligned} \quad (4.47)$$

For satisfactory convergence, the truncated basis set ( $j \leq n$ ) must contain at least the basis state corresponding to the eigenvalue  $\mathcal{E}_i$  and hence the "pole" terms in the matrix  ${}^0\tilde{R}^L$ . Thus the Buttle correction,

$$(\Delta R)_{cc'} = \sum_{j>n} \gamma_{jc}^2 (\mathcal{E}_j - E)^{-1} \delta_{cc'}, \quad (4.48)$$

does not contain any singular terms, since for  $j > n$ ,  $\mathcal{E}_j > E$ , and hence its contribution vanishes, because in Eq. (3.14) the  $R$  matrix is multiplied by a factor which vanishes for natural boundary conditions.

The essence of the Buttle method is to solve the  $H_0$  scattering problem exactly, i.e., without truncation, and then to incorporate that result into the  $R$ -matrix formalism. Another way to achieve the same result is provided by the technique of inserting an optical potential for the background scattering described in Sec. III.C. One must merely identify the "optical-model" partition Hamiltonian  $\bar{H}_\alpha$  with  $H_0$ .

## E. Finite-element method

Nordholm and Bacskay (1978) have suggested using the finite-element method (Strang and Fix, 1973) to overcome the slow convergence of the SRM method. By the addition of a small number of sine functions localized within an interval  $[a_\alpha - \Delta a_\alpha, a_\alpha]$  to a standard set of SRM basis states  $|\phi_j\rangle$ , which satisfy Eqs. (4.23) and (4.34), the boundary condition problem can be resolved. For example, if the basis states  $|\phi_j\rangle$  obey Eq. (4.23) with  $B_c = 0$ , then the added sine functions might be

$$\phi_l(r_\alpha) = \left[ \frac{2}{\Delta a_\alpha} \right]^{1/2} \sin[\pi(l-n)(r_\alpha - a_\alpha + \Delta a_\alpha)/\Delta a_\alpha], \quad (4.49)$$

where  $l = n+1, n+2, \dots$ , so that these added basis states correspond to  $B_c$  values of plus or minus infinity. Nordholm and Bacskay have found that about five such sine functions and an interval  $\Delta a_\alpha \approx 2a_\alpha/n$  produces about optimal efficiency. Applying this method to potential scattering, they obtained results comparable in accuracy with the BCRM method.

## F. Extended (or generalized) $R$ -matrix method

The extended (or generalized)  $R$ -matrix (ERM) method was initiated by Tobocman and Nagarajan (1965) and was further developed and tested by others (Nagarajan, Shah, and Tobocman, 1965; Adams, 1967; Garside and Tobocman, 1968, 1969; Lane and Robson, 1969a, 1969b; Purcell, 1969a). The method was devised in an attempt to extend nuclear structure calculations based on the shell model and generalizations thereof to multichannel nuclear reaction calculations. The SRM approach has an inherent obstacle to such a unified reaction theory: It employs basis states which fulfill "homogeneous" boundary conditions at the channel entrance surface, so that it is difficult to comply with the nuclear structure boundary conditions in all but the simplest calculations. The ERM formalism seeks to remedy this difficulty by using basis states which fulfill homogeneous boundary conditions on a hypersphere located external to the channel entrance surface, i.e.,

$$\left[ \frac{1}{\phi_j} \frac{\partial}{\partial r_\alpha} (r_\alpha \phi_j) \right]_{r_\alpha = a'_\alpha} = B_c \quad \text{for } a'_\alpha > a_\alpha. \quad (4.50)$$

By allowing the hypersphere to be located at infinity, one is free to use conventional nuclear structure wave functions (e.g., single-particle harmonic oscillator states). Such wave functions are nonorthogonal over the interaction region, and this is the essential difference between the ERM and SRM methods. It should be noted that the formalism of Sec. III.B, which expresses the collision matrix in terms of  $R$  matrices, is valid for such nonorthogonal basis states representing the Green's-function operators.

The use of a nonorthogonal basis set is expected to lead to more rapid convergence as the number of basis states is increased than that provided by the orthogonal basis of

the SRM method. This is because the nonorthogonal states have boundary conditions on the channel entrance surface which are usually sufficiently "inhomogeneous" to resolve the external boundary constraints. On the other hand, for such a basis, it is a nontrivial task to separate the  $R$  matrix into "nearby" and "distant" levels so that one can no longer apply the Buttle correction for distant levels.

Initially, the ERM method, employing a harmonic oscillator basis set, was tested by application to relatively simple model scattering problems (Nagarajan, Shah, and Tobocman, 1965; Adams, 1967; Purcell, 1969a). It was found that oscillator functions provided a convenient practical basis set which gave satisfactory convergence to the exact results. Moreover, in some cases—e.g., the continuum shell model (Mahaux and Weidenmüller, 1969)—oscillator functions also allow any spurious cm motion to be separated out (Philpott, 1977).

More recently, similar ERM calculations have been carried out (see, for example, Philpott and George, 1974) for more realistic problems, and satisfactory convergence has also been obtained, provided the channel radii were chosen carefully. This sensitivity to the channel radii arises because the ERM method using oscillator functions is generally only *semiconvergent*—i.e., for given channel radii the method converges quite rapidly as the size of the basis is increased to a result close to the exact one, but then diverges again fairly rapidly as the number of basis functions is increased beyond a critical value. This semi-convergence can be avoided if special care is taken to treat correctly the tail of the interaction *outside* the channel entrance surface, but this procedure is inconvenient and not in keeping with the usual philosophy of  $R$ -matrix theory.

Philpott and George (1974) have devised a criterion for choosing values for the channel radii which optimize the convergence of the ERM method when a nonorthogonal basis set is used. They find that the optimum radii have values which minimize the difference between the logarithmic derivatives of the internal and external wave functions at the channel entrance surface. In the following section (Sec. V), we shall discuss methods for which the convergence criterion of Philpott and George is automatically satisfied.

Philpott and co-workers (Philpott, 1976; Philpott, Mukhopadhyay, and Purcell, 1978) have proposed a technique to avoid the above sensitivity to the channel radii. This involves the use of two linearly independent energy-dependent radial functions in each channel, which are treated as additional basis states. These auxiliary functions are chosen in such a way that essentially they improve the form of the trial wave function only near the channel entrance surface. Thus the remaining part of the basis (set of oscillator functions) still carries the full structure content of the model. This technique of Philpott *et al.* is similar in concept to the use of localized sine functions in the finite-element method of Sec. IV.E. With the introduction of the auxiliary functions, fewer oscillator states are required to achieve the same accuracy in the calculations, and the results are much less sensitive to the

choice of channel radii.

Applications of the ERM method and comparison with other techniques are given in Sec. VIII.

## V. NATURAL BOUNDARY CONDITION METHODS

### A. Natural boundary condition parameters

As we have seen in Sec. IV.D, the Buttle correction to the SRM method vanishes when the logarithmic derivatives of the basis states  $|\phi_j\rangle$  are equal to the logarithmic derivative of the scattering wave function  $|\Psi_k\rangle$  at the channel radii and the energy  $E$  at which the  $R$ -matrix method is applied is equal to an eigenvalue of the total Hamiltonian in the internal region. In this case

$$\mathcal{L}(B_c)|\Psi_k\rangle=0, \quad (5.1)$$

$$\mathcal{L}(B_c)|\phi_j\rangle=0, \quad (5.2)$$

and

$$\{H + \mathcal{L}(B_c) - E\}|\Psi_k\rangle=0. \quad (5.3)$$

The quantities  $B_c$  which satisfy the above three equations are defined to be the *natural boundary condition* (n.b.c.) parameters for the wave function  $|\Psi_k\rangle$  at the energy  $E$ . The aim of the natural boundary condition (NBC) methods is to find a technique by which these n.b.c. parameters  $B_c$  may be determined.

The  $R$ -matrix method can be applied for any choice of the basis states  $|\phi_j\rangle$  and will yield correct results for the collision matrix, provided an adequate number of terms is retained in the expansion for  $\tilde{R}^L$  [Eq. (4.2)]. However, the convergence of this expansion clearly depends on the particular choice of basis states. The latter in turn are governed by both the nature of the scattering problem, which determines  $H_0$ , and the choice of the boundary constraints at the channel radii. The calculation and inversion of the matrix  $G^{L-1}$ , necessary for the computation of the  $R$  matrix, can require a substantial fraction of the total computing time for the problem. Any procedure which selects a set of basis states producing improved convergence in the expansion Eq. (4.2), which of necessity must be truncated, thereby also reduces the dimension of the matrix  $G^{L-1}$  to be calculated and inverted. For a given Hamiltonian  $H_0$ , the optimum convergence is obtained when the corresponding basis states of Eq. (4.34) satisfy natural boundary conditions.

That this latter statement is true is shown by the following considerations. In the general case, when the basis states satisfy parameters other than the natural boundary conditions at the channel radii, the expansion of the scattering wave function in terms of the basis states [Eq. (4.37)] does not converge *uniformly* at the channel radii. This effect corresponds to the Gibbs phenomenon of Fourier analysis (see, for instance, Carslaw, 1930), which arises due to the inability of the basis states to resolve the boundary conditions. As mentioned in Sec. IV, this lack of uniform convergence leads to a discontinuity of the



slope at the channel radii. This is particularly unfortunate for the SRM method, since some of the important quantities, namely, the partial widths  $\Gamma_{j\bar{c}}$  and thus the collision matrix, depend on the expansion of the scattering wave function just at the channel radii. The number of terms required in the expansion to represent the scattering wave function adequately in the internal region including the boundary therefore becomes large. When n.b.c. parameters are employed at the channel radii, the problems caused by the lack of uniform convergence are avoided. The internal scattering wave function, which is the eigenfunction associated with an eigenvalue of the total Hamiltonian in the internal region, joins smoothly (i.e., with no discontinuity of slope or value) to the known asymptotic form of the scattering wave function at that energy.

The main complication introduced by the NBC approach is that the n.b.c. parameters are *energy dependent*. This necessitates the calculation of the basis states  $|\phi_j\rangle$  at each energy. Clearly, the numerical procedures used to achieve this must be highly efficient; otherwise the computational advantage, gained by the reduction in size of the matrices to be manipulated, will be lost. A discussion of this problem and a comparison of the relative efficiency of the different approaches is contained in Sec. VIII. In this section we shall present the mathematical formalism of the various NBC methods.

## B. Eigenchannel method

The eigenchannel method, developed by Danos and Greiner (1966), was the first of the NBC methods to receive wide usage. This approach and its application to photonuclear reactions has already been reviewed comprehensively (Barrett *et al.*, 1973) and so will be discussed here only in order to set it in context with the other NBC methods.

In the eigenchannel method, the scattering wave function satisfies Eqs. (5.1) and (5.3), and the orthogonal basis states are given by Eq. (5.2) and the relation

$$\{H_0 + \mathcal{L}(B_c) - \mathcal{E}_j\} |\phi_j\rangle = 0, \quad (5.4)$$

where  $B_c$  are n.b.c. parameters and

$$H = H_0 + V, \quad (5.5)$$

where  $V$  is a residual interaction. As before, the scattering wave function can be expanded in terms of the basis states

$$|\Psi_k\rangle = \sum_j a_j^{(k)} |\phi_j\rangle. \quad (5.6)$$

Substitution of Eqs. (5.4) and (5.6) into Eq. (5.3) and projecting onto the basis state  $\langle\phi_i|$  lead to the infinite set of equations

$$\sum_j a_j^{(k)} [(\mathcal{E}_j - E)\delta_{ij} + V_{ij}] = 0, \quad (5.7)$$

where

$$V_{ij} = \langle\phi_i| V |\phi_j\rangle. \quad (5.8)$$

The problem is therefore to determine the expansion coefficients  $a_j^{(k)}$  for the scattering wave function by solving Eq. (5.7).

In the eigenchannel method, the additional requirement is imposed that the scattering wave function in the external region consist of a set of standing-wave solutions with a *common* phase shift, the eigenphase  $\delta_k$ , in each open channel. This asymptotic boundary condition has been discussed in Sec. II.B.3.

Numerically, the eigenchannel procedure is as follows:

- (1) An arbitrary value is assumed for the eigenphase  $\delta_k$ .
- (2) Assuming that this value chosen for the eigenphase is correct, the boundary condition parameters  $B_c$  in each channel for the scattering wave function  $|\Psi_k\rangle$  are given in terms of the known asymptotic form of the radial wave function in each channel, i.e.,

$$B_c = \frac{1}{x_{ac}^{(k)}(a_\alpha)} \frac{\partial}{\partial a_\alpha} [a_\alpha x_{ac}^{(k)}(a_\alpha)], \quad (5.9)$$

where for open channels

$$x_{ac}^{(k)}(a_\alpha) = v_{\bar{c}k} [\zeta_{ac}^{(-)}(a_\alpha) e^{-i\delta_k} - \zeta_{ac}^{(+)}(a_\alpha) e^{+i\delta_k}], \quad (5.10)$$

and for closed channels

$$x_{ac}^{(k)}(a_\alpha) = \zeta_{ac}^{(+)}(a_\alpha). \quad (5.11)$$

The wave functions  $\zeta_{ac}^{(\pm)}$  are defined by Eqs. (2.9) and (2.10) and are known.

- (3) Using the values of the parameters  $B_c$  obtained in step (2), a set of basis states  $|\phi_j\rangle$  can be determined which obey Eqs. (5.2) and (5.4).
- (4) The matrix  $h$  with elements

$$h_{ij} = \mathcal{E}_j \delta_{ij} + V_{ij} \quad (5.12)$$

can then be computed and diagonalized to obtain a set of eigenvalues  $E_j$ .

- (5) If by chance one of the eigenvalues obtained in step (4) is equal to the energy  $E$ , then the value chosen for  $\delta_k$  is indeed an eigenphase. Normally this will not be the case and a search procedure is required to vary the assumed value for  $\delta_k$  until one of the eigenvalues  $E_j$  is equal to the energy  $E$ . From the associated wave function, the amplitudes  $v_{\bar{c}k}$  are determined.
- (6) In this manner, each member of the total set of  $m$  eigenphases (for  $m$  open channels)—i.e.,  $\delta_k$  ( $k=1, 2, \dots, m$ )—can be obtained in turn.
- (7) Once the complete set of eigenphases  $\delta_k$  and corresponding amplitudes  $v_{\bar{c}k}$  has been obtained, the collision matrix at energy  $E$  and hence the various reaction cross sections can be calculated using the relation [Eq. (2.44)]

$$\tilde{U} = v e^{2i\Delta} v^{-1}, \quad (5.13)$$

where  $v$  and  $\Delta$  are matrices whose elements are  $v_{\bar{c}k}$  and  $\delta_k \delta_{\bar{c}k}$ , respectively.

Although extremely simple in principle, the eigenchan-

nel method suffers from two major disadvantages. First, since the n.b.c. parameters are energy dependent, it is necessary to repeat all of the steps (1)–(7) for each energy at which a calculation of the scattering cross sections is desired. Second, the method involves an iteration procedure, each stage of which requires the determination of a new set of basis states  $|\phi_j\rangle$ , as well as the computation and diagonalization of a  $\nu m \times \nu m$  matrix, where  $\nu$  is the number of basis states retained in each channel (it is assumed that  $\nu$  is independent of  $c$ ). The time required for matrix diagonalization increases rapidly as the size of the matrix increases, so that, for problems involving many coupled channels, most of the computing time is spent handling matrix diagonalizations. Thus any numerical advantage over the SRM method, obtained by the improved convergence of the expansion of Eq. (5.6) when n.b.c. parameters are used to define the basis states  $|\phi_j\rangle$ , is largely lost by the inefficiency of a technique requiring many diagonalizations of large matrices. The second NBC method, which will be discussed in the following section, was designed to minimize this numerical inefficiency of the iteration procedure of the eigenchannel approach while retaining the superior convergence properties of the basis states resulting from the use of n.b.c. parameters.

### C. Barrett-Delsanto method

As indicated in Sec. II.B, the eigenchannel boundary conditions are just one of an infinite set of possible standing-wave boundary conditions which can be imposed on the scattering wave function at the channel radii. In the more general case, the phase shifts between incoming and outgoing waves in each open channel,  $\delta_{\bar{c}k}$ , are not equal. It is the requirement of the eigenchannel method that these phase shifts be the same for each open channel—i.e., be eigenphases—which leads directly to the numerical inefficiency of the method.

As can be seen from Eq. (5.9), any change in the eigenphase  $\delta_k$  which occurs for an iteration in the eigenchannel method involves a recalculation of the boundary condition parameters  $B_{\bar{c}}$  for *all* the open channels considered. Thus for each iteration a different set of basis states is employed for each open channel, so that the matrix  $h$  must be substantially recalculated (only the closed channel basis states remain constant) and diagonalized. In the Barrett-Delsanto (BD) method (Barrett and Delsanto, 1974), the eigenchannel requirement that the phase shifts  $\delta_{\bar{c}k}$  be the same for all open channels is dropped. In this case, the boundary condition parameters for  $(m-1)$  of the  $m$  open channels can be arbitrarily chosen and kept constant and an iteration carried out only for the boundary condition parameter for the remaining open channel until one of the

eigenvalues  $E_j$  of the matrix  $h$  coincides with the energy  $E$  at which the collision matrix is to be calculated. The set of parameters  $B_{\bar{c}}$  so determined are n.b.c. parameters in the sense of Eqs. (5.1)–(5.3) for the particular set of asymptotic standing-wave solutions chosen. From the associated wave function [Eq. (5.6)], the corresponding quantities  $v_{\bar{c}k}$  and  $\delta_{\bar{c}k}$  can be obtained, using Eqs. (5.7) and (5.9). This procedure is repeated by carrying out the iteration for each of the open channels in turn, with arbitrary boundary conditions imposed on the remaining  $(m-1)$  open channels. In this way a set of degenerate wave functions  $|\psi_k\rangle$  ( $k=1, 2, \dots, m$ ) is obtained and hence a complete set of amplitudes  $v_{\bar{c}k}$  and phase shifts  $\delta_{\bar{c}k}$ . The collision matrix  $\tilde{U}$  can then be calculated using Eq. (2.41), i.e.,

$$\tilde{U} = A^* A^{-1}, \quad (5.14a)$$

where

$$A_{\bar{c}k} = v_{\bar{c}k} e^{-i\delta_{\bar{c}k}}. \quad (5.14b)$$

The numerical advantage of the BD approach over the eigenchannel method is twofold. First, since arbitrary boundary conditions are imposed on all but one of the open channels, it is necessary to recalculate the basis states  $|\phi_j\rangle$  in only that one channel during the search procedure for the n.b.c. parameters. Second, as a result of this, a large block of the  $h$  matrix is left unchanged during the iteration procedure, and a different technique can be employed to find the eigenvalues of the  $h$  matrix [Eq. (5.12)]. This technique involves the diagonalization of a  $\nu \times \nu$  matrix rather than the  $\nu m \times \nu m$  matrix of the eigenchannel method. For most applications,  $\nu$  is of the order of 4 or 5, while  $m$  can be quite large ( $> 20$ ) (see Barrett *et al.*, 1973). It is this dramatic reduction in size of the basic matrix to be diagonalized in the iteration procedure, which results in a large saving of computing time in the BD method when compared with the eigenchannel method. The special matrix diagonalization technique employed in the BD method will now be presented.

In the matrix diagonalization, it is convenient to separate the matrix  $h$  given by Eq. (5.12) into submatrices corresponding to the nature of the boundary conditions applied to the basis states used in the calculation of the matrix. In one channel—say,  $c=1$ —the boundary conditions are to be changed during the iteration procedure; in the others they remain fixed, being arbitrary values for the remaining open channels and the known n.b.c. values for the closed channels. Accordingly, the matrix  $h$  can be written as

$$h = \begin{pmatrix} P & V \\ V^\dagger & Q \end{pmatrix}, \quad (5.15)$$

where

$$P = \begin{pmatrix} \mathcal{E}_1 + V_{11} & V_{12} & \cdots & V_{12} \\ V_{21} & \mathcal{E}_2 + V_{22} & \cdots & V_{22} \\ \vdots & \vdots & \ddots & \vdots \\ V_{\nu 1} & V_{\nu 2} & \cdots & \mathcal{E}_\nu + V_{\nu\nu} \end{pmatrix}, \quad (5.16)$$

$$Q = \begin{pmatrix} \mathcal{E}_{v+1} + V_{v+1v+1} & V_{v+1v+2} & \cdots & V_{v+1vm} \\ V_{v+2v+1} & \mathcal{E}_{v+2} + V_{v+2v+2} & \cdots & V_{v+2vm} \\ \vdots & \vdots & \ddots & \vdots \\ V_{vmv+1} & V_{vmv+2} & \cdots & \mathcal{E}_{vm} + V_{vmvm} \end{pmatrix}, \quad (5.17)$$

and

$$V = \begin{pmatrix} V_{1v+1} & V_{1v+2} & \cdots & V_{1vm} \\ V_{2v+1} & V_{2v+2} & \cdots & V_{2vm} \\ \vdots & \vdots & \ddots & \vdots \\ V_{vv+1} & V_{vv+2} & \cdots & V_{vvm} \end{pmatrix}. \quad (5.18)$$

Defining the two column vectors  $x$  and  $y$  by

$$x = \begin{pmatrix} a_1^{(1)} \\ a_2^{(1)} \\ \vdots \\ a_v^{(1)} \end{pmatrix} \quad (5.19)$$

and

$$y = \begin{pmatrix} a_{v+1}^{(1)} \\ a_{v+2}^{(1)} \\ \vdots \\ a_{vm}^{(1)} \end{pmatrix}, \quad (5.20)$$

Eq. (5.12) can be rewritten in matrix notation as

$$\begin{pmatrix} P & V \\ V^\dagger & Q \end{pmatrix} \begin{pmatrix} x \\ y \end{pmatrix} = E \begin{pmatrix} x \\ y \end{pmatrix}. \quad (5.21)$$

The procedure is now to “prediagonalize” the matrix  $Q$ , a process which is performed only once and not at each step of the iteration procedure. This is accomplished by making use of the transformation

$$y = Cz, \quad (5.22)$$

where  $C$  is a unitary matrix such that

$$C^\dagger Q C = \Lambda, \quad (5.23)$$

and  $\Lambda$  is the diagonal matrix with elements

$$\Lambda_{ij} = \lambda_i \delta_{ij}. \quad (5.24)$$

Multiplying Eq. (5.21) on the left by the matrix

$$\begin{pmatrix} 1 & 0 \\ 0 & C^\dagger \end{pmatrix},$$

and applying Eqs. (5.22) and (5.23) yields the results

$$\begin{pmatrix} P & W \\ W^\dagger & \Lambda \end{pmatrix} \begin{pmatrix} x \\ z \end{pmatrix} = E \begin{pmatrix} x \\ z \end{pmatrix}, \quad (5.25)$$

where

$$W = VC \quad (5.26)$$

and

$$z = C^\dagger y. \quad (5.27)$$

The system of equations (5.25) can be written as two simultaneous equations:

$$Px + Wz = Ex, \quad (5.28)$$

$$W^\dagger x + \Lambda z = Ez, \quad (5.29)$$

where  $E$  is the diagonal matrix with elements  $E_{ij} = E \delta_{ij}$ . Neglecting the possibility of  $E$  being exactly equal to one of the eigenvalues  $\lambda_i$  of the matrix  $Q$  [although this possibility can be easily treated (Barrett and Delsanto, 1974)], Eqs. (5.28) and (5.29) can be combined to give

$$[(P - E) + W(E - \Lambda)^{-1}W^\dagger]x = 0. \quad (5.30)$$

For a given set of boundary condition parameters  $B_c$ , the matrix  $\bar{h}$  with elements

$$\bar{h}_{ij} = P_{ij} + \sum_k \frac{W_{ik}W_{jk}}{E - \lambda_k} \quad (5.31)$$

can be calculated and diagonalized. In general, none of the eigenvalues of  $\bar{h}$  will be equal to the energy  $E$ . As before, an iteration procedure can be set up to vary the boundary constraint for channel  $c=1$  until the energy  $E$  coincides with one of the eigenvalues of  $\bar{h}$ , in which case one set of n.b.c. parameters has been found. The expansion coefficients  $a_j^{(1)}$  ( $j=1, 2, \dots, v$ ) of the total wave function in the first channel are simply the elements of the eigenvector  $x$  associated with the particular eigenvalue of  $\bar{h}$  which is equal to  $E$ . The coefficients  $a_{j>v}^{(1)}$  in the other channels are the elements of the vector  $y$  and can be obtained using Eqs. (5.27)–(5.29) from the relation

$$y = C(E - \Lambda)^{-1}W^\dagger x. \quad (5.32)$$

Other sets of n.b.c. parameters may be obtained by a different choice of the open channel upon which the iteration is to be performed. In this way,  $m$  independent sets of n.b.c. parameters can be determined. The collision matrix  $\bar{U}$  is then given by Eq. (5.14), where the amplitudes  $v_{c\bar{c}}$  can be obtained by matching the internal and external total wave functions  $|\Psi_k\rangle$  at the channel radii and where the phase shifts  $\delta_{c\bar{c}}$  are given in terms of the n.b.c. parameters by Eq. (5.9).

#### 1. Energy correction to the BD method

It is possible to make a simple correction to the energy eigenvalues and wave functions obtained in the BD

method to allow approximately for the effect of the neglected higher levels with a consequent improvement in accuracy (Ahmad, Barrett, and Robson, 1976b). This is done in the following manner.

Let us assume that the BD method has been carried out using a set of basis states truncated to  $\nu$  levels in each channel. The iteration of the boundary condition parameter for one open channel has been completed, so that one of the eigenvalues  $E_i$  of the matrix  $h$  [Eq. (5.12)] is equal to the energy  $E$  and the boundary constraints are natural. Then the eigenfunction  $|\Psi_i\rangle$ , associated with the eigenvalue  $E_i$ , can be expanded in terms of the basis states  $|\phi_j\rangle$ , which satisfy n.b.c. parameters:

$$|\Psi_i\rangle = \sum_j a_j^{(i)} |\phi_j\rangle, \quad (5.33)$$

and the secular equation [Eq. (5.7)] may be written

$$\sum_j a_j^{(i)} \langle \phi_k | H | \phi_i \rangle = \langle \phi_k | H | \Psi_i \rangle = E_i a_k^{(i)}. \quad (5.34)$$

We now investigate the effect of including a previously neglected level,  $\phi_m$ . The addition of this level modifies Eq. (5.33) for the wave function, which is now given by

$$|\bar{\Psi}_i\rangle = \sum_j b_j^{(i)} |\phi_j\rangle + b_m^{(i)} |\phi_m\rangle. \quad (5.35)$$

The sum in Eq. (5.35) (and in subsequent equations) runs over only those levels  $|\phi_j\rangle$  which are treated exactly; the extra level  $|\phi_m\rangle$  being written explicitly.

The secular equation now becomes

$$\sum_j b_j^{(i)} \langle \phi_k | H | \phi_j \rangle + b_m^{(i)} \langle \phi_k | H | \phi_m \rangle = \bar{E}_i b_k^{(i)} \quad (5.36)$$

and

$$\sum_j b_j^{(i)} \langle \phi_m | H | \phi_j \rangle + b_m^{(i)} \langle \phi_m | H | \phi_m \rangle = \bar{E}_i b_m^{(i)}, \quad (5.37)$$

where  $\bar{E}_i$  are the new eigenvalues, which have been slightly shifted from the old values  $E_i$  by the introduction of the extra level. Let us define  $Z_{il}$  by the relationship

$$Z_{il} = \sum_j b_j^{(i)} a_j^{(l)}, \quad (5.38)$$

where the  $a_j^{(l)}$  are given by Eq. (5.34). Then

$$b_j^{(i)} = \sum_l a_j^{(l)} Z_{il}, \quad (5.39)$$

since the coefficients  $a_j^{(l)}$  are the elements of an orthogonal matrix. Using Eq. (5.34) we may write Eqs. (5.36) and (5.37) in the form

$$E_l Z_{il} + b_m^{(i)} \langle \Psi_l | H | \phi_m \rangle = \bar{E}_i Z_{il} \quad (5.40)$$

and

$$\sum_l Z_{il} \langle \phi_m | H | \Psi_l \rangle + b_m^{(i)} \langle \phi_m | H | \phi_m \rangle = \bar{E}_i b_m^{(i)}. \quad (5.41)$$

Rearrangement of Eq. (5.40) yields

$$Z_{il} = b_m^{(i)} \langle \Psi_l | H | \phi_m \rangle / (\bar{E}_i - E_l), \quad (5.42)$$

which upon substitution into Eq. (5.41) gives

$$\bar{E}_i = \langle \phi_m | H | \phi_m \rangle + \sum_l \frac{|\langle \Psi_l | H | \phi_m \rangle|^2}{(\bar{E}_i - E_l)}. \quad (5.43)$$

Since we are interested only in the eigenvalue  $\bar{E}_i$ , which is closest to the original eigenvalue  $E_i = E$ , one term is expected to dominate the sum in Eq. (5.43), i.e.,

$$\bar{E}_i \approx \langle \phi_m | H | \phi_m \rangle + \frac{|\langle \Psi_i | H | \phi_m \rangle|^2}{(\bar{E}_i - E_i)}. \quad (5.44)$$

The solution of this equation for  $\bar{E}_i$  is

$$\bar{E}_i = \frac{1}{2} \{ \langle \phi_m | H | \phi_m \rangle + E_i \pm [(\langle \phi_m | H | \phi_m \rangle - E_i)^2 + 4 |\langle \phi_m | H | \Psi_i \rangle|^2]^{1/2} \}. \quad (5.45)$$

If we assume

$$|\langle \phi_m | H | \Psi_i \rangle| \ll (\langle \phi_m | H | \phi_m \rangle - E_i)$$

and expand the square root by the binomial theorem, the solution for  $\bar{E}_i$  near  $E_i$  is given by

$$\bar{E}_i \approx E_i - \frac{|\langle \phi_m | H | \Psi_i \rangle|^2}{\langle \phi_m | H | \phi_m \rangle - E_i}. \quad (5.46)$$

The effect of as many higher levels as necessary may be approximately included by successive application of Eq. (5.46) without increasing the dimensions of the matrices to be diagonalized and thus without a substantial effect on the computation time. The iteration procedure in the BD method is now continued until the corrected value of one of the eigenvalues,  $\bar{E}_i$ , is equal to  $E$ . The small correction to the energy leads to slightly different values for the n.b.c. parameters,  $B_c$ , and hence for the phase shifts,  $\delta_{\bar{c}k}$ , in the asymptotic region.

The expansion coefficients,  $b_j^{(i)}$  and  $b_m^{(i)}$ , in Eq. (5.35) must also be calculated in order to obtain the corresponding "corrected" values for the amplitudes  $v_{\bar{c}k}$ . From Eqs. (5.39) and (5.42), we have, assuming  $\bar{E}_i \approx E_i$ , that

$$\begin{aligned} b_j^{(i)} &= b_m^{(i)} \sum_l a_j^{(l)} \frac{\langle \Psi_l | H | \phi_m \rangle}{(\bar{E}_i - E_l)} \\ &\approx b_m^{(i)} \frac{\langle \Psi_i | H | \phi_m \rangle}{(\bar{E}_i - E_i)} a_j^{(i)}. \end{aligned} \quad (5.47)$$

Since the normalization is arbitrary, it is convenient to choose

$$b_m^{(i)} = (\bar{E}_i - E_i) / \langle \Psi_i | H | \phi_m \rangle, \quad (5.48)$$

so that

$$b_j^{(i)} = a_j^{(i)}. \quad (5.49)$$

Thus, with this choice of normalization, the expansion coefficients,  $b_j^{(i)}$ , for the components of the wave function treated exactly remain unchanged by the correction, and

the coefficient for the additional component is given approximately by Eq. (5.48). These coefficients may be employed to yield improved estimates of the amplitudes  $v_{\bar{c}k}$  and hence of the collision matrix  $\tilde{U}$ .

## 2. Perturbation treatment for the BD method

If the residual interaction  $V$  [Eq. (5.5)] is very small, then using second-order perturbation theory (Delsanto and Quarati, 1979), the BD method may be implemented without any iteration or search process. The procedure is as follows.

First, one chooses a set of values for *all* the boundary condition parameters  $B_{\bar{c}}$  and n.b.c. values  $B_{\bar{c}}$  for the closed channels. These determine a set of basis states  $|\phi_j\rangle$  and eigenenergies  $\mathcal{E}_i$  given by Eq. (5.4). As a result of the residual interaction, the eigenvalue  $\mathcal{E}'_i$  of the matrix  $\bar{h}$  of Eq. (5.31), which is required to be equal to the energy of the system  $E$ , will be slightly shifted from the corresponding unperturbed eigenvalue  $\mathcal{E}_i$ . To second order we have

$$\mathcal{E}'_i = \mathcal{E}_i + V_{ii} + \sum_k \frac{|W_{ik}|^2}{(\mathcal{E}_i - \lambda_k)}, \quad (5.50)$$

where  $V_{ii}$ ,  $W_{ik}$ , and  $\lambda_k$  are given by Eqs. (5.8), (5.26), and (5.24), respectively. This eigenenergy  $\mathcal{E}'_i$  is the energy  $E$  corresponding to the chosen boundary condition values  $B_{\bar{c}}$ , which form one set— $k$ , say—of n.b.c. parameters. The phase shifts  $\delta_{\bar{c}k}$  are given directly in terms of these parameters  $B_{\bar{c}}$  by Eq. (5.9), and the corresponding amplitudes  $v_{\bar{c}k}$  can be obtained as before by matching the internal and external total wave functions  $|\Psi_k\rangle$  at the channel

radii. Thus, by choosing  $m$  (the number of open channels) independent sets of n.b.c. parameters and using Eq. (5.50), we can obtain the collision matrix  $\tilde{U}$  without any iteration process, provided the residual interaction is sufficiently small.

In the generalized nuclear shell model in which arbitrary finite single-particle potentials  $U_i$  are added to the kinetic energy  $T$  and subtracted from the potential energy  $\mathcal{V}$ , the residual interaction

$$V = \mathcal{V} - \sum_{i=1}^N U_i \quad (5.51)$$

is often small. In such cases, the above procedure can be employed, thus avoiding very many lengthy and complex iterations, with a substantial saving of computing time.

## D. Iterated $R$ -matrix method

It is possible (Ahmad, Barrett, and Robson, 1976a, 1976b) to incorporate n.b.c. parameters into the standard calculable  $R$ -matrix method discussed in Sec. IV.C. Instead of employing, as is customary, a fixed set of basis states for all energies, an energy-dependent basis is chosen by an iterative procedure based explicitly upon the fact that a finite set of basis states with n.b.c. parameters provides the best estimate of the collision matrix. This is the iterative  $R$ -matrix (IRM) method.

The IRM method is closely related to the BD method in that it employs the same standing-wave asymptotic boundary conditions. Substituting Eq. (2.28) into Eq. (4.1) and assuming for convenience that  $b_c = 0$  (all  $c$ ), we have for  $r_\alpha = a_\alpha$

$$\begin{aligned} \left[ \frac{\hbar^2 a_\alpha}{2m_{\bar{c}}} \right]^{1/2} (\bar{c}, a_\alpha | \Psi_k \rangle &= \left[ \frac{\hbar^2 a_\alpha}{2m_{\bar{c}}} \right]^{1/2} v_{\bar{c}k} [\zeta_{\alpha\bar{c}}^{(-)}(a_\alpha) e^{-i\delta_{\bar{c}k}} - \zeta_{\alpha\bar{c}}^{(+)}(a_\alpha) e^{+i\delta_{\bar{c}k}}] \\ &= \sum_\beta \sum_{\bar{c}' \in \beta} \tilde{R}_{\bar{c}\bar{c}'}^L(a_\alpha, a_\beta) \left[ \frac{\hbar^2 a_\beta}{2m_{\bar{c}'}} \right]^{1/2} \left[ \frac{\partial}{\partial a_\beta} a_\beta \right] v_{\bar{c}'k} [\zeta_{\beta\bar{c}'}^{(-)}(a_\beta) e^{-i\delta_{\bar{c}'k}} - \zeta_{\beta\bar{c}'}^{(+)}(a_\beta) e^{+i\delta_{\bar{c}'k}}] \\ &\quad - \sum_\beta \sum_{\bar{c}' \in \beta} \tilde{R}_{\bar{c}\bar{c}'}^L(a_\alpha, a_\beta) \left[ \frac{\hbar^2 a_\beta}{2m_{\bar{c}'}} \right]^{1/2} \left[ \frac{\partial}{\partial a_\beta} a_\beta \right] [\zeta_{\beta\bar{c}'}^{(+)}(a_\beta) U_{\bar{c}'k}] \end{aligned} \quad (5.52)$$

and

$$\begin{aligned} \left[ \frac{\hbar^2 a_\alpha}{2m_{\bar{c}}} \right]^{1/2} (\bar{c}, a_\alpha | \Psi_k \rangle &= - \left[ \frac{\hbar^2 a_\alpha}{2m_{\bar{c}}} \right]^{1/2} \zeta_{\alpha\bar{c}}^{(+)}(a_\alpha) U_{\bar{c}k} \\ &= \sum_\beta \sum_{\bar{c}' \in \beta} \tilde{R}_{\bar{c}\bar{c}'}^L(a_\alpha, a_\beta) \left[ \frac{\hbar^2 a_\beta}{2m_{\bar{c}'}} \right]^{1/2} \left[ \frac{\partial}{\partial a_\beta} a_\beta \right] v_{\bar{c}'k} [\zeta_{\beta\bar{c}'}^{(-)}(a_\beta) e^{-i\delta_{\bar{c}'k}} - \zeta_{\beta\bar{c}'}^{(+)}(a_\beta) e^{+i\delta_{\bar{c}'k}}] \\ &\quad - \sum_\beta \sum_{\bar{c}' \in \beta} \tilde{R}_{\bar{c}\bar{c}'}^L(a_\alpha, a_\beta) \left[ \frac{\hbar^2 a_\beta}{2m_{\bar{c}'}} \right]^{1/2} \left[ \frac{\partial}{\partial a_\beta} a_\beta \right] [\zeta_{\beta\bar{c}'}^{(+)}(a_\beta) U_{\bar{c}'k}]. \end{aligned} \quad (5.53)$$

Here

$$\tilde{R}_{cc'}^L(a_\alpha, a_\beta) = \sum_{j, j'} \gamma_{jc} (G^L)_{jj'} \gamma_{j'c'}, \quad (5.54)$$

$$\gamma_{jc} = \left[ \frac{\hbar^2 a_\alpha}{2m_c} \right]^{1/2} (c, a_\alpha | \phi_j), \quad (5.55)$$

the quantities  $(c, a_\alpha | \phi_j)$  are radial basis functions at  $r_\alpha = a_\alpha$ , and  $G^L$  is the matrix whose inverse has elements  $\langle \phi_j | H + \mathcal{L}(0) - E | \phi_{j'} \rangle$ .

The  $\tilde{U}$ -matrix elements  $U_{\bar{c}k}$  and hence the cross sections may be determined in the following manner. The known n.b.c. parameters for the closed channels, arbitrary values of the  $B_{\bar{c}}$  (and hence of the phase shifts  $\delta_{\bar{c}k}$ ) for all except one of the open channels  $k$ , together with an initial guess for the value of  $B_k$  are used to construct a finite set of basis states (say,  $\nu$  levels/channel). The  $\tilde{R}^L$ -matrix elements are calculated in this basis and the coupled Eqs. (5.52) and (5.53) are solved to obtain the remaining phase shift  $\delta_{kk}$  (as well as the  $m-1$  relative amplitudes  $v_{\bar{c}k}/v_{kk}$ ). From this derived value of  $\delta_{kk}$ , a new value of  $B_k$  may be obtained using Eq. (5.9) and the calculation repeated with new basis states for the channel  $k$ . This defines an iteration procedure which in general converges to the identical result obtained by the BD method for the same boundary conditions. The procedure has to be repeated  $m$  times, corresponding to a different choice of the open channel  $k$  for which  $B_k$  is varied. In this way the matrix elements  $A_{\bar{c}k}$ , depending upon the phase shifts  $\delta_{\bar{c}k}$  and amplitudes  $v_{\bar{c}k}$ , are obtained and the  $\tilde{U}$ -matrix determined from Eq. (5.14a).

In both the IRM and BD methods two or three iterations usually suffice to obtain the n.b.c. value for the parameter  $B_k$  being varied. However, for some excitation energies, the IRM method does not necessarily converge to the corresponding BD result. If during the iteration process the boundary condition parameter  $B_k$  becomes large (say  $|B_k| > 100$ ), the method often "converges" to a value of  $|B_k| \rightarrow \infty$  and not to the n.b.c. value. This is a disadvantage of the IRM method, although the problem is readily overcome by employing a better initial guess (e.g., based upon knowledge of the n.b.c. value at adjacent excitation energies) for the parameter  $B_k$ . The problem appears to arise partly from numerical difficulties associated with the small  $R^L$ -matrix elements associated with large values of  $|B_k|$ .

The BD and IRM methods are closely related techniques using basis states, obtained by an iterative procedure, which satisfy n.b.c. parameters  $B_c$  for the same form of asymptotic wave-function boundary constraints. However, the BD method uses a matrix diagonalization procedure to solve Eq. (5.7), which requires the Bloch parameters  $b_c$  in Eq. (3.8) to be chosen so that  $b_c = B_c$ , while the IRM method employs the  $R$ -matrix formalism and requires matrix inversion to solve Eq. (3.10), i.e.,

$$|\Psi_k\rangle = G^L \mathcal{L}(b_c) |\Psi_k\rangle \quad (5.56)$$

at the channel radii ( $r_\alpha = a_\alpha$ ). In order to solve Eq. (5.56), it is essential that the n.b.c. parameters  $B_c$ , satisfied by

both the basis states and the scattering wave function  $|\Psi_k\rangle$  on the channel entrance surface, should not be equal to the Bloch parameters  $b_c$ ; otherwise, the right-hand side of Eq. (5.56) would be *indeterminate*. On the other hand, the BD method requires that  $b_c = B_c$  (all  $c$ ) and hence, in this sense, is "complementary" to the IRM method.

## VI. VARIATIONAL METHODS

### A. Hulthén-Kohn variational methods for the $K$ matrix

Several variational approaches have been employed to solve the many-body scattering problem, especially for atomic systems. Comprehensive reviews of such methods and their applications have been given recently (Callaway, 1978; Nesbet, 1977, 1980). In this review, we shall therefore give only a brief summary of those methods which are related to or have been compared with the methods previously discussed. In particular, we shall discuss the Hulthén (1944, 1948) and Kohn (1948) variational methods for determining the  $K$  matrix. Since the  $K$  matrix is real and symmetric, it provides a very convenient representation of the open-channel asymptotic boundary conditions for the scattering wave function (see Sec. II.B.4). Once the  $K$  matrix is known, the collision matrix  $\tilde{U}$  is given by Eq. (2.37), i.e., by the relation

$$\tilde{U} = \Sigma (1 - iK)^{-1} (1 + iK) \Sigma, \quad (6.1)$$

where the matrices  $1$ ,  $\Sigma$ ,  $K$ , and  $\tilde{U}$  have elements  $\delta_{\bar{c}k}$ ,  $e^{i\sigma_{\bar{c}}}\delta_{\bar{c}k}$ ,  $K_{\bar{c}k}$ , and  $U_{\bar{c}k}$ , respectively.

In the calculable  $R$  matrix (Sec. IV) and NBC methods (Sec. V) the scattering wave function  $|\Psi_k\rangle$  in the internal region is expanded in terms of a set of basis states, which are chosen to be eigenstates of some simpler Hamiltonian  $H_0$ , which is often single particle in nature. In the variational methods, the basis states ( $\nu$  per channel)

$$|\phi_j\rangle \equiv |\phi_{ci}\rangle \quad (i=1, 2, \dots, \nu)$$

are assumed to be arbitrary linearly independent functions but subject to the following constraints in the external region ( $r_\alpha > a_\alpha$ ):

$$(\tilde{c} | \phi_{\bar{c}1}) = \left[ \frac{m_{\bar{c}}}{\hbar k_{\bar{c}}} \right]^{1/2} F_{l_{\bar{c}}}(k_{\bar{c}} r_\alpha) r_\alpha^{-1}, \quad (6.2)$$

$$(\tilde{c} | \phi_{\bar{c}2}) = \left[ \frac{m_{\bar{c}}}{\hbar k_{\bar{c}}} \right]^{1/2} G_{l_{\bar{c}}}(k_{\bar{c}} r_\alpha) r_\alpha^{-1}, \quad (6.3)$$

and

$$(\tilde{c} | \phi_{\bar{c}i>2}) = 0. \quad (6.4)$$

Then for  $r_\alpha > a_\alpha$

$$(\tilde{c} | \Psi_k) = \left[ \frac{m_{\bar{c}}}{\hbar k_{\bar{c}}} \right]^{1/2} [a_{\bar{c}1}^{(k)} F_{l_{\bar{c}}}(k_{\bar{c}} r_\alpha) + a_{\bar{c}2}^{(k)} G_{l_{\bar{c}}}(k_{\bar{c}} r_\alpha)] r_\alpha^{-1}. \quad (6.5)$$

In principle, the coefficients  $a_{\bar{c}i}^{(k)}$  can be determined by the solution of the Schrödinger equation

$$(H - E)\Psi_k = 0. \quad (6.6)$$

This is in fact the procedure adopted in the calculable  $R$ -matrix and NBC methods. In the variational approach, the  $a_{\bar{c}1}^{(k)}$  and  $a_{\bar{c}2}^{(k)}$  coefficients are chosen so that

$$a_{\bar{c}1}^{(k)} = \delta_{\bar{c}k} = D_{\bar{c}}^{(k)} \quad (6.7)$$

and

$$a_{\bar{c}2}^{(k)} = K_{\bar{c}k} = K_{\bar{c}}^{(k)}, \quad (6.8)$$

i.e., the wave functions  $(\bar{c} | \Psi_k)$  are assumed to satisfy  $K$ -matrix standing-wave asymptotic boundary conditions [Eq. (2.33)].

Writing Eq. (6.6) in the Bloch-Schrödinger form

$$\{H + \mathcal{L}(b_c) - E\}\Psi_k = \mathcal{L}(b_c)\Psi_k, \quad (6.9)$$

where  $\mathcal{L}(b_c)$  is defined by Eq. (3.4), and using the expansion

$$|\Psi_k\rangle = \sum_{ci} a_{ci}^{(k)} |\phi_{ci}\rangle, \quad (6.10)$$

we have

$$\sum_{ci} a_{ci}^{(k)} \{H + \mathcal{L}(b_c) - E\} |\phi_{ci}\rangle = \mathcal{L}(b_c) |\Psi_k\rangle. \quad (6.11)$$

Projecting both sides of Eq. (6.11) onto the basis state  $\langle \phi_{c'i'} |$  gives

$$\sum_{ci} a_{ci}^{(k)} \langle \phi_{c'i'} | H + \mathcal{L}(b_c) - E | \phi_{ci} \rangle = \langle \phi_{c'i'} | \mathcal{L}(b_c) | \Psi_k \rangle. \quad (6.12)$$

Equation (6.12) can also be obtained "variationally" by considering the functional

$$\begin{aligned} I &= \langle \Psi_k | H - E | \Psi_k \rangle \\ &= \langle \Psi_k | H + \mathcal{L}(b_c) - E | \Psi_k \rangle - \langle \Psi_k | \mathcal{L}(b_c) | \Psi_k \rangle \\ &= \sum_{c'i'ci} a_{c'i'}^{(k)*} a_{ci}^{(k)} \langle \phi_{c'i'} | H + \mathcal{L}(b_c) - E | \phi_{ci} \rangle \\ &\quad - \sum_{c'i'} a_{c'i'}^{(k)*} \langle \phi_{c'i'} | \mathcal{L}(b_c) | \Psi_k \rangle. \end{aligned} \quad (6.13)$$

Then for arbitrary infinitesimal variations of the coefficients  $a_{c'i'}^{(k)*}$ , the functional  $I$  is stationary if

$$\begin{aligned} \frac{\partial I}{\partial a_{c'i'}^{(k)*}} &= \sum_{ci} a_{ci}^{(k)} \langle \phi_{c'i'} | H + \mathcal{L}(b_c) - E | \phi_{ci} \rangle \\ &\quad - \langle \phi_{c'i'} | \mathcal{L}(b_c) | \Psi_k \rangle = 0, \end{aligned} \quad (6.14)$$

which is Eq. (6.12).

Equation (6.12) can be rewritten in the form

$$\begin{pmatrix} M^{FF} & M^{FG} & P \\ M^{GF} & M^{GG} & Q \\ P^\dagger & Q^\dagger & N \end{pmatrix} \begin{pmatrix} a^{(k)} \\ b^{(k)} \\ c^{(k)} \end{pmatrix} = \begin{pmatrix} L^F \\ L^G \\ 0 \end{pmatrix}, \quad (6.15)$$

where the submatrices and their dimensions are tabulated in Table I. In Eq. (6.15) the relations

$$\langle \phi_{\bar{c}'i'>2} | \mathcal{L}(b_c) | \Psi_k \rangle = 0 \quad (6.16)$$

and

$$\langle \phi_{\bar{c}'i'} | \mathcal{L}(b_c) | \Psi_k \rangle = 0 \quad (6.17)$$

arising from the constraint Eq. (6.4) and the assumption of the known n.b.c. values for the closed-channel parameters  $b_{\bar{c}}$ , respectively, have been employed. Also,

$$M^{GF} = (M^{FG})^\dagger. \quad (6.18)$$

Equation (6.15) is equivalent to the following three matrix equations:

$$M^{FF}D^{(k)} + M^{FG}K^{(k)} + Pc^{(k)} = L^F, \quad (6.19)$$

$$M^{GF}D^{(k)} + M^{GG}K^{(k)} + Qc^{(k)} = L^G, \quad (6.20)$$

$$P^\dagger D^{(k)} + Q^\dagger K^{(k)} + Nc^{(k)} = 0, \quad (6.21)$$

where Eqs. (6.7) and (6.8) have been substituted. Multiplying Eq. (6.21) from the left by the matrix  $N^{-1}$  yields

$$c^{(k)} = -N^{-1}P^\dagger D^{(k)} - N^{-1}Q^\dagger K^{(k)}, \quad (6.22)$$

and substituting into Eq. (6.19) and (6.20) gives

$$m^{FF}D^{(k)} + m^{FG}K^{(k)} = 0 \quad (6.23)$$

and

$$m^{GF}D^{(k)} + m^{GG}K^{(k)} = 0, \quad (6.24)$$

where

$$m^{FF} = M^{FF} - PN^{-1}P^\dagger - Y^{FF}, \quad (6.25)$$

$$m^{FG} = M^{FG} - PN^{-1}Q^\dagger - Y^{FG}, \quad (6.26)$$

$$m^{GF} = M^{GF} - QN^{-1}P^\dagger - Y^{GF}, \quad (6.27)$$

and

$$m^{GG} = M^{GG} - QN^{-1}Q^\dagger - Y^{GG}. \quad (6.28)$$

Here the diagonal matrices  $Y^{FF}$ ,  $Y^{FG}$ ,  $Y^{GF}$ , and  $Y^{GG}$  have elements

$$Y_{\bar{c}\bar{c}'}^{FF} = \frac{1}{2} \hbar \{ F_{l_{\bar{c}}} [ F_{l_{\bar{c}}} - b_{\bar{c}} F_{l_{\bar{c}}} (k_{\bar{c}} a_{\alpha})^{-1} ] \} \delta_{\bar{c}\bar{c}'}, \quad (6.29)$$

$$Y_{\bar{c}\bar{c}'}^{FG} = \frac{1}{2} \hbar \{ F_{l_{\bar{c}}} [ G_{l_{\bar{c}}} - b_{\bar{c}} G_{l_{\bar{c}}} (k_{\bar{c}} a_{\alpha})^{-1} ] \} \delta_{\bar{c}\bar{c}'}, \quad (6.30)$$

$$Y_{\bar{c}\bar{c}'}^{GF} = \frac{1}{2} \hbar \{ G_{l_{\bar{c}}} [ F_{l_{\bar{c}}} - b_{\bar{c}} F_{l_{\bar{c}}} (k_{\bar{c}} a_{\alpha})^{-1} ] \} \delta_{\bar{c}\bar{c}'}, \quad (6.31)$$

and

$$Y_{\bar{c}\bar{c}'}^{GG} = \frac{1}{2} \hbar \{ G_{l_{\bar{c}}} [ G_{l_{\bar{c}}} - b_{\bar{c}} G_{l_{\bar{c}}} (k_{\bar{c}} a_{\alpha})^{-1} ] \} \delta_{\bar{c}\bar{c}'}, \quad (6.32)$$

where the prime denotes the derivative with respect to the argument  $k_{\bar{c}} a_{\alpha}$ . Using the Wronskian relation

TABLE I. Dimensions and elements of various matrices.

Matrix	Element	Dimension
$M^{FF}$	$M_{\bar{c}\bar{c}'}^{FF} = \langle \phi_{\bar{c}1}   H + \mathcal{L}(b_c) - E   \phi_{\bar{c}'1} \rangle$	$m \times m^a$
$M^{FG}$	$M_{\bar{c}\bar{c}'}^{FG} = \langle \phi_{\bar{c}1}   H + \mathcal{L}(b_c) - E   \phi_{\bar{c}'2} \rangle$	$m \times m$
$M^{GF}$	$M_{\bar{c}\bar{c}'}^{GF} = \langle \phi_{\bar{c}2}   H + \mathcal{L}(b_c) - E   \phi_{\bar{c}'1} \rangle$	$m \times m$
$M^{GG}$	$M_{\bar{c}\bar{c}'}^{GG} = \langle \phi_{\bar{c}2}   H + \mathcal{L}(b_c) - E   \phi_{\bar{c}'2} \rangle$	$m \times m$
$P$	$P_{\bar{c}(\bar{c}'>2)} = \langle \phi_{\bar{c}1}   H + \mathcal{L}(b_c) - E   \phi_{\bar{c}'>2} \rangle$ $P_{\bar{c}(\bar{c}'')} = \langle \phi_{\bar{c}1}   H + \mathcal{L}(b_c) - E   \phi_{\bar{c}''} \rangle$	$m \times [(\nu-2)m + \nu\bar{m}]^b$
$Q$	$Q_{\bar{c}(\bar{c}'>2)} = \langle \phi_{\bar{c}2}   H + \mathcal{L}(b_c) - E   \phi_{\bar{c}'>2} \rangle$ $Q_{\bar{c}(\bar{c}'')} = \langle \phi_{\bar{c}2}   H + \mathcal{L}(b_c) - E   \phi_{\bar{c}''} \rangle$	$m \times [(\nu-2)m + \nu\bar{m}]$
$N$	$N_{(\bar{c}i>2)(\bar{c}'i>2)} = \langle \phi_{\bar{c}i>2}   H + \mathcal{L}(b_c) - E   \phi_{\bar{c}'i>2} \rangle$ $N_{(\bar{c}i>2)(\bar{c}'i)} = \langle \phi_{\bar{c}i>2}   H + \mathcal{L}(b_c) - E   \phi_{\bar{c}'i} \rangle$ $N_{(\bar{c}i)(\bar{c}'i>2)} = \langle \phi_{\bar{c}i}   H + \mathcal{L}(b_c) - E   \phi_{\bar{c}'i>2} \rangle$ $N_{(\bar{c}i)(\bar{c}'i)} = \langle \phi_{\bar{c}i}   H + \mathcal{L}(b_c) - E   \phi_{\bar{c}'i} \rangle$	$[(\nu-2)m + \nu\bar{m}] \times [(\nu-2)m + \nu\bar{m}]$
$a^{(k)}$	$a_{\bar{c}}^{(k)} = \delta_{k\bar{c}}$	$m \times 1$
$b^{(k)}$	$b_{\bar{c}}^{(k)} = K_{k\bar{c}}$	$m \times 1$
$c^{(k)}$	$c_{(\bar{c}i>2)}^{(k)} = a_{\bar{c}i>2}^{(k)}$ $c_{(\bar{c}i)}^{(k)} = a_{\bar{c}i}^{(k)}$	$[(\nu-2)m + \nu\bar{m}] \times 1$
$L^F$	$L_{\bar{c}}^F = \langle \phi_{\bar{c}1}   \mathcal{L}(b_c)   \Psi_k \rangle$	$m \times 1$
$L^G$	$L_{\bar{c}}^G = \langle \phi_{\bar{c}2}   \mathcal{L}(b_c)   \Psi_k \rangle$	$m \times 1$

<sup>a</sup> $m$  ( $\bar{m}$ ) is number of open (closed) channels.

<sup>b</sup> $\nu$  is number of levels/channel.

$G_{l\bar{c}} F'_{l\bar{c}} - F_{l\bar{c}} G'_{l\bar{c}} = 1$ , we can see that

$$m^{FG} - (m^{GF})^\dagger = (Y^{GF})^\dagger - Y^{FG} = \frac{1}{2} \hbar, \quad (6.33)$$

since  $M^{FG}$  satisfies Eq. (6.18) and since the matrix  $N$  is Hermitian.

Noting that  $m^{FF}$ ,  $m^{FG}$ ,  $m^{GF}$ , and  $m^{GG}$  are independent of the index  $k$ , we can generalize the column matrices  $D^{(k)}$  and  $K^{(k)}$  in Eqs. (6.23) and (6.24) to the corresponding square matrices  $\mathbb{1}$  and  $K$ , respectively, and write

$$m^{FF} + m^{FG}K = 0 \quad (6.34)$$

and

$$m^{GF} + m^{GG}K = 0. \quad (6.35)$$

Equations (6.34) and (6.35) have nontrivial solutions only when the determinant

$$\det m \equiv \begin{vmatrix} m^{FF} & m^{FG} \\ m^{GF} & m^{GG} \end{vmatrix} = 0. \quad (6.36)$$

The aim of the variational approach is to determine the  $K$  matrix from Eqs. (6.34) and (6.35). It is not generally possible to do this unambiguously, since there are two independent equations in only one unknown. Unless the determinant in Eq. (6.36) vanishes, which is the case when the trial wave function  $|\Psi_k\rangle$  is the exact scattering func-

tion, two different values for  $K$  will be obtained from the two equations. However, if the set of basis states used in the calculation is sufficiently complete, Eq. (6.36) will be approximately satisfied and the two values obtained for  $K$  will be approximately equal.

In the method of Hulthén (1944), the two equations (6.34) and (6.35) are combined into one equation by taking the sum of the first equation and the product of  $K^\dagger$  with the second equation, i.e., the functional

$$I(K) = m^{FF} + m^{FG}K + K^\dagger m^{GF} + K^\dagger m^{GG}K \quad (6.37)$$

is considered. If Eqs. (6.34) and (6.35) are satisfied, then

$$I(K) = 0, \quad (6.38)$$

although the reverse is not necessarily true. Hulthén proposed that  $K$  be chosen so that Eq. (6.38) is satisfied. The functional  $I(K)$  is obtained from the functional  $I$  of Eq. (6.13) when both the wave functions  $\Psi_k$  and  $\Psi_{k'}$  are constrained to obey  $K$ -matrix standing-wave asymptotic boundary conditions. In this case, the coefficients  $a_{\bar{c}'1}^{(k')}$  and  $a_{\bar{c}'2}^{(k')}$  are held fixed and  $I$  is stationary, provided Eq. (6.14) holds for the remaining coefficients  $c^{(k')}$ , i.e.,

$$\frac{\partial I}{\partial c_{\bar{c}'i}^{(k')*}} = 0. \quad (6.39)$$

These conditions, when substituted into Eq. (6.13) for the



functional  $I$ , yield the functional  $I(K)$ .

When only one reaction channel is open, the matrices  $m^{FF}$ ,  $m^{FG}$ ,  $m^{GF}$ ,  $m^{GG}$ , and  $K$  reduce to simple variables, and Eq. (6.38) becomes a simple quadratic in  $K$ . In this case,  $K$  is  $\tan\delta$ , where  $\delta$  is the elastic scattering phase shift. Thus the phase shift  $\delta$  and hence the elastic scattering cross section can be calculated from Eq. (6.38), provided one knows which of the two solutions for  $\tan\delta$  to discard. This constitutes a fundamental disadvantage of the Hulthén method. Furthermore, the extension of the method to the multichannel scattering problem is not straightforward, so that its use has been confined to single-channel scattering calculations.

An alternative variational approach which does not suffer from the above disadvantages is that of Kohn (1948). In Kohn's method, variations with respect to  $K$  are allowed, so that the corresponding variation of  $I(K)$ ,

$$\delta I(K) = (m^{FG} + K^\dagger m^{GG})\delta K + \delta K^\dagger (m^{GF} + m^{GG}K). \quad (6.40)$$

Then  $I(K)$  is stationary with respect to  $\delta K^\dagger$  if Eq. (6.35) is satisfied, i.e.,

$$K = -(m^{GG})^{-1}m^{GF}. \quad (6.41)$$

In this case,  $I(K)$  is *not* stationary with respect to  $\delta K$ , since

$$m^{FG} + K^\dagger m^{GG} = \frac{1}{2}\hbar\mathbb{1}, \quad (6.42)$$

where we have used Eq. (6.33). Thus Kohn considers the functional

$$\mathcal{J}(K) = I(K) - \frac{1}{2}\hbar K, \quad (6.43)$$

which is stationary for all infinitesimal variations of  $K$ . Setting  $I(K)$  equal to zero, which is true for the exact wave function  $\Psi_k$ , we find that Eq. (6.43) yields the Kohn formula for the  $K$  matrix, i.e.,

$$\begin{aligned} K &= -2\hbar^{-1}\mathcal{J}(K) \\ &= -2\hbar^{-1}[m^{FF} - (m^{GF})^\dagger(m^{GG})^{-1}m^{GF}], \end{aligned} \quad (6.44)$$

where Eqs. (6.35), (6.37), and (6.41) have been used.

A related method, known as the inverse Kohn or Rubinow procedure (Hulthén and Skavlem, 1952; Feshbach and Rubinow, 1952; Rubinow, 1955), is derived similarly.

The functional  $I$  of Eq. (6.13) can be written in terms of  $K^{-1}$ , rather than  $K$ , by choosing the coefficients

$$a_{\bar{c}1}^{(k)} = (K^{-1})_{\bar{c}k} \quad (6.45)$$

and

$$a_{\bar{c}2}^{(k)} = \delta_{\bar{c}k}. \quad (6.46)$$

Then, corresponding to  $I(K)$  of Eq. (6.37), we have the functional

$$\begin{aligned} I(K^{-1}) &= m^{GG} + m^{GF}K^{-1} \\ &\quad + (K^{-1})^\dagger m^{FG} + (K^{-1})^\dagger m^{FF}K^{-1}. \end{aligned} \quad (6.47)$$

The variation of  $I(K^{-1})$  for small changes in  $K^{-1}$  is

given by

$$\begin{aligned} \delta I(K^{-1}) &= [m^{GF} + (K^{-1})^\dagger m^{FF}]\delta K^{-1} \\ &\quad + \delta(K^{-1})^\dagger (m^{FG} + m^{FF}K^{-1}). \end{aligned} \quad (6.48)$$

Choosing

$$K^{-1} = -(m^{FF})^{-1}m^{FG} \quad (6.49)$$

so that  $I(K^{-1})$  is stationary with respect to  $\delta(K^{-1})^\dagger$  and substituting into Eq. (6.48) gives

$$\delta I(K^{-1}) = -\frac{1}{2}\hbar\delta K^{-1}. \quad (6.50)$$

Thus the functional

$$\mathcal{J}(K^{-1}) = I(K^{-1}) + \frac{1}{2}\hbar K^{-1} \quad (6.51)$$

is stationary with respect to all infinitesimal variations of  $K^{-1}$ . If we set  $I(K^{-1})$  equal to zero, which is true for the exact wave functions  $\Psi_k$ , Eq. (6.51) yields the inverse-Kohn formula for  $K^{-1}$ , i.e.,

$$\begin{aligned} K^{-1} &= 2\hbar^{-1}\mathcal{J}(K^{-1}) \\ &= 2\hbar^{-1}[m^{GG} - (m^{FG})^\dagger(m^{FF})^{-1}m^{FG}], \end{aligned} \quad (6.52)$$

from which the  $K$  matrix is obtained by matrix inversion.

In the numerical application of the Kohn method, difficulties are often encountered near those energies where the matrix  $m^{GG}$  becomes singular. In fact, near these energies, spurious resonances can appear in the scattering cross sections calculated by the Kohn procedure. For similar reasons, difficulties arise with the inverse Kohn method at energies where  $m^{FF}$  becomes singular. Nesbet (1968) has suggested a procedure whereby the Kohn method is employed whenever the determinant  $|m^{GG}| > |m^{FF}|$  and the inverse Kohn method for  $|m^{FF}| > |m^{GG}|$ . This technique successfully eliminates the problem of spurious resonances.

Once the  $K$  matrix has been determined, the collision matrix  $\tilde{U}$  may be obtained from Eq. (6.1) and hence the cross sections calculated. If  $\det m = 0$ , the Hulthén, Kohn, and inverse-Kohn methods all give the same result. For single-channel problems, Malik (1962) and Rudge (1973) have proposed including in the trial wave function an extra parameter which can be adjusted so that  $\det m = 0$ . This avoids the anomalous singularities of the Kohn method by ensuring that if  $m^{GG} = 0$ , then  $m^{GF} = 0$ , also, so that  $(m^{GG})^{-1}m^{GF}$  is finite. It should be noted that the NBC methods automatically yield  $\det m = 0$ .

The above variational methods have usually been used in the limit that the channel radii become very large. In this case, the operator  $\mathcal{L}(b_c) \rightarrow 0$  and integral operators such as  $(H - E)^{-1}$  assume their Cauchy principal values.

## B. Kohn variational method for the $\tilde{U}$ matrix

The methods discussed in the preceding section can also be employed to obtain the collision matrix  $\tilde{U}$  directly. If, instead of Eqs. (6.2)–(6.4), the basis states satisfy the following constraints in the external region:

$$(\tilde{c} | \phi_{\tilde{c}1} \rangle = \zeta_{\alpha\tilde{c}}^{(-)}(k_{\tilde{c}}r_{\alpha}), \quad (6.53)$$

$$(\tilde{c} | \phi_{\tilde{c}2} \rangle = -\zeta_{\alpha\tilde{c}}^{(+)}(k_{\tilde{c}}r_{\alpha}), \quad (6.54)$$

and

$$(\tilde{c} | \phi_{\tilde{c}i>2} \rangle = 0, \quad (6.55)$$

then for  $r_{\alpha} > a_{\alpha}$ ,

$$(\tilde{c} | \Psi_k \rangle = a_{\tilde{c}1}^{(k)} \zeta_{\alpha\tilde{c}}^{(-)}(k_{\tilde{c}}r_{\alpha}) - a_{\tilde{c}2}^{(k)} \zeta_{\alpha\tilde{c}}^{(+)}(k_{\tilde{c}}r_{\alpha}). \quad (6.56)$$

If we choose the coefficients  $a_{\tilde{c}1}^{(k)}$  and  $a_{\tilde{c}2}^{(k)}$  so that

$$a_{\tilde{c}1}^{(k)} = \delta_{\tilde{c}k} \quad (6.57)$$

and

$$a_{\tilde{c}2}^{(k)} = U_{\tilde{c}k}, \quad (6.58)$$

the wave functions  $(\tilde{c} | \Psi_k \rangle \equiv (\tilde{c} | \Psi_k^{(+)} \rangle)$  satisfy scattering boundary conditions [Eq. (2.17)].

If the functional

$$I(\tilde{U}) = \langle \Psi_k^{(-)} | H - E | \Psi_k^{(+)} \rangle \quad (6.59)$$

is considered and the wave functions  $\Psi_k^{(+)}$  and  $\Psi_k^{(-)}$  are constrained to obey outgoing and incoming scattering boundary conditions, respectively, i.e.,

$$(\tilde{c} | \Psi_k^{(\pm)} \rangle = \pm \zeta_{\alpha\tilde{c}}^{(\mp)}(k_{\tilde{c}}r_{\alpha}) \mp \zeta_{\tilde{c}}^{(\pm)}(k_{\tilde{c}}r_{\alpha}) U_{\tilde{c}k} \quad (6.60)$$

for large  $r_{\alpha}$ , then analogously to the preceding section it can be shown that the functional

$$\mathcal{J}(\tilde{U}) = I(\tilde{U}) + i\hbar\tilde{U} \quad (6.61)$$

is stationary with respect to all infinitesimal variations of  $\tilde{U}$ . Thus

$$\delta\mathcal{J}(\tilde{U}) = -I(\tilde{U}_t) + i\hbar(\tilde{U}_{st} - \tilde{U}_t) = 0, \quad (6.62)$$

where  $\tilde{U}_{st}$  and  $\tilde{U}_t$  are the "stationary" and "trial" values of  $\tilde{U}$ , respectively. Equation (6.62) gives

$$\tilde{U}_{st} = \tilde{U}_t + i\hbar^{-1}I(\tilde{U}_t). \quad (6.63)$$

Kamimura (1977) considers this expression to be superior to the corresponding one [Eq. (6.44)] for the  $K$  matrix for two reasons. First, unitarity of the approximate  $\tilde{U}$  matrices,  $\tilde{U}_{st}$  and  $\tilde{U}_t$ , is not assumed, so that the unitary nature of  $\tilde{U}_{st}$  can be used as a check on the calculations. Second, the Kohn variational procedure for the  $K$  matrix leads to difficulties near those energies where the matrix  $m^{GG}$  becomes singular: This situation does not appear to occur in the variational method for the  $\tilde{U}$  matrix.

In the limit that the channel radii become very large, the operator  $\mathcal{L}(b_c) \rightarrow -i\epsilon$ , where  $\epsilon$  is a small positive quantity and the limit  $\epsilon \rightarrow 0$  is to be taken (Robson and Robson, 1967).

### C. Hulthén-Kohn variational method for the $R$ matrix

It is instructive to derive the  $R$ -matrix relation [Eq. (3.14)] by a variational method. Consider the functional  $I$  of Eq. (6.59), i.e.,

$$\begin{aligned} I &= \langle \Psi_k^{(-)} | H - E | \Psi_k^{(+)} \rangle \\ &= \langle \Psi_k^{(-)} | H + \mathcal{L}(b_c) - E | \Psi_k^{(+)} \rangle \\ &\quad - \langle \Psi_k^{(-)} | \mathcal{L}(b_c) | \Psi_k^{(+)} \rangle \\ &= \sum_{jj'} a_j^{(k)*} a_j^{(k)} \langle \tilde{\phi}_{j'} | H + \mathcal{L}(b_c) - E | \phi_j \rangle \\ &\quad - \sum_{j'} a_j^{(k)*} \langle \tilde{\phi}_{j'} | \mathcal{L}(b_c) | \Psi_k^{(+)} \rangle, \end{aligned} \quad (6.64)$$

where the expansions

$$| \Psi_k^{(+)} \rangle = \sum_j a_j^{(k)} | \phi_j \rangle \quad (6.65)$$

and

$$\langle \Psi_k^{(-)} | = \sum_{j'} a_j^{(k)*} \langle \tilde{\phi}_{j'} | \equiv \langle \tilde{\Psi}_k^{(+)} | \quad (6.66)$$

have been used. Here the tilde denotes that the radial part of the wave function is to be complex conjugated. The functional  $I$  is stationary with respect to infinitesimal variations of the coefficients  $a_j^{(k)*}$  if

$$\begin{aligned} \frac{\partial I}{\partial a_j^{(k)*}} &= \sum_j a_j^{(k)} \langle \tilde{\phi}_{j'} | H + \mathcal{L}(b_c) - E | \phi_j \rangle \\ &\quad - \langle \tilde{\phi}_{j'} | \mathcal{L}(b_c) | \Psi_k^{(+)} \rangle = 0. \end{aligned} \quad (6.67)$$

This gives

$$a_j^{(k)} = \sum_{j'} (G^L)_{jj'} \langle \tilde{\phi}_{j'} | \mathcal{L}(b_c) | \Psi_k^{(+)} \rangle, \quad (6.68)$$

where the elements  $(G^L)_{jj'}$  belong to a matrix whose inverse has elements  $\langle \tilde{\phi}_{j'} | H + \mathcal{L}(b_c) - E | \phi_j \rangle$ , so that

$$| \Psi_k^{(+)} \rangle = \sum_{jj'} | \phi_j \rangle (G^L)_{jj'} \langle \tilde{\phi}_{j'} | \mathcal{L}(b_c) | \Psi_k^{(+)} \rangle. \quad (6.69)$$

Consequently, using Eq. (3.4) for the Bloch operator  $\mathcal{L}(b_c)$  and matching at  $r_{\alpha} = a_{\alpha}$ , we have

$$\begin{aligned} (c, a_{\alpha} | \Psi_k^{(+)} \rangle &= \sum_{\beta} \sum_{c' \in \beta} R_{cc'}^L(a_{\alpha}, a_{\beta}) \\ &\quad \times \left[ \frac{\partial}{\partial a_{\beta}} a_{\beta} - b_{c'} \right] (c', a_{\beta} | \Psi_k^{(+)} \rangle, \end{aligned} \quad (6.70)$$

where  $R_{cc'}^L(a_{\alpha}, a_{\beta})$  is the  $R$  matrix defined by Eq. (3.15). Equation (6.70) is identical with Eq. (3.14).

The above derivation of the  $R$ -matrix formalism places no restriction on the basis states other than *linear independence*, unlike the usual  $R$ -matrix theory (Lane and Thomas, 1958), in which the basis states satisfy a set of fixed boundary conditions at the channel radii, i.e.,

$$\mathcal{L}(B_c) | \phi_j \rangle = 0. \quad (6.71)$$

In general, nonorthogonal basis states may be used as in the ERM method (Sec. IV.F).

When the Buttler correction (see Sec. IV.D) is included

in the SRM approach (see Sec. IV.C), the trial wave function  $\Psi_k^{(+)}$  of Eq. (6.64) is a linear combination of the finite set of basis states  $\phi_j$  and the function  ${}^0\Psi_k$ , which is the regular solution of Eq. (6.9) with  $H$  replaced by  $H_0$ . Zvijac, Heller, and Light (1975) have shown that an additional improvement to the BCRM can be achieved by obtaining this combination variationally. As pointed out by Nesbet (1980), the variational correction of Zvijac *et al.* can be obtained more directly than in their paper by using Eq. (6.70) with the function  ${}^0\Psi_k^{(+)}$  included as one of the basis states. It should be noted that if the basis states  $\phi_j$  satisfy natural boundary condition parameters at the channel radii (see Sec. V) then both the Buttle and variational corrections vanish for the reason discussed in Sec. IV.D.

#### D. Schwinger variational methods for the $T$ matrix

In Secs. VI.A and VI.B we have discussed Hulthén-Kohn variational methods based upon the Schrödinger equation for obtaining the  $K$  matrix and  $\tilde{U}$  matrix, respectively. In this section we shall indicate briefly alternative methods based upon the Schwinger variational principle (see, for instance, Joachain, 1975), which uses the Lippmann-Schwinger (1950) integral equation for deriving the  $T$  matrix in the single-partition case. The multipartition case will be considered in Sec. XI.

We define the transition matrix  $T$  to have elements

$$T_{\tilde{c}\tilde{c}'} = \frac{1}{2\hbar} \langle \Phi_{\tilde{c}}^{(-)} | \bar{V}_\alpha | \Psi_{\tilde{c}'}^{(+)} \rangle = \frac{1}{2\hbar} \langle \Psi_{\tilde{c}}^{(-)} | \bar{V}_\alpha | \Phi_{\tilde{c}'}^{(+)} \rangle, \quad (6.72)$$

where  $\Phi_{\tilde{c}}^{(+)}$  is the regular solution of the equation

$$(\bar{H}_\alpha - E)\Phi_{\tilde{c}}^{(+)} = 0 \quad (6.73)$$

having unit current incident in channel  $\tilde{c}$  and purely outgoing current in all other channels. The states  $\Phi_{\tilde{c}}^{(-)}$  and  $\Psi_{\tilde{c}}^{(-)}$  are the states  $\tilde{\Phi}_{\tilde{c}}^{(+)}$  and  $\tilde{\Psi}_{\tilde{c}}^{(+)}$ , respectively, where the tilde denotes that the radial part of the wave function is to be complex conjugated. The states  $\Psi_{\tilde{c}}^{(\pm)}$  satisfy the Lippmann-Schwinger equations:

$$|\Psi_{\tilde{c}}^{(+)}\rangle = |\Phi_{\tilde{c}}^{(+)}\rangle + \bar{G}_\alpha \bar{V}_\alpha |\Psi_{\tilde{c}}^{(+)}\rangle \quad (6.74)$$

and

$$\langle \Psi_{\tilde{c}}^{(-)} | = \langle \Phi_{\tilde{c}}^{(-)} | + \langle \Psi_{\tilde{c}}^{(-)} | \bar{V}_\alpha \bar{G}_\alpha, \quad (6.75)$$

where  $\bar{G}_\alpha$  is defined by Eq. (3.27). The above definition of the transition matrix  $T$  is a generalization of the conventional transition matrix, in that a background potential  $U_\alpha$  is allowed so that distorted waves,  $\Phi_{\tilde{c}}^{(\pm)}$ , replace the usual plane waves and the integration is restricted to the internal region. In the limit that the channel radii become infinitely large and  $U_\alpha \rightarrow 0$ , the  $T$  matrix of Eq. (6.72) becomes the conventional transition matrix.

Let us now consider the following functional for the transition matrix elements:

$$\mathcal{J}_{\tilde{c}\tilde{c}'} = \frac{1}{2\hbar} (\langle \Phi_{\tilde{c}}^{(-)} | \bar{V}_\alpha | \Psi_{\tilde{c}'}^{(+)} \rangle + \langle \Psi_{\tilde{c}}^{(-)} | \bar{V}_\alpha | \Phi_{\tilde{c}'}^{(+)} \rangle - \langle \Psi_{\tilde{c}}^{(-)} | \bar{V}_\alpha - \bar{V}_\alpha \bar{G}_\alpha \bar{V}_\alpha | \Psi_{\tilde{c}'}^{(+)} \rangle), \quad (6.76)$$

where  $\Psi_{\tilde{c}}^{(\pm)}$  are trial functions for  $\Psi_{\tilde{c}}^{(\pm)}$ . First, this functional gives the correct expression for the  $T$ -matrix element  $T_{\tilde{c}\tilde{c}'}$  when  $\Psi_{\tilde{c}}^{(\pm)} = \Psi_{\tilde{c}}^{(\pm)}$ . Second, for arbitrary infinitesimal variations of  $\Psi_{\tilde{c}}^{(-)}$  near the correct state  $\Psi_{\tilde{c}}^{(-)}$ , we have

$$\delta \mathcal{J}_{\tilde{c}\tilde{c}'} = \frac{1}{2\hbar} (\langle \delta \Psi_{\tilde{c}}^{(-)} | \bar{V}_\alpha | \Phi_{\tilde{c}'}^{(+)} \rangle - \langle \delta \Psi_{\tilde{c}}^{(-)} | \bar{V}_\alpha - \bar{V}_\alpha \bar{G}_\alpha \bar{V}_\alpha | \Psi_{\tilde{c}'}^{(+)} \rangle), \quad (6.77)$$

which vanishes if  $\Psi_{\tilde{c}}^{(+)} = \Psi_{\tilde{c}}^{(+)}$ , thus satisfying Eq. (6.74). Similarly, for small changes in  $\Psi_{\tilde{c}}^{(-)}$  around its correct value, we have

$$\delta \mathcal{J}_{\tilde{c}\tilde{c}'} / \delta \Psi_{\tilde{c}}^{(+)} = 0, \quad (6.78)$$

if  $\Psi_{\tilde{c}}^{(-)} = \Psi_{\tilde{c}}^{(-)}$ , which satisfies Eq. (6.75).

An alternative variational functional for the transition matrix elements is

$$\mathcal{J}_{\tilde{c}\tilde{c}'} = \frac{\langle \Psi_{\tilde{c}'}^{(-)} | \bar{V}_\alpha | \Phi_{\tilde{c}}^{(+)} \rangle \langle \Phi_{\tilde{c}}^{(-)} | \bar{V}_\alpha | \Psi_{\tilde{c}'}^{(+)} \rangle}{2\hbar \langle \Psi_{\tilde{c}}^{(-)} | \bar{V}_\alpha - \bar{V}_\alpha \bar{G}_\alpha \bar{V}_\alpha | \Psi_{\tilde{c}'}^{(+)} \rangle}. \quad (6.79)$$

This form has the same properties as the previous expression [Eq. (6.76)] and is also independent of the normalizations of the trial wave functions  $\Psi_{\tilde{c}}^{(\pm)}$ . It is interesting to note that the functional of Eq. (6.79) also agrees with the Born series for the transition matrix in terms of distorted waves up to second order, i.e.,

$$\mathcal{J}_{\tilde{c}\tilde{c}'} = \frac{1}{2\hbar} (\langle \Phi_{\tilde{c}}^{(-)} | \bar{V}_\alpha | \Phi_{\tilde{c}'}^{(+)} \rangle + \langle \Phi_{\tilde{c}}^{(-)} | \bar{V}_\alpha \bar{G}_\alpha \bar{V}_\alpha | \Phi_{\tilde{c}'}^{(+)} \rangle + \dots), \quad (6.80)$$

when  $|\Psi_{\tilde{c}'}^{(+)}\rangle$  and  $\langle \Psi_{\tilde{c}}^{(-)} |$  are approximated by  $|\Phi_{\tilde{c}'}^{(+)}\rangle$  and  $\langle \Phi_{\tilde{c}}^{(-)} |$ , respectively, and when the second term is small compared with the first term. The first term,  $(2\hbar)^{-1} \langle \Phi_{\tilde{c}}^{(-)} | \bar{V}_\alpha | \Phi_{\tilde{c}'}^{(+)} \rangle$ , constitutes the distorted-wave Born approximation to the  $T$  matrix (Tobocman, 1961).

## VII. CALCULABLE METHODS FOR COMPOSITE PARTICLE SCATTERING

In this section we shall consider the scattering of composite particles in more detail. In any attempt to describe processes such as nuclear heavy-ion scattering from a microscopic point of view, the composite nature of both the target and the projectile must be taken into account. In particular, the correct antisymmetrization of the wave

function with respect to the interchange of nucleons between the target and the projectile is important. Two closely related ways of including nucleon clustering in nuclear structure and scattering calculations are the resonating group method (RGM) (Wheeler, 1937a, 1937b) and the generator coordinate method (GCM) (Hill and Wheeler, 1953; Griffin and Wheeler, 1957). In the following we shall outline several ways in which the GCM has been combined with one or another of the calculable reaction theories discussed previously to obtain composite particle scattering cross sections. First, however, we shall give a brief description of both the RGM and GCM necessary for this purpose. For full details of these techniques, the reader is referred to the recent review articles of Wong (1975), Saito (1977), Horiuchi (1977), and Tang, LeMere, and Thompson (1978).

### A. Resonating group and generator coordinate methods

In the RGM the scattering wave function  $\Psi_k$  is written in terms of the channel (or cluster) function for *all* configuration space. For simplicity we limit the discussion to two-spin-zero-cluster systems. Then the scattering function  $\Psi_k$  can be written [see Eq. (2.5)]

$$\Psi_k = \mathcal{A} \sum_{\alpha} \sum_{c \in \alpha} \chi_{ac} u_{ac}^{(k)}(\mathbf{r}_{\alpha}), \quad (7.1)$$

where (as in Sec. II) the cm motion is assumed to have been factored out and has been omitted for convenience. Here the channel states  $\chi_{ac}$  are eigenstates of the Hamiltonian  $h_{\alpha}^{(1)} + h_{\alpha}^{(2)}$  describing the internal degrees of freedom [Eq. (2.4)] of the two-cluster system in partition  $\alpha$ , i.e.,

$$(h_{\alpha}^{(1)} + h_{\alpha}^{(2)} - \epsilon_{ac}) \chi_{ac} = 0, \quad (7.2)$$

the function  $u_{ac}^{(k)}(\mathbf{r}_{\alpha})$  is the wave function of relative motion, and  $\mathcal{A}$  is the antisymmetrization operator. It is convenient to write

$$\mathcal{A} = \mathcal{A}' \mathcal{A}_1 \mathcal{A}_2, \quad (7.3)$$

where  $\mathcal{A}_i$  is the antisymmetrization operator for the nucleons in cluster  $i$  and  $\mathcal{A}'$  is an operator which antisymmetrizes the nucleons of one cluster with those of the other cluster. Then we have [Eq. (2.14)]

$$\hat{\chi}_{ac} = \mathcal{A}_1 \mathcal{A}_2 \chi_{ac} = \mathcal{A}' \chi_{ac}^{(1)} \mathcal{A}_2 \chi_{ac}^{(2)} = \hat{\chi}_{ac}^{(1)} \hat{\chi}_{ac}^{(2)}, \quad (7.4)$$

where  $\hat{\chi}_{ac}^{(i)}$  are antisymmetrized cluster wave functions. In the general case, the vector coupling of any internal angular momenta of the clusters has to be taken into account.

An equation for the relative motion wave functions can be obtained by projecting the Schrödinger equation for  $\Psi_k$  onto the channel state  $\hat{\chi}_{ac}$ :

$$\langle \hat{\chi}_{ac} | H - E | \sum_{\beta} \sum_{c' \in \beta} \mathcal{A}' \hat{\chi}_{\beta c'} u_{\beta c'}^{(k)}(\mathbf{r}_{\beta}) \rangle = 0, \quad (7.5)$$

where the integration is over all coordinates except  $\mathbf{r}_{\beta}$ . Introducing the parameter coordinate  $\mathbf{r}'_{\beta}$  (Wildermuth and Kanellopoulos, 1958/59), we can write Eq. (7.5)

$$\langle \hat{\chi}_{ac} | H - E | \sum_{\beta} \sum_{c' \in \beta} \mathcal{A}' \hat{\chi}_{\beta c'} u_{\beta c'}^{(k)}(\mathbf{r}'_{\beta}) \delta(\mathbf{r}_{\beta} - \mathbf{r}'_{\beta}) \rangle = 0, \quad (7.6)$$

where the angular brackets denote integration over *all* configuration space but not the parameter coordinate  $\mathbf{r}_{\beta}$ . Defining

$$\mathcal{A}' = \delta_{\alpha\beta} \delta_{cc'} + \mathcal{A}'' , \quad (7.7)$$

we can write Eq. (7.6) as a set of simultaneous linear integrodifferential equations:

$$\left[ -\frac{\hbar^2}{2m_c} \nabla_{\mathbf{r}'_{\alpha}}^2 + V_c^D(\mathbf{r}'_{\alpha}) - E_{ac} \right] u_{ac}^{(k)}(\mathbf{r}'_{\alpha}) + \sum_{\beta} \sum_{c' \in \beta} \int K_{cc'}(\mathbf{r}'_{\alpha}, \mathbf{r}'_{\beta}) u_{\beta c'}^{(k)}(\mathbf{r}'_{\beta}) d\mathbf{r}'_{\beta} = 0, \quad (7.8)$$

where

$$K_{cc'}(\mathbf{r}'_{\alpha}, \mathbf{r}'_{\beta}) = \langle \hat{\chi}_{ac} \delta(\mathbf{r}_{\alpha} - \mathbf{r}'_{\alpha}) | H - E | \mathcal{A}'' \hat{\chi}_{\beta c'} \delta(\mathbf{r}_{\beta} - \mathbf{r}'_{\beta}) \rangle \quad (7.9)$$

and  $V_c^D(\mathbf{r}'_{\alpha})$  is a "direct" potential given by

$$K_c^D(\mathbf{r}'_{\alpha}) = \left[ -\frac{\hbar^2}{2m_c} \nabla_{\mathbf{r}'_{\alpha}}^2 + V_c^D(\mathbf{r}'_{\alpha}) - E_{ac} \right] \langle \hat{\chi}_{ac} \delta(\mathbf{r}_{\alpha} - \mathbf{r}'_{\alpha}) | H - E | \hat{\chi}_{ac} \rangle. \quad (7.10)$$

In principle, the RGM is very satisfactory, since it employs completely antisymmetric wave functions which contain no spurious cm motion. However, due to the complicated nature of the RG wave function [Eq. (7.1)], the calculation of the kernels  $K_{cc'}$  becomes very tedious for a large number of nucleons if the kernels are evaluated using integration over the natural cluster coordinates, i.e., the internal and relative coordinates of the clusters. This is because a different coordinate transformation is necessary for every permutation of the nucleons in the different clusters arising from antisymmetrization.

Another approach, which is physically equivalent to the RGM, is the GCM. This method was proposed as an alternative formalism in the hope of simplifying the calculations. For the single-channel case ( $c \in \alpha$ ), the GCM employs total wave functions (i.e., including cm motion) for the  $N$ -body system of the form

$$\Psi_k^T(\mathbf{R}_i) = \int f^{(k)}(\mathbf{S}) \Phi(\mathbf{R}_i, \mathbf{S}) d\mathbf{S}, \quad (7.11)$$

where

$$\Phi(\mathbf{R}_i, \mathbf{S}) = \mathcal{A}' \left[ \hat{\chi}_{ac}^{(1)} \left[ \mathbf{R}_i + \frac{N_2}{N} \mathbf{S} \right] \hat{\chi}_{ac}^{(2)} \left[ \mathbf{R}_i - \frac{N_1}{N} \mathbf{S} \right] \right] \quad (7.12)$$

is an antisymmetrized product of the Slater determinants  $\hat{\chi}_{ac}^{(1)}$  and  $\hat{\chi}_{ac}^{(2)}$  representing the ground states of the two clusters and where  $\mathbf{R}_i$  is the position of the  $i$ th nucleon. The two Slater determinants are usually assumed to be composed of harmonic oscillator orbitals centered at

$-N_2\mathbf{S}/N$  and  $N_1\mathbf{S}/N$ , respectively, where  $N_j$  is the number of nucleons in cluster  $j$  and where each orbital is multiplied by a spin-isospin function. The generator coordinate  $\mathbf{S}$  thus corresponds to the separation of the centers of the harmonic oscillator potentials, i.e., the *mean* position of the cluster cm coordinates. This form of the GCM was initiated by Margenau (1941) and developed by Brink (1966). If the *same* oscillator length parameter  $b$  is used for each cluster, the function  $\Phi(\mathbf{R}_i, \mathbf{S})$  can also be written

$$\Phi(\mathbf{R}_i, \mathbf{S}) = \Phi_{\text{cm}} \mathcal{A}' [\Gamma(\mathbf{r}_\alpha, \mathbf{S}) \hat{\chi}_{\alpha c}], \quad (7.13)$$

where

$$\Gamma(\mathbf{r}_\alpha, \mathbf{S}) = \left[ \frac{N_1 N_2}{\pi b^2 N} \right]^{3/4} \exp[-N_1 N_2 (\mathbf{r}_\alpha - \mathbf{S})^2 / (2b^2 N)] \quad (7.14)$$

and  $\Phi_{\text{cm}}$  is the cm wave function.

The basic idea of the GCM (Griffin and Wheeler, 1957) is to permit "collective" degrees of freedom to be introduced into the  $N$ -particle scattering wave function without any specific dependence upon collective coordinates appearing in the wave function. The generating wave (or weight) function  $f^{(k)}(\mathbf{S})$  of Eq. (7.11) which describes such collective effects is to be determined by the Ritz variational principle  $\delta E = 0$  for infinitesimal variations  $\delta f^{(k)}(\mathbf{S})$ . This leads to the Hill-Wheeler equation:

$$\int K(\mathbf{S}, \mathbf{S}') f^{(k)}(\mathbf{S}') d\mathbf{S}' = 0, \quad (7.15)$$

where the GCM kernels  $K(\mathbf{S}, \mathbf{S}')$  are given by

$$K(\mathbf{S}, \mathbf{S}') = \langle \hat{\chi}_{\alpha c} \Gamma(\mathbf{r}_\alpha, \mathbf{S}) | H - E | \mathcal{A}' \hat{\chi}_{\alpha c} \Gamma(\mathbf{r}_\alpha, \mathbf{S}') \rangle. \quad (7.16)$$

The angular brackets denote integration over all configuration space, but not the generator coordinates  $\mathbf{S}$  and  $\mathbf{S}'$ . The same result can be obtained by projecting the Schrödinger equation onto the function  $\Phi$  and integrating over the same space.

Comparison of Eq. (7.16) with Eq. (7.9) yields a relationship between the RG and GC kernels:

$$K(\mathbf{S}, \mathbf{S}') = \int \Gamma(\mathbf{r}_\alpha, \mathbf{S}) [K_{cc}(\mathbf{r}_\alpha, \mathbf{r}'_\alpha) + K_c^D(\mathbf{r}_\alpha) \delta(\mathbf{r}_\alpha - \mathbf{r}'_\alpha)] \Gamma(\mathbf{r}'_\alpha, \mathbf{S}') d\mathbf{r}_\alpha d\mathbf{r}'_\alpha. \quad (7.17)$$

The RG relative motion wave function  $u_{\alpha c}^{(k)}(\mathbf{r}_\alpha)$  is also simply related to the weight function  $f^{(k)}(\mathbf{S})$ :

$$u_{\alpha c}^{(k)}(\mathbf{r}_\alpha) = \int \Gamma(\mathbf{r}_\alpha, \mathbf{S}) f^{(k)}(\mathbf{S}) d\mathbf{S}, \quad (7.18)$$

or more simply in terms of an integral operator  $\Gamma_{\alpha c}$ ,

$$u_{\alpha c}^{(k)} = \Gamma_{\alpha c} f^{(k)}. \quad (7.19)$$

Thus for the conditions discussed above, the RGM and GCM are essentially equivalent, being related by an integral transformation, and one may either solve the Hill-Wheeler equation [Eq. (7.15)] with GC kernels or the

RGM integrodifferential equation [Eq. (7.8)] with RG kernels.

In general, the GC kernels of Eq. (7.16) are much easier to calculate than the corresponding RG kernels of Eq. (7.9), since they involve only the evaluation of matrix elements between single-particle wave functions. However, for large clusters, calculation of the GC kernels is still laborious due to the nonorthogonal basis and the large number of terms which arise from antisymmetrization. Furthermore, in a numerical treatment, problems can arise in the GCM due to rounding-off errors if the basis states are almost linearly dependent (Galetti and de Toledo Piza, 1978) [in practice, the right-hand side of Eq. (7.11) is discretized]. The solution of the Hill-Wheeler equation is also hampered by the singular character of the weight function  $f^{(k)}(\mathbf{S})$  (Giraud and LeTourneaux, 1972).

Another major difficulty with the GC approach is how to choose the appropriate weight function in order to impose the correct asymptotic boundary condition on the scattering function  $\Psi_k$ . In those methods which solve the Hill-Wheeler equation in the whole configuration space either by direct procedures [de Takacs, 1972; Tanabe, Tohsaki, and Tamagaki, 1973; Friedrich, Hüsken, and Weiguny, 1974; Canto and Brink, 1977 (method 1)] or by using variational techniques (Beck *et al.*, 1975a), it is necessary to transform the known asymptotic RG relative wave function into an appropriate weight function. This procedure becomes tedious for large clusters. An alternative approach is to solve the Hill-Wheeler equation only for the interaction region of configuration space and to employ the known asymptotic RG wave function in the channel region. Methods using this approach are the microscopic  $R$ -matrix method (MRM) (Horiuchi, 1970; Baye and Heenen, 1974, 1977c), several Kohn variational techniques [Mito and Kamimura, 1976; Kamimura, 1977; Canto and Brink, 1977 (method 2); Nagata and Yamamoto, 1977], and the natural boundary condition method of Baldock, Barrett, and Robson (1979). The above methods will be discussed briefly in the following sections and their application to  $\alpha$ - $\alpha$  elastic scattering in Sec. VIII.D.

When the two clusters are represented by harmonic oscillator orbitals with *different* length parameters, as is physically more reasonable for clusters of different sizes, Eq. (7.13) is no longer valid and the cm and relative motion are coupled together. In this case the GCM wave functions may contain spurious components of cm excitation. However, Fiebig and Timm (1981) have recently given a simple technique based upon a single-momentum projection method of Rouhaninejad and Yoccoz (1966) for eliminating spurious cm effects in GC kernels and furthermore have shown that in general such effects are very small. Alternative procedures for treating the case of unequal oscillator length parameters have been suggested (Sünkel and Wildermuth, 1972; Kamimura and Matsuse, 1974; Giraud and LeTourneaux, 1975; Thompson and Tang, 1975, 1976; Horiuchi, 1977; Tohsaki-Suzuki, 1978). These methods involve various transformations between GC and RG kernels and generally depend upon employing analytical forms for the kernels.

This requirement is not very practical for two large clusters, even when algebraic computer techniques (Tohsaki-Suzuki, 1977) are adopted. One of the more successful of these methods, the so-called "complex GC technique" has been reviewed in detail (Tang, LeMere, and Thompson, 1978; Tang, 1981), and, since it is not closely related to the calculable reaction theories of the present review, we shall not discuss it further here.

If there are several channels, it is natural to extend the GCM wave function of Eq. (7.11) to the more general form (Griffin and Wheeler, 1957)

$$\Psi_k^T(\mathbf{R}_i) = \sum_c \int \Phi_c(\mathbf{R}_i, \mathbf{S}) f_c^{(k)}(\mathbf{S}) d\mathbf{S}, \quad (7.20)$$

and application of the Ritz variational principle leads to a set of coupled equations for the weight functions  $f_c^{(k)}(\mathbf{S})$ :

$$\sum_{c'} \int K_{cc'}(\mathbf{S}, \mathbf{S}') f_{c'}^{(k)}(\mathbf{S}') d\mathbf{S}' = 0. \quad (7.21)$$

However, the latter equations are very difficult to interpret physically and are probably meaningless (Giraud and LeTourneaux, 1975). Thus, in this more general case, the GC formalism applied to the whole configuration space breaks down and it seems necessary to return to the RGM. However, as in the case of unequal harmonic oscillator length parameters, it is convenient to obtain the necessary RG kernels from the simpler GC kernels. These kernel transformations, which form the basis of methods such as the complex GC technique, have been reviewed by Horiuchi (1977). On the other hand, if the oscillator length parameters are equal for the two clusters and the GC formalism is restricted to the interaction region of configuration space as in the MRM, the generalization to multichannel scattering is straightforward (Baye, Heenen and Libert-Heinemann, 1977). In the following sections we shall outline several methods for calculating the simple one-channel case of the elastic scattering of two spinless closed-shell clusters.

## B. Solution of Hill-Wheeler equation in whole configuration space

### 1. Direct solution (method of de Takacsy)

It is convenient to make a partial wave expansion:

$$K(\mathbf{S}, \mathbf{S}') = (SS')^{-1} \sum_{lm} K_l(S, S') Y_l^m(\Omega_S) Y_l^{m*}(\Omega_{S'}), \quad (7.22)$$

$$K_l^0(S, S') = [1 + (-1)^l \delta_{N_1 N_2}] \int \Gamma_l(r_\alpha, S) [T_l + V_C(R_\alpha) - E_{\text{rel}}] \Gamma_l(r_\alpha, S') dr_\alpha \quad (7.30)$$

on the right-hand side of Eq. (7.26), they obtained

$$\begin{aligned} X_l(S) &= -[1 + (-1)^l \delta_{N_1 N_2}] \int \Gamma_l(r_\alpha, S) [T_l + V_C(r_\alpha) - E_{\text{rel}}] \int \Gamma_l(r_\alpha, S') f_l^0(S') dS' dr_\alpha \\ &= -[1 + (-1)^l \delta_{N_1 N_2}] \int \Gamma_l(r_\alpha, S) [T_l + V_C(r_\alpha) - E_{\text{rel}}] u_l^0(r_\alpha) dr_\alpha. \end{aligned} \quad (7.31)$$

Here

$$f^{(k)}(\mathbf{S}) = S^{-1} \sum_l f_l^{(k)}(S) Y_l^0(\Omega_S). \quad (7.23)$$

Then the Hill-Wheeler equation [Eq. (7.15)] becomes

$$\int K_l(S, S') f_l^{(k)}(S') dS' = 0. \quad (7.24)$$

In the method of de Takacsy (1972), it is assumed that for sufficiently large  $S$  ( $> S_0$ , say) that

$$f_l^{(k)}(S) = f_l^0(S), \quad (7.25)$$

where  $f_l^0(S)$  is the known asymptotic form of the GC weight function. Then Eq. (7.24) can be written

$$\begin{aligned} \int_0^{S_0} K_l(S, S') f_l^{(k)}(S') dS' &= - \int_{S_0}^{\infty} K_l(S, S') f_l^0(S') dS' \\ &\equiv X_l(S). \end{aligned} \quad (7.26)$$

This integral equation is transformed into a set of algebraic equations for the values  $f^{(k)}(S_i)$  corresponding to a discrete set of  $\bar{N}$  points  $S_i$  over the range  $0 \leq S \leq S_0$  by the use of a Gauss-Legendre quadrature formula with weight factors  $w_i$ . This gives  $\bar{N}$  simultaneous linear equations:

$$\sum_{i=1}^{\bar{N}} K_l(S_j, S_i) f_l^{(k)}(S_i) w_i = X_l(S_j) \quad (j = 1, \dots, \bar{N}). \quad (7.27)$$

de Takacsy, neglecting the Coulomb interaction, assumed that

$$f_l^0(S) = j_l(kS) + n_l(kS) \tan(\delta_l - \frac{1}{2}l\pi), \quad (7.28)$$

where  $j_l$  and  $n_l$  are regular and irregular spherical Bessel functions,  $k$  is the wave number for the relative motion, and  $\delta_l$  is the phase shift. In order to determine the phase shift, one more equation is required: de Takacsy took this to be Eq. (7.28) for some value of  $S = S_n$  slightly larger than  $S_0$ . The resultant  $\bar{N} + 1$  simultaneous linear equations are then solved for the  $\bar{N} + 1$  unknowns,  $f_l^{(k)}(S_i)$  and  $\delta_l$ . Tanabe, Tohsaki, and Tamagaki (1973) suggested that one can include the Coulomb interaction by expressing the asymptotic weight function  $f_l^0(S)$  in terms of the Coulomb functions:

$$f_l^0(S) = F_l(kS) + G_l(kS) \tan \delta_l. \quad (7.29)$$

In order to avoid the requirement for a matching condition for the GC weight function which does not seem to have been justified theoretically, Canto and Brink (1977) in their method 1 eliminated any explicit dependence on  $f_l^0(S)$ . By employing the asymptotic form of the GC kernel, i.e.,

$$T_l = -\frac{\hbar^2}{2m_c} \left[ \frac{d^2}{dr_\alpha^2} - \frac{l(l+1)}{r_\alpha^2} \right], \quad (7.32)$$

$$\Gamma_l(r_\alpha, S) = \left[ \frac{N_1 N_2}{\pi b^2 N} \right]^{3/4} 4\pi S r_\alpha \exp[-N_1 N_2 (r_\alpha^2 + S^2)/2b^2 N] i_l(N_1 N_2 S r_\alpha / b^2 N), \quad (7.33)$$

$\delta_{N_1 N_2}$  has the value 0 or 1 if the clusters are different or identical, respectively,  $V_C(r_\alpha)$  is the Coulomb interaction,  $E_{\text{rel}}$  is the energy of relative motion,  $m_c$  is the reduced mass of the system, and  $i_l$  is the modified spherical Bessel function.

Canto and Brink took

$$u_l^0(r_\alpha) = \eta(r_\alpha) [F_l(kr_\alpha) + G_l(kr_\alpha) \tan \delta_l], \quad (7.34)$$

with

$$\eta(r_\alpha) = \begin{cases} 0, & \text{if } r_\alpha \leq a_0 \\ \left[ (r_\alpha - a_0) - \frac{(a_1 - a_0)}{2\pi} \sin \left[ \frac{2\pi(r_\alpha - a_0)}{(a_1 - a_0)} \right] \right] / (a_1 - a_0), & \text{if } a_0 \leq r_\alpha \leq a_1 \\ 1, & \text{if } r_\alpha \geq a_1. \end{cases} \quad (7.35)$$

Thus by using the RGM relative partial wave function

$$u_l(r_\alpha) = \sum_{i=1}^{\bar{N}} \Gamma_l(r_\alpha, S_i) c_i^l + u_l^0(r_\alpha), \quad (7.36)$$

one can obtain a set of  $\bar{N}$  simultaneous linear equations of the form of Eq. (7.27) with the functions  $X_l(S_i)$  given by Eq. (7.31) in terms of  $u_l^0(r_\alpha)$ , rather than the GC weight function  $f_l^0(S)$  of the de Takacs method. Instead of a matching condition for the GC weight function [e.g., Eq. (7.28)], Canto and Brink employed Eq. (7.36) for some value of  $r_\alpha = R > a_1$ . The resultant  $\bar{N} + 1$  equations can then be solved for the  $\bar{N} + 1$  unknowns  $c_i^l$  and  $\delta_l$ .

## 2. Variational method

Beck *et al.* (1975a) have used the GCM wave function as a trial function in a Kohn-type variational method (see Sec. VI.A). Using the functional  $I$  of Eq. (6.13), one finds the variational principle to be

$$\delta I = \langle \delta \Psi_k^T | H - E | \Psi_k^T \rangle = 0, \quad (7.37)$$

where here the angular brackets will denote integration over all configuration space. In partial wave form this is

$$\int \int \delta f_l^{(k)}(S) K_l(S, S') f_l^{(k)}(S') dS' dS = 0. \quad (7.38)$$

Thus if the weight function  $f_l^{(k)}(S)$  could be chosen arbitrarily, Eq. (7.38) would give the Hill-Wheeler equation for  $f_l^{(k)}(S')$ . However, it is necessary that  $f_l^{(k)}(S)$  should lead to the correct asymptotic boundary condition on  $u_l(r_\alpha)$  via Eq. (7.18). On the other hand, if the Hill-Wheeler equation [Eq. (7.24)] does have a solution with the proper asymptotic form, then this solution is also a solution of Eq. (7.38).

Beck *et al.* employed a trial function for the RGM partial wave function of the form of Eq. (7.36) with  $u_l^0(r_\alpha)$  given in terms of  $f_l^0(S)$  by the relation

$$u_l^0(r_\alpha) = \int \Gamma_l(r_\alpha, S) f_l^0(S) dS, \quad (7.39)$$

where (for the special case  $\eta_0 = 0$  in their paper)

$$f_l^0(S) = f_{lr}^0(S) + f_{li}^0(S) \tan \delta_l \quad (7.40)$$

and

$$\begin{Bmatrix} f_{lr}^0(S) \\ f_{li}^0(S) \end{Bmatrix} = \exp \left[ (k^2 b^2 N_1 N_2 / 2N) \sum_{n=0}^P d_{ln} S^{-n} \right] \begin{Bmatrix} F_l(kS) \\ G_l(kS) \end{Bmatrix}. \quad (7.41)$$

The coefficients  $d_{ln}$  are to be chosen so that a proper asymptotic form is obtained for  $u_l^0(r_\alpha)$ . The variational principle of Eq. (7.38) leads to the set of equations of Eq. (7.27) plus an additional Hill-Wheeler equation involving the phase shift

$$\sum_{i=1}^{\bar{N}} \int K_l(S_i, S) f_{li}^0(S) dS + X_{lr} + X_{li} \tan \delta_l = 0, \quad (7.42)$$

where

$$\begin{Bmatrix} X_{lr} \\ X_{li} \end{Bmatrix} = \int f_{li}^0(S) \int K_l(S, S') \begin{Bmatrix} f_{lr}^0(S') \\ f_{li}^0(S') \end{Bmatrix} dS' dS. \quad (7.43)$$

The  $\bar{N} + 1$  equations [Eqs. (7.27) and (7.43)] can then be solved for the  $\bar{N} + 1$  unknowns  $c_i^l$  and  $\delta_l$ .

## C. Solution of Hill-Wheeler equation in interaction region only

### 1. Microscopic $R$ -matrix method

In the preceding section we have seen various attempts to solve the Hill-Wheeler equation in the whole configura-

tion space. This has the disadvantage that it requires the evaluation of GC kernels in the channel region as well as special care to obtain the correct asymptotic boundary condition on the scattering function. An alternative procedure, initiated by Horiuchi (1970) and developed by Baye and Heenen (1974) is the microscopic  $R$ -matrix method (MRM). In this approach, the GCM wave function is used only in the interaction region and the known RG wave function is employed in the external region.

In the MRM, the total scattering wave function is expanded in terms of a discrete set of GC basis states  $\Phi(\mathbf{R}_i, \mathbf{S}_j)$  within the interaction region

$$\Psi_k^T(\mathbf{R}_i) = \sum_j f^{(k)}(\mathbf{S}_j) \Phi(\mathbf{R}_i, \mathbf{S}_j), \quad \text{if } r_\alpha \leq a_\alpha. \quad (7.44)$$

For this antisymmetrized basis, the definition of the relative coordinate  $r_\alpha$  is not unique: Other forms are given by exchanging nucleons between the two clusters. Since the  $N$  nucleons are indistinguishable, there are

$$n = \frac{1}{1 + \delta_{N_1 N_2}} \frac{N!}{N_1! N_2!} \quad (7.45)$$

equivalent independent definitions of the relative coordinate  $r_\alpha^{(p)}$  ( $p = 1, \dots, n$ ). The interaction region is defined to be that region of configuration space for which

$$r_\alpha^{(p)} \leq a_\alpha, \quad \text{for all } p. \quad (7.46)$$

In order to deal in a straightforward manner with integrals involving antisymmetrized states of the complete system, it is expedient to introduce (Barrett and Robson, 1979) the antisymmetrized channel states

$$|\hat{c}\rangle = \Phi_{\text{cm}, \mathcal{A}} |c\rangle, \quad (7.47)$$

where  $|c\rangle$  is defined by Eq. (2.14) and where for convenience we have included the cm wave function  $\Phi_{\text{cm}}$ . Then the "reduced width amplitude"

$$\begin{aligned} \langle \hat{c}, a_\alpha | \Phi(\mathbf{R}_i, \mathbf{S}_j) \rangle &= \langle \hat{c}, a_\alpha | \Phi_{\text{cm}, \mathcal{A}} \Gamma(\mathbf{r}_\alpha, \mathbf{S}_j) \hat{\chi}_{\alpha c} \rangle \\ &= \Gamma_l(a_\alpha, \mathbf{S}_j). \end{aligned} \quad (7.48)$$

Here (as in Sec. III), the notation  $\langle \hat{c}, a_\alpha | \rangle$  denotes integration over all coordinates except  $r_\alpha^{(p)}$ , which is set equal to  $a_\alpha$ . Thus, in analogy to Eq. (3.14), we have

$$\begin{aligned} \langle \hat{c}, a_\alpha | \Psi_k^T \rangle &= \sum_{jj'} \langle \hat{c}, a_\alpha | \Phi(\mathbf{R}_i, \mathbf{S}_j) \rangle \langle G^L \rangle_{jj'} \\ &\quad \times \langle \Phi(\mathbf{R}_i, \mathbf{S}_{j'}) | \hat{\mathcal{L}}(b_c) \Psi_k^T \rangle, \end{aligned} \quad (7.49)$$

where  $\hat{\mathcal{L}}(b_c)$  is a generalization of the Bloch operator [Eq. (3.4)]

$$\begin{aligned} \hat{\mathcal{L}}(b_c) &= \sum_\alpha \sum_{c \in \alpha} |\hat{c}\rangle \frac{\hbar^2}{2m_c a_\alpha} \\ &\quad \times \sum_{p=1}^n \delta(r_\alpha^{(p)} - a_\alpha) \left[ \frac{\partial}{\partial r_\alpha^{(p)}} r_\alpha^{(p)} - b_c \right] |\hat{c}\rangle \end{aligned} \quad (7.50)$$

and  $G^L$  is a matrix whose inverse has elements

$$\langle G^{L^{-1}} \rangle_{jj'} = \langle \Phi(\mathbf{R}_i, \mathbf{S}_j) | H + \hat{\mathcal{L}}(b_c) - E | \Phi(\mathbf{R}_i, \mathbf{S}_{j'}) \rangle. \quad (7.51)$$

For the elastic scattering of two spinless clusters, this gives

$$\begin{aligned} &[\zeta_l^{(-)}(a_\alpha) - \zeta_l^{(+)}(a_\alpha) U_l] \\ &= R_l^T \left[ \frac{d}{da_\alpha} a_\alpha - b_c \right] [\zeta_l^{(-)}(a_\alpha) - \zeta_l^{(+)}(a_\alpha) U_l], \end{aligned} \quad (7.52)$$

with

$$R_l^T = \frac{\hbar^2}{2m_c a_\alpha} \sum_{jj'} (\mathbf{S}_j \mathbf{S}_{j'})^{-1} \Gamma_l(a_\alpha, \mathbf{S}_j) \langle G^L \rangle_{jj'} \Gamma_l(a_l, \mathbf{S}_{j'}) \quad (7.53)$$

and

$$\zeta_l^{\pm}(a_\alpha) = \left[ \frac{m_c}{\hbar k} \right]^{1/2} i e^{\mp i \sigma_l} [G_l(ka_\alpha) \pm i F_l(ka_\alpha)] a_\alpha^{-1}. \quad (7.54)$$

For identical clusters, only *even*  $l$  values occur, since the asymptotic radial relative wave function has an additional factor  $[1 + (-1)^l]$ . Equation (7.52) is readily solved for the collision matrix  $U_l = \exp(2i\delta_l)$ . A similar expression for the collision function is obtained for the alternative formulation based on the Green's-function operator  $G$  of Eq. (3.6) and the use of Eq. (3.7).

The MRM has been extended to multichannel scattering by Baye, Heenen, and Libert-Heinemann (1977) and has been applied to a wide range of (but mostly single-channel) heavy-ion scattering problems (Baye and Heenen, 1974; Heenen, 1976; Baye, 1976; Baye and Heenen, 1977a, 1977b; Baye, Heenen, and Libert-Heinemann, 1978; Baye and Salmon, 1979a, 1979b).

In the special case where one of the clusters consists only of a single nucleon, it is sometimes more convenient to employ a single-particle continuum wave function, which is defined relative to the same potential well used to describe the single-particle bound states of the other cluster, i.e., to take  $\mathbf{S}=0$  in Eq. (7.12). In this case,  $\Phi(\mathbf{R}_i, \mathbf{S}) \equiv \Phi(\mathbf{R}_i, 0)$  is simply a single antisymmetrized Slater determinant of single-particle orbitals and there are just  $N$  equivalent independent definitions of the relative coordinate  $r_\alpha^{(p)}$ . Equations (7.46)–(7.51) are essentially valid (provided the vector coupling of the internal angular momenta of the target cluster and single nucleon is taken into account) and represent the  $R$ -matrix approach to the continuum shell model (Mahaux and Weidenmüller, 1969). In such an approach, neglecting the cm motion, Takeuchi and Moldauer (1970) employed a finite spherically symmetric potential with a spin-orbit term to describe the single-particle states for neutron scattering from  $^{17}\text{O}$ . On the other hand, for  $n$ - $^{14}\text{C}$  scattering, Philpott (1973) used harmonic oscillator orbitals for both the bound valency and continuum nucleons. This permits the



separation of any spurious cm motion (Philpott, 1977), which is important for nucleons incident upon light targets.

## 2. Variational methods

Canto and Brink (1977) in their method 2 have employed a Kohn variational method to solve the one-channel partial wave form of the RGM equation [Eq. (7.8)], using a trial function

$$u_l(r_\alpha) = \sum_{i=1}^N c_i^l \Gamma_l(r_\alpha, S_i) \quad (7.55)$$

with mesh points  $S_i$  within the interaction region. This leads to an expression for the collision function  $U_l$  which is identical with Eq. (7.52) of the MRM, so that the two methods are equivalent. Nagata and Yamamoto (1977) have also proposed such a variational approach. The equivalence of the Kohn variational method and the MRM follows from a generalization of the variational derivation of the  $R$ -matrix formalism as given in Sec. VI.C.

Mito and Kamimura (1976) and Kamimura (1977) have proposed Kohn variational methods to obtain the collision matrix  $\tilde{U}$  directly, rather than the  $K$  matrix (see Sec. VI.B). For the trial function of Eq. (7.55), this technique gives similar results but is not equivalent to the other methods since unitarity of the  $\tilde{U}$  matrix is not guaranteed. Thus the unitary nature of the calculated  $\tilde{U}$  matrix can be employed as a check on the accuracy of the calculations.

### D. Natural boundary condition method

The natural boundary condition (NBC) methods of Sec. V have been extended to treat composite particle scattering by Baldock, Barrett, and Robson (1979). In this approach, the GCM is used to construct a set of basis wave functions rather than the total wave function  $\Psi_k^T$  of Eq. (7.11). An arbitrary choice can therefore be made for the GC weight function  $f(\mathbf{S})$ . However, to ensure a rapid convergence of the expansion of the scattering wave function,  $f(\mathbf{S})$  is chosen so that the basis states have a suitable asymptotic form. For the single-channel case and spin-zero clusters, the basis states are taken to be

$$\phi_j^{(l)}(\mathbf{R}_i) = \int j_l(k_j S) Y_l^m(\Omega_S) \Phi(\mathbf{R}_i, \mathbf{S}) d\mathbf{S}, \quad (7.56)$$

where  $j_l(k_j S)$  is the regular spherical Bessel function and  $\Phi(\mathbf{R}_i, \mathbf{S})$  is an antisymmetrized product of Slater determinants representing the ground states of the two clusters given by Eq. (7.12). If the same length parameter is assumed for the single-particle harmonic oscillator states of each cluster, then Eq. (7.13) is valid, so that the cm motion separates out. For large values of the relative coordinate  $r_\alpha$ , it can be shown that

$$\phi_j^{(l)} \sim \phi_j^{0(l)} \propto [1 + (-1)^l \delta_{N_1 N_2}] j_l(k_j r_\alpha) Y_l^m(\Omega_{r_\alpha}) \hat{\chi}_{ac} \Phi_{cm}, \quad (7.57)$$

where  $N_i$  is the number of nucleons in cluster  $i$ .

The use of the function  $j_l(k_j S) Y_l^m(\Omega_S)$  for the GC weight function  $f(\mathbf{S})$  has several advantages. First, it projects out states of good angular momentum so that a separate angular momentum projection is not required. Such a projection is necessary when other than closed-shell clusters are considered. Second, the basis states have an appropriate asymptotic form which is suitable for the application of NBC methods to obtain the scattering cross section. Third, the use of standard functions allows most of the matrix elements involved in the calculations to be evaluated analytically.

The NBC methods require that the basis states satisfy the condition

$$\left[ \frac{a_\alpha}{j_l(k_j a_\alpha)} \frac{\partial j_l(k_j a_\alpha)}{\partial a_\alpha} \right] = B_c, \quad (7.58)$$

which gives a set of discrete values  $k_j$  defining the basis states for the interaction region. The constant  $B_c$  for the given channel  $c$  is the natural boundary condition for the total scattering wave function  $\Psi_k^T$ , which for large separations of the two clusters can be written as a sum of partial waves of definite angular momentum given by

$$\Psi_k^{T(l)} \sim \mathcal{A} [\xi_l^{(-)}(r_\alpha) - \xi_l^{(+)}(r_\alpha) U_l] Y_l^m(\Omega_{r_\alpha}) \chi_{ac}^{(1)} \chi_{ac}^{(2)} \Phi_{cm}, \quad (7.59)$$

where  $\xi_l^{(\pm)}(r_\alpha)$  are defined by Eq. (7.54). Thus

$$B_c = \left[ \frac{a_\alpha}{\Psi_k^{T(l)}} \frac{\partial \Psi_k^{T(l)}}{\partial a_\alpha} \right]. \quad (7.60)$$

The eigenfunctions  $\Psi_k^{T(l)}$  of the Hamiltonian describing the two-cluster system in the interaction region may be expanded in terms of the basis states, i.e.,

$$\Psi_k^{T(l)} = \sum_j c_{kj}^{(l)} \phi_j^{(l)}, \quad \text{for } r_\alpha \leq a_\alpha. \quad (7.61)$$

The expansion coefficients  $c_{kj}^{(l)}$  may be obtained by solving the set of equations:

$$\sum_j c_{kj}^{(l)} (\langle \phi_i^{(l)} | H_T | \phi_j^{(l)} \rangle - E_k \langle \phi_i^{(l)} | \phi_j^{(l)} \rangle) = 0, \quad (7.62)$$

where  $H_T$  is the total Hamiltonian of the system,  $E_k$  are the eigenvalues of the total energy when the wave functions  $\Psi_k^{T(l)}$  satisfy the boundary condition of Eq. (7.60), and the angular brackets denote integration over the interaction region.

Asymptotically, the allowed values of the kinetic energy of separation of the two clusters,  $T_k$ , are given by

$$T_k = E_k - B_1 - B_2, \quad (7.63)$$

where  $B_i$  is the binding energy of cluster  $i$ . From the calculated values of  $T_k$ , corresponding to a given value of  $B_c$ , the wave number  $k$  of relative motion implicit in Eq. (7.59) and hence the collision function  $U_l = \exp(2i\delta_l)$  may be calculated using Eq. (7.60). By letting  $B_c$  vary through the range  $-\infty$  to  $+\infty$ , one can obtain the phase shift  $\delta_l$

at all energies.

The above method does not suffer from the instabilities associated with the singular character of the GC weight function  $f^{(k)}(\mathbf{S})$  employed in those methods, which solve the Hill-Wheeler equation by discretizing the interaction region of coordinate space. The method also has the advantages of the NBC methods, which minimize the number of basis states required in the interaction region. However, compared with the microscopic  $R$ -matrix method (see Sec. VII.C.1), the NBC method involves additional integrations over two generator coordinates,  $\mathbf{S}$  and  $\mathbf{S}'$ , in the evaluation of the Hamiltonian and overlap matrix elements,  $\langle \phi_i^{(l)} | H_T | \phi_j^{(l)} \rangle$  and  $\langle \phi_i^{(l)} | \phi_j^{(l)} \rangle$ , of Eq. (7.62). This means that, except for the simplest closed-shell systems, the calculations are extremely tedious even when symbolic algebra computer codes are employed. Applications of the technique have so far been limited to  $\alpha$ - $\alpha$  (Baldock, Barrett, and Robson, 1979) and  $^{16}\text{O}$ - $^{16}\text{O}$  (Baldock, Robson, and Barrett, 1981) elastic scattering.

### VIII. PRACTICAL APPLICATION OF $R$ -MATRIX AND RELATED THEORIES

The reaction theories described in this review are receiving widespread and increasing application in several areas of physics. The standard  $R$ -matrix method (Sec. IV.C), including the Buttle correction (Sec. IV.D), the extended  $R$ -matrix approaches (Sec. IV.F), and the various natural boundary condition methods (Sec. V), have been employed with considerable success for the dynamical description of resonance phenomena observed in nucleon elastic and inelastic scattering and in photonuclear reactions. The applications have ranged from a calculation of the structure of  $^4\text{He}$  (Bevelacqua and Philpott, 1977) to studies of polarization-analyzing power differences—e.g., in the reaction  $^{15}\text{N}(p,n)^{15}\text{O}^*$  (Philpott and Halderson, 1980). For composite particle scattering, the microscopic  $R$ -matrix (Sec. VII.C.1) and natural boundary condition (Sec. VII.D) methods, which use a combination of generator coordinate and  $R$ -matrix techniques, have been employed to investigate the scattering of both light systems—e.g.,  $\alpha + \alpha$  (see Sec. VIII.D) and heavier systems such as  $^{40}\text{Ca} + ^{40}\text{Ca}$  (Baye and Salmon, 1979b). In atomic and molecular physics, the  $R$ -matrix approach has been applied both to comparatively simple systems like  $e^-$ -H scattering and to more complex problems, such as electron scattering from molecular nitrogen (Burke and Robb, 1975; Buckley, Burke, and Lan, 1979). However, a comprehensive survey of the many examples where calculable reaction theories have been applied to the solution of real physical scattering problems is too large in scope to be contemplated here. Instead, in this section, we shall present a fairly detailed discussion of a few selected examples where several different methods have been applied to the same scattering problem. This allows a critical comparison of the alternative approaches.

The first example is an exactly soluble model consisting of two coupled square-well potentials. This model has been employed by a number of authors to determine the

convergence and accuracy of their numerical techniques before applying the method to more realistic situations. A reliable comparison of the accuracies of the various techniques can be obtained with the model because of the availability of an exact analytic solution.

The second example which will be considered is the elastic scattering of neutrons from the  $^{12}\text{C}$  nucleus. This is also a problem which has been approached using a number of different techniques. Again, the availability of a coupled-channels calculation enables a meaningful comparison to be made of the convergence rates of the various reaction theories with each other. Furthermore, the problem is typical of many which arise in low-energy nuclear physics.

The third example has been selected as a representative of the application of reaction theory to problems in atomic physics. The problem which will be considered is the elastic scattering of low-energy electrons from the helium atom. This is a topic to which a considerable amount of experimental and theoretical effort has been directed in recent years, in an attempt to establish a standard reference cross section for the calibration of other experiments. A number of high-precision calculations have been performed for the  $e^-$ -He elastic scattering cross section.

The last example is typical of an area of nuclear physics which is currently receiving increasing attention, namely, the scattering of composite particles. To calculate successfully the scattering cross sections for such a process, the reaction theories previously outlined in this review need to be combined with some method of describing the cluster nature of the particles as described in Sec. VII. In this section, we shall present the results of the application of these techniques to the calculation of the  $\alpha$ - $\alpha$  elastic scattering cross section.

#### A. Coupled square wells

An exactly soluble model comprising two square-well potentials coupled by a square-well interaction has been used by many authors (Newton, 1959, 1961; Fonda and Newton, 1960; Weidenmüller, 1964, 1965; Haglund and Robson, 1965; Mahaux and Weidenmüller, 1965, 1967; Glöckle, 1966, Glöckle, Hüfner, and Weidenmüller, 1967; Garside and Tobocman, 1969; Purcell, 1969a; Lejeune and Mahaux, 1970; Lejeune and Nagarajan, 1970, 1971; Schmittroth and Tobocman, 1971; Philpott, 1976; Ahmad, Barrett, and Robson, 1976b) as a test of various reaction theories. The parameters of the model may be varied to simulate bound states embedded in the continuum, and both elastic and inelastic scattering cross sections can be calculated. By comparing the results obtained from reaction theory calculations with the exact analytic solutions, one can compare the rates of convergence of the various formulations of reaction theory.

In this model, the system is described by the Schrödinger equation

$$(H - E)\Psi = 0, \quad (8.1)$$

which in matrix notation can be written

$$\begin{bmatrix} T + V_{11}(r) - E & V_{12}(r) \\ V_{12}(r) & T + V_{22}(r) - E + Q \end{bmatrix} \begin{bmatrix} \Psi^{(1)} \\ \Psi^{(2)} \end{bmatrix} = 0. \quad (8.2)$$

Here,  $T$  is the kinetic energy operator,  $Q$  is the reaction threshold energy in the second channel, and the potentials  $V_{ij}(r)$  are of the form

$$\begin{aligned} V_{ij}(r) &= -V_{ij}, \quad r \leq R \\ &= 0, \quad r > R. \end{aligned} \quad (8.3)$$

The basic coupled radial equations for the model, assuming  $s$ -wave scattering, are

$$\frac{d^2 u_1(r)}{dr^2} + \frac{2m}{\hbar^2} [E - V_{11}(r)] u_1(r) = \frac{2m}{\hbar^2} V_{12}(r) u_2(r) \quad (8.4a)$$

and

$$\frac{d^2 u_2(r)}{dr^2} + \frac{2m}{\hbar^2} [E - Q - V_{22}(r)] u_2(r) = \frac{2m}{\hbar^2} V_{12}(r) u_1(r), \quad (8.4b)$$

where  $m$  is the reduced mass of the scattered particle. These equations can be solved exactly to obtain the radial wave functions  $u_1(r)$  and  $u_2(r)$  for channels 1 and 2, respectively. From these solutions, the collision matrix and the associated elastic scattering and reaction cross sections can be calculated. The parameters of the model can be varied to simulate cases of weak, intermediate, and strong coupling. We shall now investigate the application of several of the reaction theories discussed in this review to the solution of the above two-channel problem.

### 1. Wigner-Eisenbud $R$ -matrix theory

In the Wigner-Eisenbud form of the  $R$ -matrix theory (see Sec. IV.B), the eigenstates  $\phi_j$  and their eigenvalues  $\mathcal{E}_j$ , which play a basic role in this theory of multichannel scattering, are solutions of the full Schrödinger equation in the internal region, subject to chosen boundary conditions  $B_c$  at the channel radii  $a_c$ . The validity of the one-level approximation to Eq. (4.24) has been tested by Mahaux and Weidenmüller (1965, 1967) and Lejeune and

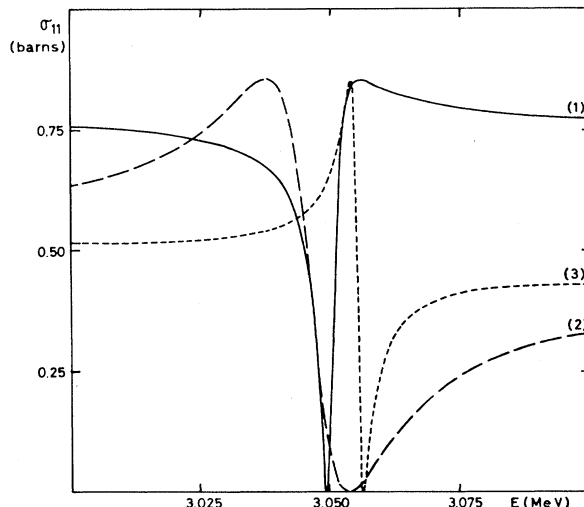


FIG. 1. Curve 1 represents the exact value of the elastic scattering cross section vs energy for the model parameters of Table II. Curve 2 shows the one-level approximation for  $a_1 = a_2 = 6.0$  fm,  $B_1 = 0$ , and  $B_2 = -2.262$ . Curve 3 corresponds to the one-level approximation with  $a_1 = a_2 = 6.0$  fm,  $B_1 = 4.6$ , and  $B_2 = -2.262$  (from Lejeune and Mahaux, 1970).

Mahaux (1970). Some of their results for a weak coupling model are presented in Fig. 1. The model parameters are listed in Table II:  $a_1 = a_2 = 6.0$  fm,  $B_1 = 0$  (curve 2) and 4.6 (curve 3), and  $B_2 = -2.262$ .

It is seen that the one-level approximation is unsatisfactory. There appear to be two main reasons for this failure. First, the background scattering phase shift differs considerably from the hard-sphere phase shift, and the one-level formula is unable to reproduce this difference. Second, the theoretical width of the resonance is too large. Only if the interaction radius in the open channel is arbitrarily chosen, such that the hard-sphere scattering phase shift is approximately equal to the potential scattering phase shift in the vicinity of the resonance, is the one-level approximation adequate. Results for such a case are shown in Fig. 2 for  $a_1 = 11.537$  fm,  $a_2 = 6.0$  fm,  $B_1 = 0$  (long dashes) and 7.5 (short dashes), and  $B_2 = -2.262$ .

The deficiencies of the one-level approximation are largely removed and its accuracy is dramatically im-

TABLE II. Interaction parameters for coupled square-well problem.

Figs./Table	$V_{11}$ (MeV)	$V_{22}$ (MeV)	$V_{12}$ (MeV)	$Q$ (MeV)	$R$ (fm)	Refs. <sup>a</sup>
1-4, 10	31.0	41.0	0.1	6.0	6.0	1-3
5, 6, 11, 12	32.0	39.0	1.0	3.5	6.0	4
7, Table III	32.161	39.022	1.072	3.5	6.0	3
8, 9	32.161	39.022	20.0	3.5	6.0	3
13, 14, 19, 20	42.0	39.0	1.0	3.5	6.0	6
15-18, 23, 24	10.0	15.0	4.0	3.5	6.0	5, 6
21, 22	32.0	39.0	1.0	3.5	6.0	5

<sup>a</sup>Reference: 1. Lejeune and Mahaux (1970); 2. Lejeune and Nagarajan (1970); 3. Ahmad, Barrett, and Robson (1976b); 4. Garside and Tobocman (1969); 5. Philpott (1976); 6. Schmittroth and Tobocman (1971).

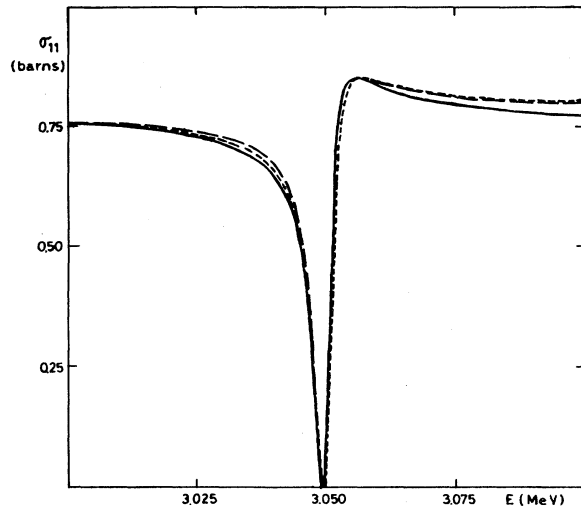


FIG. 2. All curves refer to the model parameters of Table II. The full curve is the exact elastic scattering cross section. The other curves represent the one-level approximation with  $a_2=6.0$  fm,  $B_2=-2.262$ ,  $a_1=11.537$  fm,  $B_1=0$  (long dashes), and  $B_1=7.5$  (short dashes) (from Lejeune and Mahaux, 1970).

proved by the inclusion of a constant background term in the expression for the  $R$  matrix. This term approximates the effect of distance levels which are neglected in the single-level expression. It was found to be important to choose natural boundary condition parameters and a large channel radius for the closed channel. In this case theory gives a good description of the exact solution. The results for the parameters listed in Table II are plotted in Fig. 3. Here  $a_1=6.0$  fm,  $B_1=0$ ,  $B_2=-2.262$ , and  $a_2=6.0$  fm

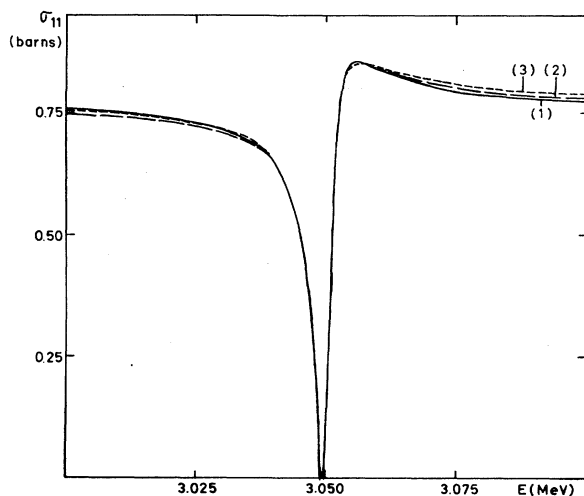


FIG. 3. The full curve (1) represents the exact elastic scattering cross section for the model parameters of Table II. Curve 2 represents the one-level approximation plus a constant background term evaluated at 3.050 MeV for  $a_1=a_2=6.0$  fm,  $B_1=0$ , and  $B_2=-2.262$ . Curve 3 represents the one-level approximation plus a constant background term in channel 1 only evaluated at 3.050 MeV for  $a_1=6.0$  fm,  $a_2=12.0$  fm,  $B_1=0$ , and  $B_2=-2.262$  (from Lejeune and Mahaux, 1970).

(curve 2) and 12.0 fm (curve 3).

The results displayed in Figs. 1–3 indicate that caution must be exercised when employing the one-level approximation to obtain fits to experimental data if one wishes to derive resonance widths and energies which have a clear physical meaning. A similar conclusion is reached in the discussion of  $^{12}\text{C}(n,n)^{12}\text{C}$  scattering in Sec. VIII.B. In general, for the weak-coupling case, the one-level approximation plus a constant background term gives a satisfactory description of an isolated resonance. However, as pointed out by Lejeune and Mahaux (1970), for some choices of the open-channel boundary condition parameter, two eigenstates are important in the  $R$ -matrix expansion so that usage of the single-level approximation with a constant background term would lead to the extraction of meaningless resonance parameters. In this case, a two-level approximation without any background term yields a good description of the resonance.

## 2. Kapur-Peierls theory

The Kapur-Peierls dispersion theory has been discussed in Sec. IV.A. This approach differs from the Wigner-Eisenbud method in that outgoing wave boundary conditions are applied to all open channels with the result that the energy eigenvalues and eigenstates are complex and energy dependent. As a consequence, the Kapur-Peierls formalism has not found extensive application, although the expression for the  $\tilde{U}$  matrix [Eq. (4.21)] is simpler than the corresponding expression in the Wigner-Eisenbud theory [Eqs. (4.17) and (4.26)].

Lejeune and Nagarajan (1970) have investigated the validity of the single-level approximation in the framework of the Kapur-Peierls formalism using the two-channel model of Eqs. (8.2) and (8.3). The results of their calculations for the model parameters of Table II and  $a_1=a_2=6.0$  fm are given in Fig. 4, where they are compared with the exact solution. No background phase shift was introduced to allow for the contribution from distant levels. It is seen that the agreement between the exact and the Kapur-Peierls value for the resonance energy is excellent, although the magnitude for the peak cross section is grossly overestimated.

Although the method does not preserve unitarity, it was found that the resonance energy in the single-level Kapur-Peierls formalism is practically independent of the open-channel radius. Moreover, Lejeune and Mahaux (1970) have shown, for the weak-coupling case, that the violation of unitarity occurs mainly in the elastic channel. For these reasons, they have suggested that for sharp resonances the Kapur-Peierls formalism is likely to be more useful for multichannel resonance analysis than the Wigner-Eisenbud method. However, in order to obtain a satisfactory unitarized  $\tilde{U}$  matrix, Lejeune and Mahaux found that it was necessary to employ essentially a two-level approximation. In addition, the complications introduced by the complex and energy-dependent boundary conditions have limited the widespread usage of the Kapur-Peierls approach.

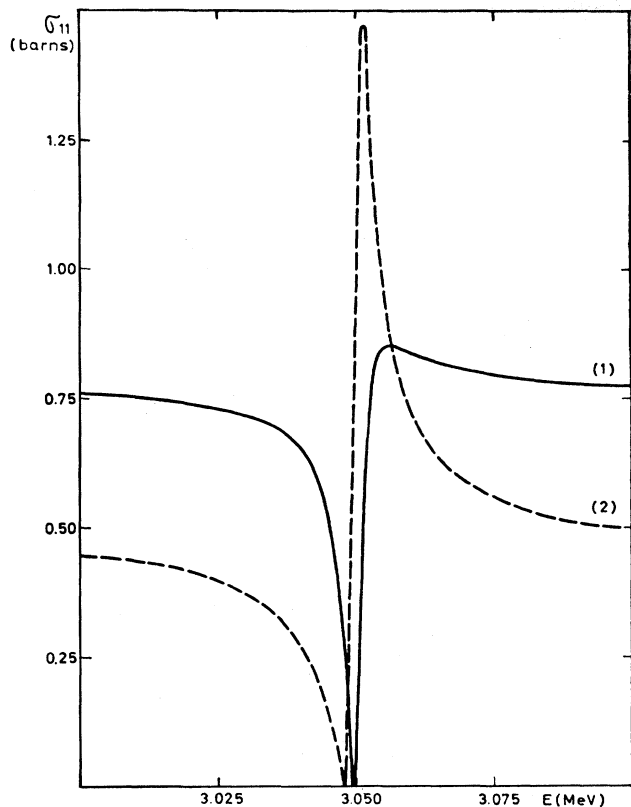


FIG. 4. The exact elastic scattering cross section (curve 1) and the one-level approximation Kapur-Peierls result (curve 2) for  $a_1 = a_2 = 6.0$  fm. The model parameters of Table II are plotted vs the incident energy (from Lejeune and Nagarajan, 1970).

### 3. Standard calculable $R$ -matrix method

The standard  $R$ -matrix (SRM) method described in Sec. IV.C has also been investigated using the two-channel model of Eqs. (8.2) and (8.3) with the coupling potential being treated as the residual interaction by Garside and Tobocman (1969) and Ahmad, Barrett, and Robson (1976b). The model parameters employed in these two studies are listed in Table II.

The results obtained by Garside and Tobocman (1969) for the elastic and inelastic scattering cross sections are presented in Figs. 5 and 6 for  $a_1 = a_2 = 8.0$  fm and  $B_1 = B_2 = 0$ . The convergence of the SRM method is seen to be quite slow, with 20 terms in the  $R$ -matrix expansion still not producing an adequately converged result. While the neglected distant levels may not be important for determining the rapid energy variation of the collision matrix over a narrow resonance energy range, the coherent effect of these terms is necessary to alter the nonresonant background part of the collision matrix from the otherwise hard-sphere scattering form. The Buttler correction (see Sec. IV.D) to the SRM method allows in an approximate way for the contribution of the neglected distant levels.

The effect of the Buttler correction (BCRM) in this model has been investigated by Ahmad, Barrett, and Robson (1976b) for two different values of the coupling parameter. The results for an intermediate-coupling strength using four levels/channel are shown in Table III and Fig. 7 and for stronger coupling with six levels/channel in Figs. 8 and 9. In each case, the Buttler correction results in a marked improvement over the SRM method. Channel radii  $a_1 = a_2 = 7.5$  fm and boundary condition parameters  $B_c = 0$  were employed.

An SRM calculation using the same weak-coupling parameters as employed by Lejeune and Mahaux (1970) has been carried out by Ahmad, Barrett, and Robson (1976b). The results of these calculations using one level/channel are given in Fig. 10. Provided that natural boundary condition parameters are employed in the closed channel, the resonance position and shape are well reproduced (curve SRM<sub>2</sub>). This is in agreement with the corresponding results obtained with the Wigner-Eisenbud and Kapur-Peierls methods.

### 4. Extended $R$ -matrix method

Three extensive studies of the application of the extended  $R$ -matrix (ERM) method (see Sec. IV.F) to the coupled square-well problem have been made by Garside and Tobocman (1969), Schmittroth and Tobocman (1971), and Philpott (1976).

In the first investigation the basis states were taken to be eigenstates of the channel Hamiltonians  $T + V_{ii}(r)$ , which fulfilled homogeneous boundary conditions at a radius  $r = a'$ . The channel radii  $a_i = a$  were chosen such that  $a < a'$ , so that these eigenstates satisfied inhomogeneous boundary conditions at  $r = a$ . The results for  $a = 6$  fm,  $a' = 8$  fm, and the model parameters of Table II are presented in Figs. 11 and 12. Comparison with Figs. 5 and 6 leads to two conclusions. First, the convergence of the ERM method is faster than that of the corresponding SRM calculation. Although this is partially aided by the smaller channel radii, a nearly perfect fit to the exact solution is obtained with only six levels in the  $R$ -matrix expansion. Second, a narrow "spurious" resonance appears in the elastic scattering results for the ERM method. This false resonance tends to disappear as the number of levels in the  $R$ -matrix expansion is increased.

Schmittroth and Tobocman (1971) have also applied the ERM formalism to the coupled square-well problem. They have investigated the two formulations of  $R$ -matrix theory involving the matrices  $R_{cc'}^L$  and  $R_{cc'}$  of Eqs. (3.15) and (3.22), respectively, described in Sec. III.B. In the latter case, the operator  $G$  defined in Eq. (3.6) and appearing in the expression [Eq. (3.22)] for the  $R$  matrix was calculated in two ways.

In the first method, the Hamiltonian was diagonalized in a truncated set of harmonic oscillator basis states to give a set of approximate Hamiltonian eigenfunctions  $\{\Psi_N\}$  with eigenvalues  $E_N$ . The Green's-function operator is then given by

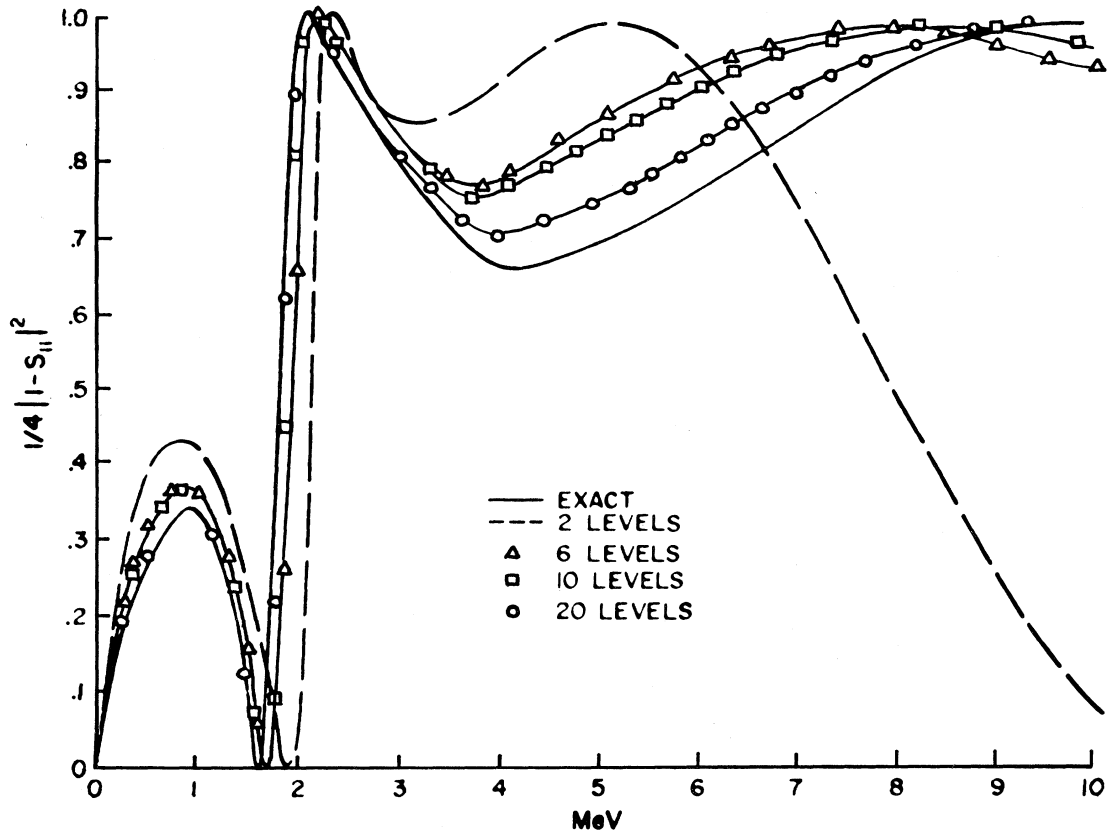


FIG. 5.  $2mE(4\pi\hbar^2)^{-1} \times$  elastic scattering cross section for the model parameters of Table II,  $a_1=a_2=8.0$  fm, and  $B_1=B_2=0$ . Shown are the exact result and several SRM calculations (from Garside and Tobocman, 1969).

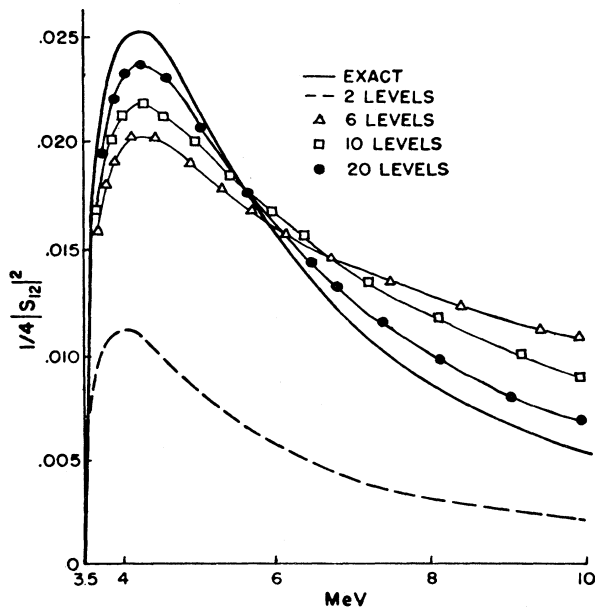


FIG. 6.  $2mE(4\pi\hbar^2)^{-1} \times$  inelastic scattering cross section for the model parameters of Table II,  $a_1=a_2=8.0$  fm, and  $B_1=B_2=0$ . Shown are the exact result and several SRM calculations (from Garside and Tobocman, 1969).

$$G = \sum_{NM} |\Psi_N\rangle \mathcal{N}_{NM} (E - E_M)^{-1} \langle \Psi_M|, \quad (8.5)$$

where

$$(\mathcal{N}^{-1})_{NM} = \langle \Psi_N | \Psi_M \rangle. \quad (8.6)$$

Since the Hamiltonian  $H$  is not Hermitian for harmonic oscillator basis states when integration is restricted to the internal region, the diagonalization was carried out for simplicity using Hamiltonian matrix elements calculated by integration over all configuration space. The basic idea of this approach is that direct use of Hamiltonian eigenstates and eigenvalues provided by an independent nuclear structure calculation could be employed. In the second method, the matrix elements of  $E-H$  were evaluated over the finite volume of the internal region and then the matrix was inverted at each required energy to obtain the operator  $G$ . In a truncated basis space one would normally expect the diagonalization and inversion procedures to give the same answer. However, the different regions of integration employed for the calculation of the matrix elements in the two techniques introduce a difference in their respective rates of convergence. Calculations using these methods are denoted by  $E$ -RM(DIAG) and  $E$ -RM(INV), respectively, in Figs. 13–18.

TABLE III. Elastic scattering cross sections (b) for coupled square-well problem.

$E$ (MeV)	Exact	SRM	BCRM	NBC	BD + correction
0.2	1.869 52	2.302 09	1.871 82	1.870 30	1.869 50
0.6	1.484 36	1.741 91	1.487 03	1.485 13	1.484 22
1.0	1.136 14	1.282 33	1.139 71	1.137 05	1.136 14
1.4	0.754 26	0.850 81	0.760 32	0.755 41	0.754 28
1.8	0.113 60	0.284 96	0.123 19	0.115 04	0.113 60
2.2	1.093 83	0.686 16	1.090 21	1.093 08	1.093 74
2.6	0.982 61	1.000 62	0.982 26	0.982 83	0.982 62
3.0	0.788 05	0.791 96	0.787 43	0.788 33	0.788 03
3.4	0.648 54	0.657 80	0.648 10	0.648 83	0.648 53
3.8	0.524 66	0.554 07	0.525 07	0.525 16	0.524 61
4.2	0.462 70	0.507 22	0.463 07	0.463 23	0.462 64
4.6	0.420 98	0.476 67	0.421 21	0.421 47	0.420 93
5.0	0.391 56	0.453 97	0.391 65	0.391 99	0.391 52
5.4	0.370 38	0.435 12	0.370 36	0.370 74	0.370 34
5.8	0.354 77	0.417 92	0.354 67	0.355 06	0.354 74
6.2	0.342 84	0.401 12	0.342 68	0.343 08	0.342 82
6.6	0.333 23	0.384 07	0.333 04	0.333 41	0.333 21
7.0	0.324 95	0.366 48	0.324 73	0.325 09	0.324 94

The insertion of an optical potential to account for distant levels in the  $R$ -matrix formalism has been described in Sec. III.C. A numerical investigation of the accuracy of this approach for both of the  $R$ -matrix formulations was also carried out by Schmittroth and Tobocman. Calculations of this type for the  $R$ - and  $R^L$ -matrix formulations are indicated by  $E$ -RM(INV) + O.M. and  $L$ -OP + O.M., respectively, in Figs. 13–18.

The results of their investigation are presented in Figs.

13–18. Harmonic oscillator wave functions were used as basis states with an oscillator parameter chosen so that  $\hbar\omega = 10.46$  MeV. The model parameters are listed in Table II; an intermediate-strength channel coupling being used for the results presented in Figs. 13 and 14 and a stronger coupling for those in Figs. 15–18. The channel radii were 7.0 fm, and the boundary condition parameters were set to zero in the  $\mathcal{L}$ -operator calculations.

The results for the elastic and inelastic scattering cross

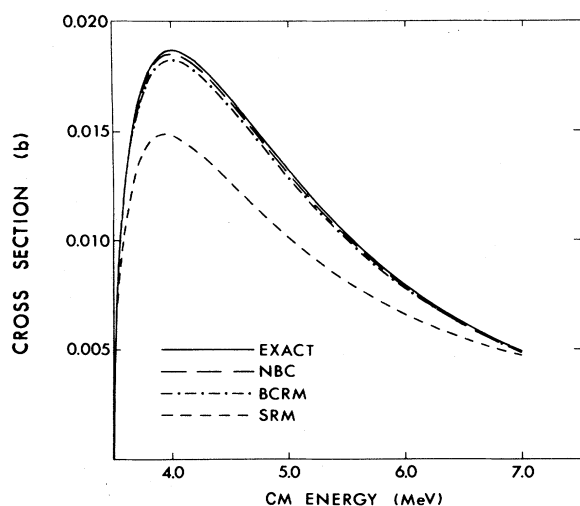


FIG. 7. Total inelastic scattering cross section for coupled square-well model calculated by several methods for the parameters of Table II. Each method employed  $B_c = 0$  for the fixed boundary condition parameters, channel radii of 7.5 fm, and the lowest four basis states/channel. The result for the BD method, including the energy correction with eight additional higher basis states/channel is indistinguishable from the exact calculation (from Ahmad, Barrett, and Robson, 1976b).

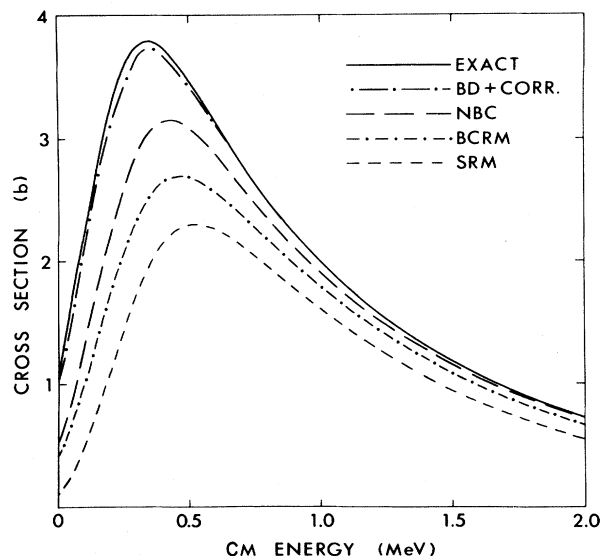


FIG. 8. Total elastic scattering cross section for coupled square-well model calculated by several methods for the parameters of Table II. Each method employed  $B_c = 0$  for the fixed boundary condition parameters, channel radii of 7.5 fm, and the lowest six basis states/channel. The energy correction to BD method used six additional higher basis states/channel (from Ahmad, Barrett, and Robson 1976b).

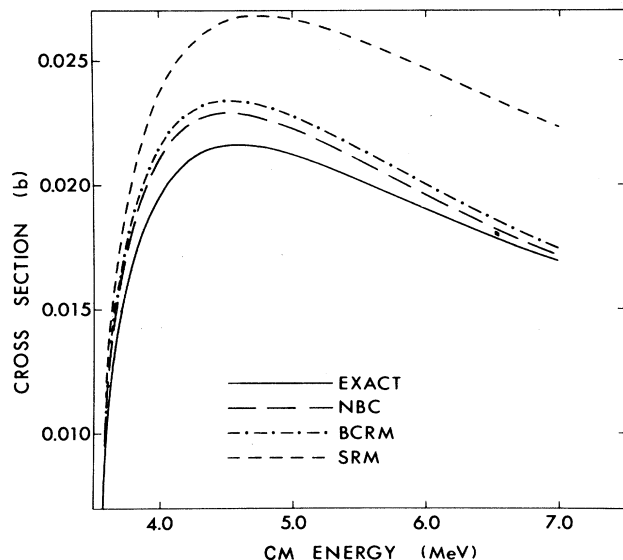


FIG. 9. Total inelastic scattering cross section for coupled square-well model calculated by several methods for the parameters of Table II (see Fig. 8 caption for explanation of curves). The result for the BD method including the energy correction is indistinguishable from the exact calculation (from Ahmad, Barrett, and Robson, 1976b).

sections in Figs. 13–18 show that the ERM calculations converge with approximately ten levels/channel, provided the inversion technique is used. For a smaller number of basis states, the inclusion of an optical potential generally

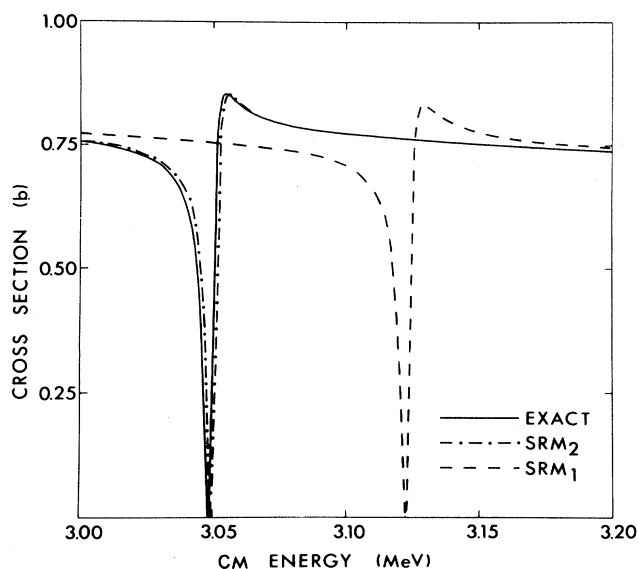


FIG. 10. Total elastic scattering cross section for coupled square-well model calculated by several methods for the parameters of Table II. Each method employed channel radii of 6.0 fm and only the basis state in each channel closest to 3.05 MeV. Curves SRM<sub>1</sub> and SRM<sub>2</sub> are SRM calculations with  $B_1=B_2=0$  and with  $B_1=0$  and natural boundary condition parameters in closed channel 2, respectively (from Ahmad, Barrett, and Robson, 1976b).

improves the results but can lead to the appearance of spurious resonances in the calculated cross sections. One can show that with no optical potential both the E-RM(INV) and L-OP techniques give the same results. Figures 17 and 18 show that the inversion technique produces results which are distinctly more reliable than the diagonalization procedure.

Schmittroth and Tobocman have also studied the  $X$ -matrix forms of both  $R$ -matrix formalisms which have been described in Sec. III.D. Figures 19 and 20 show typical results which they obtained for the elastic and inelastic scattering cross sections using the intermediate-coupling parameters of Table II. They employed three methods to calculate the  $X$  matrix. In two of these methods, the Green's-function operator  $G$  of Eq. (3.6) was represented by the relations (Hüfner and Lemmer, 1968; Garside and Tobocman, 1969)

$$G = (\bar{V} - \bar{V} \bar{G} \bar{V})^{-1} - \bar{V}^{-1} \quad (8.7)$$

and

$$G = (\bar{V} - \bar{V} \bar{G} \bar{V})^{-1} \bar{V} \bar{G}, \quad (8.8)$$

respectively, where  $\bar{V}$  denotes the optical potential matrix with elements  $V_{ii} \delta_{ij}$  and  $\bar{G}$  is the corresponding optical-model Green's-function operator. Calculations using these two forms to obtain the  $X$ -matrix operator

$$\hat{X} = \bar{V} + \bar{V} G \bar{V} \quad (8.9)$$

corresponding to the operator of Eq. (3.44) with the  $\Delta$  term set to zero (see Appendix A) are denoted by  $X1$  and  $X2$ , respectively, in Figs. 19 and 20. The third method (denoted by  $XL$ ) employed Eq. (3.24) for the operator  $G^L$ , i.e.,

$$G^L = [H + \mathcal{L}(b_c) - E]^{-1}, \quad (8.10)$$

to obtain the corresponding  $X$ -matrix operator [Eq. (3.43)]

$$\hat{X}^L = -\bar{V} + \bar{V} G^L \bar{V}. \quad (8.11)$$

In all three methods, the matrix elements were computed using the same harmonic oscillator basis as for the ERM calculations of Figs. 13–18, and the parameters  $s_c$  of Eq. (3.35) were chosen equal to zero so that the  $X$  matrix is identical with the  $K$  matrix of Sec. II.B.4. The  $X$ -matrix calculations do not depend on the channel radii. Comparison with Figs. 13 and 14 shows that the methods  $X1$  and  $X2$  converge faster than the  $R$ -matrix calculations even with the optical potential included and that there is no problem with false resonances. On the other hand, for reasons which are not immediately apparent, the  $XL$  method does poorly. It was found that false resonances appear and convergence is poor near narrow resonances or near the threshold cusp in elastic cross sections.

In the calculations of Philpott (1976), both harmonic-oscillator eigenfunctions and energy-dependent wave functions obtained from the solution of the Schrödinger equation for an auxiliary potential were considered as basis states. The auxiliary potentials were taken to be the channel potentials  $V_{11}$  and  $V_{22}$ , so that the residual in-



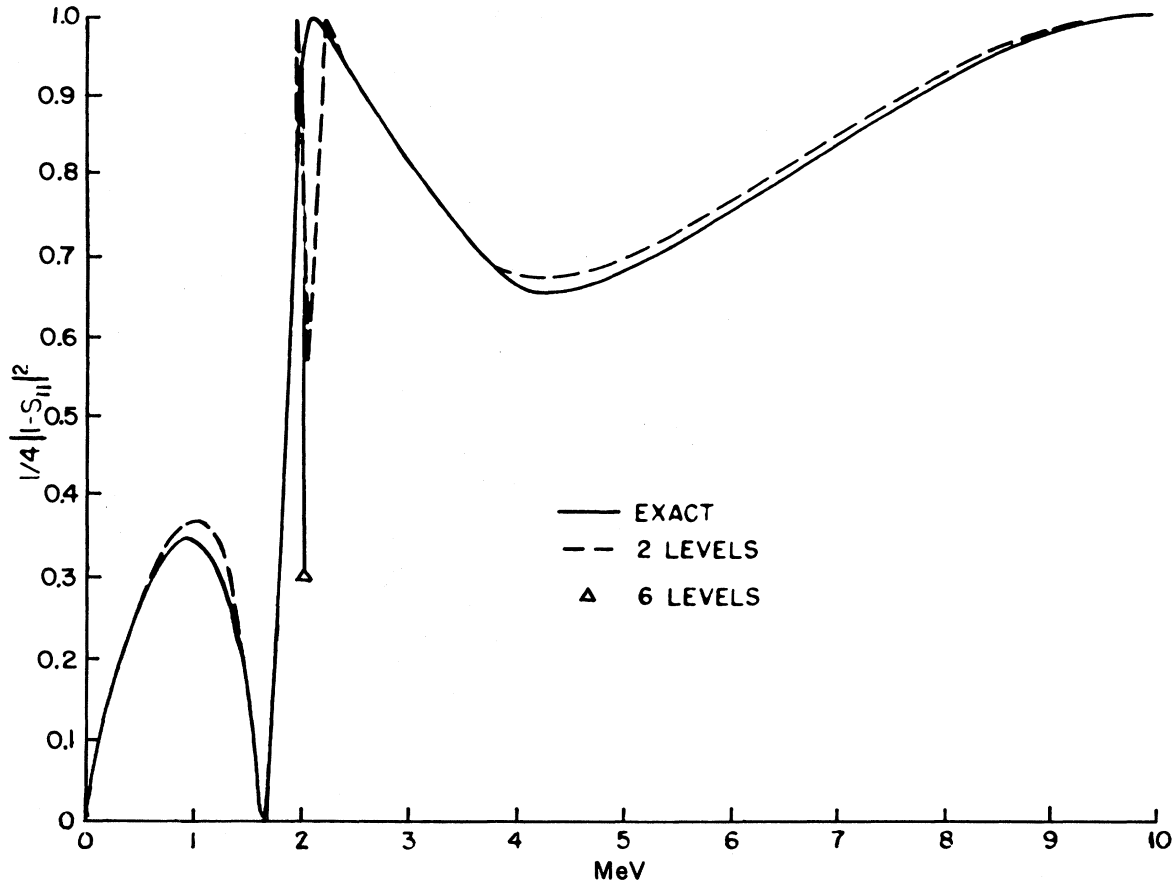


FIG. 11.  $2mE(4\pi\hbar^2)^{-1} \times$  elastic scattering cross section for the model parameters of Table II,  $a_1=a_2=6.0$  fm, and  $a'_1=a'_2=8.0$  fm. Shown are the exact result and ERM calculations for two levels (one level/channel) and six levels (three levels/channel) in the  $R$ -matrix expansion (from Garside and Tobocman, 1969).

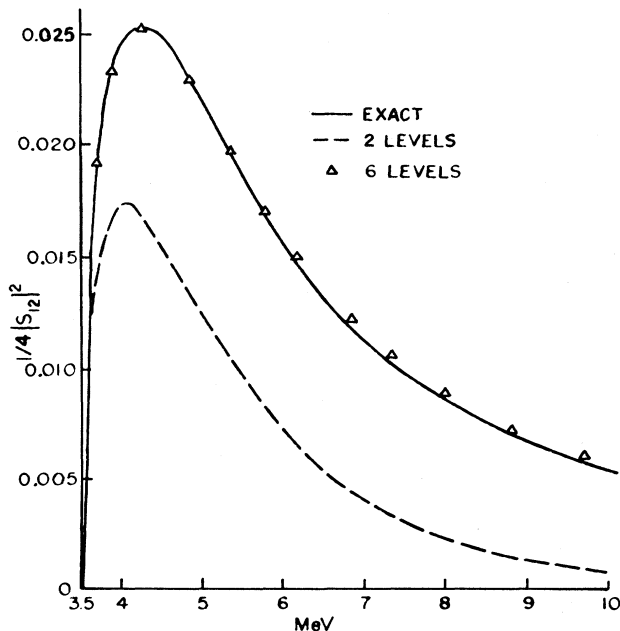


FIG. 12.  $2mE(4\pi\hbar^2)^{-1} \times$  inelastic scattering cross section for the model parameters of Table II,  $a_1=a_2=6.0$  fm and  $a'_1=a'_2=8.0$  fm (see Fig. 11 caption for explanation of curves) (from Garside and Tobocman, 1969).

teraction was the coupling potential  $V_{12}$ . The energy-dependent functions were defined to have radial wave functions satisfying the following equations:

$$(T_r + V_{ii} - E + Q\delta_{i2})v_i(r) = 0 \quad (8.12)$$

and

$$(T_r + V_{ii} - E + Q\delta_{i2})w_i(r) + \beta_i V_{ii}v_i(r) = 0, \quad (8.13)$$

where  $T_r$  is the radial kinetic energy operator. For open channels, these functions satisfy the following relations at large radii:

$$v_i(r) = \sin(k_i r + \bar{\delta}_i) \quad (8.14)$$

and

$$w_i(r) = \cos(k_i r + \bar{\delta}_i), \quad (8.15)$$

where

$$k_i^2 = 2m\hbar^{-2}(E - Q\delta_{i2}). \quad (8.16)$$

The boundary constraint on  $w_i(r)$  serves to determine the constant factor  $\beta_i$  of the term involving  $v_i(r)$  in Eq. (8.13), which ensures the linear independence of  $v_i$  and  $w_i$ . Thus for each open channel the functions  $v_i$  and  $w_i$  provide two energy-dependent basis functions which are ca-

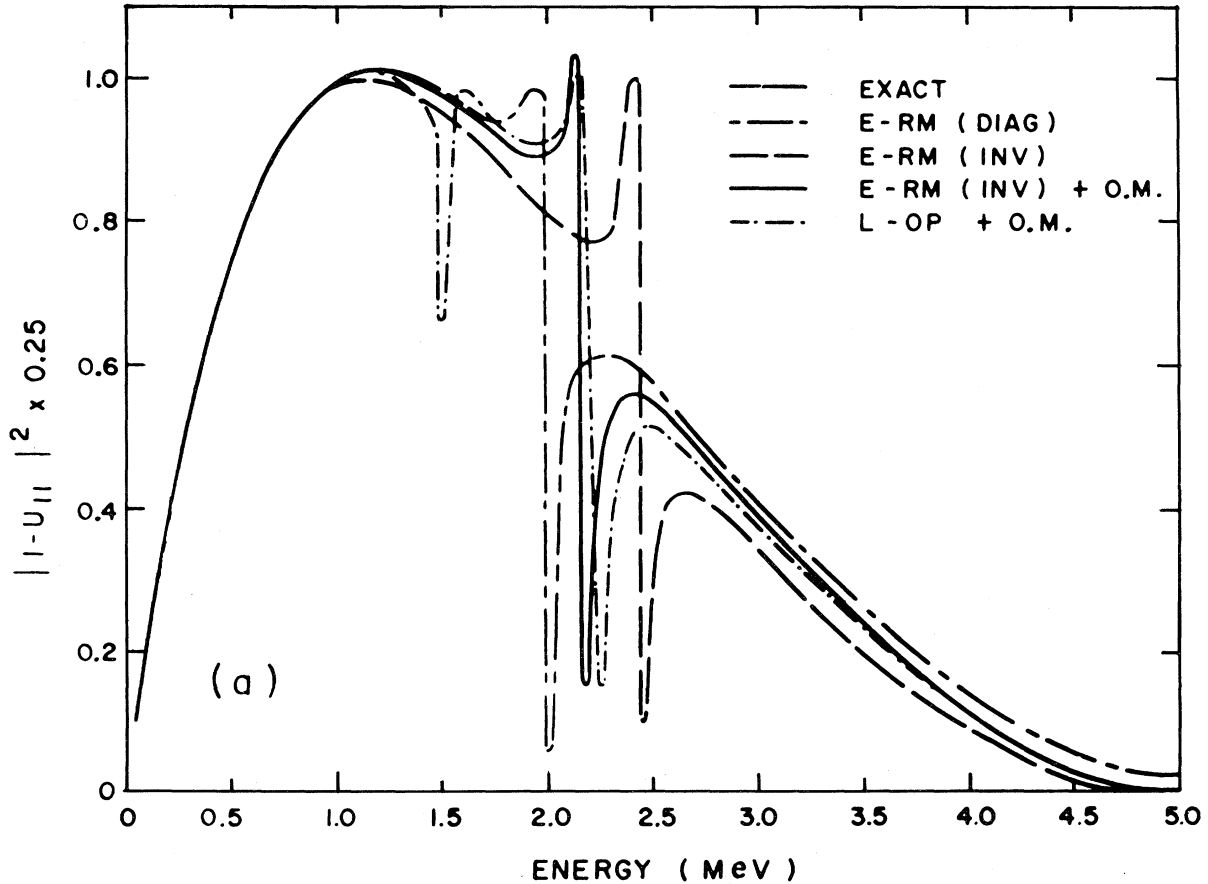


FIG. 13.  $2mE(4\pi\hbar^2)^{-1} \times$  elastic scattering cross section for ten-level (five levels/channel)  $R$ -matrix calculations for the model parameters of Table II. The following methods are compared with the exact result: ERM with diagonalization, ERM with inversion, ERM with inversion plus optical model, and  $\mathcal{L}$  operator plus optical model. These curves are identified by  $E$ -RM(DIAG),  $E$ -RM(INV),  $E$ -RM(INV) + O.M., and  $L$ -OP + O.M., respectively. Each method employed channel radii of 7.0 fm and  $B_c=0$  for the  $\mathcal{L}$ -operator result (from Schmittroth and Tobocman, 1971).

pable of describing all possible asymptotic forms of the desired physical solution in that channel.

If channel 2 is closed, the asymptotic dependence is described by a single energy-dependent function, which is built upon the function  $w_2(r)$ , satisfying the asymptotic form for large radii:

$$w_2(r) = e^{-\kappa r}, \quad (8.17)$$

where

$$\kappa^2 = 2m\hbar^{-2}(Q - E). \quad (8.18)$$

When no auxiliary energy-dependent functions were employed, it was found that using four oscillator functions/channel for the model parameters of Table II and  $a_1 = a_2 = 6.0$  fm already gives qualitative agreement with the exact solution (see Figs. 21–24). Complete convergence (not shown) was obtained for both eight and ten oscillator functions/channel.

When the energy-dependent channel functions were introduced, complete convergence was achieved in the “intermediate-coupling” case with no additional oscillator functions. In the “strong-coupling” case, the same result

was achieved, using two additional oscillator functions.

Figures 21–24 also show results when the matrix elements of the residual interaction are treated more approximately, by using a smaller basis set ( $\bar{N}$ /channel) of harmonic oscillator functions, than the remainder of the operator  $H-E$  (eight oscillator functions/channel). The curves illustrate the convergence of this method as the number of contributing matrix elements of the residual interaction is increased. It is seen that excellent agreement with the exact result is obtained in all cases for  $\bar{N}=3$ . Complete convergence was found for  $\bar{N}=4$ .

The resonance near 2.2 MeV in the intermediate-coupling case (Fig. 21) is associated with a  $3s$  quasibound state in channel 2. Thus it is necessary to include this state (i.e.,  $\bar{N}=3$ ) before convergence can be expected. In general, it is essential to include as many oscillator basis functions as are necessary to account for the “structure” problem associated with the internal region. The additional auxiliary energy-dependent functions are sufficient to describe the “reaction” problem in each of the two-channel regions, which otherwise would require a comparatively large number of higher oscillator functions. In

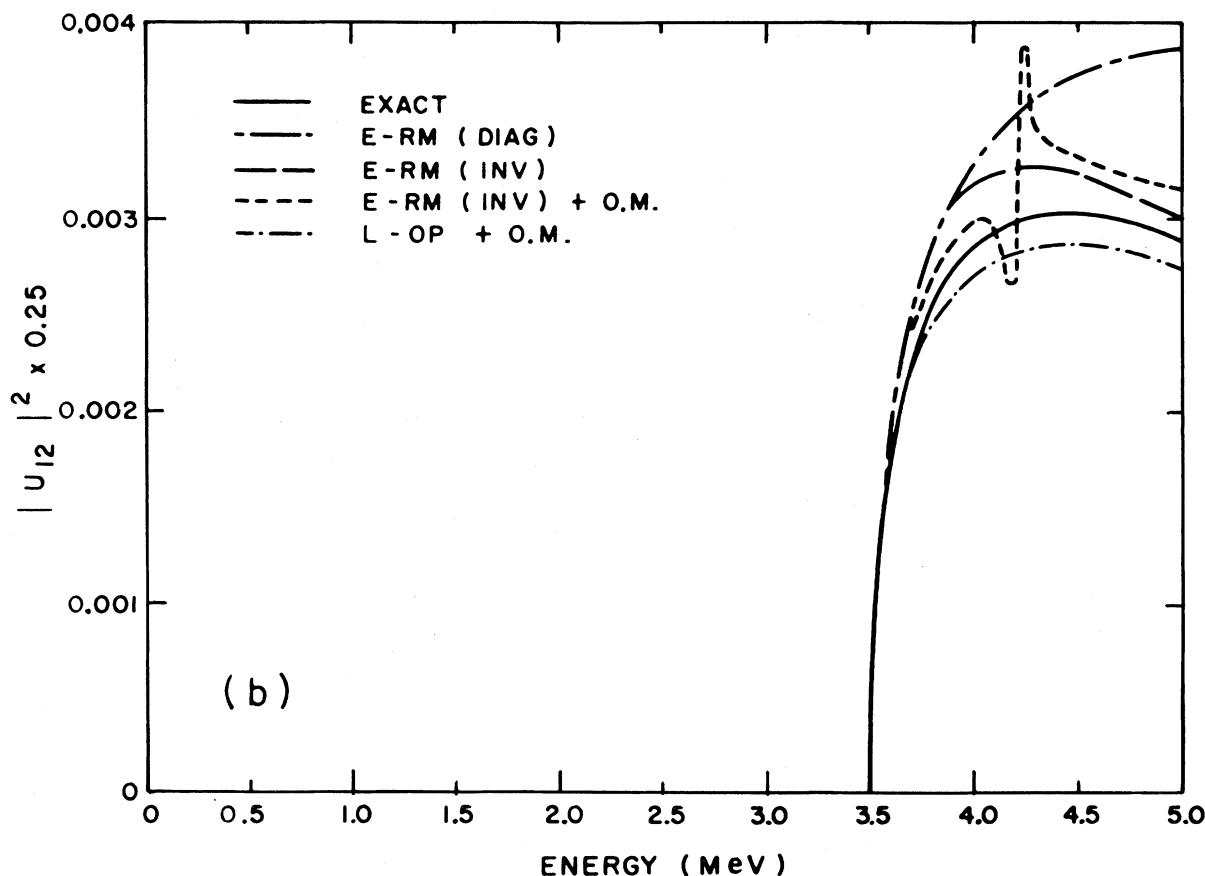


FIG. 14.  $2mE(4\pi\hbar^2)^{-1} \times$  inelastic scattering cross section for ten-level (five levels/channel)  $R$ -matrix calculations for the model parameters of Table II (see Fig. 13 caption for explanation of curves) (from Schmittroth and Tobocman, 1971).

the latter case, the actual number depends rather critically upon the channel radii employed. The use of the auxiliary functions causes the results to be essentially independent of the channel radii.

This hybrid technique of Philpott is analogous to the use of localized auxiliary sine functions by Nordholm and Bacskay (1978) in their finite-element method as discussed in Sec. IV.E. The method (like the SRM approach) is noniterative and requires significantly fewer matrix elements involving the residual interaction than the corresponding SRM calculation. However, the basis states are no longer completely energy independent. There is no evidence in Figs. 21–24 of any spurious resonances similar to those found by Garside and Tobocman (1969).

##### 5. Natural boundary condition methods

The Barrett-Delsanto (BD) (see Sec. V.C) and the iterative  $R$ -matrix (see Sec. V.D) methods have been applied to the coupled square-well problem by Ahmad, Barrett, and Robson (1976b). Both NBC methods produce identical results, which are presented in Table III and Figs. 7–10 for the parameters of Table II. The basis states were tak-

en to be eigenfunctions of the channel Hamiltonians  $T + V_{ii}(r)$ . For the intermediate-coupling (Table III and Fig. 7) and strong-coupling (Figs. 8 and 9) cases, four and six basis states/channel were used, respectively. In these cases, the channel radii were 7.5 fm. It was found that the convergence of the NBC methods is considerably better than either the SRM or BCRM methods for the strong-coupling case. For the weak-coupling example (Fig. 10) with channel radii of 6.0 fm, one level/channel produced a result indistinguishable from the exact one.

The energy correction to the BD method (see Sec. V.C.1) was also used, resulting in a significant improvement in the corresponding calculations with little associated increase in computing time. For the intermediate-coupling case, four levels/channel plus the energy correction with eight additional higher basis states/channel produced accurate results, and for the strong-coupling case, six levels/channel plus six additional levels/channel treated in the energy correction were sufficient.

##### B. Neutron elastic scattering from $^{12}\text{C}$

The elastic scattering of neutrons from the  $^{12}\text{C}$  nucleus below the inelastic scattering threshold has been often

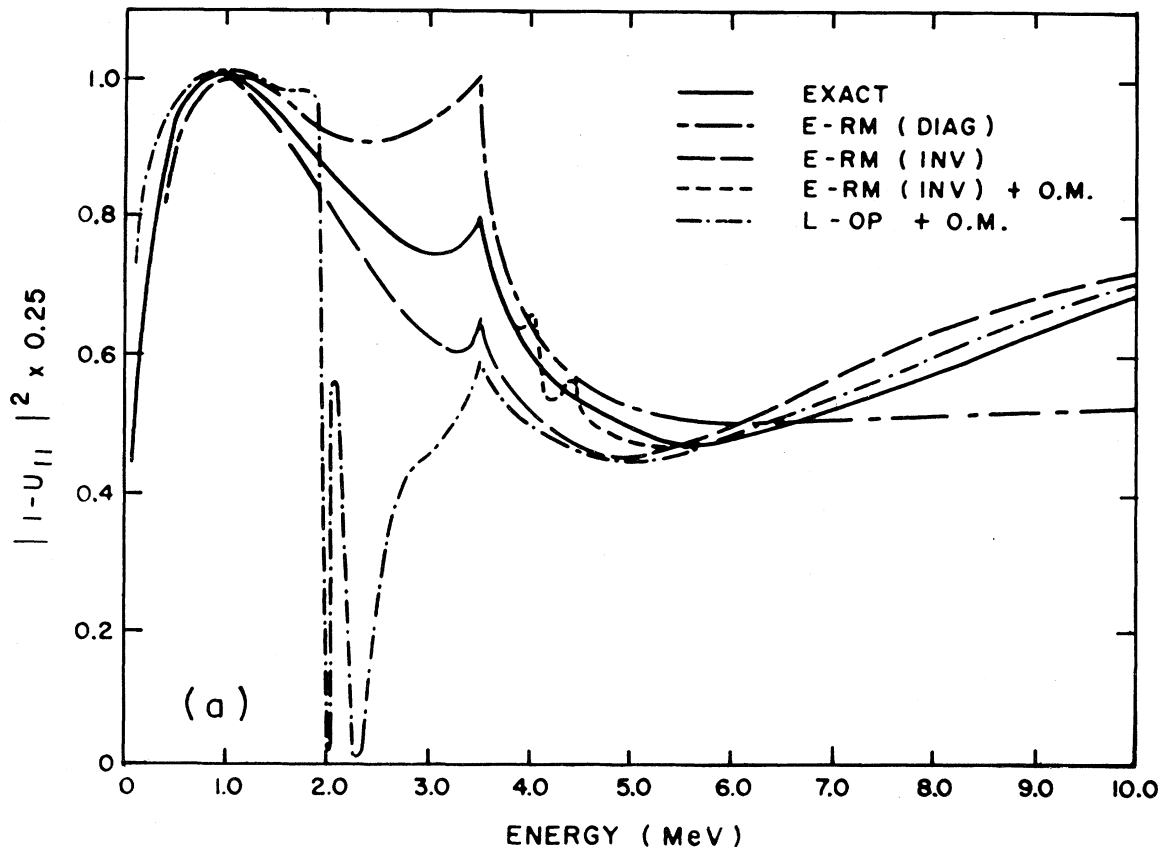


FIG. 15.  $2mE(4\pi\hbar^2)^{-1} \times$  elastic scattering cross section for ten-level (five levels/channel)  $R$ -matrix calculations for the model parameters of Table II (see Fig. 13 caption for explanation of curves) (from Schmittroth and Tobocman, 1971).

used as a test of reaction theories. The semimagic nature of  $^{12}\text{C}$  results in a relatively large level spacing in the  $^{13}\text{C}$  compound nucleus. As a consequence, a good theoretical description of the experimental low-energy elastic scattering cross section is possible when only a few reaction channels are treated explicitly. A number of coupled-channels calculations based on either the shell model or various collective models have been carried out. In some cases, the same model has been employed in several independent calculations; we shall examine some of these for comparative purposes. First, however, we shall consider a parametrized multilevel  $R$ -matrix fit to the experimental data.

### 1. Multilevel $R$ -matrix fit

Westin and Adams (1971) have carried out a two-level  $R$ -matrix fit to the  $^{12}\text{C}(n,n)^{12}\text{C}$  total elastic scattering cross section in the energy range 2.5–4.5 MeV (lab.). Their aim was to determine the resonance energies and associated reduced widths of the  $d_{3/2}$  double resonance which exists in this energy region.

The two-level single-channel approximation to Eq. (4.33), which may be written

$$R = R_0 + \gamma_1^2(\mathcal{E}_1 - E)^{-1} + \gamma_2^2(\mathcal{E}_2 - E)^{-1}, \quad (8.19)$$

where  $\mathcal{E}_1$  and  $\mathcal{E}_2$  are the resonance energies,  $\gamma_1^2$  and  $\gamma_2^2$  are the reduced widths, and  $R_0$  is a background term representing the contribution from all the other distant levels, was used to fit the data as compiled by Stehn *et al.* (1964). A preliminary potential scattering calculation with a Woods-Saxon potential was performed to determine an optimum choice for the channel radius  $a$  and the boundary condition parameter  $B$  such that the energy dependence of the background term  $R_0$  was minimized. The term  $R_0$  was not treated as an arbitrary parameter in the  $R$ -matrix fitting procedure; instead the value obtained from the potential scattering calculation was employed.

The calculation immediately revealed a major difficulty associated with this method of resonance analysis. Figures 25 and 26 show two equally good fits to the data using quite different resonance parameters. These are listed in lines 1 and 2 of Table IV, respectively. In using a multilevel  $R$ -matrix fitting procedure to determine the reduced widths, one can obtain significantly different results, depending on the arbitrarily chosen parameters  $a$  and  $B$ . These differences propagate through to the spectroscopic factors associated with the resonances and hence to the physical interpretation of the resonances.

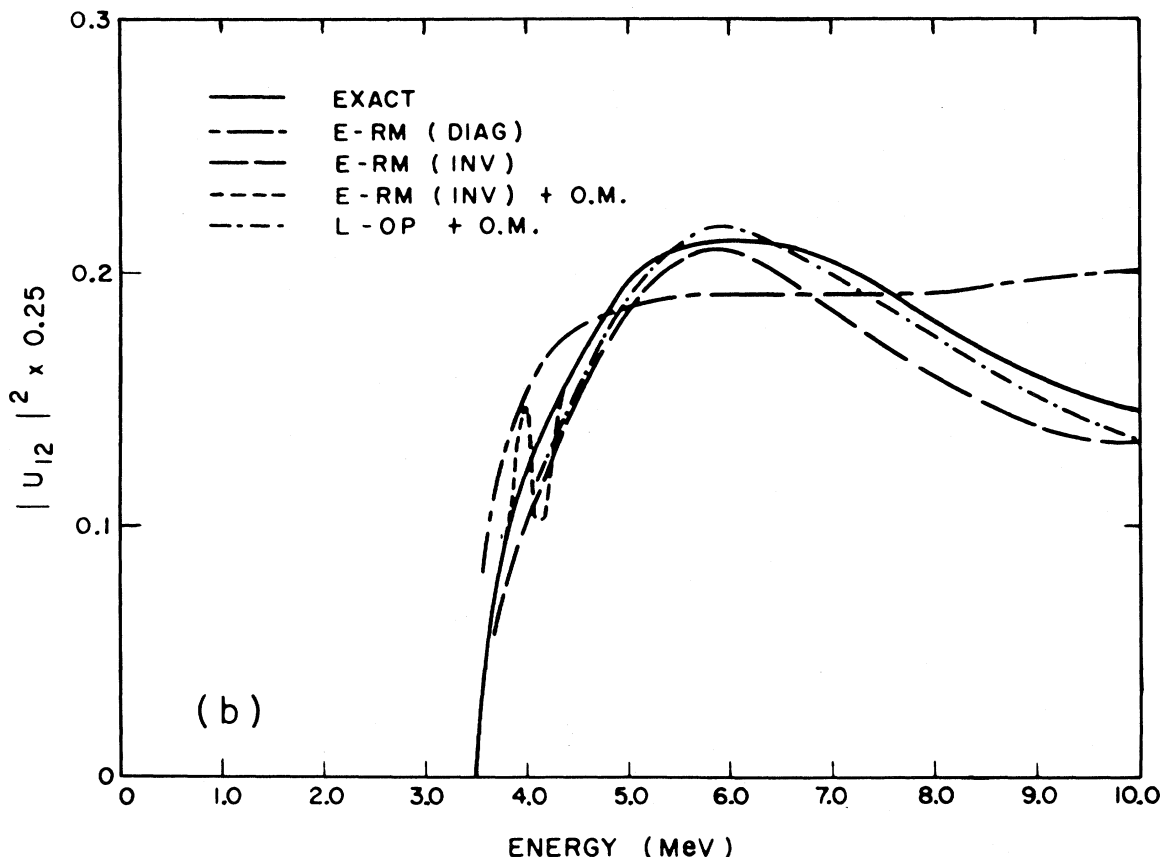


FIG. 16.  $2mE(4\pi\hbar^2)^{-1} \times$  inelastic scattering cross section for ten-level (five levels/channel)  $R$ -matrix calculations for the model parameters of Table II (see Fig. 13 caption for explanation of curves) (from Schmittroth and Tobocman, 1971).

In a later paper, Westin and Adams (1973) investigated the effect of using the extended  $R$ -matrix (ERM) formalism for two-level fits to the elastic scattering cross section. This approach allows one to employ different boundary condition parameters for each level. In this case, however, it is more difficult to calculate the background term  $R_0$ , and the method results in a larger number of arbitrary parameters for only a slight improvement in the fit to the data. A typical set of results is presented in Fig. 27 for the parameters listed in lines 3 and 4 of Table IV.

The fact that the energies and reduced widths of levels in the  $R$ -matrix theory are dependent on arbitrarily chosen channel radii and boundary condition parameters is well known. However, the calculated cross sections are independent of these parameters provided that the series expansion for the  $R$  matrix [Eq. (4.33)] has converged adequately. An investigation by Barker (1972) has shown, even when only a small number of terms is retained in this expansion, that the cross sections can be made independent of the choice of boundary condition parameters. It is not necessary, therefore, to treat these parameters as adjustable. However, if the values of the resonance energies and reduced widths obtained from a multilevel  $R$ -matrix fit are to be compared with values calculated from some nuclear model, the boundary condition param-

eters should be chosen to have the most appropriate values. A common method in the single-channel case is to set the boundary condition parameter equal to the shift function [as defined in Eq. (4.4)] calculated at the average energy of the resonances.

## 2. Standard calculable $R$ -matrix method

An early  $R$ -matrix calculation of the scattering of nucleons from  $^{12}\text{C}$  was carried out by Buttle (1967). The model employed was a collective model of Buck (1963) in which the full Hamiltonian is

$$H = H_I + T + V_{\text{diag}} + V_{\text{coupl}}, \quad (8.20)$$

where  $H_I$  is the internal part of the Hamiltonian giving rise to the different target states and projectile states occurring in channel  $|c\rangle$  and  $T$  is the relative kinetic energy. The interaction consists of a part,  $V_{\text{diag}}$ , which is diagonal in channel space and a part,  $V_{\text{coupl}}$ , which is not. For the diagonal part of the potential, a real Woods-Saxon potential plus a spin-orbit term of Thomas form was used, and the coupling potential was described by a derivative Woods-Saxon interaction with a coupling parameter  $\beta$ , which is a measure of the permanent quadrupole deformation in the rotational model of Buck.

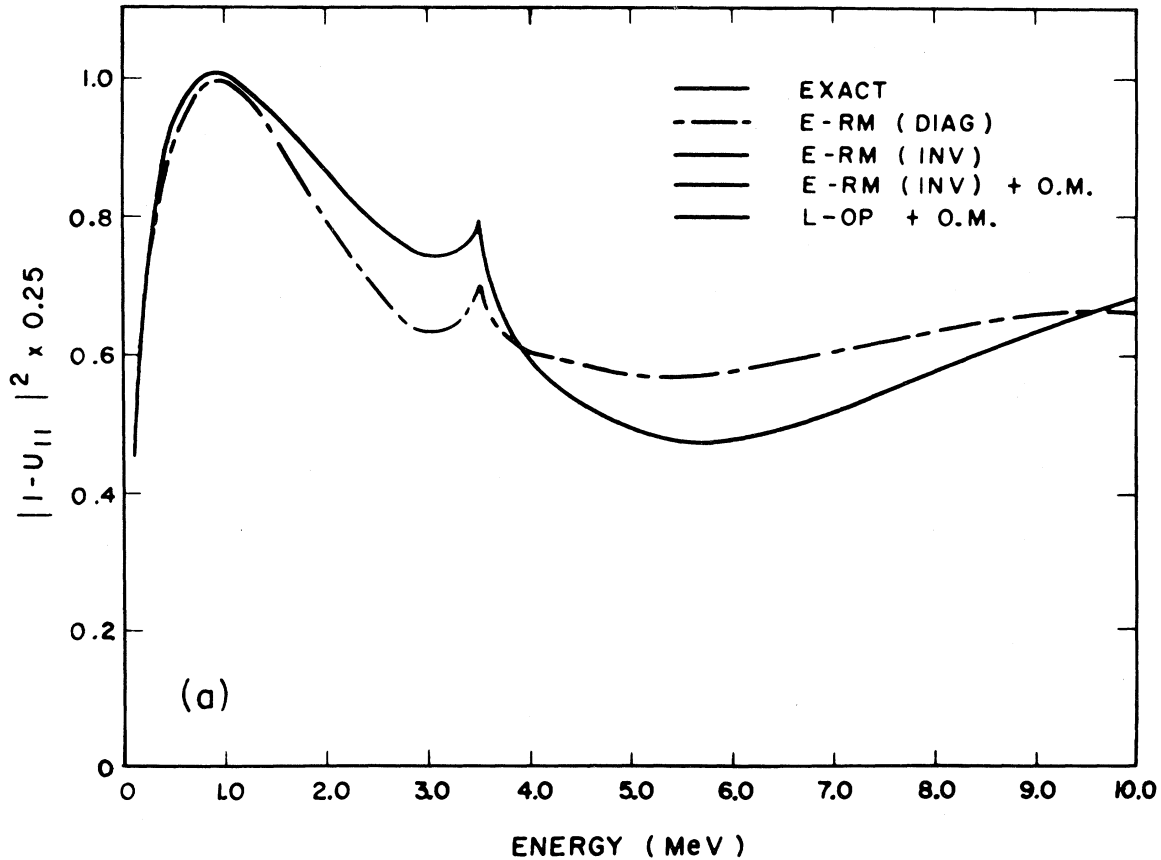


FIG. 17.  $2mE(4\pi\hbar^2)^{-1} \times$  elastic scattering cross section for 20-level (ten levels/channel)  $R$ -matrix calculations for the model parameters of Table II (see Fig. 13 caption for explanation of curves) (from Schmittroth and Tobocman, 1971).

Buttle investigated three levels of approximation in the  $R$ -matrix method and compared his results with the corresponding coupled-channels calculations performed, using the program of Buck. In the first method (method I), the basis states were taken to be eigenstates of that part of the Hamiltonian  $H$  which is diagonal in channel space, and distant levels were ignored. This is the standard calculable  $R$ -matrix method (SRM) described in Sec. IV.C. In the second approximation (method II), the effect of distant levels is partially included, using the Buttle correction (BCRM) of Sec. IV.D. In method III, distant levels are taken into account by using distorted waves in the entrance and exit channels within the  $X$ -matrix formalism of Sec. III.D. In this case, the optical potential employed to describe the background was taken to be  $V_{\text{diag}}$  so that the residual interaction was simply the coupling potential  $V_{\text{coupl}}$ . The second term on the right-hand side of either Eq. (3.41) or Eq. (3.42) gives rise to the conventional distorted-wave Born approximation (DWBA) to the  $T$  matrix [see also Eq. (6.80)]. The values of the parameters  $a_\alpha$  and  $B_c$  were fixed at  $a_\alpha = 5.4$  fm and  $B_c = 0$ . Little effect was observed by varying them. No attempt was made to compare the results of any of the calculations with the experimental data.

Figure 28 shows the results obtained by Buttle for the

$^{12}\text{C}(n,n)^{12}\text{C}$  differential cross sections compared with the "exact" coupled-channels calculation and the DWBA result in a nonresonant energy region. The inelastic scattering is to the  $2^+$  first excited state in  $^{12}\text{C}$  at 4.433 MeV. In the model, the target states were limited to the  $0^+$  ground state and this  $2^+$  state. Three levels/channel were used in the SRM method. It is seen that method I gives qualitative agreement with the "exact" results but tends to overestimate the elastic scattering forward peak. Inclusion of the Buttle correction (method II) greatly improves the results. Method III does not represent any improvement over the BCRM method. For the strong-coupling case of Fig. 28, the DWBA is not a good first approximation and method III gives poorer results than method II. Furthermore, it was found that method III sometimes gives rise to spurious resonances and therefore is unreliable. Figure 29 shows some corresponding results for the  $^{12}\text{C}(p,p')^{12}\text{C}$  reaction in a resonant region. A spurious resonance is clearly visible near 6.25 MeV.

### 3. Extended $R$ -matrix method

The extended (or generalized)  $R$ -matrix (ERM) method has been described in Sec. IV.F. It was first applied to the elastic scattering of neutrons at low bombarding ener-

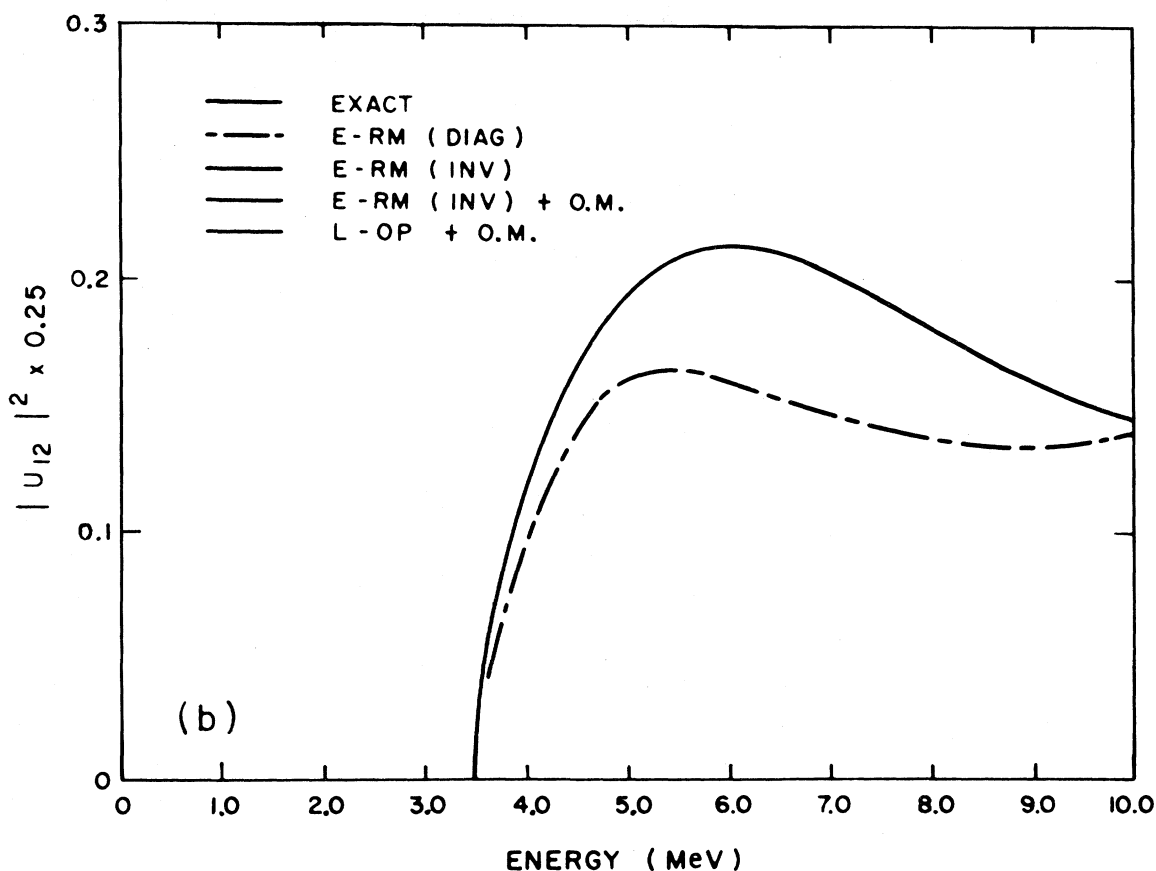


FIG. 18.  $2mE(4\pi\hbar^2)^{-1} \times$  inelastic scattering cross section for 20-level (ten levels/channel)  $R$ -matrix calculations for the model parameters of Table II (see Fig. 13 caption for explanation of curves) (from Schmittroth and Tobocman, 1971).

gies ( $< 4.4$  MeV) by Purcell (1969b). Purcell employed a model for the positive parity states of  $^{13}\text{C}$ , which consisted of a neutron weakly coupled to a deformed axially symmetric  $^{12}\text{C}$  core. The basis states for the construction of the  $R$ -matrix comprised the simple rotator states for the  $^{12}\text{C}$  target (limited to the  $0^+$  ground state and  $2^+$  4.433-MeV first excited state) coupled to the single-particle neutron states assumed to be moving in a spherically symmetrical harmonic-oscillator potential. The use of these harmonic-oscillator states results in a nonorthogonal basis set, necessitating the application of the ERM formalism developed by Tobocman and co-workers (Tobocman and Nagarajan, 1965; Nagarajan, Shah, and Tobocman, 1965; Garside and Tobocman, 1968, 1969).

The results obtained by Purcell for a suitably chosen set of model parameters are shown in Fig. 30. Here the calculated total elastic scattering cross section for the reaction  $^{12}\text{C}(n,n)^{12}\text{C}$ , using four levels/channel, is presented and compared with the experimental data. The convergence of the method is illustrated in Fig. 31, where the cross section for the  $d_{3/2}$  partial wave is plotted as a function of the number of basis states/channel ( $N_r$ ). Little change is observed as  $N_r$  is increased above four, indicating that the procedure has converged satisfactorily. The channel radius was set at 5.7 fm.

A similar calculation to that of Purcell was performed by Robson and van Meegen (1972b), in which both the  $R$ -matrix theory and the Feshbach (1958, 1962) unified theory were studied. In this case, however, the harmonic-oscillator potential used by Purcell for the neutron single-particle well is replaced by a more realistic Woods-Saxon potential. The results for this calculation are shown in Fig. 32 for two different values of the channel radii.

In the calculations both of Purcell and of Robson and van Meegen, the calculated width of the  $d_{3/2}$  resonance near 3.3 MeV is too small. This discrepancy is attributed by Robson and van Meegen to the neglect of the distant levels, which is a consequence of the severe truncation of basis states and to the inadequacy of the model Hamiltonian. Robson and van Meegen used up to two levels/channel.

To remove any ambiguity created by the inadequacy of the physical model employed for the  $^{13}\text{C}$  system, Philpott and George (1974) have performed an ERM-type calculation using a collective model due to Reynolds *et al.* (1968). The latter authors used this model in a coupled-channels calculation to obtain a good fit to the low-energy elastic scattering  $^{12}\text{C}(n,n)^{12}\text{C}$  data. An  $R$ -matrix—or, for that matter, any reaction theory—calculation should give

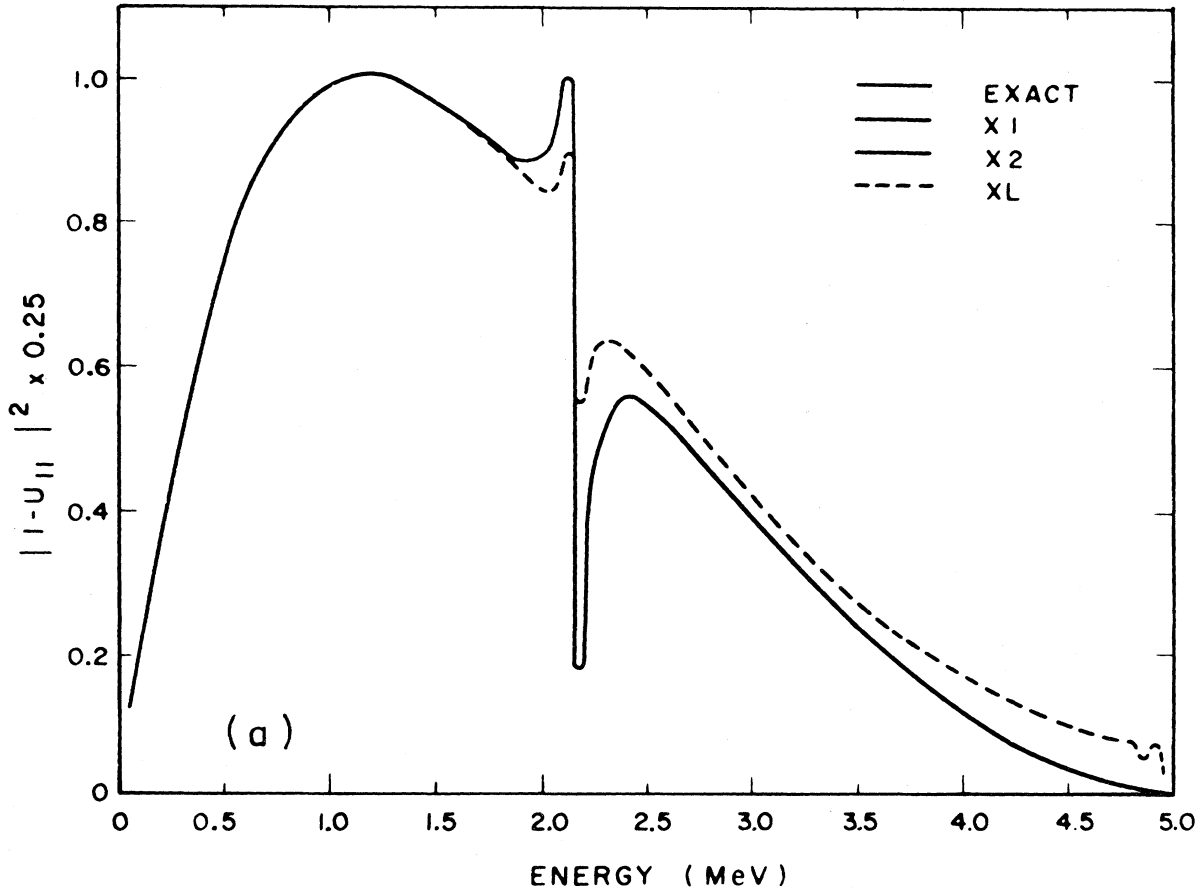


FIG. 19.  $2mE(4\pi\hbar^2)^{-1} \times$  elastic scattering cross section for six-level (three levels/channel)  $X$ -matrix calculations for the model parameters of Table II. The following methods are used to obtain the Green's function for the  $X$  matrix: the Hufner-Lemmer method [Eq. (8.7)], the iterated Hufner-Lemmer method [Eq. (8.8)], and the  $\mathcal{L}$ -operator method [Eq. (8.10)]. The results of these methods are denoted by  $X1$ ,  $X2$ , and  $XL$ , respectively. For the  $\mathcal{L}$ -operator method, the  $B_c$  were chosen compatible with  $s_c=0$  boundary conditions (from Schmittroth and Tobocman, 1971).

identical results to the corresponding coupled-channels calculation, if identical model parameters are used in both cases. The model of Reynolds *et al.* is similar to the collective model employed by Robson and van Meegen (1972b), except that the internal  $^{12}\text{C}$  excitations are represented by the surface oscillations of a liquid drop instead of the rotation of a deformed core. The single neutron moves in a Woods-Saxon potential.

The results obtained by Philpott and George are shown in Fig. 33 and are essentially identical to those of the coupled-channels calculation. Philpott and George employed eight harmonic-oscillator functions/channel for the single-neutron basis states, and the channel radii were 7.0 fm. The convergence of the method as the number of basis states is increased is illustrated in Fig. 34. It is seen that in this case eight basis functions/channel are required for satisfactory convergence. In addition, it was found that the rate of convergence depends on the choice of the channel radius, with the best choice being such that the internal and external logarithmic derivatives of the wave functions in each channel are as nearly matched as

possible.

In some cases, it was found that the convergence of the method is initially quite rapid but does not last beyond a certain finite number of functions. In this mode, the method is only semiconvergent. This semiconvergence arises in the work of Philpott and George for two reasons. First, for simplicity, the radial integrals involving the nuclear Woods-Saxon potential were not terminated at the channel radius and, second, the nuclear potential was omitted (as is usual) from the "asymptotic" external wave function. Apparently, the higher-order harmonic-oscillator basis functions penetrate to larger radii where the tail of the nuclear potential, although very small, is not sufficiently negligible and a significant error may be introduced into the calculation. Thus to avoid the semiconvergence problem, special care is necessary in dealing with the tail of the interaction. However, Philpott and George conclude that the ERM method, despite its ultimate divergence as the number of harmonic-oscillator basis states is increased, is a viable and accurate tool for the calculation of nuclear reaction cross sections.



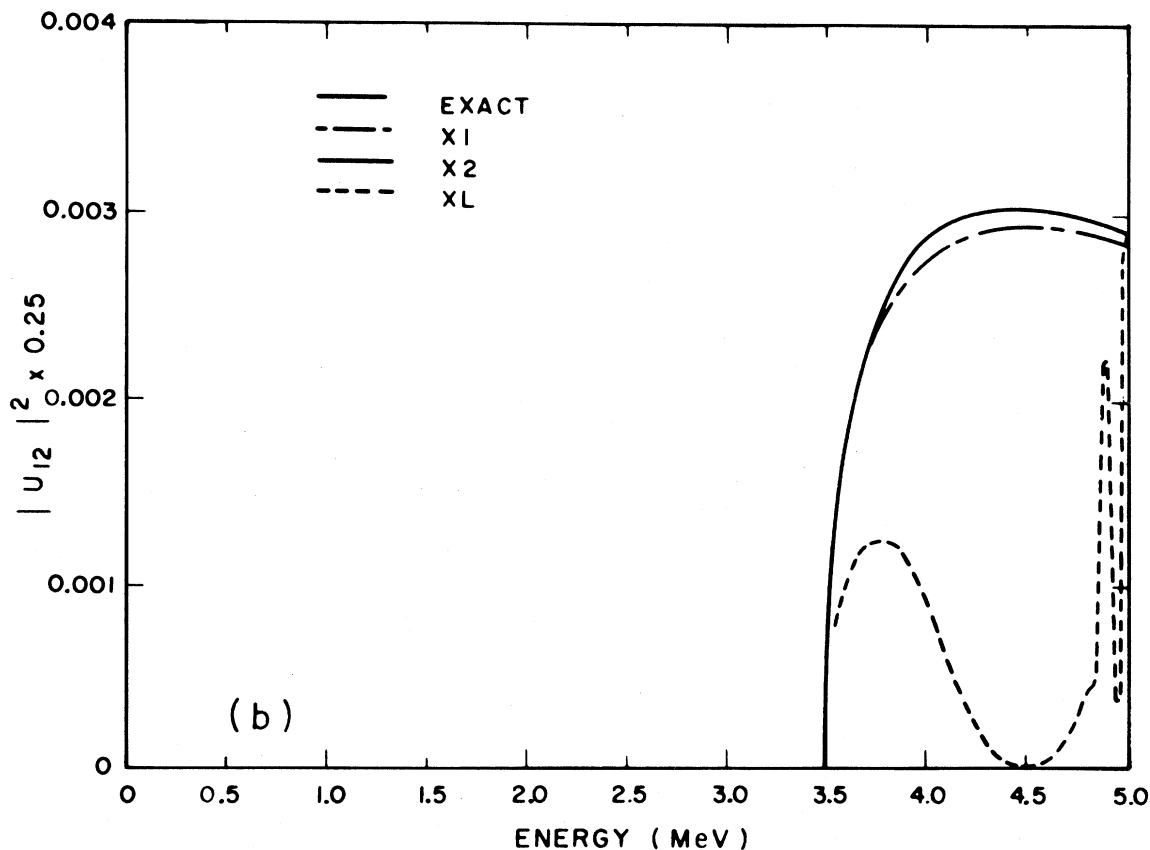


FIG. 20.  $2mE(4\pi\hbar^2)^{-1} \times$  inelastic scattering cross section for six-level (three levels/channel)  $X$ -matrix calculations for the model parameters of Table II (see Fig. 19 caption for explanation of curves) (from Schmittroth and Tobocman, 1971).

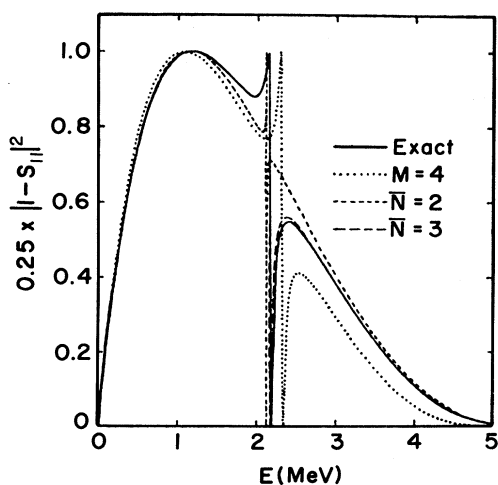


FIG. 21.  $2mE(4\pi\hbar^2)^{-1} \times$  elastic scattering cross section for the model parameters of Table II. Various approximations are compared with the exact result. The  $M=4$  approximation corresponds to the use of exact matrix elements within a basis which contains four oscillator functions/channel. Channel convergence is not achieved. The  $\bar{N}=2$  and  $3$  approximations correspond to the use of a smaller basis set ( $\bar{N}$ /channel) of oscillator functions for the matrix elements of the residual interaction within a basis large enough (eight levels/channel) to assure convergence when exact matrix elements are introduced (from Philpott, 1976).

The three calculations described so far in this section are similar in that a collective model of the  $^{13}\text{C}$  system was used. Other workers (Robson and van Megen, 1972a; Mori, 1973) have employed a shell model to describe  $^{13}\text{C}$ , which allows the antisymmetrization of the incoming neutron with the  $^{12}\text{C}$  to be properly included. The inclusion of such exchange effects is relatively simple for

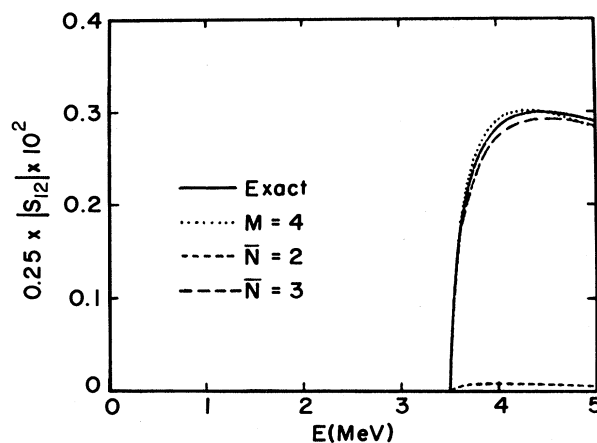


FIG. 22.  $200mE(4\pi\hbar^2)^{-1} \times$  inelastic scattering cross section for the model parameters of Table II (see Fig. 21 caption for explanation of curves) (from Philpott, 1976).

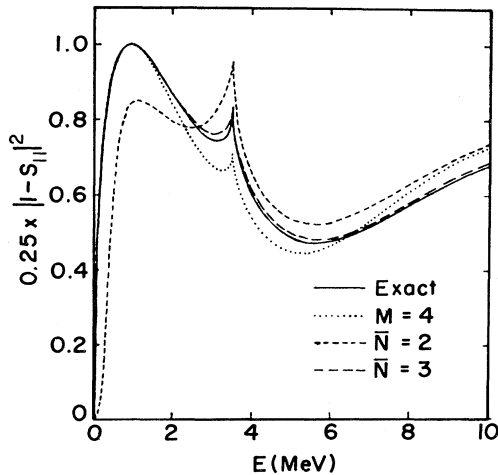


FIG. 23.  $2mE(4\pi\hbar^2)^{-1} \times$  elastic scattering cross section for the model parameters of Table II (see Fig. 21 caption for explanation of curves) (from Philpott, 1976).

reaction theories using the  $R$ -matrix approach in comparison with coupled-channels calculations and represents a major attraction of the  $R$ -matrix method.

Figure 35 shows some typical results for the  $^{12}\text{C}(n,n)^{12}\text{C}$  total cross section calculated by Mori (1973), using a two-body interaction (BJ) due to Blatt and Jackson (1949), which are compared with both the experimental data and calculations employing matrix elements obtained with a macroscopic phenomenological form factor for quadrupole deformation (Mori and Terasawa, 1972). The calculations included antisymmetrization either exactly (DE) or by using renormalized matrix elements (DN). It is seen that the resonance widths of the higher-energy resonances are too small compared with the experimental values even when the channel radius is reduced to 5.0 fm. This discrepancy is probably attributable to the small number of levels (four) per channel used in the calculations. The same comment also applies to the earlier

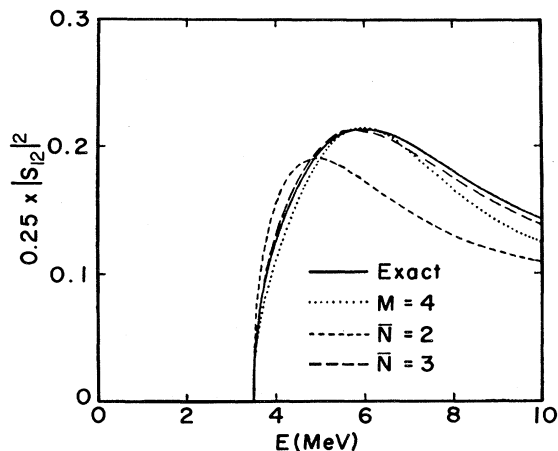


FIG. 24.  $2mE(4\pi\hbar^2)^{-1} \times$  inelastic scattering cross section for the model parameters of Table II (see Fig. 21 caption for explanation of curves) (from Philpott, 1976).

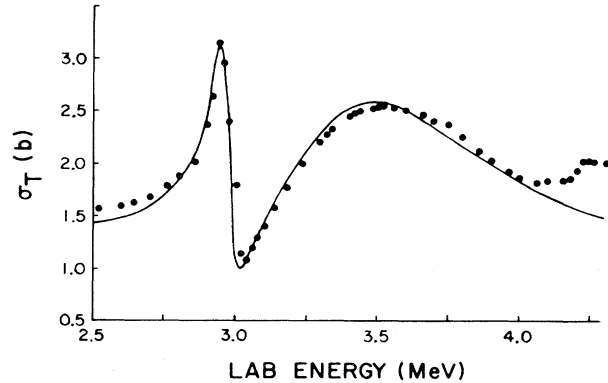


FIG. 25. A fit to the  $d_{3/2}$  double resonance in  $^{12}\text{C}(n,n)^{12}\text{C}$  using the  $R$ -matrix formulation. The dots are the experimental data from Stehn *et al.* (1964), and the solid line is a fit using the parameters in line 1 of Table IV (from Westin and Adams, 1971).

calculations of Robson and van Meegen (1972a, 1972b), in which similar results were obtained. Both sets of results are analogous to those of Philpott and George (1974) presented in Fig. 34, when only four levels/channel are employed. The resonance widths are very sensitive to the scattering wave function of the system near the channel entrance surface, and a sufficient number of harmonic-oscillator basis functions must be used to adequately represent the scattering wave function near the channel radii. On the other hand, some of the discrepancy may arise from the use of an inadequate model Hamiltonian. The calculations of Mori show that antisymmetrization effects can be important.

#### 4. Natural boundary condition methods

The weak-coupling collective model of Reynolds *et al.* (1968) has also been used by Ahmad, Barrett, and Robson

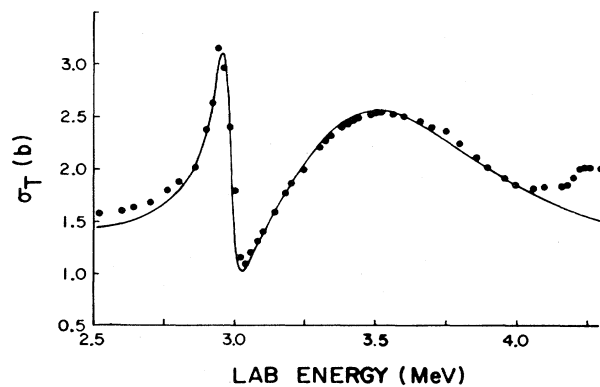


FIG. 26. A fit to the  $d_{3/2}$  double resonance in  $^{12}\text{C}(n,n)^{12}\text{C}$  using the  $R$ -matrix formulation. The dots are the experimental data from Stehn *et al.* (1964), and the solid line is a fit using the parameters in line 2 of Table IV (from Westin and Adams, 1971).

TABLE IV. Parameters for the  $d_{3/2}$  double resonance.

$a$ (fm)	$B_1$	$B_2$	$R_0$	$\mathcal{E}_1$ (MeV)	$\mathcal{E}_2$ (MeV)	$\gamma_1^2$ (keV)	$\gamma_2^2$ (keV)
5.5	-0.926	-0.926	0.21	2.95	3.50	68	460
5.5	-0.561	-0.561	0.21	2.90	3.30	180	440
5.5	-0.810	-0.810	0.0	2.95	3.50	90	593
5.5	-0.870	-0.760	0.0	2.95	3.50	78	640

(1976a) to investigate the convergence of two natural boundary condition (NBC) methods. The first of the NBC methods is essentially the Barrett and Delsanto (1974) approach (see Sec. V.C), while the second is the iterative  $R$ -matrix method discussed in Sec. V.D. A Woods-Saxon potential was employed in these calculations to generate the single-particle basis states.

The results of the two NBC methods are essentially identical and are presented in Fig. 36. Satisfactory convergence was obtained using only two levels/channel. In Fig. 37 the sum of the  $J^\pi = \frac{1}{2}^+$  and  $\frac{3}{2}^+$  contributions to the total cross section for the reaction  $^{12}\text{C}(n,n)^{12}\text{C}$  calculated by the NBC methods is compared with the corresponding result of Philpott and George (1974) obtained with the ERM theory. In the NBC methods only one level/channel was employed, while the ERM calculation used eight harmonic oscillator states/channel. A comparison of Figs. 31, 34, and 37 illustrates the very rapid convergence of the NBC methods.

Figure 38 shows a comparison of the relative convergence of the NBC and SRM methods for the  $J^\pi = \frac{3}{2}^+$  contribution to the total elastic neutron cross section of  $^{12}\text{C}$ . In this case, the channel-coupling parameter of the model of Reynolds *et al.* was increased by a factor of about 5 in order to give a more stringent test of the methods. The channel radii were set at 7.2 fm, and bound-

dary condition parameters  $B_c = 0$  were employed in the SRM calculations. The NBC methods give convergence using two levels/channel, while the SRM results, with four levels/channel, have not fully converged.

Several points emerge from consideration of the convergence properties of the NBC methods. First, the criterion for optimum convergence formulated by Philpott and George in the case of the ERM theory is automatically satisfied by the NBC basis states at each energy. In fact, the success of the iterative  $R$ -matrix method, which depends explicitly on the natural boundary condition parameters providing the best rate of convergence, implies that such boundary conditions require the minimum number of basis states for a given Hamiltonian. Both the Buttle correction to the SRM method (see Sec. IV.D) and the additional variational correction proposed by Zvijac, Heller, and Light (1975) (see Sec. VI.B) vanish automati-

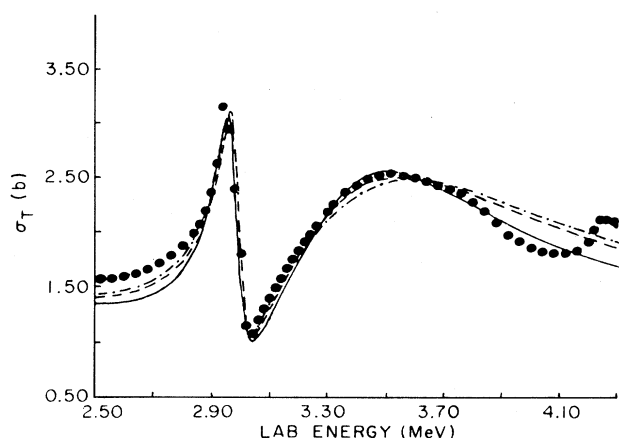


FIG. 27. Various ERM fits to the two  $\frac{3}{2}^+$  interfering levels in  $^{12}\text{C}(n,n)^{12}\text{C}$ . The dots are the experimental data from Stehn *et al.* (1964). The solid curve uses the parameters in line 1 of Table IV but with  $R_0 = 0.0$ . The dashed curve uses the parameters in line 3 of Table IV, while the dot-dashed curve is from line 4 of Table IV (from Westin and Adams, 1973).

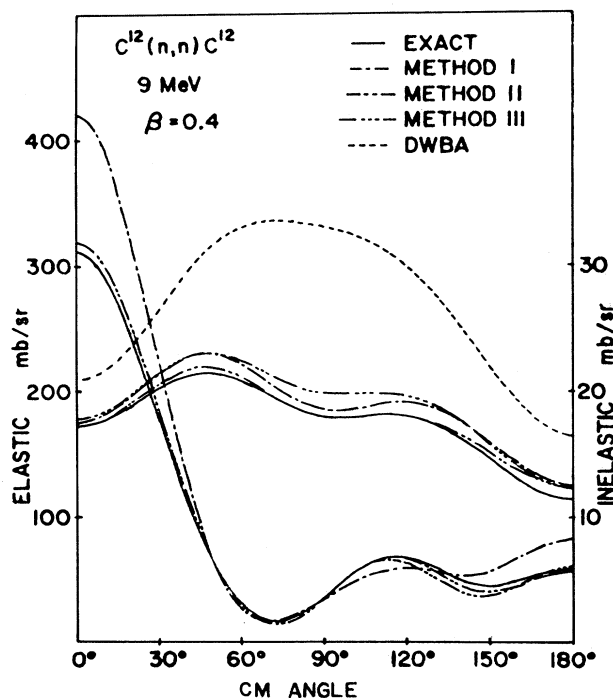


FIG. 28. Differential cross sections for  $^{12}\text{C}(n,n)^{12}\text{C}$  at 9 MeV with strong coupling ( $\beta = 0.4$ ). The solid curve is the exact result. Three levels/channel are included in the various calculations: METHOD I (SRM), METHOD II (BCRM), and METHOD III ( $X$  matrix), and the boundary conditions are  $a_a = 5.4$  fm,  $B_c = 0$ . The dashed curve is the DWBA result (from Buttle, 1967).

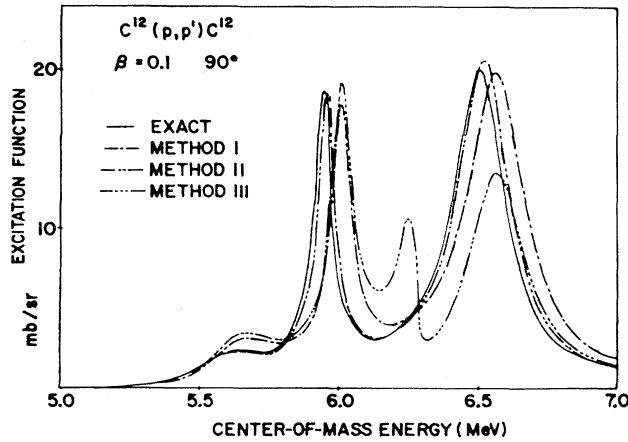


FIG. 29. Inelastic scattering  $90^\circ$  excitation functions for  $^{12}\text{C}(p,p')^{12}\text{C}$  in a region of resonances for  $\beta=0.1$  (see Fig. 28 caption for explanation of curves) (from Buttle, 1967).

cally when n.b.c. parameters are used.

In applying the NBC methods, the Barrett-Delsanto approach requires no more than four iterations to determine the n.b.c. parameters; the iterative  $R$ -matrix method also requires only a few iterations at most energies, although when  $B_c$  approaches  $\pm\infty$ , some numerical difficulties are experienced. These can be easily overcome (Ahmad, Barrett, and Robson, 1976a).

Recent application and extension of the Barrett-Delsanto approach to nuclear reaction problems has been made by Delsanto and co-workers (Delsanto and Quarati, 1976, 1978, 1979; Delsanto, Pompei, and Quarati, 1977), and Ahmad (1978, 1979) has further developed and applied the iterative  $R$ -matrix method.

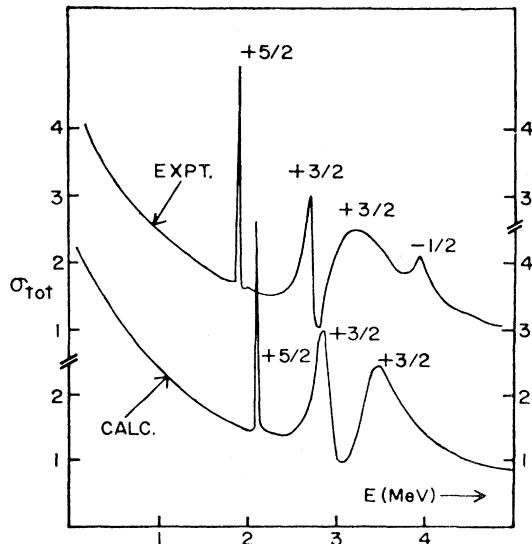


FIG. 30. Total cross section for  $^{12}\text{C}(n,n)^{12}\text{C}$ . The upper curve and scale show the experimental total neutron cross section. The lower curve and scale show the result of an ERM calculation using four oscillator functions (length parameter  $b=1.67$  fm)/channel and channel radii of 5.7 fm (from Purcell, 1969b).

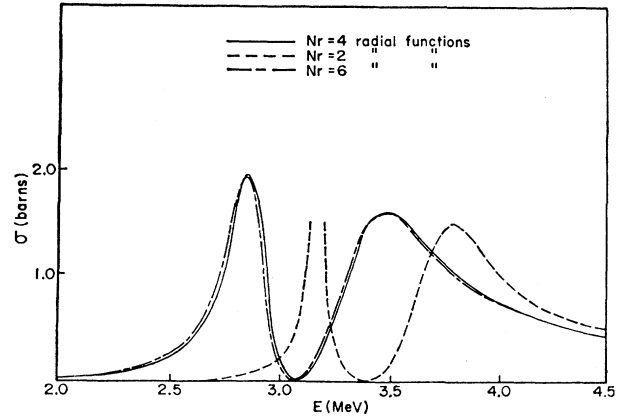


FIG. 31. Cross section for  $d_{3/2}$  partial wave as a function of the number of oscillator basis states/channel ( $N_r$ ) (from Purcell, 1969b).

### C. Low-energy electron-helium scattering

The elastic scattering of low-energy ( $< 19$  eV) electrons from the helium atom has received considerable experimental and theoretical attention. From an experimental point of view, it is desirable to have a standard reference cross section for the precise calibration of electron scattering apparatus. Helium is a promising choice for the standard, because it is chemically inert and because the scattering cross section is free from structure below 19 eV. Helium also presents a challenging problem to theorists, because it is sufficiently simple that an *ab initio* calculation of the  $e^-$ -He scattering cross section can be contemplated with some hope of accurately describing the experimental data. In this section we shall describe the various *ab initio* calculations which have been made using the reaction theories previously discussed in this paper, and we shall discuss the comparison of the calculated results with the experimental data.

#### 1. Experimental measurements

Until recently an uncertainty of approximately 10–15% existed in the experimental determination of the  $e^-$ -He elastic scattering cross section (Bederson and Kieffer, 1971). The direct measurements of Golden and Bandel (1965) were in disagreement with the results of Crompton and co-workers (Crompton, Elford, and Robertson, 1970; Milloy and Crompton, 1977). The latter group employed an electron swarm technique which necessitates a considerable amount of numerical analysis of the experimental data. A discrepancy of 10–15% is obviously undesirable in a cross-section measurement which is to be used as a standard reference.

Since 1974, however, there have been a considerable number of new direct measurements (Andrick and Bitsch, 1975; Kauppila *et al.*, 1977; Stein *et al.*, 1978; Kennerly and Bonham, 1978; Blaauw *et al.*, 1980; Charlton *et al.*, 1980), which are all in agreement to within a few per cent

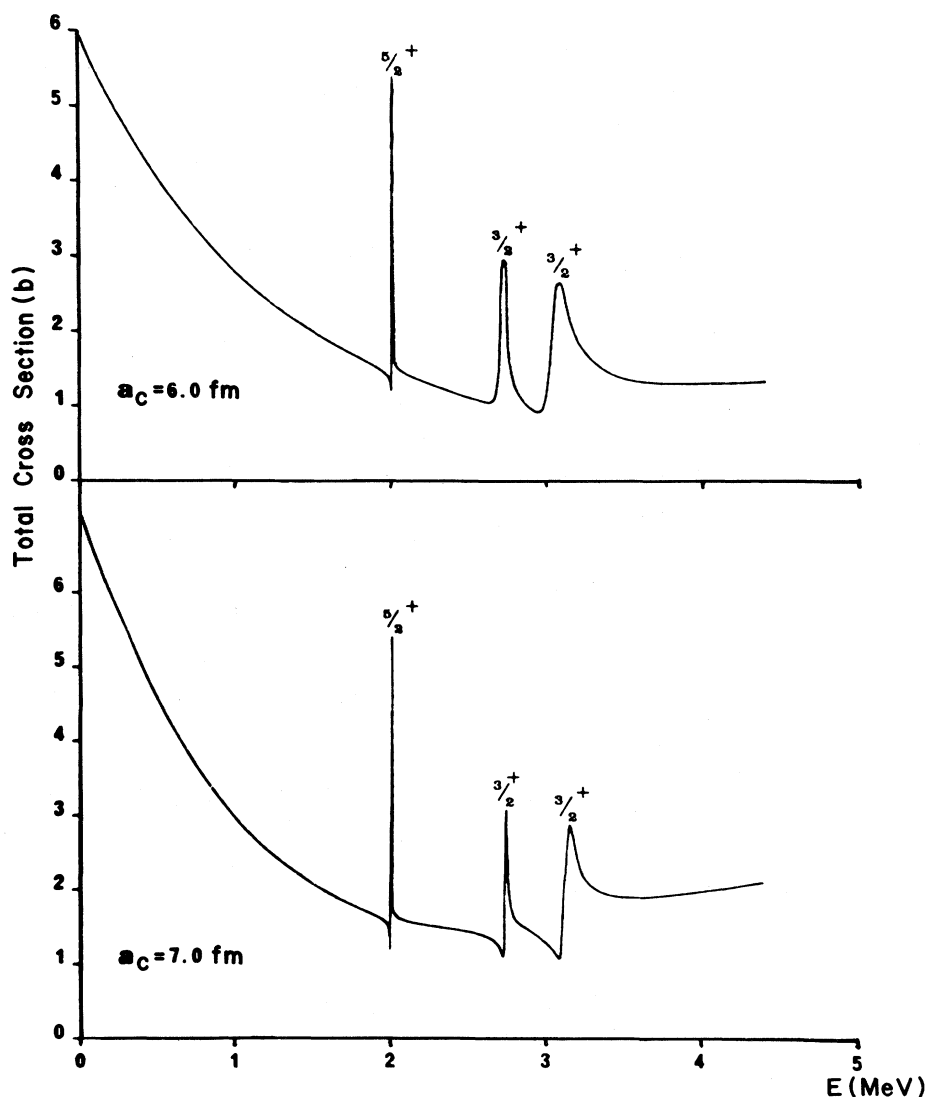


FIG. 32. Total elastic scattering cross section for  $R$ -matrix method using Woods-Saxon basis states (one level/channel) for channel radii of 6.0 and 7.0 fm (from Robson and van Megen, 1972b).

with the measurements of Crompton and co-workers. Figure 39, which is reprinted from Blaauw *et al.* (1980) indicates the state of agreement of the post-1970 experiments. The existence of reliable experimental data provides an opportunity for a meaningful test of *ab initio* calculations and an investigation of the number of excited states of helium to be included in the close-coupling approximation. We shall now look in some detail at the various approaches to the solution of this coupled-channels problem.

## 2. $R$ -matrix method

The application of the  $R$ -matrix method to problems in atomic physics was pioneered by Burke, Hibbert, and Robb (1971). This topic has been reviewed (Burke and Robb, 1975), and the approach is being extended to

electron-molecule collisions (Burke, Mackay, and Shimamura, 1977). The specific application of the  $R$ -matrix method to electron-helium scattering has been made by Burke and Robb (1972) and O'Malley, Burke, and Berrington (1979).

In the earlier work, the static exchange approximation, in which the helium atom is confined to its ground state throughout the collision process, was used. This is a fairly simple model which neglects the polarization of the atom produced by the incoming electron. The polarization effect is important and can be treated by the inclusion of inelastic excitations of the helium atom. In particular, the  $2p$  excitation is largely responsible for the dipole polarizability of the atom. Instead of including the continuum of  $2p, 3p, \dots$ , etc., physical states, it is often preferable to include one state to represent as nearly as possible the complete  $p$ -wave continuum. This state is referred to as the  $2\bar{p}$  pseudostate.

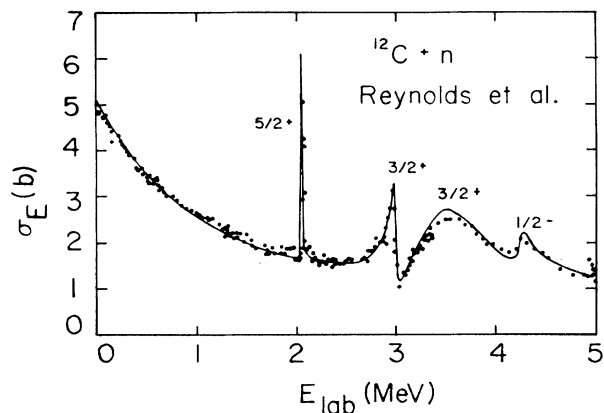


FIG. 33. Total elastic scattering cross section for  $^{12}\text{C}(n,n)^{12}\text{C}$  calculated by the ERM method from a coupled-channels model with parameters chosen by Reynolds *et al.* (1968) to fit the experimental data over the energy range from 0 to 5 MeV. The ERM calculation employs eight (nine for  $s$ -wave channels) oscillator functions/channel. The channel radii are 7.0 fm and the oscillator length parameter  $b=1.67$  fm (from Philpott and George, 1974).

In the latter, much more sophisticated  $R$ -matrix calculation of O'Malley, Burke, and Berrington (1979), and a multiconfiguration helium ground state was used, and pseudo  $P$  and  $D$  states were constructed from optimized  $1s$  through to  $4f$  pseudo-orbitals. The estimated error in the calculated cross sections is about 1%. The results of this calculation are compared with the experimental data for the momentum-transfer cross section and the total elastic scattering cross section in Figs. 40 and 41, respectively. As can be seen, the agreement between the theoretical and experimental results is excellent.

### 3. Natural boundary condition methods

An application of the NBC approach to electron-helium scattering at low bombarding energies ( $< 10$  eV)

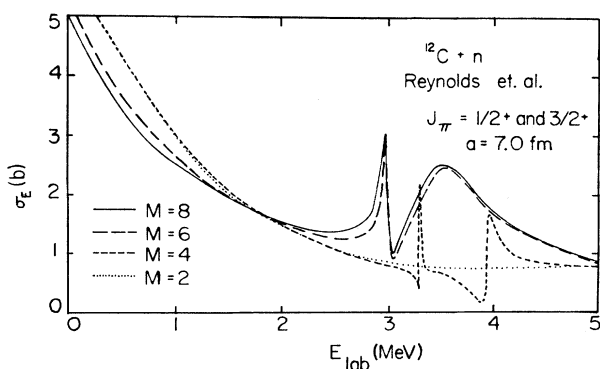


FIG. 34. Calculated  $J^\pi = \frac{1}{2}^+$  and  $\frac{3}{2}^+$  contributions to the total elastic neutron cross section from  $^{12}\text{C}$  plotted against energy for various numbers of oscillator functions/channel. The channel radii are 7.0 fm and the oscillator length parameter  $b=1.67$  fm (from Philpott and George, 1974).

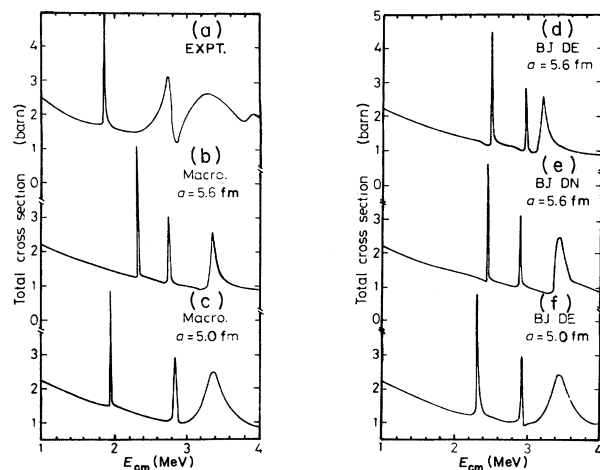


FIG. 35. Total neutron cross sections from  $^{12}\text{C}$ : (a) experimental [from Reynolds *et al.* (1968)] and calculated ones by (b) macroscopic matrix elements with  $a_\alpha(\equiv a)=5.6$  fm; (c) with  $a_\alpha=5.0$  fm and by BJ potential with (d) DE matrix elements and  $a_\alpha=5.6$  fm; (e) DN matrix elements and  $a_\alpha=5.6$  fm; and (f) DE matrix elements and  $a_\alpha=5.0$  fm. The calculations employed four oscillator functions (length parameter  $b=1.67$  fm)/channel (from Mori, 1973).

has been made by Barrett and Robson (1979). Both the Barrett-Delsanto and iterative  $R$ -matrix methods (see Secs. V.C and V.D) were used, and the results of both techniques were found to be in excellent agreement with one another. Two models were employed for the

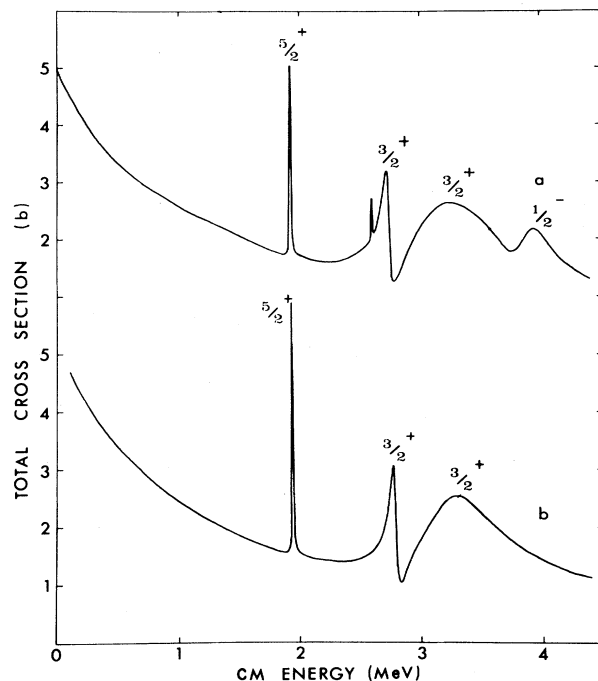


FIG. 36. Total elastic cross section for  $^{12}\text{C}(n,n)^{12}\text{C}$ . The curves are (a) experiment, (b) sum of the  $J^\pi = \frac{1}{2}^+$ ,  $\frac{3}{2}^+$ , and  $\frac{5}{2}^+$  contributions calculated by the NBC methods with two basis states/channel for the weak-coupling collective model of Reynolds *et al.* (1968) (from Ahmad, Barrett, and Robson, 1976a).

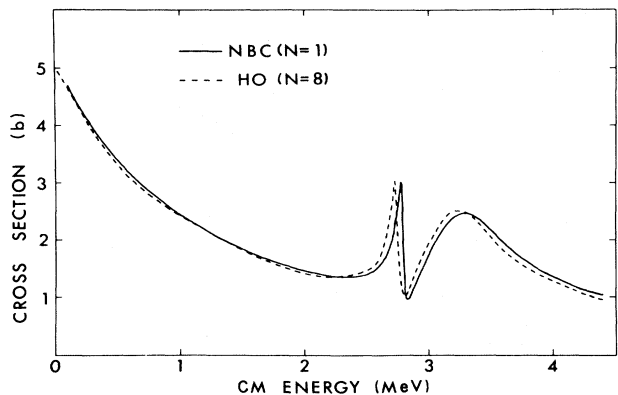


FIG. 37. Sum of  $J^\pi = \frac{1}{2}^+$  and  $\frac{3}{2}^+$  contributions to the total elastic cross section for  $^{12}\text{C}(n,n)^{12}\text{C}$ , calculated by the NBC methods with one basis state/channel, compared with the ERM result of Philpott and George (1974) with eight harmonic-oscillator states/channel for the weak-coupling collective model of Reynolds *et al.* (1968) (from Ahmad, Barrett, and Robson, 1976a).

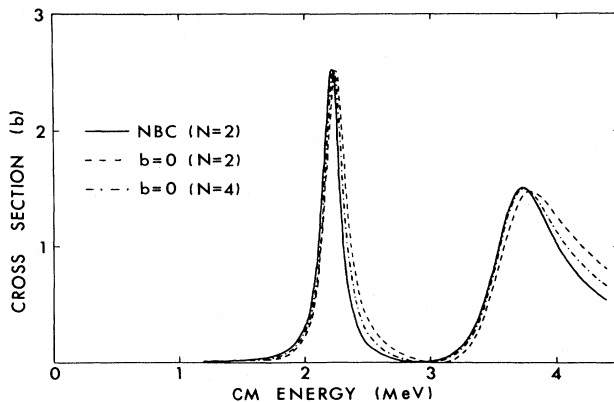


FIG. 38. Calculated  $J^\pi = \frac{3}{2}^+$  contribution to the total elastic cross section for  $^{12}\text{C}(n,n)^{12}\text{C}$  using the SRM method for  $B_c(\equiv b) = 0$  in all channels with two or four basis states/channel, compared with the NBC methods with two basis states/channel for the collective model of Reynolds *et al.* (1968) with the deformation parameter increased to  $\beta = 0.168$  (from Ahmad, Barrett, and Robson, 1976a).

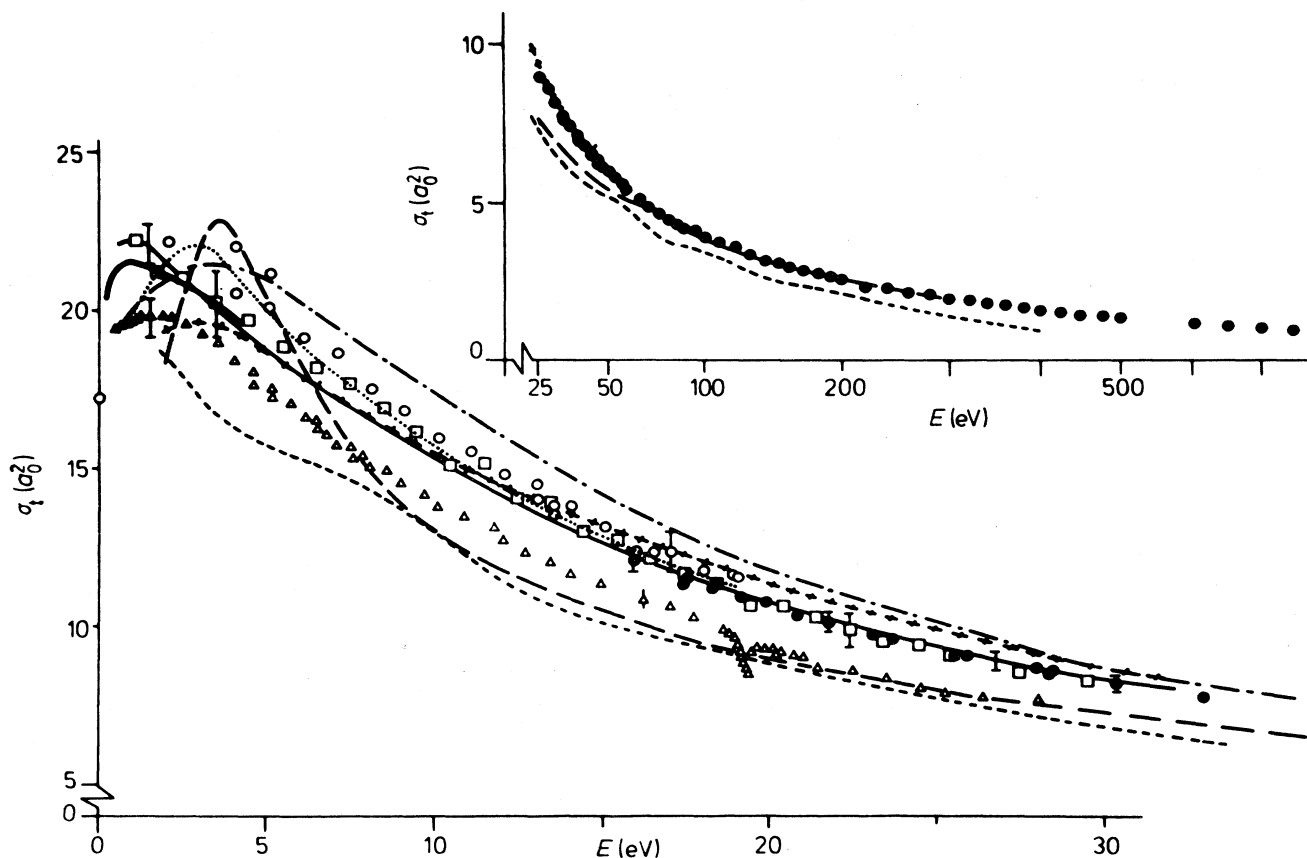


FIG. 39. Total cross sections for electron-helium elastic scattering:  $\bullet$ , Blaauw *et al.* (1980);  $\circ$ , Andrick and Bitsch (1975);  $\triangle$ , Golden and Bandel (1965);  $\square$ , Kauppila *et al.* (1977);  $\text{---}$ , Kennerly and Bonham (1977);  $\text{---}$ , Crompton, Elford, and Robertson (1970);  $\cdots$ , Ramsauer and Kollath (1932);  $\times \times \times \times$ , Brüche, Lilienthal, and Schrödter (1927);  $\text{---}\text{---}\text{---}$ , Ramsauer (1921a, 1921b);  $\text{---}$ , Normand (1930);  $\text{---}$ , Brode (1925) (from Blaauw *et al.*, 1980).

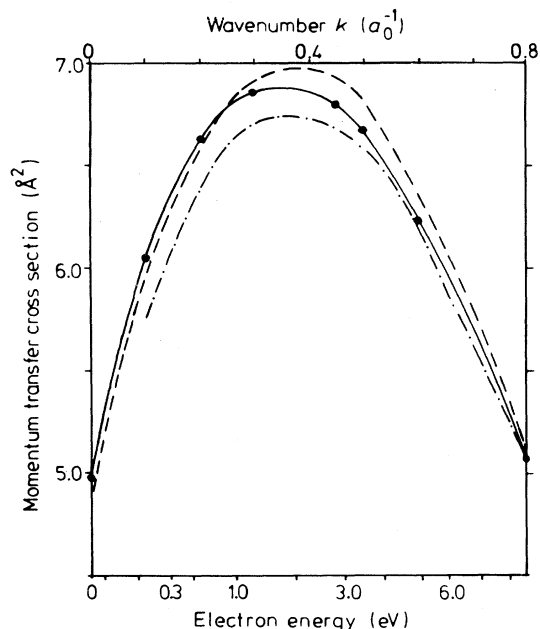


FIG. 40. Momentum-transfer cross sections for electron-helium elastic scattering plotted against wave number and energy: —○—, variational calculation of O'Malley, Burke, and Berrington (1979); - - - -, variational calculation of Sinfailam and Nesbet (1972); - · - · -, experimental results of Crompton, Elford, and Robertson (1970) and Milloy and Crompton (1977) (from O'Malley, Burke, and Berrington, 1979).

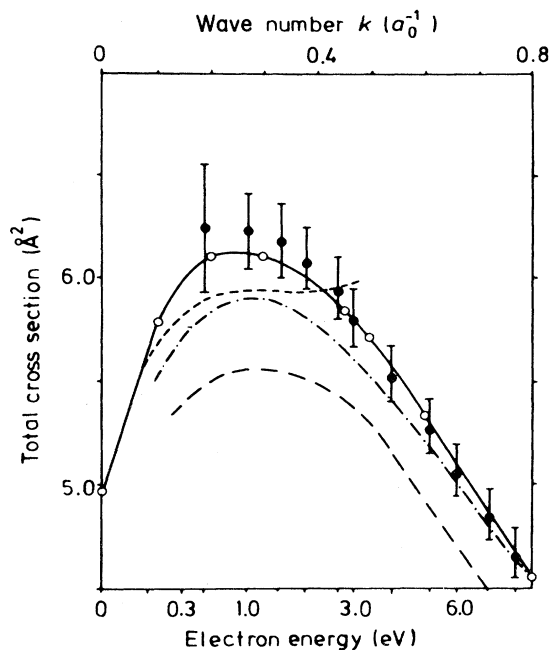


FIG. 41. Total cross sections for electron-helium elastic scattering plotted against wave number and energy: —○—, variational calculation of O'Malley, Burke, and Berrington (1979); - - - -, variational calculation of Sinfailam and Nesbet (1972); - · - · -, theoretical semiempirical result of O'Malley (1963); - - - -, older experimental results of Golden and Bandel (1965); Φ, recent experimental results of Kennerly and Bonham (1978) (from O'Malley, Burke, and Berrington, 1979).

electron-helium system: (i) the static exchange approximation and (ii) the  $1s-2\bar{p}$  approximation in which virtual excitation of a  $p$ -wave pseudostate of the target is allowed. In both cases, the helium atom ground state was described by a Hartree-Fock wave function assuming a simple  $(1s)^2$  configuration, and exchange effects were fully taken into account in the calculation of the  $s$ - and  $p$ -wave phase shifts. Convergence of the NBC treatment was achieved with four radial quantum numbers/channel for channel radii of 6 a.u. The higher partial wave phase shifts were calculated using the Born approximation.

The results of the calculations are compared with the experimental total elastic scattering cross section and momentum-transfer cross section in Figs. 42 and 43, respectively. It is seen that the agreement with experiment is good, considering the simplicity of the models employed. The  $p$ -wave phase shifts were found to be more sensitive than the  $s$ -wave phase shifts to the details of the model representing the helium atom. This accounts for the better agreement obtained for the total elastic scattering cross section than for the momentum-transfer cross section, which is affected more by the  $p$ -wave and higher partial wave phase shifts.

The above calculations were the first application of the NBC methods to an atomic system and demonstrated that these methods provide a useful approach to such problems. Furthermore, the calculations indicate that the extension of the NBC methods to include particle exchange effects, while nontrivial, is nevertheless essentially straightforward.

#### 4. Variational calculations

An early variational calculation of the low-energy  $e^-$ -He scattering cross section based on the Kohn variational method (see Sec. VI.A) was made by Sinfailam and

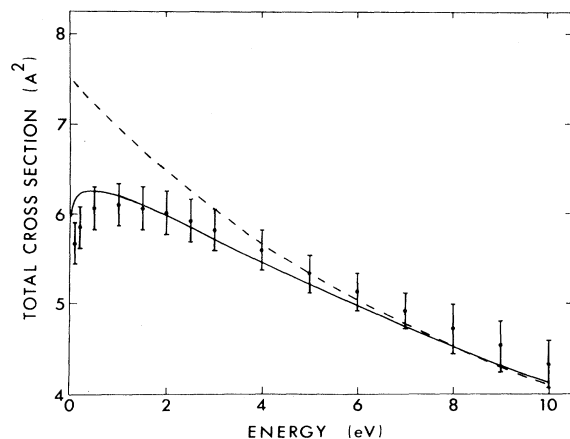


FIG. 42. Total cross section for electron-helium elastic scattering. The data points are derived from the momentum-transfer cross section measurements of Crompton, Elford, and Robertson (1970) and Milloy and Crompton (1977). The broken and full curves are the predictions of the static-exchange and  $1s-2\bar{p}$  models, respectively (from Barrett and Robson, 1979).



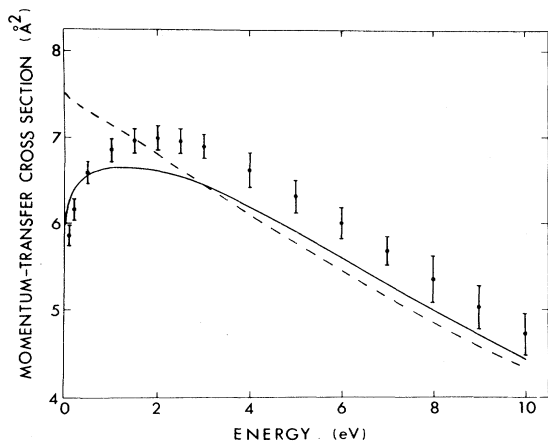


FIG. 43. Momentum-transfer cross section for electron-helium elastic scattering. The data points are the measurements of Crompton, Elford, and Robertson (1970) and Milloy and Crompton (1977). The broken and full curves are the predictions of the static-exchange and  $1s-2p$  models, respectively (from Barrett and Robson, 1979).

Nesbet (1972). The so-called "optimized anomaly free" modification of Kohn's method (Nesbet and Oberoi, 1972) was employed. The polarization and correlation effects were taken into account using Bethe-Goldstone equations (see Nesbet, 1980) in which all significant virtual excitations of a single-target  $1s$  orbital were included. The basis states for the one-electron orbitals were chosen to have exponential radial form factors  $r^n \exp(-\alpha r)$  with both a decreasing geometric sequence and an increasing arithmetic sequence of coefficients  $\alpha$ . Exchange symmetry was fully taken into account. The results of the calculation are compared with the data available at the time in Figs. 44 and 45.

A variational calculation of similar scope to the above has been performed by Wichmann and Heiss (1974) using the  $1s-2s-2p$  close-coupling approximation. They employed both the Kohn and inverse-Kohn techniques. The results of the two methods were identical to at least three figures, implying that there were no problems with singular matrices. Up to 15 trial functions were used to describe the scattering wave function. The  $p$  and  $d$  phase shifts obtained by Wichmann and Heiss are appreciably lower than those of Sinfailam and Nesbet. This was attributed to a difference in the choice of the helium wave function in the two calculations. The results of the Wichmann and Heiss calculation for the total cross section are shown in Fig. 46, where they are compared with the measurements of Golden and Bandel (1965). The calculated cross section is in fact larger than these early experimental results and is in much better agreement with the more recent data shown in Fig. 39.

A recent, much more sophisticated calculation using the Kohn variational procedure has been carried out by Nesbet (1979a, 1979b). This work is comparable in scope and complexity with the  $R$ -matrix calculation of O'Malley, Burke, and Berrington (1979) discussed in Sec.

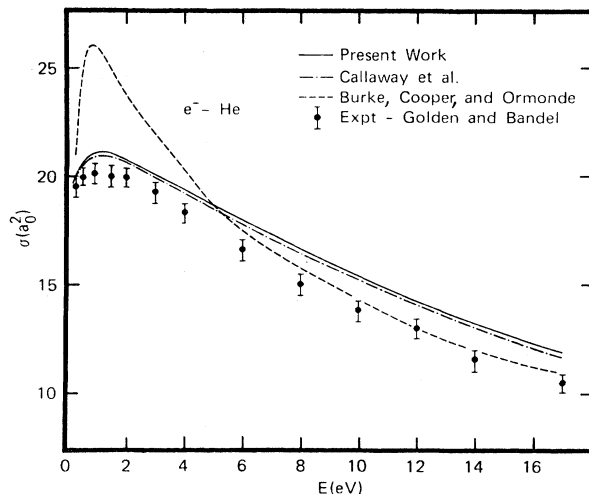


FIG. 44. Total cross section for electron-helium elastic scattering. The data points are the measurements of Golden and Bandel (1965). The solid curve shows the variational calculation of Sinfailam and Nesbet (1972); the dashed curve denotes the static-exchange close coupling calculation of Burke, Cooper, and Ormonde (1969), and the open circles are the results of Callaway *et al.* (1968) using the polarized orbital method (from Sinfailam and Nesbet, 1972).

VIII.C.2. The variational wave function represents target-atom electronic correlation, electric dipole and quadrupole polarizability response, and short-range electron-atom correlation at a level of accuracy sufficient for 1% accuracy in the differential scattering cross section. Levels up to  $5s$ ,  $5p$ ,  $5d$ , and  $5f$  were included in the excited-atom wave function.

The results of Nesbet's calculation are displayed in Figs. 47 and 48. The agreement with experiment is seen to be excellent, and it would appear that the  $e^-$ -He scattering cross sections at bombarding energies  $< 19$  eV are now known both experimentally and theoretically to a

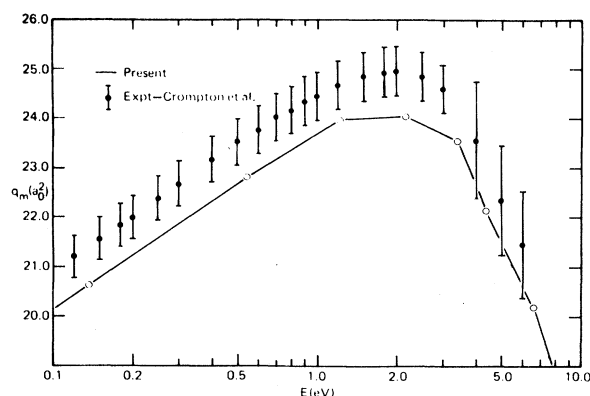


FIG. 45. Momentum-transfer cross section for electron-helium elastic scattering. The data points are the measurements of Crompton, Elford, and Jory (1967) and Crompton, Elford, and Robertson (1970); —○— denotes the variational calculation of Sinfailam and Nesbet (1972) (from Sinfailam and Nesbet, 1972).

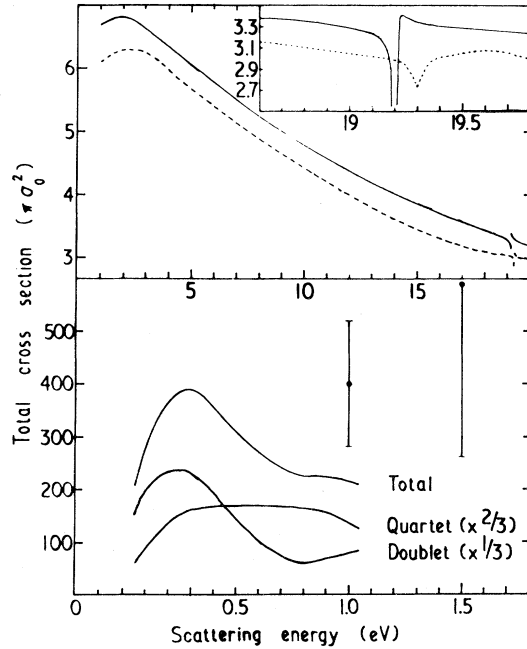


FIG. 46. Upper portion: elastic  $e$ -He scattering from ground state; dashed curve denotes the experimental results of Golden and Bandel (1965); solid curve shows the variational calculation of Wichmann and Heiss (1974). Lower portion: elastic  $e$ -He scattering from  $2^3S$  state; data points are the measurements of Neynaber *et al.* (1964); solid curves are the variational results of Wichmann and Heiss (1974) (from Wichmann and Heiss, 1974).

precision of several percent. The earlier disagreements between experimental results and between experiment and theory have been removed.

Although most of the variational calculations of electron-atom scattering have been made using the Hulthén-Kohn and associated methods, the Schwinger variational method (see Sec. VI.D) has been applied to  $e^-$ -He scattering by Lucchese and McKoy (1979). However, their calculation is more in the nature of a test of the Schwinger approach than an attempt to accurately describe the experimental data. The results obtained by Lucchese and McKoy using the static exchange approximation to represent the electron-helium system are in good agreement with the corresponding calculation of Sinfailam and Nesbet (1972). Lucchese and McKoy claim that the Schwinger variational approach gives accurate results with small discrete basis sets. The method has been applied to an exactly soluble multichannel problem by Takatsuka and McKoy (1980), and it was found to yield accurate results with a convergence superior to those of other variational methods. Its application to more realistic physical problems is expected in the near future.

#### D. $\alpha$ - $\alpha$ elastic scattering

In Sec. VII we have outlined several ways in which the generator coordinate method (GCM) has been combined with one or other of the calculable reaction theories to en-

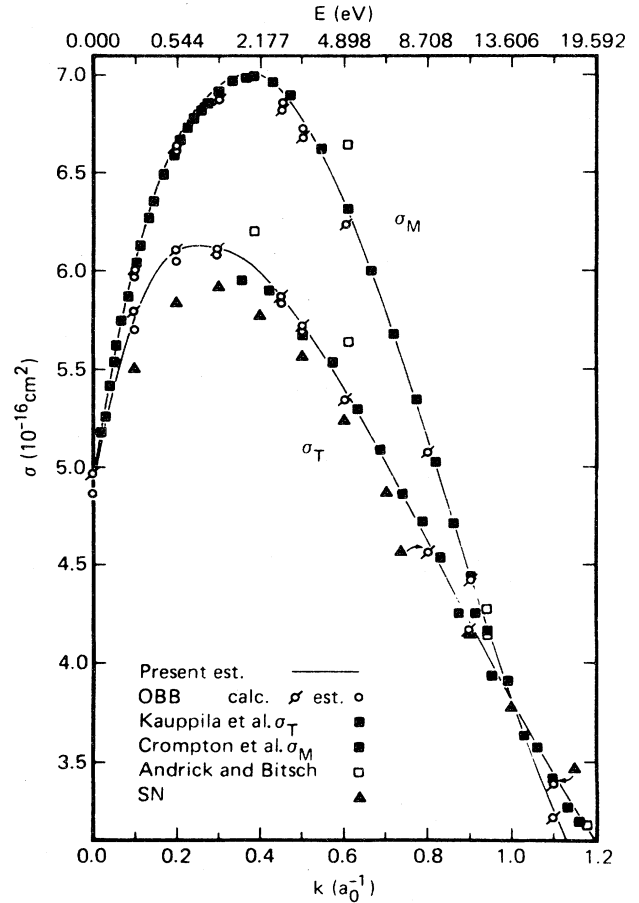


FIG. 47. Total and momentum-transfer cross sections for electron-helium elastic scattering. Full curves: variational results of Nesbet (1979a, 1979b);  $\circ$  and  $\circ$  calculated and estimated values, respectively, of O'Malley, Burke, and Berrington (1979);  $\blacksquare$   $\sigma_T$ , Kauppila *et al.* (1977) and  $\sigma_M$ , Crompton, Eilford, and Robertson (1970);  $\square$ , Andrick and Bitsch (1975);  $\blacktriangle$ , Sinfailam and Nesbet (1972) (from Nesbet, 1979b).

able the numerical computation of composite particle scattering cross sections. In this section we shall describe the application of these techniques to  $\alpha$ - $\alpha$  elastic scattering. The  $\alpha$ - $\alpha$  system has often been used as a test of the various methods because of its relative simplicity involving identical clusters, which are well represented by  $(1s)^4$  closed-shell model configurations and because the high energy of the first excited state of the  $\alpha$  particle ensures that the inelastic reaction channels can be reasonably neglected at sufficiently low bombarding energies.

#### 1. Direct solution of Hill-Wheeler equation

It was seen in Sec. VII.A that the formulation of the GCM leads to the Hill-Wheeler equation [Eq. (7.15)], an integral equation for the GC amplitude or weight function  $f^{(k)}(\mathbf{S})$ . In what is probably the most direct approach towards a solution, de Takacsy (1972) transformed this integral equation into a set of algebraic equations by

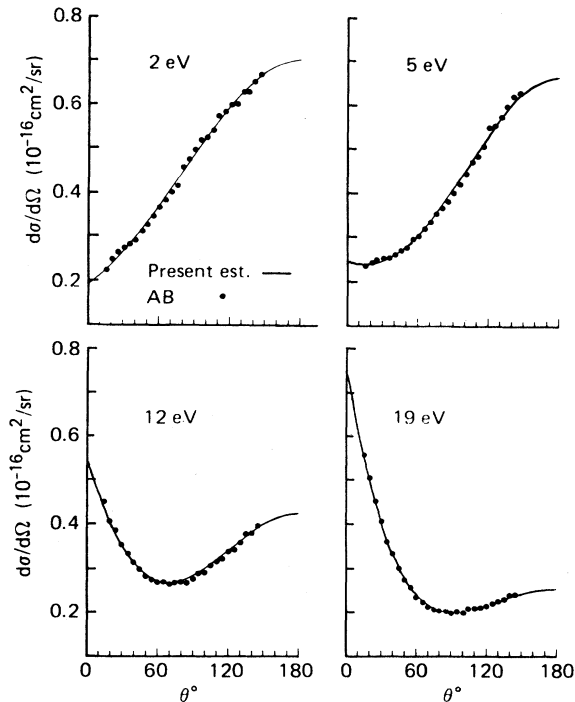


FIG. 48. Differential cross sections for electron-helium elastic scattering. Full curves are variational results of Nesbet (1979a, 1979b). The data points are the measurements of Andrick and Bitsch (1975) scaled to give the same total cross section as the calculation of Nesbet (from Nesbet, 1979b).

a discretization of the range of integration over the interaction region and the use of a Gauss-Legendre quadrature formula (see Sec. VII.B). The result is a set of simultaneous linear equations for the GC amplitude at each of the discrete points. de Takacsy applied this method, neglecting the Coulomb interaction, to the  $\alpha$ - $\alpha$  elastic scattering problem to demonstrate the usefulness of the approach. In the external region, he assumed that the partial-wave GC weight function could be represented in terms of regular and irregular spherical Bessel functions by the relation

$$f_l(S) = j_l(kS) + n_l(kS) \tan(\delta_l - \frac{1}{2}l\pi), \quad (8.21)$$

where  $k$  is the wave number for the relative motion and  $\delta_l$  is the phase shift. A typical set of mesh points was obtained by using spacings 0.3 fm for the range  $0 \leq S \leq 2.4$  fm and 0.6 fm for the range  $2.4 \leq S \leq 6.0$  fm ( $\equiv S_0$ ), while the integral over the external region was performed with a step size of 0.6 fm for the range  $6.0 \leq S \leq 12.0$  fm. A four-point Gauss-Legendre quadrature formula was employed for each step. de Takacsy concluded that this direct solution of the Hill-Wheeler equation provides a practical method for composite particle scattering.

Tanabe, Tohsaki, and Tamagaki (1973), using the de Takacsy method, pointed out that one can include the Coulomb interaction in the  $\alpha$ - $\alpha$  elastic scattering problem by assuming that in the asymptotic region one can express the partial-wave GC weight function in terms of Coulomb

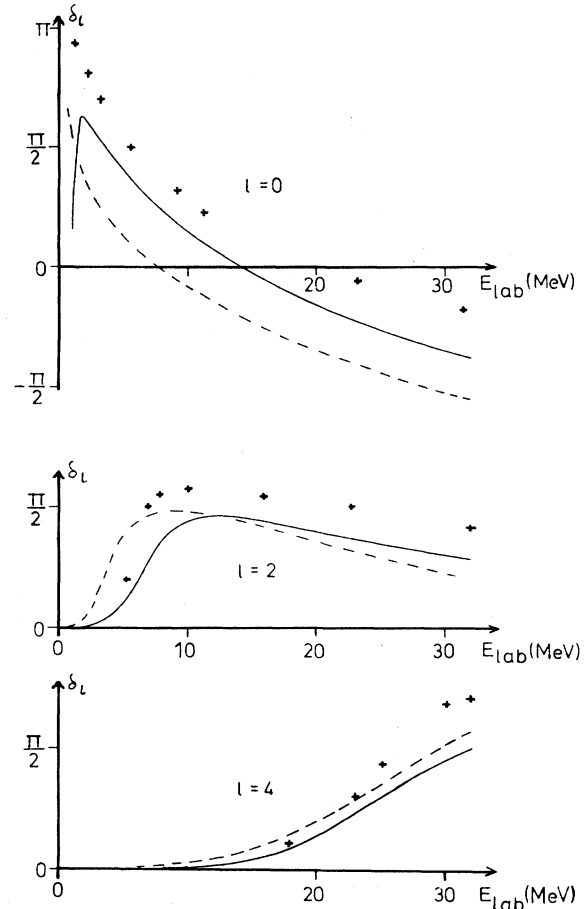


FIG. 49. The  $\alpha$ - $\alpha$  phase shifts calculated by direct solution of the Hill-Wheeler equation using a harmonic-oscillator length parameter  $b = 1.38$  fm for the  $1s$  orbitals and the Volkov force 1 (Volkov, 1965). The dashed curve was calculated without, the solid curve with the Coulomb interaction. The crosses represent the experimental values (from Friedrich, Hüsken, and Weiguny, 1974).

wave functions:

$$f_l(S) = F_l(kS) + G_l(kS) \tan \delta_l. \quad (8.22)$$

They also found it unnecessary to employ as many mesh points as de Takacsy.

Friedrich, Hüsken, and Weiguny (1974) also extended the method of de Takacsy to include the Coulomb interaction using a different and more complicated representation of the asymptotic GC weight function. Their results, employing 14 mesh points equidistant in the range  $0 \leq S \leq 12.0$  fm, a harmonic oscillator length parameter  $b = 1.38$  fm for the  $1s$  orbitals, and the Volkov force 1 (Volkov, 1965), are shown in Fig. 49.

Apart from the difficulty of obtaining an appropriate form of the GC weight function to give the correct asymptotic boundary condition on the scattering wave function, the direct solution of the Hill-Wheeler equation also has convergence problems associated with the singular character of the weight function (Giraud and LeTour-

neaux, 1972): As the mesh size decreases, the amplitudes  $f_l(S_i)$  oscillate more and more violently. Lumbroso (1974, 1976) has avoided this trouble by formulating the problem in a momentum representation. He has calculated the  $\alpha$ - $\alpha$  elastic scattering phase shifts for  $l=0, 2, 4,$  and  $6$  partial waves using a Volkov force 2 with Majorana component  $m=0.56$  for the nucleon-nucleon interaction and a harmonic-oscillator length parameter  $b=1.36$  fm. The results are shown in Fig. 50. Comparison of Figs. 49 and 50 shows a substantial disagreement between the two sets of results, although similar models were used. However, the results of Lumbroso appear to be in close agreement with those of Tanabe, Tohsaki, and Tamagaki (1973) (not shown), implying that the de Takacsy method provides a satisfactory approach to composite particle scattering. The above discrepancy has been investigated by Beck *et al.* (1975b), who employed a variational technique which will be discussed in the next section.

## 2. Variational techniques

As indicated above, the direct procedures for solving the Hill-Wheeler equation are not ideal. The use of a

momentum representation involves much labor and the formulation in coordinate space tends to be unstable. The disagreement between the results of Friedrich *et al.* and Lumbroso motivated the development by Beck *et al.* (1975a) of an alternative technique employing the Kohn variational method (see Sec. VI.A). This approach has been discussed in Sec. VII.B.2.

The Kohn variational method has been applied by Beck *et al.* (1975b) to  $\alpha$ - $\alpha$  elastic scattering and their results for the  $l=0$  phase shift are shown in Fig. 51. It is seen that good agreement is obtained with the earlier work of Lumbroso when a Volkov force 2 is used (curve 1), but that there is considerable disagreement (curve 2) with the results of Friedrich *et al.* (curve 3). Both curves 2 and 3 employed a Volkov force 1 and nearly the same oscillator length parameters,  $b=1.36$  and  $1.38$  fm, respectively. However, Friedrich *et al.* used a Majorana component  $m=0.60$ , while Beck *et al.* employed  $m=0.55$ . Thus the disagreement in the calculated results could be due to the use of different exchange parameters. Beck *et al.* concluded that the discrepancy may arise from different approximations made in introducing the scattering boundary condition into the Hill-Wheeler equation and that

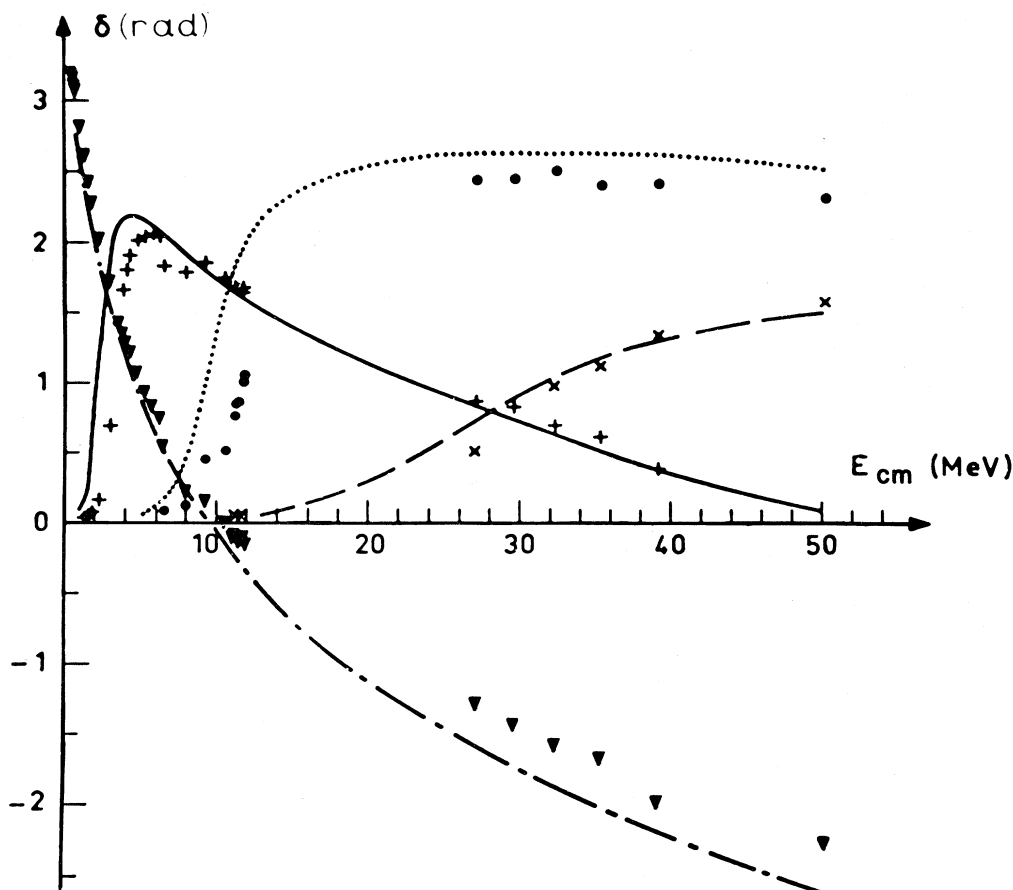


FIG. 50. The  $\alpha$ - $\alpha$  phase shifts for  $l=0(\blacktriangle)$ ,  $2(+)$ ,  $4(\bullet)$ , and  $6(\times)$  partial waves calculated by Lumbroso (1974, 1976) using a momentum representation for the direct solution of the Hill-Wheeler equation. A Volkov force 2 with Majorana component  $m=0.56$  for the nucleon-nucleon interaction and a harmonic-oscillator length parameter  $b=1.36$  fm were used (from Lumbroso, 1976).

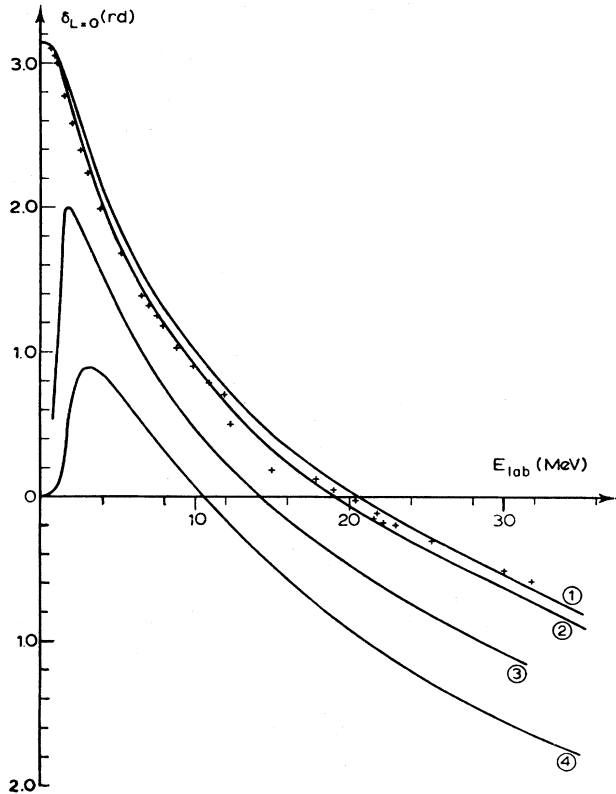


FIG. 51. The  $\alpha$ - $\alpha$  phase shift for the  $l=0$  partial wave. Curves 1, 2, and 4 denote calculations of Beck *et al.* (1975b) using the Kohn variational method with a Volkov force 2, a Volkov force 1, and the Brink-Boeker force *B* 1, respectively. Curve 3 shows the results of Friedrich *et al.* (1974) with a Volkov force 2. The crosses represent the experimental values (from Beck *et al.*, 1975b).

those of Friedrich *et al.* may not be quite adequate. Figure 51 shows that while the Volkov forces 1 and 2 give nearly the same result (curves 2 and 1, respectively), the potential *B* 1 of Brink and Boeker (1967) gives quite a different result (curve 4). Thus the result is quite sensitive to the nucleon-nucleon interaction employed.

Other calculations based on Kohn variational methods have been carried out by Mito and Kamimura (1976) and Canto and Brink (1977). The results of Canto and Brink obtained with their method 2 (see Sec. VII.C.2), using a Volkov force 1 with Majorana component  $m=0.55$  and an oscillator length parameter  $b=1.36$  fm, are shown in Fig. 52, where comparison is made with the phase-shift

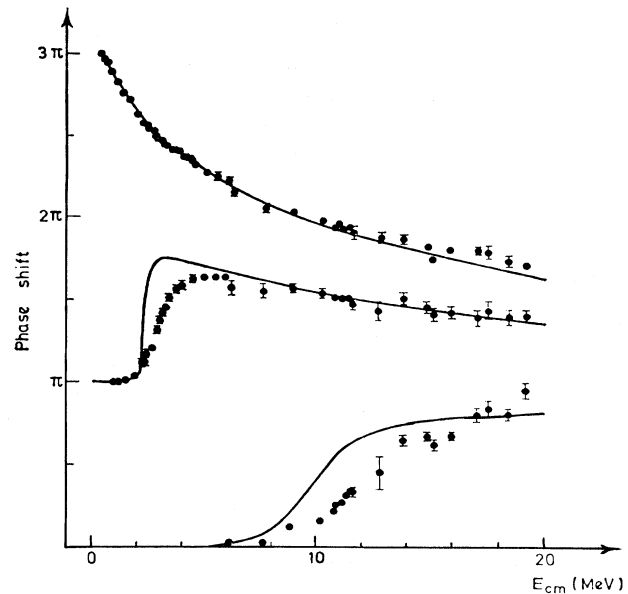


FIG. 52. The  $\alpha$ - $\alpha$  elastic scattering phase shifts for  $l=0, 2$ , and  $4$  partial waves. The solid curves are the calculations of Canto and Brink (1977), and the points denote the phase-shift analysis results of Afzal, Ahmad, and Ali (1969) (from Canto and Brink, 1977).

analysis of Afzal, Ahmad, and Ali (1969). In the variational calculation, seven mesh points and a channel radius  $a_\alpha=7.0$  fm were employed. The corresponding phase shifts obtained by Canto and Brink in their method 1 (see Sec. VII.B.2) are almost the same as those of method 2. This is shown in Table V, where the convergence of the two methods is compared for the  $l=0$  phase shift. In this table,  $\bar{N}_i$  denotes the number of internal mesh points used,  $\bar{N}_j^T$  the total number of mesh points used for method  $j$ , and  $\delta_0^j$  the corresponding  $l=0$  phase shift in radians. Overall, the convergence of method 2 seems preferable, although both techniques appear to require the same number of internal mesh points, which for larger clusters will mainly determine the amount of computing time involved in the calculation. It was found that the results of both methods were stable to changes in the channel radius  $a_\alpha$  within the range 6.1–11.6 fm, provided a sufficient number ( $\geq 3$ ) of internal mesh points was used.

### 3. Microscopic *R*-matrix method

The microscopic *R*-matrix method (MRM) (see Sec. VII.C.1) has also been applied to  $\alpha$ - $\alpha$  elastic scattering by

TABLE V. Convergence of  $l=0$  phase shifts at  $E_{cm}=1, 12$ , and  $20$  MeV.

$\bar{N}_i$	$\bar{N}_1^T$	$\bar{N}_2^T$	1 MeV		12 MeV		20 MeV	
			$\delta_0^1$	$\delta_0^2$	$\delta_0^1$	$\delta_0^2$	$\delta_0^1$	$\delta_0^2$
6	12	8	-0.456	-0.459	-0.334	-0.335	-1.101	-1.104
5	10	7	-0.458	-0.464	-0.354	-0.341	-1.167	-1.106
4	8	6	-0.464	-0.470	-0.339	-0.357	-1.090	-1.108
3	5	4	-0.547	-0.473	-0.407	-0.415	-0.985	-1.132
2	4	3	-0.768	-0.507	0.189	-0.833	-0.243	-1.398

Horiuchi (1970) and Baye and Heenen (1974). For simplicity Horiuchi evaluated the Hamiltonian and overlap matrix elements by integration over all configuration space rather than the required interaction region. This approximation is analogous to the method  $E$ -RM(DIAG) of Schmittroth and Tobocman (1971) described in Sec. VIII.A.4. However, it leads to a strong dependence of the results on the channel radius. Baye and Heenen avoided the approximation made by Horiuchi and obtained satisfactory results for the  $l=0, 2, 4,$  and  $6$  partial waves.

Figure 53 shows their results (curve 1) for the  $l=0$  phase shift compared with those obtained by Lumbroso (1976) (curve 2) and Friedrich, Hüsken, and Weiguny (1974) (curve 3) (see Sec. VIII.D.1). Baye and Heenen used a Volkov force 1 with Majorana component  $m=0.56$  and an oscillator length parameter  $b=1.36$  fm. The same model was also employed by Tanabe, Tohsaki, and Tamagaki (1973) as described in Sec. VIII.D.1, and their results (not shown) are very close to curve 1. Curve 4 shows the corresponding results using Horiuchi's approximate treatment of the matrix elements. It is seen that this curve oscillates around curve 1, becoming less reliable with increasing energy.

Baye and Heenen attributed the differences in the results to the use of either different nucleon-nucleon interactions or more approximate treatments: Lumbroso calculated the Coulomb matrix elements approximately,

and Friedrich *et al.* used only 14 mesh points, compared with the 32 mesh points of Tanabe *et al.* In the MRM, it was found that only four mesh points were necessary for convergence. This is one of the main advantages of the MRM compared with direct solutions of the Hill-Wheeler equation. Another is that only numerical values of the GC kernels are required, since there is no need for further integral transforms of these kernels. This allows the Coulomb matrix elements to be computed without approximation.

#### 4. Natural boundary condition method

A combination of the NBC and GC methods has been developed for the treatment of composite particle scattering by Baldock, Barrett, and Robson (1979). This technique has been described in Sec. VII.D. The basic difference between this approach and that of the MRM discussed above is that the GCM is used to generate basis states for the solution of the many-body Schrödinger equation rather than the solution of the Schrödinger equation itself. This difference ensures that there is no problem associated with numerical instabilities arising from the singular character of the GC weight function. In addition, the NBC method automatically carries out the projection over angular momentum, which is a separate procedure in the other methods.

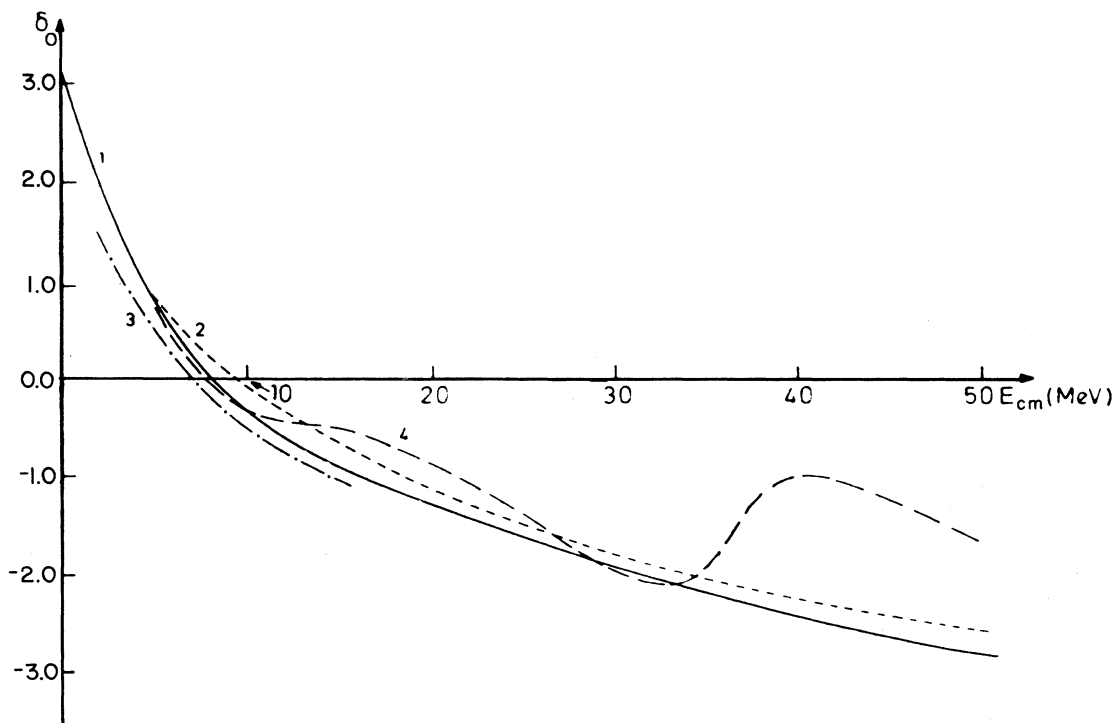


FIG. 53. The  $\alpha$ - $\alpha$  phase shift for the  $l=0$  partial wave. Curve 1 (solid curve): MRM calculation of Baye and Heenen (1974); curve 2 (short-dashed curve): calculation of Lumbroso (1976); curve 3 (dot-dashed curve): calculation of Friedrich, Hüsken, and Weiguny (1974); curve 4 (long-dashed curve): calculation of Baye and Heenen (1974) with the method of Horiuchi (1970) (from Baye and Heenen, 1974).

The results of an NBC calculation (Baldock, 1980) for  $\alpha$ - $\alpha$  elastic scattering using a Volkov force 1 with Majorana component  $m=0.56$  and an oscillator length parameter  $b=1.36$  fm are shown in Figs. 54 and 55 (solid curves). Also shown for comparison are the phase-shift analysis results of Afzal, Ahmad, and Ali (1969) and the corresponding calculations of Canto and Brink (1977) (dashed curves) and Baye and Heenen (1974) (dot-dashed curves) which have been described in the previous sections, VIII.D.2 and VIII.D.3, respectively. Both these calculations employed the same model as the NBC calculation, except that the exchange parameter was slightly less ( $m=0.55$ ) in the case of Canto and Brink. It is seen that the NBC results are in good agreement with the earlier calculations. It was found that the phase shifts were independent of the channel radius for  $r_\alpha > 5.5$  fm, provided a sufficient number of basis states was employed. For energies  $< 30$  MeV and  $a_\alpha = 6.0$  fm, only three basis functions were required. At higher energies, converged phase shifts were obtained with only three basis states, provided the energy correction of Sec. V.C.1 was employed.

## 5. Discussion

From the previous sections, it is apparent that there are several useful techniques for the application of reaction theories to the calculation of composite particle scattering cross sections and that the use of these methods is a viable alternative to the direct solution of the Hill-Wheeler equation in the GCM. In general, the methods have been ap-

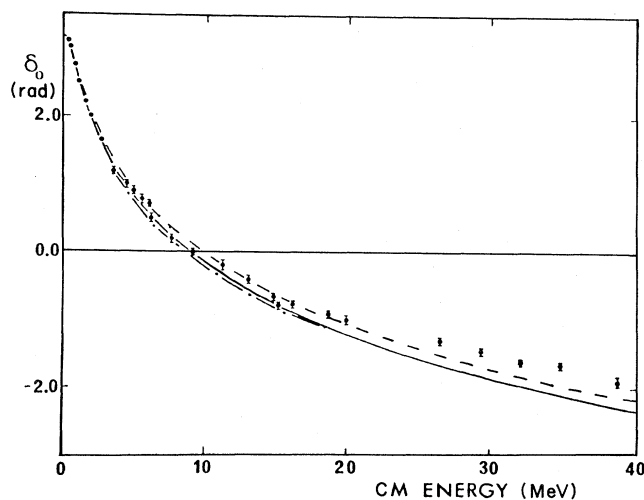


FIG. 54. The  $\alpha$ - $\alpha$  phase shift for the  $l=0$  partial wave. Solid curve denotes the NBC calculation of Baldock (1980) using a Volkov force 1 with Majorana component  $m=0.56$  and an oscillator length parameter  $b=1.36$  fm. The dashed and dot-dashed curves are the calculations of Canto and Brink (1977) and Baye and Heenen (1974), respectively. The points denote the phase-shift analysis results of Afzal, Ahmad and Ali (1969) (from Baldock, 1980).

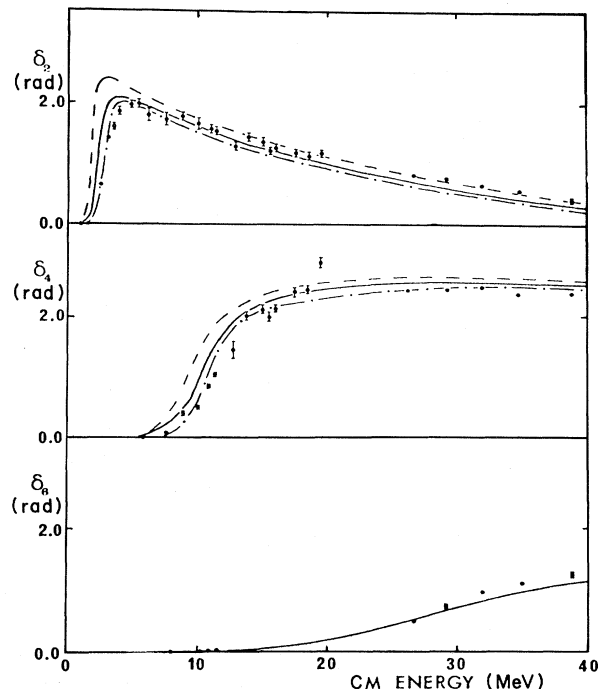


FIG. 55. The  $\alpha$ - $\alpha$  phase shifts for  $l=2, 4$ , and  $6$  partial waves (for further details see Fig. 54 caption) (from Baldock, 1980).

plied successfully to  $\alpha$ - $\alpha$  elastic scattering. However, in the case of larger clusters, the neglect of inelastic channels usually cannot be justified and the resultant increase in the complexity of the scattering problem leads to large and very tedious calculations. Nevertheless, some progress in this direction is being made (Baye, Heenen, and Libert-Heinemann, 1978), although only qualitative agreement with experiment is possible with the simple models employed. The extension of the methods to more realistic models involving different oscillator length parameters and more complicated shell-model configurations is hampered by a further large increase in the complexity of the many-body microscopic calculations. It seems likely that the use of more realistic models will become possible only if an adequate approximate treatment of the Pauli principle can be found.

## E. Conclusion

In this section we have investigated the application of calculable reaction theories to four selected problems in different areas of physics. In each of these applications, the reaction theory techniques have provided attractive alternatives to the direct solution of a system of coupled integrodifferential equations.

A comparison of the results when different methods are applied to the same scattering problem indicates that most of the methods are accurate if sufficient basis states have been included in the calculation. However, the rate of convergence of the various approaches can be quite dif-

ferent, and the practicability of a given method needs to be investigated in the context of the problem being studied before a decision is made as to which technique represents the optimum procedure for obtaining the solution.

Of all the calculable theories investigated, the natural boundary condition (NBC) methods have the fastest rate of convergence with increasing number of basis states. However, these methods suffer from the disadvantage of requiring basis states which are energy dependent and which therefore must be calculated at each energy of interest. Thus sophisticated computer programs are required and have been developed to enable the basis states to be determined very quickly. The eigenchannel method (see Sec. V.B) was the first of the NBC procedures to receive wide application. Its use (Barrett and Delsanto, 1971) for the calculation of photon absorption in  $^{208}\text{Pb}$  involved the solution of a 31 coupled-channels problem. The Barrett-Delsanto method (see Sec. V.C) has superseded the eigenchannel method because it represents a substantial improvement in terms of the computing time involved to achieve the same result. This method also permits—via the energy correction of Sec. V.C.1—allowance to be made for the effect of neglected higher levels with a consequent improvement in accuracy.

The  $R$ -matrix approach was developed in nuclear physics but is now receiving considerable attention also in atomic and molecular physics. In general, the convergence of the standard calculable  $R$ -matrix (SRM) method (see Sec. IV.C) is quite poor. However, the use of the Buttle correction (see Sec. IV.D) greatly improves the accuracy of this technique with only a small increase in the numerical complexity and should therefore be regarded as a mandatory requirement of the SRM method. The iterative  $R$ -matrix method (see Sec. V.D), which is equivalent to the Barrett-Delsanto method, optimizes the basis states to maximize the rate of convergence in an  $R$ -matrix calculation and is thus worthy of consideration in such an approach.

The extended  $R$ -matrix (ERM) method was developed primarily to enable the use of harmonic oscillator basis functions, which are widely employed in bound-state nuclear structure calculations, to be carried over directly into scattering calculations. Thus this approach has been employed mostly in low-energy nuclear physics. For such problems, the ERM method has enjoyed considerable success, although care must be exercised to ensure that proper convergence has been obtained. It was found that approximations (see Secs. VIII.B.4 and VIII.D.3) in which the Hamiltonian and overlap matrix elements are calculated by integration over all configuration space, so that direct use can be made of shell-model bound-state calculations, rather than only the required interaction region, are unsatisfactory. The ERM method converges faster than the SRM method but the Buttle correction is no longer available to correct for distant levels. However, the convergence rate of the ERM approach can often be improved by using either an optical potential, which may lead to spurious resonances, or auxiliary energy-dependent

wave functions to allow a better description of the scattering wave function in the channel region (see Sec. VIII.A.3). Calculations based on the  $X$  matrix formalism (see Sec. III.D) appear to converge faster than the ERM calculations even with an optical potential included and do not give rise to false resonances (see Sec. VIII.A.3). This is true provided that the calculation is done by solving the Lippmann-Schwinger equation [inverting  $\bar{V} - \bar{V} \bar{G} \bar{V}$  in Eqs. (8.7) and (8.8)] rather than by solving the Schrödinger equation [inverting  $H + \mathcal{L}(b_c) - E$  in Eq. (8.10)].

The variational approach (see Sec. VI) is an old technique, which is currently receiving considerable application in nuclear, atomic, and molecular physics, and high-precision results have been obtained.

In this section, we have presented selected examples of the application of the various calculable reaction theories discussed previously in this review. The advantage to a particular investigator of one method over another depends to a large degree on the problem under investigation and the availability of computer software. It is apparent, however, that most of the methods are satisfactory when properly applied so that they represent viable alternatives to the more direct approach, which involves the numerical solution of a system of coupled integrodifferential equations.

## IX. CALCULABLE TRANSITION OPERATOR FORMALISM

In Sec. VII.A.4 we have seen that the calculations of Schmittroth and Tobocman indicate that  $X$ -matrix formalism calculations can give very good results provided they are based on solution of the Lippmann-Schwinger (LS) equation rather than the inversion of  $H + \mathcal{L} - E$ . The LS equation is the dynamical equation for the  $X$  matrix. We designate formalisms based on the solution of an equation for the transition operator as transition operator formalisms to distinguish them from the  $R$ -matrix formalisms which are based on the evaluation of the inverse of  $E - H$  or  $H + \mathcal{L} - E$ .

In Sec. III.D we saw how the  $R$ -matrix formalism can yield an expression for the collision matrix in terms of a transition matrix operator  $X$ . The result followed from the use of the iterated resolvent relation for the Green's-function operator. We now address the task of deriving the resolvent relation and obtaining dynamical equations for the transition matrix operator.

Our analysis is based on the use of an explicit expression for the partition Green's-function operator. This will be the following spectral decomposition:

$$\bar{G}_\alpha = \sum_{c \in \alpha} |c\rangle g_c(r_\alpha, r'_\alpha) \langle c|, \quad \text{for } r_\alpha, r'_\alpha < a_\alpha, \quad (9.1)$$

where

$$g_c(r, r') = -2\hbar^{-1} \bar{u}_{ac}(r_<) \bar{v}_{ac}(r_>), \quad (9.2)$$

$$\bar{v}_{ac}(r) = \bar{h}_{ac}(r) - s_c \bar{u}_{ac}(r), \quad (9.3)$$

and  $r_<$  ( $r_>$ ) is the smaller (larger) of  $r$  and  $r'$ . The radial



functions  $\bar{u}_{\alpha c}$  and  $\bar{v}_{\alpha c}$  are regular and irregular eigenstates of the partition  $\alpha$  Hamiltonian:

$$(\bar{H}_\alpha - E) |c\rangle \begin{cases} \bar{u}_{\alpha c}(r_\alpha) \\ \bar{v}_{\alpha c}(r_\alpha) \end{cases} = 0 \quad (9.4)$$

and are solutions of the radial wave equation

$$\left[ -\frac{\hbar^2}{2m_c} \left( \frac{1}{r_\alpha} \frac{d^2}{dr_\alpha^2} r_\alpha - \frac{l_c(l_c+1)}{r_\alpha^2} \right) + U_\alpha(r_\alpha) + \frac{Z_\alpha^{(1)} Z_\alpha^{(2)} e^2}{r_\alpha} - E_{\alpha c} \right] \begin{cases} \bar{u}_{\alpha c}(r_\alpha) \\ \bar{v}_{\alpha c}(r_\alpha) \end{cases} = 0. \quad (9.5)$$

The background potential  $U_\alpha$  is a real short-range function of  $r_\alpha$ , which is introduced to provide an additional degree of flexibility in the formalism. For open channels, the asymptotic forms of these radial functions are

$$\bar{u}_{\alpha c}(r_\alpha) \sim \left( \frac{m_{\bar{c}}}{\hbar k_{\bar{c}}} \right)^{1/2} r_\alpha^{-1} \sin(\theta_{\bar{c}} + \bar{\delta}_{\bar{c}}) \quad (9.6)$$

and

$$\bar{v}_{\alpha c}(r_\alpha) \sim \left( \frac{m_{\bar{c}}}{\hbar k_{\bar{c}}} \right)^{1/2} r_\alpha^{-1} \cos(\theta_{\bar{c}} + \bar{\delta}_{\bar{c}}) - s_{\bar{c}} \bar{u}_{\alpha c}, \quad (9.7)$$

where

$$\theta_{\bar{c}} = k_{\bar{c}} r_\alpha - \eta_{\bar{c}} \ln 2k_{\bar{c}} r_\alpha - \frac{1}{2} l_{\bar{c}} \pi \quad (9.8)$$

and

$$k_{\bar{c}} = (2m_{\bar{c}} \hbar^{-2} E_{\alpha c})^{1/2}. \quad (9.9)$$

The phase shift  $\bar{\delta}_{\bar{c}}$  is due to the potential  $U_\alpha$  and the Coulomb interaction, and the remaining quantities are as defined in Sec. II. The parameters  $s_{\bar{c}}$  in Eq. (9.7) can be adjusted to give the desired asymptotic form. The choice  $s_{\bar{c}} = -i$  gives pure outgoing wave asymptotic behavior.

The partition Green's-function operator  $\bar{G}_\alpha$  of Eq. (9.1) is defined to be nonzero only in that part of the inside region where the channel states  $|c\rangle (c \in \alpha)$  are nonvanishing. This region is a cylinder in configuration space having as its cross section the partition  $\alpha$  channel entrance. On the sides of this cylinder  $\bar{G}_\alpha$  will fulfill the same homogeneous boundary conditions as those imposed on the channel states  $|c\rangle$  at the outer boundary of channel entrance  $\alpha$ . Thus Eq. (3.27) must be replaced by

$$\bar{G}_\alpha (E - \bar{H}_\alpha^\dagger) = (E - \bar{H}_\alpha) \bar{G}_\alpha = P_\alpha, \quad (9.10)$$

where

$$P_\alpha = \sum_{c \in \alpha} |c\rangle \langle c|. \quad (9.11)$$

$P_\alpha$  is clearly the projector on to the cylindrical volume within which  $\bar{G}_\alpha$  exists.

To incorporate these partition Green's-function operators into the scattering formalism we need a kind of resol-

vent equation relating them to the system Green's-function operator. This is found by multiplying Eq. (9.10) on the right or left by  $G$  and using Eq. (3.6). The result is a generalized resolvent relation:

$$P_\alpha G = \bar{G}_\alpha + \bar{G}_\alpha (\bar{V}_\alpha + \Delta) G \quad (9.12)$$

or

$$G P_\alpha = \bar{G}_\beta + G (\bar{V}_\beta - \Delta) \bar{G}_\beta, \quad (9.13)$$

where

$$\Delta = H - H^\dagger = \bar{H}_\alpha - \bar{H}_\alpha^\dagger = H_0 - H_0^\dagger. \quad (9.14)$$

The  $\Delta$  arises because  $G$  and the partition Green's-function operators fulfill different asymptotic boundary conditions. The presence of the projectors is due to the fact that the partition Green's-function operator  $\bar{G}_\alpha$  is nonvanishing only in that part of the internal region which is projected onto by  $P_\alpha$ .

In Appendix A we shall present arguments supporting the claim that the  $\Delta$  terms in the resolvent relations become negligible in the limit as the channel radii all become very large. Therefore, we shall ignore such terms in what follows and take the resolvent relations to be

$$P_\alpha G = \bar{G}_\alpha + \bar{G}_\alpha \bar{V}_\alpha G \quad (9.15)$$

and

$$G P_\alpha = \bar{G}_\beta + G \bar{V}_\beta \bar{G}_\beta. \quad (9.16)$$

If we substitute Eq. (9.16) into Eq. (9.15), we find

$$P_\alpha G P_\alpha = \bar{G}_\alpha P_\alpha + \bar{G}_\alpha \hat{X}_{\alpha\beta} \bar{G}_\beta, \quad (9.17)$$

where

$$\hat{X}_{\alpha\beta} = \bar{V}_\alpha + \bar{V}_\alpha G \bar{V}_\beta. \quad (9.18)$$

The quantity  $\hat{X}_{\alpha\beta}$  is the reaction matrix operator of Eq. (3.44). If Eq. (9.17) is substituted into Eq. (3.22) for the  $R$  matrix (the projection operators being quite appropriate in that expansion), which in turn is inserted into Eq. (3.23), the result is

$$Z_{\bar{c}\bar{c}'}^{(\pm)} = \bar{v}_{\alpha c}(a_\alpha) [\delta_{\bar{c}\bar{c}'} - (s_{\bar{c}} \pm i) X_{\bar{c}\bar{c}'}] e^{\mp i \bar{\delta}_{\bar{c}'}} \quad (9.19)$$

where

$$X_{\bar{c}\bar{c}'} = -2\hbar^{-1} \langle \bar{u}_{\alpha c} | \hat{X}_{\alpha\beta} | \bar{u}_{\alpha c'} \rangle \quad (9.20)$$

is identical with Eq. (3.48) with the ket defined by Eq. (3.39).

If all the parameters  $s_{\bar{c}}$  are equal to  $-i$ , the matrix  $X$  is equal to the  $T$  matrix of Eq. (6.72) multiplied by a phase factor  $-e^{-i(\bar{\delta}_{\bar{c}} + \bar{\delta}_{\bar{c}'})}$ . In this case, the reaction matrix operator  $\hat{X}_{\alpha\beta}$  of Eq. (9.18) becomes the transition matrix operator  $\hat{T}_{\alpha\beta}$ , which satisfies the relation

$$\hat{T}_{\alpha\beta} \Phi_{\bar{c}'}^{(+)} = \bar{V}_\alpha \Psi_{\bar{c}'}^{(+)} \quad (\bar{c}' \in \beta). \quad (9.21)$$

Thus, noting that the states  $\Phi_{\bar{c}'}^{(\pm)}$  defined in Sec. IV. D are just

$$2e^{\pm\bar{\delta}_{\bar{c}}}|u_{\alpha\bar{c}}\rangle = 2e^{\pm i\bar{\delta}_{\bar{c}}}|c\rangle u_{\alpha\bar{c}}(r_{\alpha}),$$

we can write Eq. (6.72)

$$\begin{aligned} T_{\bar{c}\bar{c}'} &= (2\hbar)^{-1} \langle \Phi_{\bar{c}}^{(-)} | \hat{T}_{\alpha\beta} | \Phi_{\bar{c}'}^{(+)} \rangle \\ &= 2\hbar^{-1} \langle u_{\alpha\bar{c}} | \hat{T}_{\alpha\beta} | u_{\beta\bar{c}'} \rangle e^{i(\bar{\delta}_{\bar{c}} + \bar{\delta}_{\bar{c}'})} \\ &= -X_{\bar{c}\bar{c}'} e^{i(\bar{\delta}_{\bar{c}} + \bar{\delta}_{\bar{c}'})}. \end{aligned} \quad (9.22)$$

Substituting Eq. (9.22) into Eq. (3.49) for the collision matrix gives

$$\begin{aligned} U_{\bar{c}\bar{c}'} &= \delta_{\bar{c}\bar{c}'} e^{2i\bar{\delta}_{\bar{c}}} - 2iT_{\bar{c}\bar{c}'}, \\ &= \delta_{\bar{c}\bar{c}'} - 2i(\bar{T}_{\bar{c}\bar{c}'} + T_{\bar{c}\bar{c}'}), \end{aligned} \quad (9.23)$$

where

$$\bar{T}_{\bar{c}\bar{c}'} = -\delta_{\bar{c}\bar{c}'} e^{i\bar{\delta}_{\bar{c}}} \sin \bar{\delta}_{\bar{c}} \quad (9.24)$$

is the background potential transition amplitude. For  $s_{\bar{c}}=0$  (all  $\bar{c}$ ) and  $U_{\alpha}=0$ ,  $X$  is the reactance or  $K$  matrix of Sec. II.B.4.

Finally, we shall derive dynamical equations for the reaction matrix operator. This is done by substituting the resolvent relations of Eqs. (9.15) and (9.16) into the definition of the operator  $\hat{X}_{\alpha\beta}$  [Eq. (9.18)]. When the resolvent relation of Eq. (9.15) is used, we find

$$\begin{aligned} \hat{X}_{\alpha\beta} &= \bar{V}_{\alpha} + \bar{V}_{\alpha}(1-P_{\gamma})G\bar{V}_{\beta} + \bar{V}_{\alpha}P_{\gamma}G\bar{V}_{\beta} \\ &= \bar{V}_{\alpha}[1 + (1-P_{\gamma})G\bar{V}_{\beta} + \bar{G}_{\gamma}(\bar{V}_{\beta} - \bar{V}_{\gamma}) + \bar{G}_{\gamma}\hat{X}_{\gamma\beta}], \end{aligned} \quad (9.25)$$

and when Eq. (9.16) is used, we obtain

$$\begin{aligned} \hat{X}_{\alpha\beta} &= \bar{V}_{\alpha} + \bar{V}_{\alpha}G(1-P_{\gamma})\bar{V}_{\beta} + \bar{V}_{\alpha}GP_{\gamma}\bar{V}_{\beta} \\ &= \bar{V}_{\alpha} + \bar{V}_{\alpha}G(1-P_{\gamma})\bar{V}_{\beta} + \hat{X}_{\alpha\gamma}\bar{G}_{\gamma}\bar{V}_{\beta}. \end{aligned} \quad (9.26)$$

If one sets  $(1-P_{\gamma})$  equal to zero in the above equations, the result is what we shall call the Lippmann-Schwinger equations for the reaction matrix operator:

$$\hat{X}_{\alpha\beta} = \bar{V}_{\alpha} + \bar{V}_{\alpha}\bar{G}_{\gamma}(\bar{V}_{\beta} - \bar{V}_{\gamma}) + \bar{V}_{\alpha}\bar{G}_{\gamma}\hat{X}_{\gamma\beta} \quad (9.27a)$$

$$\begin{aligned} &= \bar{V}_{\alpha}\bar{G}_{\gamma}\bar{G}_{\beta}^{-1} + \bar{V}_{\alpha}\bar{G}_{\gamma}\hat{X}_{\gamma\beta} \\ &= \bar{V}_{\alpha}\bar{G}_{\gamma}(E - \bar{H}_{\beta}^{\dagger}) + \bar{V}_{\alpha}\bar{G}_{\gamma}\hat{X}_{\gamma\beta} \end{aligned} \quad (9.27b)$$

and

$$\hat{X}_{\alpha\beta} = \bar{V}_{\alpha} + \hat{X}_{\alpha\gamma}\bar{G}_{\gamma}\bar{V}_{\beta}. \quad (9.27c)$$

Equations (9.27) refer to the "post" form of the reaction matrix operator. The "prior" form would have resulted if we had derived Eqs. (9.17) and (9.18) by substituting Eq. (9.15) into Eq. (9.16) instead of doing the reverse. The "prior" form of the equations is

$$\hat{X}_{\alpha\beta}^{(-)} = \bar{V}_{\beta} + \bar{V}_{\alpha}G\bar{V}_{\beta} \quad (9.28a)$$

$$= \bar{V}_{\beta} + \bar{V}_{\alpha}\bar{G}_{\gamma}\hat{X}_{\gamma\beta}^{(-)} \quad (9.28b)$$

$$= \bar{G}_{\alpha}^{-1}\bar{G}_{\gamma}\bar{V}_{\beta} + \hat{X}_{\alpha\gamma}^{(-)}\bar{G}_{\gamma}\bar{V}_{\beta}. \quad (9.28c)$$

The equations of the above calculable transition operator formalism are identical in form with the equations of the conventional version of many-body scattering theory derived using a time-dependent approach (see, for examples, Ekstein, 1956; Kouri, Krüger, and Levin, 1977b). However, the definitions of the Green's-function operators differ in a significant way. The partition Green's-function operator  $\bar{G}_{\gamma}$  implicitly contains the projector  $P_{\gamma}$ , which approaches the identity as the channel radii become very large. In conventional many-body scattering theory the Green's-function operators contain a convergence parameter  $i\epsilon$ , which is associated with the extension of the wave packets used to define the scattering wave function. The limit  $i\epsilon \rightarrow 0$  is to be performed on the final result, and special care is required when this limit is performed on expressions containing products of Green's-function operators.

The similarity of the equations in both the "calculable" and "conventional" formalisms is a consequence of neglecting terms containing  $(1-P_{\gamma})$  and  $\Delta$  in the former approach. Clearly it is necessary to justify the neglect of these terms. Arguments justifying such neglect are presented in Appendix A.

## X. BKL EQUATIONS

### A. The BKL reaction matrix operator equations

We have succeeded thus far in relating the collision matrix  $\tilde{U}$  to a reaction matrix operator  $\hat{X}$ . The elements of the reaction matrix operator are related to each other by a set of inhomogeneous linear integral equations, the Lippmann-Schwinger (LS) equations. However, the LS equations displayed in Eqs. (9.27) resist any direct attempt at solution.

Equations (9.27) represent a very large set of coupled integral equations due to the complete freedom one has in the choice of indices  $\alpha$ ,  $\beta$ , and  $\gamma$ . The kernel of each of the equations is a nonconnected operator so that it cannot be compact. In addition, while the set of equations as a whole embodies the complete set of asymptotic boundary condition constraints, this may not be true of particular subsets. Thus single LS equations or arbitrary sets of these equations will generally be unsatisfactory choices for scattering dynamical equations. The selection must be made with some care.

The Baer, Kouri, Levin, and Tobocman (BKLT) equations represent a selection of LS equations which should provide a set of dynamical equations that are soluble by standard methods. The BKLT method consists of choosing a set of LS equations such that all two-cluster partitions are coupled to each other sequentially in a closed cycle. By including all two-cluster partitions, one uses all two-cluster partition Green's-function operators, and thus reference is made to every channel entrance. This brings all the asymptotic boundary condition constraints into play. By requiring sequential cyclic coupling we force the equations to be of the connected kernel type.



formulation the property that its first-order approximation is the usual Born approximation  $\hat{V}\hat{U}$  rather than the  $\hat{V}\hat{W}$  term given by the Kouri-Levin formulation.

### B. The BKLT and LS wave-function equations

In this section we shall show how the BKLT reaction matrix operator equations can be transformed into a set of coupled wave-function equations. Ultimately, as shown in Eq. (9.22), one calculates the matrix element of the reaction matrix operator with respect to "distorted"-wave functions  $\Phi_k^{(+)}$ , i.e., regular solutions of Eq. (9.4):

$$(\bar{H}_\gamma - E)\Phi_k^{(+)} = 0 \quad (k \in \gamma) \quad (10.14)$$

having unit current incident in channel  $k (\in \gamma)$  and purely outgoing current in all other channels. So we define system wave-function components that show the effect of the reaction matrix operator acting on such a distorted wave:

$$\hat{X}_{\alpha\gamma}\Phi_k^{(+)} = \bar{V}_\alpha\Psi_{\alpha-1k}^{(+)} \quad (k \in \gamma). \quad (10.15)$$

Combining this equation with Eq. (10.2) gives the result

$$\begin{aligned} \Psi_{\alpha k}^{(+)} &= \bar{G}_\alpha \bar{G}_\gamma^{-1} \Phi_k^{(+)} + \bar{G}_\alpha \bar{V}_\alpha \Psi_{\alpha-1k}^{(+)} \\ &= \Phi_k^{(+)} \delta_{\alpha\gamma} + \bar{G}_\alpha \bar{V}_\alpha \Psi_{\alpha-1k}^{(+)}, \end{aligned} \quad (10.16)$$

where we have used the Lippmann identity (Lippmann, 1956). See Appendix B for a proof of the Lippmann identity. More explicitly, we have the following  $\mathcal{N}$  integral equations:

$$\begin{aligned} \Psi_{\alpha k}^{(+)} &= \bar{G}_\alpha \bar{V}_\alpha \Psi_{\alpha k}^{(+)} \\ \Psi_{\beta k}^{(+)} &= \bar{G}_\beta \bar{V}_\beta \Psi_{\alpha k}^{(+)} \\ \Psi_{\gamma k}^{(+)} &= \Phi_k^{(+)} + \bar{G}_\gamma \bar{V}_\gamma \Psi_{\beta k}^{(+)} \\ \Psi_{\delta k}^{(+)} &= \bar{G}_\delta \bar{V}_\delta \Psi_{\gamma k}^{(+)} \\ &\dots \end{aligned} \quad (10.17)$$

At first sight it appears that the elements of the wave-function matrix can be identified with the system wave function itself. It seems that the greek letter subscript on the system wave-function component is superfluous. However, following the definition we have chosen for the partition Green's-function operators [Eq. (9.1)], it would seem that these components should more properly be identified with projections of the system wave function, i.e.,

$$\Psi_{\alpha k}^{(+)} = P_\alpha \Psi_k^{(+)} \quad (10.18)$$

Equations (10.15) and (10.16) have a convenient form in matrix notation. Equation (10.15) is

$$\hat{X}\Phi_{(k)}^{(+)} = \hat{V}\hat{W}\Psi_{(k)}^{(+)}, \quad (10.19)$$

while Eq. (10.16) is

$$\Psi_{(k)}^{(+)} = \hat{G}\hat{U}\hat{G}^{-1}\Phi_{(k)}^{(+)} + \hat{G}\hat{V}\hat{W}\Psi_{(k)}^{(+)}, \quad (10.20)$$

where

$$(\Phi_{(k)}^{(+)})_\alpha = \Phi_{\alpha k}^{(+)} = \delta_{\alpha\gamma} \Phi_k^{(+)} \quad (k \in \gamma). \quad (10.21)$$

An alternative set of wave-function equations can be derived from Eq. (10.5), which has the formal solution

$$\hat{X} = \hat{V}\hat{U}(\mathbb{1} - \hat{G}\hat{W}\hat{V})^{-1}. \quad (10.22)$$

Substituting this equation into Eq. (10.19) yields

$$\hat{V}\hat{W}\Psi_{(k)}^{(+)} = \hat{V}\hat{U}(\mathbb{1} - \hat{G}\hat{W}\hat{V})^{-1}\Phi_{(k)}^{(+)}. \quad (10.23)$$

Then defining

$$\hat{W}\Psi_{(k)}^{(+)} = \hat{U}\chi_{(k)}^{(+)}, \quad (10.24)$$

we have

$$\begin{aligned} \chi_{(k)}^{(+)} &= (\mathbb{1} - \hat{G}\hat{W}\hat{V})^{-1}\Phi_{(k)}^{(+)} \\ &= \Phi_{(k)}^{(+)} + \hat{G}\hat{W}\hat{V}\chi_{(k)}^{(+)}. \end{aligned} \quad (10.25)$$

In component form these equations read

$$\Psi_k^{(+)} = \sum_\alpha \chi_{\alpha k}^{(+)}, \quad (10.26)$$

where

$$\chi_{\alpha k}^{(+)} = \delta_{\alpha\gamma} \Phi_k^{(+)} + \bar{G}_\alpha \bar{V}_{\alpha-1} \chi_{\alpha-1k}^{(+)} \quad (10.27)$$

and

$$\chi_{(k)}^{(+)T} = (\chi_{\alpha k}^{(+)}, \chi_{\beta k}^{(+)}, \chi_{\gamma k}^{(+)}, \dots). \quad (10.28)$$

These coupled wave-function equations derived from the BKLT reaction operator equations are due to Hahn, Kouri, and Levin (1974). In Eq. (10.26) we have ignored the projector  $P_\alpha$ . Thus Eqs. (10.26)–(10.28) must be understood to hold in the region of configuration space where all the projectors  $P_\alpha, P_\beta, \dots$  overlap.

We shall end this section by deriving the calculable transition operator formalism analog of the LS wave-function equations. We can do this by defining the scattering wave function  $\Psi_k^{(+)}$  by [Eq. (9.21)]:

$$\hat{T}_{\beta\gamma}\Phi_k^{(+)} = \bar{V}_\beta \Psi_k^{(+)} \quad (k \in \gamma). \quad (10.29)$$

Then from the definition of  $\hat{T}$  given by Eq. (9.18) when all the parameters  $s_\epsilon = -i$ , one can deduce that

$$\Psi_k^{(+)} = (1 + G\bar{V}_\gamma)\Phi_k^{(+)}. \quad (10.30)$$

This result is valid for the case where  $G$  fulfills causal or outgoing wave asymptotic boundary conditions. The corresponding expression for a general choice of  $G$  is given by Tobocman (1972).

From Eq. (10.30) we have

$$\Psi_k^{(+)} = G\bar{G}_\gamma^{-1}\Phi_k^{(+)} = G\Delta\Phi_k^{(+)}. \quad (10.31)$$

Operating with  $P_\alpha$  on this equation and using the resolvent relation of Eq. (9.15) gives

$$\begin{aligned} P_\alpha \Psi_k^{(+)} &= \bar{G}_\alpha \bar{G}_\gamma^{-1} \Phi_k^{(+)} + \bar{G}_\alpha \bar{V}_\alpha \Psi_k^{(+)} \\ &= \Phi_k^{(+)} \delta_{\alpha\gamma} + \bar{G}_\alpha \bar{V}_\alpha \Psi_k^{(+)}. \end{aligned} \quad (10.32)$$

This equation is identical in form with the conventional Lippmann-Schwinger wave-function equation except for

the presence of the projection operator  $P_\alpha$  and the definition of  $\bar{G}_\alpha$  [Eq. (9.1)].

### C. Alternative many-body scattering theories

Several other many-body scattering formalisms have been proposed in addition to the BKLT theory and we shall briefly describe some of these.

The formalism of Chandler and Gibson (1977) yields the following dynamical equations for the elements of the transition matrix:

$$\begin{aligned} T_{\tilde{c}\tilde{c}'} &= P_{\tilde{c}} \hat{T}_{\alpha\beta} P_{\tilde{c}'} \\ &= P_{\tilde{c}} \bar{V}_\beta P_{\tilde{c}'} + P_{\tilde{c}} \bar{V}_\alpha (JJ^\dagger)^{-1} \sum_{\gamma} \sum_{\tilde{c}'' \in \gamma} \bar{G}_\gamma P_{\tilde{c}''} T_{\tilde{c}''\tilde{c}'} . \end{aligned} \quad (10.33)$$

Here  $P_{\tilde{c}}$  ( $P_{\tilde{c}'}$ ) is the projector on to channel  $\tilde{c} \in \alpha$  ( $\tilde{c}' \in \beta$ ) and  $J$  is the projector onto that part of Hilbert space spanned by the asymptotic states  $\Phi_{\tilde{c}}^{(+)}$ . The attractive feature of this equation is that  $\bar{G}_\gamma P_{\tilde{c}''}$  appears in place of  $\bar{G}_\gamma$  so that only those terms in the spectral decomposition of  $\bar{G}_\gamma$  belonging to open channels need to be included. The disadvantages are the difficulty in interpreting and calculating the quantity  $(JJ^\dagger)^{-1}$  and the fact that the kernel does not become connected upon iteration.

In the formalism of Bencze (1973), Redish (1974), and Sloan (1972) (BRS), the dynamical equations for the elements of the transition matrix operator are

$$\hat{T}_{\alpha\beta} = V_\beta^\alpha + \sum_{\gamma} K_\gamma^{\alpha 0} G_0 \hat{T}_{\gamma\beta} . \quad (10.34)$$

Here  $V_\beta^\alpha$  is the sum of those interaction potentials which are internal to partition  $\beta$  and external to partition  $\alpha$  and  $G_0$  is the free  $N$ -particle Green's-function operator

$$G_0 = (E - T)^{-1} . \quad (10.35)$$

The operator  $K_\gamma^{\alpha 0}$  is the  $\gamma$ -connected part of the reduced scattering operator

$$K_{\alpha 0}^{(\gamma)} = V_\gamma^\alpha + V_\gamma^\alpha \bar{G}_\gamma \mathcal{Y}_\gamma , \quad (10.36)$$

where  $\mathcal{Y}_\gamma = \mathcal{Y} - \bar{V}_\gamma$ . Thus to evaluate the BRS kernel, it is necessary to calculate the transition amplitude for  $N$  free particles to scatter into a partition  $\alpha$  channel when the Hamiltonian is  $\bar{H}_\gamma = T + \mathcal{Y}_\gamma$  and then to find that part of it which has connectivity  $\gamma$ .

The BRS equations are similar to the Faddeev three-body equations in that in place of the residual interaction  $\bar{V}_\gamma$  and partition Green's-function operators  $\bar{G}_\alpha$  one finds reduced scattering operators and free-particle propagators. However, in the Faddeev equation the reduced scattering operator is the readily calculable two-particle transition operator, while for the BRS many-body equa-

tion it is a rather complicated many-body operator.

In any many-body theory it is necessary to use the solutions of reduced or fewer-than- $N$ -body problems as input for the calculation of the  $N$ -body transition operators. In the BKLT and Chandler-Gibson theories, this fewer-than- $N$ -body information is contained in the partition Green's-function operators. To construct  $\bar{G}_\alpha$  one needs all the eigenstates of  $\bar{H}_\alpha$ . It is expected that those eigenstates of  $\bar{H}_\alpha$  which have energies closest to the energy of the  $N$ -body system being analyzed will make the most important contribution. Thus in these theories one might expect that in dealing with Hamiltonian eigenstates of relatively low excitation one might be better able to use physical intuition to obtain appropriate models and approximations than one would in dealing with the operators  $K_{\alpha 0}^{(\gamma)}$  of the BRS kernel.

Finally, we shall mention the formalism of Yakubovskii (1967). In this method, one is obliged to solve a hierarchical set of equations for operator matrices whose indices label chains of partitions. Consequently, the number of equations to be solved increases rapidly with the number of particles in the system. However, the great advantage of the Yakubovskii formalism is the fact that the solution of the equations is unique. In the other many-body scattering formalisms, one has the possibility of the admixture of spurious solutions which could be generated in a numerical calculation. The possibility of finding spurious solutions for the BKLT equations is discussed in Sec. XV.

In this article we shall discuss in more detail only the BKLT formalism, which is mathematically the simplest of all the many-body  $T$ -matrix formalisms that have been proposed so far. This approach also has the advantage that it is particularly simple to introduce into the BKLT equations the few cluster and the restricted basis approximations.

## XI. VARIATIONAL PRINCIPLES FOR TRANSITION AMPLITUDE

In this section we shall present some variational functionals for the many-body transition amplitude. The requirement that these functionals be stationary will be fulfilled by requiring that the variational scattering wave functions be solutions of either the  $\mathcal{N}$  simultaneous Lippmann-Schwinger (LS) equations [Eq. (10.32)] or the coupled Hahn-Kouri-Levin equations [Eq. (10.25)]. Variational principles of this kind have been published by Tobocman (1974b) and by Kouri and Levin (1975a). However, the functionals that are presented in these papers have some unsatisfactory aspects (Goldflam, Thaler, and Tobocman, 1981). The variational functionals presented here, therefore, will be alternative forms which avoid these difficulties.

### A. Variational functional based on LS equations [Eq. (10.32)]

Consider the following functional for the transition amplitude:

$$\mathcal{F}_{\tilde{c}\tilde{c}'} = \frac{1}{2\hbar} \langle \Phi_{\tilde{c}'}^{(-)} | \bar{V}_\beta | \Phi_{\tilde{c}}^{(+)} \rangle + \frac{\langle \Psi_{\tilde{c}'}^{(-)} | \Lambda_\beta^T \bar{V}_\beta \bar{G}_\beta \bar{V}_\alpha | \Phi_{\tilde{c}}^{(+)} \rangle \langle \Phi_{\tilde{c}'}^{(-)} | \bar{V}_\beta \bar{G}_\alpha \bar{V}_\alpha \Lambda_\alpha | \Psi_{\tilde{c}}^{(+)} \rangle}{2\hbar \langle \Psi_{\tilde{c}'}^{(-)} | \Lambda_\beta^T \bar{V}_\beta \bar{G}_\beta G^{-1} \bar{G}_\alpha \bar{V}_\alpha \Lambda_\alpha | \Psi_{\tilde{c}}^{(+)} \rangle} , \quad (11.1)$$

where

$$\Lambda_\alpha = \prod_{\gamma \neq \alpha} \bar{G}_\gamma \bar{V}_\gamma \quad (11.2)$$

and channels  $\tilde{c}$  and  $\tilde{c}'$  belong to partitions  $\alpha$  and  $\beta$ , respectively. The states  $\Psi_{\tilde{c}}^{(\pm)}$  are trial wave functions corresponding to the states  $\Psi_{\tilde{c}'}^{(\pm)}$ . An arrow over  $G^{-1}$  is unnecessary because the quantity  $\bar{G}_\beta \Delta \bar{G}_\alpha \equiv \bar{G}_\beta (\bar{G}^{-1} - \bar{G}^{-1}) \bar{G}_\alpha$  can be shown to vanish by the same argument used in Appendix A to show that the contribution  $G \Delta \bar{G}_\beta$  to the resolvent relation [Eq. (9.13)] is zero.

The requirement that the first variation of  $\mathcal{T}_{\tilde{c}'\tilde{c}}$ , due to small changes in  $\Psi_{\tilde{c}'}^{(-)}$  near the correct state  $\Psi_{\tilde{c}'}^{(-)}$ , should vanish, i.e.,

$$\delta \mathcal{T}_{\tilde{c}'\tilde{c}} / \delta \Psi_{\tilde{c}'}^{(-)} = 0, \quad (11.3)$$

is satisfied if

$$\bar{V}_\alpha \Phi_{\tilde{c}}^{(+)} = \bar{G}^{-1} \bar{G}_\alpha \bar{V}_\alpha \Lambda_\alpha \Psi_{\tilde{c}}^{(+)} \quad (11.4)$$

Similarly, the requirement that

$$\delta \mathcal{T}_{\tilde{c}'\tilde{c}} / \delta \Psi_{\tilde{c}}^{(+)} = 0, \quad (11.5)$$

is satisfied if

$$\bar{V}_\beta \Phi_{\tilde{c}'}^{(-)} = \bar{G}^{*-1} \bar{G}_\beta^* \bar{V}_\beta \Lambda_\beta^* \Psi_{\tilde{c}'}^{(-)}. \quad (11.6)$$

Equations (11.4) and (11.6) are essentially complex conjugates of each other. Equation (11.4) is obeyed if

$$\Lambda_\alpha \Psi_{\tilde{c}}^{(+)} = \Psi_{\tilde{c}}^{(+)} \quad (11.7)$$

and

## B. Variational functional based on Hahn-Kouri-Levin equations [Eq. (10.25)]

We now consider a variational functional based on the Hahn, Kouri, and Levin (1974) equations instead of the LS equations. Since all the wave-function components are involved, it is convenient to use matrix notation

$$\mathcal{T}_{\tilde{c}'\tilde{c}} = \frac{1}{2\hbar} \langle \Phi_{\tilde{c}'}^{(-)} | \hat{V} \hat{U} | \Phi_{\tilde{c}}^{(+)} \rangle + \frac{\langle \chi'_{\tilde{c}'}^{(-)} | \hat{V} \hat{W}^T \hat{G} \hat{U} \hat{V} | \Phi_{\tilde{c}}^{(+)} \rangle \langle \Phi_{\tilde{c}'}^{(-)} | \hat{V} \hat{U} \hat{G} \hat{W} \hat{V} | \chi'_{\tilde{c}}^{(+)} \rangle}{2\hbar \langle \chi'_{\tilde{c}'}^{(-)} | \hat{V} \hat{W}^T \hat{G} \hat{U} \hat{G}^{-1} \hat{G} \hat{W} \hat{V} | \chi'_{\tilde{c}}^{(+)} \rangle} \quad (11.11)$$

The requirement that this functional be stationary for arbitrary infinitesimal variations of the trial functions  $\chi'_{\tilde{c}'}^{(\pm)}$  yields the equation

$$\hat{U} \hat{V} \Phi_{\tilde{c}}^{(+)} = \hat{U} \mathcal{G}^{-1} \hat{G} \hat{W} \hat{V} \chi'_{\tilde{c}}^{(+)} \quad (11.12)$$

and the complex conjugate equation for  $\chi'_{\tilde{c}'}^{(-)}$ . Since  $\mathcal{G}$  is proportional to the identity matrix, i.e.,

$$\mathcal{G} = G \mathbf{1}, \quad (11.13)$$

it commutes with the matrix  $\hat{U}$ , and Eq. (11.12) can be written

$$\begin{aligned} \bar{V}_\alpha \Phi_{\tilde{c}}^{(+)} &= \bar{G}^{-1} \bar{G}_\alpha \bar{V}_\alpha \Psi_{\tilde{c}}^{(+)} \\ &= (\bar{G}_\alpha^{-1} - \bar{V}_\alpha) \bar{G}_\alpha \bar{V}_\alpha \Psi_{\tilde{c}}^{(+)} \\ &= \bar{V}_\alpha (1 - \bar{G}_\alpha \bar{V}_\alpha) \Psi_{\tilde{c}}^{(+)}. \end{aligned} \quad (11.8)$$

Equations (11.7) and (11.8) are fulfilled by the solution of Eq. (10.32), the  $\mathcal{N}$  simultaneous LS equations.

To complete the verification of Eq. (11.1) as a variational functional for the transition amplitude, we note that if Eqs. (11.4) and (11.7) are valid, then  $\mathcal{T}_{\tilde{c}'\tilde{c}}$  becomes equal to the transition amplitude  $T_{\tilde{c}'\tilde{c}}$ . Substituting Eq. (11.4) into Eq. (11.1) gives

$$\begin{aligned} \mathcal{T}_{\tilde{c}'\tilde{c}} &= \frac{1}{2\hbar} (\langle \Phi_{\tilde{c}'}^{(-)} | \bar{V}_\beta | \Phi_{\tilde{c}}^{(+)} \rangle \\ &\quad + \langle \Phi_{\tilde{c}'}^{(-)} | \bar{V}_\beta \bar{G}_\alpha \bar{V}_\alpha \Lambda_\alpha | \Psi_{\tilde{c}}^{(+)} \rangle). \end{aligned} \quad (11.9)$$

Then using Eqs. (11.7), (10.32), (9.21), and (9.22), we have, for sufficiently large channel radii,

$$\mathcal{T}_{\tilde{c}'\tilde{c}} = \frac{1}{2\hbar} \langle \Phi_{\tilde{c}'}^{(-)} | \bar{V}_\beta | \Psi_{\tilde{c}}^{(+)} \rangle = T_{\tilde{c}'\tilde{c}} \quad (11.10)$$

One of the difficulties with the variational principles of Tobocman (1974b) and of Kouri and Levin (1975a) is that they contain matrix elements of disconnected operators. This is true also of the functionals given in Eqs. (6.76) and (6.79) in the multipartition case being discussed here. These matrix elements are nonconvergent integrals. Thus such expressions appear to be too sensitive to the asymptotic behavior of the trial wave functions to be satisfactory variational functionals. On the other hand, the functional given in Eq. (11.1) has the trial wave functions appearing in matrix elements with connected operators and so should be free of such difficulties.

$$\begin{aligned} \hat{U} \hat{G} \hat{W} \hat{V} \chi'_{\tilde{c}}^{(+)} &= \hat{U} \mathcal{G} \hat{V} \Phi_{\tilde{c}}^{(+)} \\ &= \hat{U} (\hat{G}^{-1} - \hat{V})^{-1} \hat{V} \Phi_{\tilde{c}}^{(+)} \\ &= \hat{U} (\mathbf{1} - \hat{G} \hat{V})^{-1} \hat{G} \hat{V} \Phi_{\tilde{c}}^{(+)}. \end{aligned} \quad (11.14)$$

Now in matrix notation, the LS equation for the scattering wave function is

$$\Psi_{\tilde{c}}^{(+)} = \Phi_{\tilde{c}}^{(+)} + \hat{G} \hat{V} \Psi_{\tilde{c}}^{(+)}, \quad (11.15)$$

so that its formal solution is

$$\begin{aligned} \Psi_{\tilde{c}}^{(+)} &= \hat{U} (\mathbf{1} - \hat{G} \hat{V})^{-1} \Phi_{\tilde{c}}^{(+)} \\ &= \hat{U} \Phi_{\tilde{c}}^{(+)} + \hat{U} (\mathbf{1} - \hat{G} \hat{V})^{-1} \hat{G} \hat{V} \Phi_{\tilde{c}}^{(+)}. \end{aligned} \quad (11.16)$$

Combining Eqs. (11.14) and (11.16) gives

$$\Psi_{(\bar{c})}^{(+)} = \hat{U}\Phi_{(\bar{c})} + \hat{U}\hat{G}\hat{W}\hat{V}\chi_{(\bar{c})}^{(+)} \tag{11.17}$$

In this discussion we are not distinguishing between the components of the partition space vector  $\Psi_{(\bar{c})}^{(+)}$ . Therefore, Eq. (10.24) may be written here as

$$\hat{W}\Psi_{(\bar{c})}^{(+)} = \Psi_{(\bar{c})}^{(+)} = \hat{U}\chi_{(\bar{c})}^{(+)}, \tag{11.18}$$

so that Eq. (11.17) is

$$\hat{U}\chi_{(\bar{c})}^{(+)} = \hat{U}\Phi_{(\bar{c})}^{(+)} + \hat{U}\hat{G}\hat{W}\hat{V}\chi_{(\bar{c})}^{(+)} \tag{11.19}$$

when  $\chi_{(\bar{c})}^{(+)} = \chi_{(\bar{c})}^{(+)}$ . Thus the variational functional is stationary if  $\chi_{(\bar{c})}^{(\pm)}$  are solutions of the Hahn-Kouri-Levin equations [Eq. (10.25)].

If the trial functions  $\chi_{(\bar{c})}^{(\pm)}$  fulfill Eq. (10.25), we have, substituting Eq. (11.12) into Eq. (11.11),

$$\begin{aligned} \mathcal{J}_{\bar{c}'\bar{c}} = \frac{1}{2\hbar} & (\langle \Phi_{(\bar{c}')}^{(-)} | \hat{V}\hat{U} | \Phi_{(\bar{c})}^{(+)} \rangle \\ & + \langle \Phi_{(\bar{c}')}^{(-)} | \hat{V}\hat{U}\hat{G}\hat{W}\hat{V} | \chi_{(\bar{c})}^{(+)} \rangle). \end{aligned} \tag{11.20}$$

Using Eqs. (11.19) and (11.18), we find that this becomes

$$\begin{aligned} \mathcal{J}_{\bar{c}'\bar{c}} = \frac{1}{2\hbar} & \langle \Phi_{(\bar{c}')}^{(-)} | \hat{V} | \Psi_{(\bar{c})}^{(+)} \rangle \\ = \frac{1}{2\hbar} & \langle \Phi_{(\bar{c}')}^{(-)} | \bar{V}_{\beta} | \Psi_{\bar{c}}^{(+)} \rangle = T_{\bar{c}'\bar{c}}, \end{aligned} \tag{11.21}$$

so that  $\mathcal{J}_{\bar{c}'\bar{c}}$  reduces to the transition amplitude  $T_{\bar{c}'\bar{c}}$ .

The variational functional given by Eq. (11.11), unlike that of Eq. (11.1), contains matrix elements of disconnected operators. However, the requirement that the component  $\chi_{\gamma\bar{c}}^{(+)}$  vanish in all asymptotic regions except that belonging to the partition  $\gamma$  is all that is needed to make the matrix elements containing the trial wave functions convergent integrals, provided the energy is below the threshold for three-body breakup.

## XII. EXCHANGE SYMMETRY

### A. BKLT equations including exchange symmetry

In this section we describe how the BKLT many-body scattering formalism of Sec. X can be modified to include the effects of exchange symmetry. The procedure due to Goldflam and Tobocman (1978) will be followed.

Let us suppose that in fact some of the  $N$  particles of the system are physically indistinguishable from each other. If we continue to use distinct labels for all particles, we must now require the system wave functions to be symmetric in some particle coordinates and antisymmetric in others. Then, in addition, sums must be performed over the transition probabilities to physically indistinguishable final states and averages made over physically indistinguishable initial states. It has been shown (Tobocman, 1961) that the consequences of these steps for a many-body scattering formalism can be stated in very simple terms. To do this in the case of the BKLT equa-

tions, it will be necessary to expand out notation somewhat.

When the system contains some indistinguishable particles, some partitions will be physically indistinguishable. Thus we enlarge our partition labels to reflect this fact: The labels  $\alpha(1), \alpha(2), \dots, \alpha(\mathcal{N}_{\alpha})$  will identify a set of two-cluster partitions which are physically indistinguishable. Another set will be  $\beta(1), \beta(2), \dots, \beta(\mathcal{N}_{\beta})$ , and so on. Associated with partition  $\gamma(i)$  will be a set of channels  $c(i), c'(i), c''(i), \dots$ , etc. The channels  $c(1), c(2), \dots, c(\mathcal{N}_{\gamma})$  will be physically indistinguishable.

The consequences of exchange symmetry must be stated in terms of the transition matrix operator  $\hat{T}$  rather than the more general reaction matrix operator  $\hat{X}$  because of the requirements to sum and to average over transition probabilities. What is required is that each class of physically indistinguishable partitions and channels be represented by a particular member, say the one with index 1. In addition, the transition matrix operator is to be replaced by

$$\hat{T}_{\alpha(1)\beta(1)} = \mathcal{N}_{\alpha}^{-1/2} \mathcal{N}_{\beta}^{-1/2} \sum_{n=1}^{\mathcal{N}_{\beta}} (-1)^{\sigma_{\beta(n)}} \hat{T}_{\alpha(1)\beta(n)} P_{\beta}(n) \tag{12.1}$$

or by

$$\hat{T}_{\bar{\alpha}(1)\beta(1)} = \mathcal{N}_{\alpha}^{-1/2} \mathcal{N}_{\beta}^{-1/2} \sum_{n=1}^{\mathcal{N}_{\alpha}} (-1)^{\sigma_{\alpha(n)}} P_{\alpha}^{\dagger}(n) \hat{T}_{\alpha(n)\beta(1)}, \tag{12.2}$$

where  $P_{\alpha}(n)$  is the permutation operator for which

$$P_{\alpha}(n) \Phi_{\bar{c}(1)}^{(+)} = \Phi_{\bar{c}(n)}^{(+)}, \tag{12.3}$$

and  $\sigma_{\alpha(n)}$  is the parity of  $P_{\alpha}(n)$  with respect to fermion exchanges. It is understood that channels  $\bar{c}(1)$  and  $\bar{c}(n)$  belong to partition  $\alpha$ .

Let us now apply this procedure to the BKLT equations of Eq. (10.2), which for the present purposes can be written

$$\begin{aligned} \hat{T}_{\alpha(1)\mu(n)} &= \bar{V}_{\alpha(1)} \bar{G}_{\omega(\mathcal{N}_{\alpha})} (\bar{G}_{\mu(n)}^{-1} + \hat{T}_{\omega(\mathcal{N}_{\alpha})\mu(n)}), \\ \hat{T}_{\alpha(2)\mu(n)} &= \bar{V}_{\alpha(2)} \bar{G}_{\alpha(1)} (\bar{G}_{\mu(n)}^{-1} + \hat{T}_{\alpha(1)\mu(n)}), \\ &\dots \dots \dots \tag{12.4} \\ \hat{T}_{\alpha(\mathcal{N}_{\alpha})\mu(n)} &= \bar{V}_{\alpha(\mathcal{N}_{\alpha})} \bar{G}_{\alpha(\mathcal{N}_{\alpha}-1)} (\bar{G}_{\mu(n)}^{-1} + \hat{T}_{\alpha(\mathcal{N}_{\alpha}-1)\mu(n)}), \\ \hat{T}_{\beta(1)\mu(n)} &= \bar{V}_{\beta(1)} \bar{G}_{\alpha(\mathcal{N}_{\alpha})} (\bar{G}_{\mu(n)}^{-1} + \hat{T}_{\alpha(\mathcal{N}_{\alpha})\mu(n)}), \\ &\dots \dots \dots \end{aligned}$$

Carrying out a partial iteration of these equations so that explicit reference to partitions with index different from 1 is eliminated, we have

$$\begin{aligned} \hat{T}_{\alpha(1)\mu(n)} &= \bar{V}_{\alpha(1)} L_{\omega(1)} \bar{G}_{\mu(n)}^{-1} + \bar{V}_{\alpha(1)} M_{\omega(1)} \bar{G}_{\omega(1)} \hat{T}_{\omega(1)\mu(n)}, \\ \hat{T}_{\beta(1)\mu(n)} &= \bar{V}_{\beta(1)} L_{\alpha(1)} \bar{G}_{\mu(n)}^{-1} + \bar{V}_{\beta(1)} M_{\alpha(1)} \bar{G}_{\alpha(1)} \hat{T}_{\alpha(1)\mu(n)}, \\ &\dots \dots \dots \end{aligned} \tag{12.5}$$

where

$$L_{\alpha(1)} = \bar{G}_{\alpha(\mathcal{N}_\alpha)} + \bar{G}_{\alpha(\mathcal{N}_\alpha)} \bar{V}_{\alpha(\mathcal{N}_\alpha)} \bar{G}_{\alpha(\mathcal{N}_\alpha-1)} + \cdots \\ + \bar{G}_{\alpha(\mathcal{N}_\alpha)} \bar{V}_{\alpha(\mathcal{N}_\alpha)} \bar{G}_{\alpha(\mathcal{N}_\alpha-1)} \cdots \bar{G}_{\alpha(2)} \bar{V}_{\alpha(2)} \bar{G}_{\alpha(1)} \quad (12.6)$$

and

$$M_{\alpha(1)} = \bar{G}_{\alpha(\mathcal{N}_\alpha)} \bar{V}_{\alpha(\mathcal{N}_\alpha)} \bar{G}_{\alpha(\mathcal{N}_\alpha-1)} \cdots \bar{V}_{\alpha(3)} \bar{G}_{\alpha(2)} \bar{V}_{\alpha(2)} \cdot \quad (12.7)$$

Finally, combining Eqs. (12.1) and (12.5)

$$\hat{T}_{\alpha(1)\bar{\mu}(1)} = \bar{V}_{\alpha(1)} L_{\omega(1)} \bar{G}_{\bar{\mu}(1)}^{-1} \\ + \bar{V}_{\alpha(1)} \mathcal{N}_\alpha^{-1/2} M_{\omega(1)} \mathcal{N}_\omega^{-1/2} \bar{G}_{\omega(1)} \hat{T}_{\omega(1)\bar{\mu}(1)}, \quad (12.8)$$

etc., where

$$\bar{G}_{\bar{\mu}(1)}^{-1} = \mathcal{N}_\mu^{-1/2} \sum_{n=1}^{\mathcal{N}_\mu} (-1)^{\sigma_{\mu(n)}} \bar{G}_{\mu(n)}^{-1} P_\mu(n). \quad (12.9)$$

A similar process can be carried out using Eq. (10.3) instead of Eq. (10.2) and Eq. (12.2) in place of Eq. (12.1). The result is

$$\hat{T}_{\bar{\mu}(1)\alpha(1)} = \bar{V}_{\bar{\mu}(1)} \mathcal{N}_\alpha^{-1/2} J_{\alpha(1)} \\ + \hat{T}_{\bar{\mu}(1)\beta(1)} \bar{G}_{\beta(1)} \mathcal{N}_\beta^{-1/2} K_{\alpha(1)} \mathcal{N}_\alpha^{-1/2} \bar{V}_{\alpha(1)}, \quad (12.10)$$

etc., where

$$\bar{V}_{\bar{\mu}(1)} = \mathcal{N}_\mu^{-1/2} \sum_{n=1}^{\mathcal{N}_\mu} (-1)^{\sigma_{\mu(n)}} P_\mu(n)^\dagger \bar{V}_{\mu(n)}, \quad (12.11) \\ J_{\alpha(1)} = 1 + \bar{G}_{\alpha(2)} \bar{V}_{\alpha(1)} + \bar{G}_{\alpha(3)} \bar{V}_{\alpha(2)} \bar{G}_{\alpha(2)} \bar{V}_{\alpha(1)} + \cdots \\ + \bar{G}_{\alpha(\mathcal{N}_\alpha)} \bar{V}_{\alpha(\mathcal{N}_\alpha-1)} \bar{G}_{\alpha(\mathcal{N}_\alpha-2)} \cdots \bar{V}_{\alpha(2)} \bar{G}_{\alpha(2)} \bar{V}_{\alpha(1)}, \quad (12.12)$$

and

$$K_{\alpha(1)} = \bar{V}_{\alpha(\mathcal{N}_\alpha)} \bar{G}_{\alpha(\mathcal{N}_\alpha)} \bar{V}_{\alpha(\mathcal{N}_\alpha-1)} \cdots \bar{G}_{\alpha(3)} \bar{V}_{\alpha(2)} \bar{G}_{\alpha(2)} \cdot \quad (12.13)$$

In Eqs. (12.8) and (12.10) the index 1 can be suppressed, provided that it is understood that reference is made to particular physically distinguishable partitions only. The same convention can be applied to the channel indices on wave functions. Then we can write these equations in the form:

$$A = \bar{V}_{\alpha(1)} (-1)^{\sigma_{\alpha(\mathcal{N}_\alpha)}} P_{\alpha(\mathcal{N}_\alpha)} + \bar{V}_{\alpha(1)} \bar{G}_{\alpha(\mathcal{N}_\alpha)} \bar{V}_{\alpha(\mathcal{N}_\alpha)} (-1)^{\sigma_{\alpha(\mathcal{N}_\alpha-1)}} P_{\alpha(\mathcal{N}_\alpha-1)} \\ + \cdots + \bar{V}_{\alpha(1)} \bar{G}_{\alpha(\mathcal{N}_\alpha)} \bar{V}_{\alpha(\mathcal{N}_\alpha)} \bar{G}_{\alpha(\mathcal{N}_\alpha-1)} \cdots \bar{G}_{\alpha(2)} \bar{V}_{\alpha(2)} \bar{G}_{\alpha(1)} \quad (12.22)$$

and

$$B = \bar{V}_{\alpha(1)} \bar{G}_{\alpha(\mathcal{N}_\alpha)} \bar{V}_{\alpha(\mathcal{N}_\alpha)} \bar{G}_{\alpha(\mathcal{N}_\alpha-1)} \cdots \bar{V}_{\alpha(3)} \bar{G}_{\alpha(2)} \bar{V}_{\alpha(2)} \bar{G}_{\alpha(1)} \cdot \quad (12.23)$$

$$\hat{T}_{\alpha\bar{\mu}} = \hat{V}_\alpha \mathcal{N}_\alpha^{-1/2} \bar{G}_{\bar{\mu}}^{-1} + \bar{V}_\alpha \mathcal{N}_\alpha^{-1/2} M_{\omega} \mathcal{N}_\omega^{-1/2} \bar{G}_\omega \hat{T}_{\omega\bar{\mu}} \quad (12.14)$$

and

$$\hat{T}_{\bar{\mu}\alpha} = \bar{V}_{\bar{\mu}} \mathcal{N}_\alpha^{-1/2} J_\alpha + \hat{T}_{\bar{\mu}\beta} \bar{G}_{\beta} \mathcal{N}_\beta^{-1/2} K_{\alpha} \mathcal{N}_\alpha^{-1/2} \bar{V}_\alpha \cdot \quad (12.15)$$

In matrix notation these equations become

$$\tilde{T} = \hat{V} \mathcal{N}^{-1/2} \hat{W} \hat{L} \hat{U} \hat{G}^{-1} + \hat{V} \mathcal{N}^{-1/2} \hat{W} \hat{M} \mathcal{N}^{-1/2} \hat{G} \tilde{T} \quad (12.16)$$

and

$$\tilde{T} = \tilde{V} \hat{U} \mathcal{N}^{-1/2} \hat{J} + \tilde{T} \hat{G} \mathcal{N}^{-1/2} \hat{W} \hat{K} \mathcal{N}^{-1/2} \hat{V}, \quad (12.17)$$

where all matrices are diagonal in partition space except  $\hat{U}$ ,  $\hat{W}$ , and  $\tilde{T}$ .

## B. Single-clustering approximation

A frequently used approximation for low-energy nuclear scattering is the single-clustering model. In this model it is assumed that both the target and the projectile remain in their ground states throughout the collision process. When this approximation is imposed on the wave function in the Schrödinger equation, the result is a resonating group method (RGM) equation (Wheeler, 1937a, 1937b).

Let us impose the single-clustering approximation on the antisymmetrized BKLT equations. To do this we take Eq. (12.14) and (i) eliminate reference to all but one partition and (ii) in the partition Green's-function operators eliminate all the terms except the one which refers to the ground state of the target and the projectile. Thus we have

$$\hat{T}_{\alpha\bar{\alpha}} = \bar{V}_\alpha \mathcal{N}_\alpha^{-1/2} L_\alpha \bar{G}_{\bar{\alpha}}^{-1} + \bar{V}_\alpha M_\alpha \bar{G}_\alpha \hat{T}_{\alpha\bar{\alpha}}, \quad (12.18)$$

where

$$\bar{G}_\alpha = |\bar{c}\rangle g_\alpha^{(+)}(r_\alpha, r'_\alpha) \langle \bar{c}| \cdot \quad (12.19)$$

Similarly

$$\hat{T}_{\bar{\alpha}\alpha} = \bar{V}_{\bar{\alpha}} \mathcal{N}_\alpha^{-1/2} J_\alpha + \hat{T}_{\bar{\alpha}\alpha} \bar{G}_\alpha K_\alpha \bar{V}_\alpha \cdot \quad (12.20)$$

Using the definitions of  $L_\alpha$  and  $M_\alpha$  [Eqs. (12.6) and (12.7)], we can write Eq. (12.18)

$$\hat{T}_{\alpha\bar{\alpha}} = A + B \hat{T}_{\alpha\bar{\alpha}}, \quad (12.21)$$

where



Similarly, using the definitions of  $J_\alpha$  and  $K_\alpha$  [Eqs. (12.12) and (12.13)], we can write Eq. (12.20)

$$\hat{T}_{\bar{\alpha}\alpha} = C + D\hat{T}_{\bar{\alpha}\alpha}, \quad (12.24)$$

where

$$C = \sum_{n=1}^{\mathcal{N}_\alpha} (-1)^{\sigma_{\alpha(n)}} P_\alpha(n)^\dagger \bar{V}_{\alpha(n)} \\ \times (1 + \bar{G}_{\alpha(2)} \bar{V}_{\alpha(1)} + \bar{G}_{\alpha(3)} \bar{V}_{\alpha(2)} \bar{G}_{\alpha(2)} \bar{V}_{\alpha(1)} + \cdots + \bar{G}_{\alpha(\mathcal{N}_\alpha)} \bar{V}_{\alpha(\mathcal{N}_\alpha-1)} \bar{G}_{\alpha(\mathcal{N}_\alpha-1)} \cdots \bar{V}_{\alpha(2)} \bar{G}_{\alpha(2)} \bar{V}_{\alpha(1)}) \quad (12.25)$$

and

$$D = \bar{G}_{\alpha(1)} \bar{V}_{\alpha(\mathcal{N}_\alpha)} \bar{G}_{\alpha(\mathcal{N}_\alpha)} \bar{V}_{\alpha(\mathcal{N}_\alpha-1)} \cdots \bar{G}_{\alpha(3)} \bar{V}_{\alpha(2)} \bar{G}_{\alpha(2)} \bar{V}_{\alpha(1)}. \quad (12.26)$$

It is seen that in the single-clustering approximation the antisymmetrized BKLT equations represent the scattering process as a succession of knockout processes in which the system passes cyclically through all rearrangements of the incident configuration. The matrix element required in such a calculation is

$$\mathcal{M}_{\bar{c}\bar{c}'}^{(n)} = \langle \bar{u}_{\alpha\bar{c}(1)} | \bar{V}_{\alpha(1)} P_\alpha(n) | \bar{u}_{\alpha\bar{c}'(1)} \rangle, \quad (12.27)$$

where  $|\bar{u}_{\alpha\bar{c}(1)}\rangle$  is defined by Eqs. (3.39) and (9.5).

It is interesting to compare these results with the expressions given by the RGM. In the RGM, the transition matrix operator is defined by

$$\hat{T}_{\bar{\alpha}\bar{\alpha}} \Phi_{\bar{c}(1)}^{(+)} = \bar{V}_{\alpha(1)} A_\alpha \Psi_{\bar{c}(1)}^{(+)}, \quad (12.28)$$

where

$$A_\alpha = \sum_{n=1}^{\mathcal{N}_\alpha} (-1)^{\sigma_{\alpha(n)}} P_\alpha(n) \quad (12.29)$$

and

$$\Psi_{\bar{c}(1)}^{(+)} = |\bar{c}(1)\rangle w_{\alpha\bar{c}(1)}(r_\alpha). \quad (12.30)$$

The Schrödinger equation is used to determine  $w_{\alpha\bar{c}(1)}(r_\alpha)$ . Thus, since

$$[A_\alpha, H] = 0, \quad (12.31)$$

we have

$$(\bar{c}(1) | (H - E) A_\alpha | w_{\alpha\bar{c}(1)}) = 0. \quad (12.32)$$

To facilitate comparison, we transform this into an integral equation for  $\hat{T}_{\bar{\alpha}\bar{\alpha}}$ . Equation (12.32) can be written in the form

$$(\bar{c}(1) | \bar{H}_{\alpha(1)} - E | w_{\alpha\bar{c}(1)}) = (\bar{c}(1) | W_\alpha | w_{\alpha\bar{c}(1)}), \quad (12.33)$$

$$\hat{T}_{\alpha(1)\beta(1)} = \mathcal{N}_\alpha^{1/2} \mathcal{N}_\beta^{1/2} \sum_{n=1}^{\mathcal{N}_\beta} (-1)^{\sigma_{\beta(n)}} (\bar{V}_{\alpha(1)} + \hat{T}_{\alpha(1)\gamma(j)} \bar{G}_{\gamma(j)} \bar{V}_{\beta(n)}) P_\beta(n) \\ = \mathcal{N}_\alpha^{1/2} \mathcal{N}_\beta^{-1/2} (\bar{V}_{\alpha(1)} A_\beta + T_{\alpha(1)\gamma(j)} \bar{G}_{\gamma(j)} A_\beta \bar{V}_{\beta(1)}), \quad (12.38)$$

where

$$W_\alpha = (\bar{H}_{\alpha(1)} - E) - (H - E) A_\alpha \\ = (\bar{H}_{\alpha(1)} - E)(1 - A_\alpha) - \bar{V}_{\alpha(1)} A_\alpha. \quad (12.34)$$

The formal solution of Eq. (12.32) is

$$\Psi_{\bar{c}(1)}^{(+)} = \Phi_{\bar{c}(1)}^{(+)} + \bar{G}_{\alpha(1)} W_\alpha \Psi_{\bar{c}(1)}^{(+)} \\ = (1 - \bar{G}_{\alpha(1)} W_\alpha)^{-1} \Phi_{\bar{c}(1)}^{(+)}, \quad (12.35)$$

which, when substituted into Eq. (12.38), gives

$$\hat{T}_{\bar{\alpha}\bar{\alpha}} = \bar{V}_{\alpha(1)} A_\alpha (1 - \bar{G}_{\alpha(1)} W_\alpha)^{-1} \\ = \bar{V}_{\alpha(1)} A_\alpha + G_{\alpha(1)} [(\bar{H}_{\alpha(1)} - E)(1 - A_\alpha) \\ - \bar{V}_{\alpha(1)} A_\alpha] \hat{T}_{\bar{\alpha}\bar{\alpha}}. \quad (12.36)$$

The RGM equation [Eq. (12.36)] is rather different from the single-clustering approximation to the antisymmetrized BKLT (SCABKLT) equation [Eq. (12.21)]. First, the RGM has a so-called nonorthogonality interaction  $(\bar{H}_{\alpha(1)} - E)(1 - A_\alpha)$  which is absent from the SCABKLT formalism. Second, only  $\bar{G}_{\alpha(1)}$  appears in the RGM, whereas all the  $\bar{G}_{\alpha(n)}$   $\{n=1, 2, \dots, \mathcal{N}_\alpha\}$  appear in the SCABKLT equation. Thus the RGM suppresses intermediate-state propagation in the rearrangement channels, while the SCABKLT approach does not. Finally, the RGM includes in the kernel contributions from elastic processes along with the knockout contribution. The SCABKLT method has only knockout process contributions. The elastic matrix elements are

$$\mathcal{M}_{\bar{c}\bar{c}'}^{(1)} = \langle \bar{u}_{\alpha\bar{c}(1)} | \bar{V}_{\alpha(1)} | \bar{u}_{\alpha\bar{c}'(1)} \rangle. \quad (12.37)$$

We end this section by showing that if one makes an exchange symmetry reduction of the LS equations [Eqs. (9.27)] without first imposing the BKLT partition coupling scheme, then a single-clustering approximation of the reduced LS equations does give expressions which are quite similar to the RGM equation. We shall follow the method of Tobocman (1975b).

Applying exchange symmetry reduction to Eq. (9.27c), we have

where we have used

$$\bar{V}_{\beta(n)} P_{\beta}(n) = P_{\beta}(n) \bar{V}_{\beta(1)} . \quad (12.39)$$

Next we make the substitution

$$\bar{G}_{\gamma(j)} = P_{\gamma}(j) \bar{G}_{\gamma(1)} P_{\gamma}(j)^{\dagger} \quad (12.40)$$

and take note of the fact that  $P_{\gamma}(j)^{\dagger}$  will be operating to the right on the state  $A_{\beta} \bar{V}_{\beta(1)} | \Phi_{\bar{c}^{(1)}}^{(+)} \rangle$ . By virtue of the definition of  $A_{\beta}$  and the fact that  $\Phi_{\bar{c}^{(1)}}^{(+)}$  is to be chosen antisymmetric with respect to intracluster permutations, the state  $A_{\beta} \bar{V}_{\beta(1)} | \Phi_{\bar{c}^{(1)}}^{(+)} \rangle$  is completely antisymmetric with respect to fermion exchange. Thus  $P_{\gamma}(j)^{\dagger}$  acting on this state will have the same effect as its inverse  $P_{\gamma}(j)$ , namely, it will simply produce a factor of  $(-1)^{\sigma_{\gamma j}}$ . Therefore, Eq. (12.38) may be replaced by

$$\begin{aligned} \hat{T}_{\alpha(1)\bar{\beta}(1)} &= \mathcal{N}_{\alpha}^{-1/2} \mathcal{N}_{\beta}^{-1/2} [ \bar{V}_{\alpha(1)} A_{\beta} + \hat{T}_{\alpha(1)\gamma(j)} P_{\gamma}(j) \bar{G}_{\gamma(1)} P_{\gamma}(j)^{\dagger} A_{\beta} \bar{V}_{\beta(1)} ] \\ &= \mathcal{N}_{\alpha}^{-1/2} \mathcal{N}_{\beta}^{-1/2} [ \bar{V}_{\alpha(1)} A_{\beta} + \hat{T}_{\alpha(1)\gamma(j)} (-1)^{\sigma_{\gamma j}} P_{\gamma}(j) \bar{G}_{\gamma(1)} A_{\beta} \bar{V}_{\beta(1)} ] . \end{aligned} \quad (12.41)$$

This equation is valid for any choice of the  $\mathcal{N}_{\gamma}$  possible values of  $\gamma(j)$ . Thus averaging both sides of Eq. (12.41) with respect to the index  $j$  gives

$$\begin{aligned} \hat{T}_{\alpha(1)\bar{\beta}(1)} &= \mathcal{N}_{\alpha}^{-1/2} \mathcal{N}_{\beta}^{-1/2} \left[ \bar{V}_{\alpha(1)} A_{\beta} + \mathcal{N}_{\gamma}^{-1} \sum_{j=1}^{\mathcal{N}_{\gamma}} \hat{T}_{\alpha(1)\gamma(j)} (-1)^{\sigma_{\gamma j}} P_{\gamma}(j) \bar{G}_{\gamma(1)} A_{\beta} \bar{V}_{\beta(1)} \right] \\ &= \mathcal{N}_{\alpha}^{-1/2} \mathcal{N}_{\beta}^{-1/2} \bar{V}_{\alpha(1)} A_{\beta} + \mathcal{N}_{\gamma}^{-1/2} \mathcal{N}_{\beta}^{-1/2} \hat{T}_{\alpha(1)\bar{\gamma}(1)} \bar{G}_{\gamma(1)} A_{\beta} \bar{V}_{\beta(1)} . \end{aligned} \quad (12.42)$$

A similar analysis applied to Eq. (9.27b) yields

$$\hat{T}_{\bar{\alpha}(1)\beta(1)} = \mathcal{N}_{\gamma}^{-1/2} \mathcal{N}_{\alpha}^{-1/2} \bar{V}_{\alpha(1)} A_{\alpha}^{\dagger} \bar{G}_{\gamma(1)} (\mathcal{N}_{\gamma}^{-1/2} \mathcal{N}_{\beta}^{-1/2} A_{\gamma}^{\dagger} \bar{G}_{\beta}^{-1} + \hat{T}_{\bar{\gamma}(1)\beta(1)}) . \quad (12.43)$$

In the single-clustering approximation, these equations become

$$\hat{T}_{\bar{\alpha}\bar{\alpha}} = \bar{V}_{\alpha(1)} A_{\alpha} + \mathcal{N}_{\alpha}^{-1} \hat{T}_{\bar{\alpha}\bar{\alpha}} \bar{G}_{\alpha(1)} A_{\alpha} \bar{V}_{\alpha(1)} \quad (12.44)$$

and

$$\begin{aligned} \hat{T}_{\bar{\alpha}\bar{\alpha}} &= \mathcal{N}_{\alpha}^{-1} \bar{V}_{\alpha(1)} A_{\alpha}^{\dagger} \bar{G}_{\alpha(1)} (A_{\alpha}^{\dagger} \bar{G}_{\alpha(1)}^{-1} + \hat{T}_{\bar{\alpha}\bar{\alpha}}) \\ &= \mathcal{N}_{\alpha}^{-1} \bar{V}_{\alpha(1)} A_{\alpha}^{\dagger} (1 + \bar{G}_{\alpha(1)} \hat{T}_{\bar{\alpha}\bar{\alpha}}) , \end{aligned} \quad (12.45)$$

where we have used the Lippmann identity to simplify Eq. (12.45).

These equations are similar to the RGM equation in that they have the interaction  $\bar{V}_{\alpha(1)} A_{\alpha}$  in the driving term and in the kernel. They differ from the RGM equation in that the nonorthogonality term is absent and factors of  $\mathcal{N}_{\alpha}$  are present. In a test calculation of dineutron-dineutron scattering (Raphael, Tandy, and Tobocman, 1976), Eqs. (12.44) and (12.45) were compared with the RGM equation [Eq. (12.36)]. Equation (12.44) gave results which were similar to the RGM, while the cross section calculated from Eq. (12.45) was much smaller. Evidently, the factor of  $\mathcal{N}_{\alpha}^{-1}$  in the driving term of Eq. (12.45) caused the small result. Adhikari and Glöckle (1980) have suggested that the  $\mathcal{N}_{\alpha}^{-1}$  factor in the kernel will lead to important disagreement with the RGM for heavy nuclei where  $\mathcal{N}_{\alpha}$  is very large. However, it may be that the factor  $\mathcal{N}_{\alpha}^{-1}$  in the kernel acts to compensate for the missing nonorthogonality term.

### XIII. FEW-CLUSTER AND RESTRICTED BASIS MODELS

We have formulated what we call a calculable set of dynamical equations for the transition operators of a many-body system. They are calculable in the sense that we use spectral decompositions in terms of channel states for the partition Green's functions and that the integral equations decouple and acquire connected kernels when iterated. Of course, there is still the inescapable complication of having many dynamical degrees of freedom. Thus one is interested in simple models for the dynamics of many-body systems which reduce drastically the number of degrees of freedom.

One such model which has proved to be very useful is the few-cluster model. One attractive feature of the BKLT many-body scattering formalism is that the few-cluster approximation can be imposed in a very simple and natural manner. In addition, one obtains "embedding equations" which relate the model transition operators to the exact ones. The embedding equations thus provide a basis for calculating corrections to the few-cluster model.

Another model which can be treated in a similar way is the restricted basis or shell model of scattering reactions, which assumes that all dynamical processes take place in a region of Hilbert space spanned by a given set of product bound-state wave functions. The continuum state process contributions neglected by this model can be estimated with the help of the embedding equation.

The technique we use is a multipartition generalization of the Feshbach projection operator formalism (Goldflam

and Tobocman, 1979). The basic equations can be derived in just a few steps. First, Eq. (12.16) can be written in the following simplified form:

$$\tilde{T} = \hat{A} + \hat{B}\hat{G}\tilde{T}, \tag{13.1}$$

where

$$\hat{A} = \hat{V}\mathcal{N}^{1/2}\hat{W}\hat{L}\hat{U}\hat{G}^{-1}, \tag{13.2}$$

$$\hat{B} = \hat{V}\mathcal{N}^{1/2}\hat{W}\hat{M}\mathcal{N}^{-1/2}, \tag{13.3}$$

and the matrix operators  $\hat{V}$ ,  $\mathcal{N}^{1/2}$ ,  $\hat{W}$ ,  $\hat{L}$ ,  $\hat{M}$ ,  $\hat{U}$ , and  $\hat{G}$  are defined in Sec. X or XII. Next we introduce an auxiliary operator  $\tau$  which is a solution of

$$\tau = \hat{B} + \hat{B}\hat{G}\tau. \tag{13.4}$$

Then  $\tau$  and  $\tilde{T}$  are related by

$$\tilde{T} = \hat{A} + \tau\hat{G}\hat{A}. \tag{13.5}$$

Defining the wave matrix operator  $\Omega$  by

$$\tau = \Omega\hat{B}, \tag{13.6}$$

we have

$$\Omega = \mathbb{1} + \hat{B}\hat{G}\Omega \tag{13.7}$$

and

$$\tilde{T} = \hat{A} + \Omega\hat{B}\hat{G}\hat{A}. \tag{13.8}$$

Thus we have replaced our dynamical equation for the transition matrix [Eq. (13.1)] by an equation for the wave matrix operator [Eq. (13.7)].

Now let us introduce the model wave matrix operator  $\Omega^M$ , the wave matrix for the model dynamical system:

$$\Omega^M = \mathbb{1} + \hat{B}^M\hat{G}^M\Omega^M = \mathbb{1} + \Omega^M\hat{B}^M\hat{G}^M, \tag{13.9}$$

where  $\hat{B}^M\hat{G}^M$  will be the approximation to  $\hat{B}\hat{G}$  provided by the model. To relate the model wave matrix to the exact one we note that

$$\Omega^M(\hat{B}^M\hat{G}^M - \hat{B}\hat{G})\Omega = (\Omega^M - \mathbb{1})\Omega - \Omega^M(\Omega - \mathbb{1}), \tag{13.10}$$

so that

$$\Omega = \Omega^M + \Omega^M(\hat{B}\hat{G} - \hat{B}^M\hat{G}^M)\Omega. \tag{13.11}$$

This is the embedding equation.

The basic idea is as follows. First of all, Eq. (13.9) is solved for the model wave operator  $\Omega^M$ . Then the embedding equation [Eq. (13.11)] is employed to improve this approximate wave matrix operator, and the result is substituted into Eq. (13.8) to obtain the transition matrix operator.

The model system results from restricting the region of Hilbert space to which dynamical development is permitted to carry the system. This is implemented by using a projection operator matrix  $\hat{P}$  on the partition Green's-function operator matrix, i.e.,

$$\hat{G}^M = \hat{G}\hat{P}. \tag{13.12}$$

We take  $\hat{P}$  to be a diagonal matrix like  $\hat{G}$  so that

$$\hat{G}\hat{P} = \begin{pmatrix} \bar{G}_\alpha \hat{P}_\alpha & 0 & 0 & \dots \\ 0 & \bar{G}_\beta \hat{P}_\beta & 0 & \dots \\ 0 & 0 & \bar{G}_\gamma \hat{P}_\gamma & \dots \\ \dots & \dots & \dots & \dots \end{pmatrix}. \tag{13.13}$$

The operator  $\hat{B}^M$  is defined by replacing  $\hat{G}$  by  $\hat{G}^M$  in Eq. (13.13), i.e., replacing  $\bar{G}_\alpha, \bar{G}_\beta, \dots$  by  $\bar{G}_\alpha \hat{P}_\alpha, \bar{G}_\beta \hat{P}_\beta, \dots$ , respectively, in the operator  $\hat{M}$ . In addition, it may be necessary to replace the partition coupling array  $\hat{W}$  in  $\hat{B}$  by a model partition coupling array  $\hat{W}^M$ .

The Green's-function operators  $\bar{G}_\alpha, \bar{G}_\beta, \dots$  describe the propagation of the system through the various possible intermediate states between the transitions caused by  $\bar{V}_\alpha, \bar{V}_\beta, \dots$ . The projection operators  $\hat{P}_\alpha, \hat{P}_\beta, \dots$  restrict the choice of intermediate states. In the restricted basis model we take

$$\hat{P} = \hat{P}_\alpha = \hat{P}_\beta = \dots = \sum_n |\chi_n\rangle\langle\chi_n|, \tag{13.14}$$

where the  $\chi_n$  are an orthonormal set of wave functions. Ordinarily, one chooses  $\chi_n$  to be a product of harmonic-oscillator wave functions.

To implement the few-cluster approximation we first choose a set of few-cluster state configurations which we believe to have the greatest importance for the system being considered. This has been called the "reaction mechanism" by Polyzou and Redish (1979). Then we set equal to zero every partition projector  $\hat{P}_\gamma$  belonging to a partition  $\gamma$  which cannot be subdivided so as to yield one of the few-cluster configurations contained in the reaction mechanism. All other  $\hat{P}_\gamma$ 's are nonzero and are chosen to project onto those few-cluster state configurations belonging to the reaction mechanism. The projector  $\hat{P}_\gamma$  should include all open partition  $\gamma$  channel asymptotic states.

For example, suppose we are analyzing the scattering of protons by  ${}^6\text{Li}$  at energies well below the  $n + {}^6\text{Be}$  threshold. In this case the only open channels are the  $p + {}^6\text{Li}$ , the  $d + {}^5\text{Li}$ , and the  ${}^3\text{He} + {}^4\text{He}$  channels. Let us label the partitions in the following way:

$$\begin{aligned} \alpha &\equiv (p)(3p, 3n), \\ \beta &\equiv (2p, n)(2p, 2n), \\ \gamma &\equiv (p, n)(3p, 2n), \\ \delta &\equiv (n)(4p, 2n), \\ &\dots \end{aligned} \tag{13.15}$$

So for our problem we might choose the reaction mechanism to be  $\alpha + d + p$ . Then partitions  $\alpha, \beta$ , and  $\gamma$  belong to this reaction mechanism, while partition  $\delta$  does not i.e.,

$$\begin{aligned}
\alpha &\approx (p)(\alpha, d), \\
\beta &\approx (p, d)(\alpha), \\
\gamma &\approx (d)(p, \alpha).
\end{aligned} \tag{13.16}$$

For this case we would take

$$\begin{aligned}
\hat{P}_\alpha &\approx |\chi_p \chi_{6_{Li}}\rangle \langle \chi_p \chi_{6_{Li}}|, \\
\hat{P}_\beta &\approx |\chi_{3_{He}} \chi_{4_{He}}\rangle \langle \chi_{3_{He}} \chi_{4_{He}}|, \\
\hat{P}_\gamma &\approx |\chi_d \chi_{5_{Li}}\rangle \langle \chi_d \chi_{5_{Li}}|, \\
\hat{P}_\delta &\approx 0.
\end{aligned} \tag{3.17}$$

For the few-cluster approximation, the model partition coupling array  $\hat{W}^M$  must be chosen to couple only those partitions  $\gamma$  for which the partition projector  $\hat{P}_\gamma$  does not vanish. Choosing  $\hat{W}^M$  to cycle sequentially through all such partitions is sufficient to make the model dynamical equations such that they become uncoupled connected kernel equations after  $\hat{N}$  iterations (Tobocman, 1974b). Here  $\hat{N}$  is the number of partitions  $\gamma$  having a nonvanishing partition projector  $\hat{P}_\gamma$ .

For the case when none of the projection operators  $\hat{P}_\gamma$  vanishes the procedure can be simplified considerably. In this case it is not necessary to construct a model partition coupling array to replace the original. One can simply introduce  $\hat{P}$  and  $\hat{Q} = \mathbb{1} - \hat{P}$  into the dynamical equation, Eq. (13.1), directly. One obtains

$$\begin{aligned}
\tilde{T} &= \hat{A} + \hat{B}\hat{G}(\hat{P} + \hat{Q})\tilde{T} \\
&= \Omega^P \hat{A} + \Omega^P \hat{B}\hat{G}\hat{Q}\tilde{T},
\end{aligned} \tag{13.18}$$

$$\begin{aligned}
\Omega^P &= (\mathbb{1} - \hat{B}\hat{G}\hat{P})^{-1} \\
&= \mathbb{1} + \hat{B}\hat{G}\hat{P}\Omega^P.
\end{aligned} \tag{13.19}$$

Then Eq. (13.19) can be regarded as the approximate dynamical equation, and Eq. (13.18) is the embedding equation. Alternatively,  $\hat{P}$  and  $\hat{Q}$  can be interchanged. Then

$$\tilde{T} = \Omega^Q \hat{A} + \Omega^Q \hat{B}\hat{G}\hat{P}\tilde{T} \tag{13.20}$$

is the exact dynamical equation, and  $\Omega^Q \hat{A}$  and  $\Omega^Q \hat{B}$  are regarded as effective interaction potentials with

$$\begin{aligned}
\Omega^Q &= (\mathbb{1} - \hat{B}\hat{G}\hat{Q})^{-1} \\
&= \mathbb{1} + \hat{B}\hat{G}\hat{Q}\Omega^Q.
\end{aligned} \tag{13.21}$$

So instead of using the embedding equation to calculate corrections to the approximate transition operator  $\tilde{T}^P = \Omega^P \hat{A}$ , one uses Eq. (13.21) to generate the corrections  $\hat{B}\hat{G}\hat{Q}\Omega^Q \hat{A}$  and  $\hat{B}\hat{G}\hat{Q}\Omega^Q \hat{B}$  to the approximate effective interaction potentials  $\hat{A}$  and  $\hat{B}$ .

#### XIV. BREAKUP REACTION CHANNELS

In the foregoing discussion we have treated breakup channels on the same footing as two-cluster or "bound-state" channels. Both are described by asymptotic states

which are eigenstates of the same two-cluster partition Hamiltonian. In this section we show that  $n$ -cluster channels can be described by asymptotic states which are eigenstates of  $n$ -cluster partition Hamiltonians. This will represent a simplification in the specification of breakup channels.

#### A. $T$ -matrix including breakup channels explicitly

Consider the transition amplitude for a transition from channel  $\tilde{c} \in \alpha$  to channel  $\tilde{c}' \in \beta$ . We have [Eq. (9.22)]

$$\begin{aligned}
T_{\tilde{c}'\tilde{c}} &= \frac{1}{2\hbar} \langle \Phi_{\tilde{c}'}^{(-)} | \bar{V}_\beta (1 + G\bar{V}_\alpha) | \Phi_{\tilde{c}}^{(+)} \rangle \\
&= \frac{1}{2\hbar} \langle \Phi_{\tilde{c}'}^{(-)} | \bar{V}_\beta G \bar{G}_\alpha^{-1} | \Phi_{\tilde{c}}^{(+)} \rangle.
\end{aligned} \tag{14.1}$$

Suppose channel  $\tilde{c}$  is an  $n$ -cluster breakup channel. Let us make our notation more explicit in this regard by writing

$$\Phi_{\tilde{c}}^{(+)} \equiv \Phi_{\alpha_2 \tilde{c}_n}^{(+)\alpha}. \tag{14.2}$$

This notation endows the distorted-wave function with three indices and provides subscripts for both the partition and channel indices, which in turn are written as subscripts. The subscript partition index identifies the partition Hamiltonian of which the wave function is an eigenstate. The subscript on a partition index denotes the number of clusters in that partition. The subscript on a channel index indicates the number of free clusters in the incident wave part of the associated distorted-wave function. When these subscripts are omitted, they are understood to be 2. The superscript identifies the channel entrance on which the channel state associated with that distorted-wave function is defined.

Now let  $\Phi_{\gamma_n \tilde{c}_n}^{(+)\alpha}$  be a wave function for  $n$  free clusters which is identical with the incoming wave part of  $\Phi_{\alpha \tilde{c}_n}^{(+)\alpha}$ . It is clear that

$$(\bar{H}_{\gamma_n} - E)\Phi_{\gamma_n \tilde{c}_n}^{(+)\alpha} = 0. \tag{14.3}$$

From Eq. (10.30) we have

$$\begin{aligned}
\Phi_{\tilde{c}}^{(+)} &\equiv \Phi_{\alpha \tilde{c}_n}^{(+)\alpha} = (1 + \bar{G}_\alpha \bar{V}_{\gamma_n \alpha}) \Phi_{\gamma_n \tilde{c}_n}^{(+)\alpha} \\
&= \bar{G}_\alpha \bar{G}_{\gamma_n}^{-1} \Phi_{\gamma_n \tilde{c}_n}^{(+)\alpha},
\end{aligned} \tag{14.4}$$

where  $\bar{V}_{\gamma_n \alpha}$  contains all interactions internal to partition  $\alpha$  and external to partition  $\gamma_n$ . Substitution of Eq. (14.4) into Eq. (14.1) gives, using Eq. (9.13),

$$\begin{aligned}
T_{\tilde{c}'\tilde{c}_n} &= \frac{1}{2\hbar} \langle \Phi_{\tilde{c}'}^{(-)} | \bar{V}_\beta G (P_\alpha + \Delta \bar{G}_\alpha) \bar{G}_{\gamma_n}^{-1} | \Phi_{\gamma_n \tilde{c}_n}^{(+)\alpha} \rangle \\
&= \frac{1}{2\hbar} \langle \Phi_{\tilde{c}'}^{(-)} | \bar{V}_\beta G \bar{G}_{\gamma_n}^{-1} | \Phi_{\gamma_n \tilde{c}_n}^{(+)\alpha} \rangle \\
&= \frac{1}{2\hbar} \langle \Phi_{\tilde{c}'}^{(-)} | \bar{V}_\beta (1 + G\bar{V}_{\gamma_n}) | \Phi_{\gamma_n \tilde{c}_n}^{(+)\alpha} \rangle,
\end{aligned} \tag{14.5}$$

where the  $\Delta$  term has been discarded and  $P_\alpha$  replaced by one as before.

Alternatively, if we had started with  $\tilde{c}'$  being an  $n'$ -

cluster channel, we could have used post-prior equivalence to give

$$T_{\tilde{c}'_n \tilde{c}_n} = \frac{1}{2\hbar} \langle \Phi_{\beta \tilde{c}'_n}^{(-)\beta} | \vec{G}_{\beta}^{-1} G \vec{V}_{\alpha} | \Phi_{\tilde{c}_n}^{(+)} \rangle. \quad (14.6)$$

Then a similar analysis to the one just given would yield

$$T_{\tilde{c}'_n \tilde{c}_n} = \frac{1}{2\hbar} \langle \Phi_{\delta_n \tilde{c}'_n}^{(-)\beta} | (1 + \vec{V}_{\delta_n} G) \vec{V}_{\alpha} | \Phi_{\tilde{c}_n}^{(+)} \rangle. \quad (14.7)$$

Now suppose that both  $\tilde{c}$  and  $\tilde{c}'$  are multicluster channels. Then, applying the post-prior equivalence (see Appendix B) to Eq. (14.5), we have

$$T_{\tilde{c}'_n \tilde{c}_n} = \frac{1}{2\hbar} \langle \Phi_{\beta \tilde{c}'_n}^{(-)\beta} | (1 + \vec{V}_{\beta} G) \vec{V}_{\gamma_n} | \Phi_{\gamma_n \tilde{c}_n}^{(+)\alpha} \rangle, \quad (14.8)$$

and repeating the analysis leading to Eq. (14.7) gives the general result

$$T_{\tilde{c}'_n \tilde{c}_n} = \frac{1}{2\hbar} \langle \Phi_{\delta_n \tilde{c}'_n}^{(-)\beta} | (1 + \vec{V}_{\delta_n} G) \vec{V}_{\gamma_n} | \Phi_{\gamma_n \tilde{c}_n}^{(+)\alpha} \rangle. \quad (14.9)$$

Thus we have been able to express the transition amplitude in terms of asymptotic states that describe freely moving clusters. The associated channel states on channel entrance  $\alpha$ ,  $|\alpha \gamma_n \tilde{c}_n\rangle$  for various  $\gamma_n$ , do not constitute an orthonormal set of surface harmonics. However, these channel states stand in a one-to-one correspondence with a complete orthonormal set of surface harmonics  $|\tilde{c}_n\rangle \equiv |\alpha \alpha \tilde{c}_n\rangle$ . This guarantees that the above description of asymptotic fluxes is complete and involves no double counting. The price that must be paid for this simplification of multicluster motion in the asymptotic region is an increase in the number of transition matrix operators

$$\hat{T}_{\delta_n \beta \gamma_n \alpha} = P_{\beta} \vec{V}_{\delta_n} (1 + G \vec{V}_{\gamma_n}) P_{\alpha}, \quad (14.10)$$

which must be calculated. Note that the projection operators  $P_{\alpha}$  and  $P_{\beta}$  which were formerly implicit in the definition of the transition matrix operator have been made explicit in Eq. (14.10). In addition, the partition indices have been given superscripts to identify the channel entrance which is involved.

## B. Coupled LS equations for $T$ -matrix operators

We shall now present a set of coupled LS equations for the transition matrix operators of Eq. (14.10) which can be derived in just the same way as in Sec. IX. First, however, the augmented notation of the preceding section must be extended to the partition Green's-function operators. We write [cf. Eq. (9.10)]

$$\vec{G}_{\gamma_n \alpha}(E - \vec{H}_{\gamma_n}^{\dagger}) = (E - \vec{H}_{\gamma_n}) \vec{G}_{\gamma_n \alpha} = P_{\alpha}. \quad (14.11)$$

Using these definitions, the analysis of Sec. IX gives

$$\hat{T}_{\gamma_n \alpha \delta_n \beta} = P_{\alpha} \vec{V}_{\gamma_n} G_{\epsilon_n''} \vec{G}_{\delta_n}^{-1} P_{\beta} + P_{\alpha} \vec{V}_{\gamma_n} \vec{G}_{\epsilon_n''} \hat{T}_{\epsilon_n'' \delta_n \beta}, \quad (4.12)$$

and

$$\hat{T}_{\gamma_n \alpha \delta_n \beta} = P_{\alpha} \vec{V}_{\gamma_n} P_{\beta} + \hat{T}_{\gamma_n \alpha \epsilon_n''} \vec{G}_{\epsilon_n''} \vec{V}_{\delta_n} P_{\beta}. \quad (14.13)$$

These LS equations are identical to those derived in Sec. IX [Eqs. (9.27b) and (9.27c)], except that the channel projectors which originally were implicit are now explicit and that the partition indices are more complex. Alternatively, one can revert to the original notation by leaving the projectors implicit as before and understanding that a simple index  $\gamma$  represents a more complex quantity  $\gamma_n^{\alpha}$ . What has been achieved here is that one can use free-particle  $n$ -cluster channel states to calculate the elements of the transition matrix. As before, a partition coupling scheme can be introduced to give a connected kernel formalism. Note that the partition index  $\gamma_n^{\alpha}$  not only identifies a partition  $\gamma_n$  but also assigns that partition to a particular two-cluster partition  $\alpha$ . Evidently, it is necessary that partition  $\gamma_n$  be one of the  $n$ -cluster partitions that can be formed by subdividing partition  $\alpha$ .

In practice one will want to include explicit reference to all partitions  $\gamma_n$  which correspond to open  $n$ -cluster channels. This is in addition to all two-cluster channels. The choice therefore depends on the energy. Thus once one is above the threshold for any of the partition  $\gamma_n$  channels, partition  $\gamma_n$  should be included and assignments to all possible two-cluster partitions  $\alpha$  must be made for index  $\gamma_n^{\alpha}$ . Then the various partition  $\gamma_n$  Green's-function operators  $\vec{G}_{\gamma_n^{\alpha}}$  will all play a role in the set of coupled LS equations for the elements of the reaction operator matrix. These differ from each other by virtue of fulfilling boundary condition constraints on different channel entrances.

The construction of the partition  $\gamma_n$  Green's-function operator  $\vec{G}_{\gamma_n^{\alpha}}$  requires a knowledge of the wave functions for all the internal motion states for each of the  $n$  partition  $\gamma_n$  clusters. This includes the continuum states as well as the bound states. Clearly, solution of the  $n$ -body problem requires the previous solution of all the subsystem bound and scattering problems.

By extending the formalism to include explicit reference to  $n > 2$  partitions, we have first of all simplified the construction of the asymptotic states for breakup channels. A second benefit resulting from this procedure is that it provides a convenient framework for making the few-cluster or "bound-state" approximation. In this formalism the few-cluster approximation results from neglecting the continuum cluster states in the various partition Green's-function operators. This approximation has been discussed in more detail in Sec. XIII.

From the foregoing, it would appear that we are free to increase the number of partitions to which reference is made in the set of coupled LS equations beyond the number of two-cluster partitions possible for the system. All the two-cluster partitions must be included to ensure that the complete set of asymptotic boundary condition constraints have been imposed. A set of coupled LS equations which involves no more than the complete set of two-cluster partitions is said to be "minimally coupled." It turns out that the conservation of flux imposes a constraint on the content of the partition coupling scheme of the BKLT formalism. This was pointed out by Benoist-Gueutal (1975), who derived from the BKLT equations

an expression for the imaginary part of the elastic scattering amplitude. According to the optical theorem, this amplitude should be equal to minus the sum over all open channels of the squares of the magnitudes of the transition amplitudes to those channels. The analysis of the imaginary part of the transition amplitude, which is presented in Appendix C, shows that the BKLT equations do indeed give such an expression but that the sum is over all the open channels which are present in the spectral decompositions of all partition Green's functions appearing in the coupled equations. Thus the conservation of flux requires that the sum total of the spectral decompositions of all the partition Green's-function operators included in the coupling scheme must contain every open channel just once.

It is clear that one is no more allowed to have too many partitions in the coupling scheme than one is allowed to have too few. Thus it is seen that if one seeks to add a breakup channel to the partition coupling scheme, then those breakup channels belonging to that partition must be deleted from the partition Green's function of the corresponding two-cluster partition. However, this will have serious consequences. The projector associated with the depleted two-cluster partition Green's function,  $P_\alpha = (E - H_\alpha)G_\alpha$ , will no longer tend towards the identity in the limit of infinite channel radii. Thus one cannot justify setting  $(1 - P_\gamma)$  equal to zero in Eqs. (9.25) and (9.26) and one does not obtain the BKLT coupled LS equations governing the dynamical development of the system.

We conclude that, although it is possible to express breakup transition amplitudes explicitly in terms of breakup partition transition operators, it is not possible to accommodate breakup transition operators in the BKLT formalism. In brief, minimally coupled BKLT equations are also maximally coupled.

## XV. SPURIOUS SOLUTIONS

As we have seen in Sec. X, the BKLT method consists in taking  $\mathcal{N}$  sequentially coupled LS equations and iterating them. The result is  $\mathcal{N}$  decoupled connected kernel integral equations for  $\mathcal{N}$  transition amplitudes or wave-function components. It can be shown that the solutions of the original LS equations are uniquely determined by the asymptotic boundary conditions when the two-body interactions are local and short-ranged (Cattapan and Vanzani, 1979). The question naturally arises as to the uniqueness of the solutions of the BKLT equations. A lack of uniqueness would point to the existence of spurious solutions, i.e., solutions of the BKLT equations which are not solutions of the Schrödinger equation. One can demonstrate the existence of equations whose solutions constitute spurious solutions to the BKLT equations (Adhikari and Glöckle, 1979; Chandler, 1978; Vanzani, 1978). However, it has not been possible as yet to establish the existence of such solutions.

Following the method of Kowalski (1978), we shall show how these spurious solution equations may be con-

structed. We start with the BKLT equation shown in Eq. (10.4) and iterate it  $\mathcal{N} - 1$  times to obtain

$$\hat{X} = \sum_{m=1}^{\mathcal{N}} (\hat{V}\hat{W}\hat{G})^m \hat{U}\hat{G}^{-1} + (\hat{V}\hat{W}\hat{G})^{\mathcal{N}} \hat{X}. \quad (15.1)$$

The kernel of this equation is a connected operator and a diagonal matrix in partition space. The solution of Eq. (15.1) would not be unique if there existed nontrivial solutions of the homogeneous equation

$$\hat{X}^{(s)} = (\hat{V}\hat{W}\hat{G})^{\mathcal{N}} \hat{X}^{(s)}. \quad (15.2)$$

Let us also consider the associated wave-function equations. Iteration of Eq. (10.20)  $\mathcal{N} - 1$  times gives

$$\Psi_{(k)}^{(+)} = \sum_{m=0}^{\mathcal{N}-1} (\hat{G}\hat{V}\hat{W})^m \hat{G}\hat{U}\hat{G}^{-1} \Phi_{(k)}^{(+)} + (\hat{G}\hat{V}\hat{W})^{\mathcal{N}} \Psi_{(k)}^{(+)}. \quad (15.3)$$

Again, the kernel is connected and diagonal. Again, the question of uniqueness hinges on whether there exists a nontrivial solution of the homogeneous counterpart to this equation

$$\Psi_{(k)}^{(s)} = (\hat{G}\hat{V}\hat{W})^{\mathcal{N}} \Psi_{(k)}^{(s)}. \quad (15.4)$$

Following Kowalski, we start with the resolvent relation of Eq. (9.15) and write it in matrix form. We have

$$G\hat{U} = \hat{G}\hat{U} + \hat{G}\hat{V}\hat{G}\hat{U}. \quad (15.5)$$

Note that

$$\hat{V}\hat{U} = \hat{V}\hat{W}\hat{U} \quad (15.6)$$

and

$$G\hat{U} = \hat{U}G. \quad (15.7)$$

Thus the resolvent relation can be written

$$G\hat{U} = \hat{G}\hat{U} + \hat{G}\hat{V}\hat{W}\hat{G}\hat{U}. \quad (15.8)$$

Iterating this equation  $\mathcal{N} - 1$  times gives

$$G\hat{U} = \sum_{m=0}^{\mathcal{N}-1} (\hat{G}\hat{V}\hat{W})^m \hat{G}\hat{U} + (\hat{G}\hat{V}\hat{W})^{\mathcal{N}} G\hat{U}. \quad (15.9)$$

Multiplying this equation by  $G^{-1}$ ,  $\hat{G}$ , and  $\hat{G}^{-1}$  yields

$$\{1 - (\hat{G}\hat{V}\hat{W})^{\mathcal{N}}\} \hat{U} = \sum_{m=0}^{\mathcal{N}-1} (\hat{G}\hat{V}\hat{W})^m \hat{G}G^{-1}\hat{U}. \quad (15.10)$$

Now suppose that there is a vector  $\Xi$  which is not a solution of the Schrödinger matrix equation, i.e.,

$$G^{-1}\Xi \neq 0, \quad (15.11)$$

but which is a solution of

$$\sum_{m=0}^{\mathcal{N}-1} (\hat{G}\hat{V}\hat{W})^m \hat{G}\hat{U}G^{-1}\Xi = 0. \quad (15.12)$$

Then  $\hat{U}\Xi$  would be a solution of Eq. (15.4), and there would be a lack of uniqueness for the solution of Eq. (15.3).

A similar result can be found for Eq. (15.1). If we mul-

tiply Eq. (15.10) by  $\hat{G}^{-1}$  after replacing  $\mathcal{N}$  by  $\mathcal{N}+1$  and use the relation

$$(\hat{G}^{-1} - G^{-1})\hat{U} = \hat{V}\hat{U} = \hat{V}\hat{W}\hat{U}, \quad (15.13)$$

we find that

$$\{1 - (\hat{V}\hat{W}\hat{G})^{\mathcal{N}}\}\hat{V}\hat{W}\hat{U} = \sum_{m=1}^{\mathcal{N}} (\hat{V}\hat{W}\hat{G})^m \hat{U} G^{-1}. \quad (15.14)$$

Thus if we can find an operator  $\hat{Y}$  such that

$$G^{-1}\hat{Y} \neq 0 \quad (15.15)$$

and

$$\sum_{m=1}^{\mathcal{N}} (\hat{V}\hat{W}\hat{G})^m \hat{U} G^{-1} \hat{Y} = 0, \quad (15.16)$$

then  $\hat{V}\hat{W}\hat{U}\hat{Y}$  will be a solution of Eq. (15.2), and the lack of uniqueness of the solution by virtue of the existence of a spurious solution of Eq. (15.1) will have been established.

## XVI. REVIEW OF BKLT CALCULATIONS

Calculational tests and applications of the BKLT many-body scattering formalism are still in a rudimentary stage. The following is a list of what has been done to date:

- (1) A two-body system model, which has one inelastic channel. This is a one-partition two-channel model.
- (2) Collinear scattering of three particles neglecting three-body breakup.
- (3) Low-energy  $e^-$ -H scattering using the bound-state approximation.
- (4) Atomic and molecular bound-state calculations.
- (5) Nucleon transfer cross sections using the bound-state approximation.
- (6) Three-dimensional three-body problem with pure  $s$ -wave interactions.

We shall give a brief account of each of these applications of the BKLT formalism.

The first calculation on the list is due to Schmittroth and Tobocman (1971). Strictly speaking, it is not a BKLT calculation, since the two-body system has only one partition. Nevertheless, we include it because it is an example of the restricted basis method within the transition operator formalism (see Sec. XIII). In addition, it provides a comparison between the  $R$ -matrix and the transition operator formalisms. In this calculation, the coupled square-well problem of Sec. VIII.A, in which there is  $s$ -wave scattering of a particle by a two-state target, was considered. Using a harmonic-oscillator basis set, Schmittroth and Tobocman found that the level expansion converged much more rapidly for the  $X$ -matrix formalism than it did for the  $R$ -matrix formalism.

Next let us describe some of the BKLT calculations of collinear three-body scattering. In this case, the dynamical system consists of two equal-mass particles which are

constrained to move in a straight line and interact with each other and with an infinite mass, impenetrable scattering center. The Schrödinger equation is

$$\left[ E + \frac{\hbar^2}{2m} \left[ \frac{\partial^2}{\partial x^2} + \frac{\partial^2}{\partial y^2} \right] - \mathcal{V}(x,y) \right] \Psi(x,y) = 0, \quad (16.1)$$

where the wave function satisfies the boundary conditions

$$\Psi(x,0) = \Psi(0,y) = 0. \quad (16.2)$$

In the calculations of Baer and Kouri (1972), the potential was taken to be

$$\mathcal{V}(x,y) = \begin{cases} -V_0, & x < a, y > a \\ -V_0, & x > a, y < a \\ -V_0, & x < a, y > a \\ 0, & x > a, y > a. \end{cases} \quad (16.3)$$

This corresponds to both particles having a square-well potential interaction with the scattering center and experiencing, in addition, a three-body force with the scattering center and each other. Alternatively, the system can be viewed as the propagation of waves in a two-dimensional waveguide having a right-angle bend. In all the calculations described here, the energy was taken to be below the threshold for three-body breakup.

In the limit  $V_0 \rightarrow \infty$ , the Schrödinger equation can be solved by wave-function matching following the method of Hulbert and Hirschfelder (1943). This does not give the wave function in closed form but rather as an infinite sum over all possible two-body bound states. In this case there is no three-body breakup. Baer and Kouri found that the BKLT method yielded expressions identical with those of Hulbert and Hirschfelder. They also did calculations with finite  $V_0$  and found that their results agreed with those done by other methods. In calculations with finite  $V_0$ , the spectral decomposition of the partition Green's-function operator contains an integral over the continuum of breakup states which was neglected by Baer and Kouri.

The BKLT method has been tested by Lewanski and Tobocman (1978) using the collinear scattering model with the interaction potential

$$\begin{aligned} V(x,y) = & -V_x \theta(a_x - x) - V_y \theta(a_y - y) \\ & - (V_{xy} - V_x - V_y) \theta(a_x - x) \theta(a_y - y), \end{aligned} \quad (16.4)$$

where  $\theta$  is the Helmholtz step function. The constants  $V_x$ ,  $V_y$ , and  $V_{xy}$  were chosen to be infinite, but their differences were taken to be finite numbers. When these differences vanish we have the Hulbert-Hirschfelder model for which there is exact agreement between the BKLT method and the wave-function matching method. When the differences are finite, it is still possible to use wave-function matching to solve the Schrödinger equation but there is no longer exact agreement with the

BKLT result.

Lewanski and Tobocman found that the Baer-Kouri [Eq. (10.2)] and Kouri-Levin [Eq. (10.3)] versions of the BKLT method gave different results for the "finite-difference" cases. It was found that the level expansions for the wave-function matching method and the Kouri-Levin equation both converged to the same values for the transition probabilities. However, the Baer-Kouri level expansions converged to rather different values. The Kouri-Levin results fulfilled the unitarity (flux conservation) constraint, while the Baer-Kouri results did not. Explanations for this phenomenon have been proposed by Kouri *et al.* (1974) and Levin (1980), who suggested, respectively, that the nonunitary result was a consequence of either neglecting continuum states in the Green's functions or the occurrence of inhomogeneous differential equations for the Baer-Kouri wave-function components.

The third group of calculations to be discussed is those in which the BKLT method have been applied to low-energy  $e^-$ -H scattering. The first such calculation was done by Baer and Kouri (1973), using the bound-state approximation in the Baer-Kouri form of the BKLT method [Eq. (10.2)]. At low energies their results for the  $s$ -wave phase shifts agreed very well with the essentially exact results of Schwartz (1961). However, the unitarity constraint was not satisfied. These calculations were repeated by Kouri, Craigie, and Secrest (1974), who also did the calculation using the Kouri-Levin form of the equations [Eq. (10.3)]. They found that Eq. (10.3) gave the same  $s$ -wave phase shifts as Eq. (10.2), but that the Kouri-Levin transition amplitudes fulfilled unitarity. The Kouri-Levin form of the calculation of the low-energy  $e^-$ -H  $s$ -wave phase shifts was repeated by Kouri *et al.* (1974) for various choices of the partition coupling array  $\hat{W}$  [see Eq. (10.7)]. For their two-partition system, it was possible to use

$$\hat{W} = \begin{pmatrix} x & 1-x \\ 1-x & x \end{pmatrix} \quad (16.5)$$

and fulfill the requirement that the sum of the elements of any row or column is one. They found that the partition permuting choice  $x=0$ , which ensures that the iterated kernel is connected, gave the best numerical results.

The fourth item on the list is the calculation of atomic and molecular bound states. In the calculation of  $H_2^+$  bonding (Krüger and Levin, 1977; Levin and Krüger, 1977a) reference was made to the two channels

$$(1) (p_1, e) + p_2 \quad \text{and} \quad (2) p_1 + (p_2, e) .$$

The third two-cluster channel was ignored. The Hahn, Kouri, and Levin equations [Eqs. (10.25)–(10.28)] were used for the two-channel problem. These can be written

$$\Psi = \chi_1 + \chi_2 , \quad (16.6)$$

where  $\chi_1$  and  $\chi_2$  satisfy the coupled equations

$$(E - H_1)\chi_1 = V_2\chi_2 \quad (16.7)$$

and

$$(E - H_2)\chi_2 = V_1\chi_1 . \quad (16.8)$$

In addition to the two-channel approximation, it was assumed that

$$\chi_j = a_j(R)\eta_{1s}(r_j) , \quad (16.9)$$

where  $r_j$  is the distance of the electron from proton  $p_j$ ,  $R$  is the separation of the two protons, and  $\eta_{1s}$  is the hydrogenic ground-state wave function. The coupled equations were then solved for the coefficients  $a_j(R)$  and energies  $E(R)$  holding  $R$  fixed in accordance with the Born-Oppenheimer approximation. Krüger and Levin found an equilibrium separation  $R_0 = 2.07a_0$  ( $a_0 =$  Bohr radius) and a binding energy  $D_0 = 3.07$  eV, which are to be compared with the exact values of  $2.00a_0$  and 2.79 eV, respectively. Use of the same approximate wave function in a variational or degenerate-perturbational calculation gives the values  $2.50a_0$  and 1.76 eV. These results indicate that the BKLT approach may be a superior framework for applying certain types of approximations. Similar results using the same method were found for  $H_2$ , He, and  $HeH^+$  (Levin and Krüger, 1977b; Levin, 1978).

Ford and Levin (1982) have attempted to improve the  $H_2^+$  calculations by including more terms in the trial wave function. However, their expansion was found to converge to incorrect results. In an alternative approach they solved Eqs. (16.7) and (16.8) for fixed  $R$  numerically, using a configuration-space interpolation procedure (or finite-element method). With as few as 115 interpolation points, they have attained convergence to the exact ground-state energy of  $H_2^+$ .

Another application of the BKLT formalism is the analysis of nuclear rearrangement reactions using the bound-state approximation (BSA). It has been pointed out by Tobocman (1975a) and Kouri and Levin (1975b) that if one makes the BSA in the BKLT dynamical equations the result looks very similar to the equations of the coupled reaction channel (CRC) scattering formalism with two important differences. First, the awkward nonorthogonality terms of the CRC approach are absent in the BSA to the BKLT method. This situation is similar to that encountered with the resonating group method in Sec. XII. Second, the channel coupling is sequential and cyclic in the BKLT equations, while it is symmetric in the CRC equations.

Greben and Levin (1977, 1979) have carried out a series of calculations solving the coupled integrodifferential wave-function equations of both the CRC formalism and the BSA to the BKLT method. For both types of calculation, the restriction to two partitions was imposed. They compared the results for several examples of single-nucleon transfer reactions and found that both methods give differential cross sections that are very similar in both magnitude and shape. The results were also very similar to those of corresponding distorted-wave Born-approximation calculations, indicating that channel-coupling effects were relatively weak for the restrictions imposed by the approximations that were used.



Finally, the sixth item on the list is a calculation of the binding energy and scattering reactions of a three-body system with pure  $s$ -wave interactions by Tobocman (1981). This calculation attempted an essentially exact numerical solution of the BKLT integral equations [Eqs. (10.2) and (10.3)] for the transition amplitudes, using the restricted basis method (see Sec. XIII). The integral equations were converted to a set of simultaneous linear algebraic equations by expanding all operators in a harmonic-oscillator basis. These equations were then solved by matrix inversion.

Convergence with increasing size of the harmonic-oscillator basis was found to be relatively slow. While the results for the binding energy were satisfactory, those for scattering state transition amplitudes were fairly poor at low energy and deteriorated with increasing energy. However, fairly good results were obtained with the distorted-wave Baer-Kouri method.

It appears that the principal source of difficulty is an inadequate representation of the continuum contributions. This BKLT calculation, which is the first to attempt the inclusion of continuum contributions, must be judged as only partially successful. The expansion in a harmonic-oscillator basis is crudely equivalent to restricting the integrations in configuration space to a fixed volume, which only increases slowly with the size of the basis. However, the continuum-continuum matrix elements of the interaction potential, which are required in this calculation, are slowly convergent integrals which have integrands that are oscillatory and fall off slowly as one moves out to infinity. Thus expansion in a harmonic-oscillator basis is inadequate and appears to be unsatisfactory at the higher energies. It seems that it will be necessary to treat expansion in a finite basis as a projection onto a restricted basis as described in Sec. XIII so that the embedding equation [Eq. (13.11)] may be used to improve the evaluation of the continuum contributions.

We conclude that these preliminary calculations indicate that it is likely that the BKLT formalism will provide a useful tool for analyzing the dynamics of many-body systems.

#### ACKNOWLEDGMENTS

We wish to thank F. C. Barker, L. L. Foldy, K. L. Kowalski, R. J. Philpott, D. Robson, R. M. Thaler, and H. H. Wolter for helpful discussions, and the various authors and editors for permission to reproduce diagrams from their original articles. One of the authors (B.A.R.) wishes to express his appreciation to the Universität München for a position as Guest Professor for six months and to members of Sektion Physik for their kind hospitality. Part of this work was supported by the National Science Foundation under Grants Nos. PHY77-25280 and PHY78-26595.

#### APPENDIX A: JUSTIFICATION FOR NEGLECTING SURFACE TERMS IN THE RESOLVENT RELATIONS AND PROJECTION FACTORS IN THE LS EQUATIONS FOR THE REACTION MATRIX OPERATOR

In opting for the explicit spectral decomposition in terms of channel states for the partition Green's-function operator, we have caused the appearance of surface terms, those containing  $\Delta$ , and projection factors  $P_\alpha$  and  $P_\beta$  in the resolvent relations of Eqs. (9.12) and (9.13). Following the arguments of Chandler and Tobocman (1979), we shall show that  $\Delta$  can be replaced by the identity in the resolvent relations and projection operators can be ignored in the LS equations for the reaction matrix operator  $\hat{X}$  [Eqs. (9.25) and (9.26)], provided the channel radii are taken to be sufficiently large.

First, let us consider the surface terms in the generalized resolvent relations of Eqs. (9.12) and (9.13). These have the form  $\bar{G}_\alpha \Delta G$  and  $G \Delta \bar{G}_\beta$ . If the system and partition Green's-function operators were defined for the same region and fulfilled the same boundary conditions on the surface of that region, these terms would necessarily vanish. However, we have chosen to define  $\bar{G}_\alpha$  so that it vanishes outside the region projected onto by  $P_\alpha$ .

Let  $\mathcal{R}$  represent the inside or interaction region of configuration space where  $G$  is defined and let  $\mathcal{R}_\alpha$  be that portion of  $\mathcal{R}$  onto which  $P_\alpha$  projects and in which  $\bar{G}_\alpha$  is defined. The quantity  $\bar{G}_\alpha \Delta G$  is an integral over the surface of  $\mathcal{R}_\alpha$ . Part of this surface is the partition  $\alpha$  channel entrance which makes no contribution to the surface integral because  $G$  and  $\bar{G}_\alpha$  have the same behavior there. The rest of the surface of  $\mathcal{R}_\alpha$  lies interior to  $\mathcal{R}$ .

This surface of  $\mathcal{R}_\alpha$  interior to  $\mathcal{R} - \mathcal{S}_\alpha$ , say—is the boundary on which the partition  $\alpha$  channel states fulfill real homogeneous boundary conditions. Suppose the boundary condition constraint is such that the channel states vanish on the surface  $\mathcal{S}_\alpha$ . Then the quantity  $\bar{G}_\alpha \Delta G$  will be the integral over  $\mathcal{S}_\alpha$  of the product of the value of  $G$  and the normal gradient of  $\bar{G}_\alpha$ . In the limit as the channel radii are required to become arbitrarily large, the surface  $\mathcal{S}_\alpha$  gets displaced to where it is arbitrarily far from the center of the interaction region. In this limit, the quantity,  $\bar{G}_\alpha \Delta G$  becomes an arbitrarily rapidly oscillating function of the energy. Therefore, if the generalized resolvent relation [Eq. (9.12)] is averaged over a small energy interval, the surface terms average to zero. This justifies the neglect of these terms in the generalized resolvent equations and in the subsequent LS equations for the reaction matrix operator [Eqs. (9.25) and (9.26)]. This phenomenon will be illustrated by a simple example later in this Appendix.

On the basis of the foregoing argument we drop the surface terms from the resolvent relations and turn our attention to the LS equations for the reaction matrix operator:

$$\hat{X}_{\alpha\beta} = \bar{V}_\alpha [1 + \bar{G}_\gamma (\bar{V}_\beta - \bar{V}_\gamma) + \bar{G}_\gamma \hat{X}_{\gamma\beta} + (1 - P_\gamma) G \bar{V}_\beta] \quad (\text{A.1})$$

and

$$\hat{X}_{\alpha\beta} = \bar{V}_\alpha + \hat{X}_{\alpha\gamma} \bar{G}_\gamma \bar{V}_\beta + \bar{V}_\alpha G (1 - P_\gamma) \bar{V}_\beta. \quad (\text{A2})$$

The projectors produce contributions to the operator  $\hat{X}_{\alpha\beta}$  of the form

$$C = P_\alpha \bar{V}_\alpha (1 - P_\gamma) G \bar{V}_\beta P_\beta. \quad (\text{A3})$$

The projectors  $P_\alpha$  and  $P_\beta$  have been inserted to make explicit the fact that ultimately the operator  $\hat{X}_{\alpha\beta}$  will be placed in a matrix element with partition  $\alpha$  and  $\beta$  asymptotic states, which implicitly contain these projectors.

The partition  $\alpha$  region  $\mathcal{R}_\alpha$  has been defined to be that portion of the inside or interaction region of configuration space which is projected onto by  $P_\alpha$ . The various partition regions  $\mathcal{R}_\alpha, \mathcal{R}_\beta, \dots$  overlap with one another at the center of the inside region. Let  $\mathcal{R}_0$  be the intersection of all such partition regions. Within  $\mathcal{R}_0$  every projector  $P_\gamma$  is equal to the identity.

Now consider the quantities  $P_\alpha \bar{V}_\alpha, P_\beta \bar{V}_\beta, \dots$ . These quantities are nonvanishing only near the center of the inside region  $\mathcal{R}$ . In fact, the region of nonvanishing  $P_\alpha \bar{V}_\alpha$  for any partition  $\alpha$  is contained almost entirely in  $\mathcal{R}_0$ . In the limit as all the channel radii become large and all the regions  $\mathcal{R}, \mathcal{R}_0, \mathcal{R}_\alpha, \mathcal{R}_\beta, \dots$  become correspondingly large, the fraction of the region of nonvanishing  $P_\alpha \bar{V}_\alpha$  excluded from  $\mathcal{R}_0$  becomes arbitrarily small. Also, the excluded part of this region is the part which lies farthest from the center of the interaction region. The excluded portion is therefore the least important portion. Thus, in the limit of large channel radii, the region of nonvanishing  $P_\alpha \bar{V}_\alpha$  is almost entirely contained within  $\mathcal{R}_0$ . It follows that  $P_\alpha \bar{V}_\alpha (1 - P_\gamma)$  can be set equal to zero. We conclude that the  $1 - P_\gamma$  term in the LS equations for the reaction matrix operator may be safely ignored.

Finally, we present a simple example to illustrate the foregoing discussion. The system consists of three particles  $N, P$ , and  $C$  in one dimension. Particle  $C$  is infinitely massive and impenetrable for the other two particles. The interaction between the particles is described in terms of finite-range two-body potentials. The Hamiltonian for this system is

$$H = T + \mathcal{V}, \quad (\text{A4})$$

where

$$T = -\frac{\hbar^2}{2M_N} \frac{\partial^2}{\partial x_N^2} - \frac{\hbar^2}{2M_P} \frac{\partial^2}{\partial x_P^2} \quad (\text{A5})$$

and

$$\mathcal{V} = V_{NC}(x_N) + V_{PC}(x_P) + V_{NP}(|x_N - x_P|). \quad (\text{A6})$$

To discuss the asymptotic behavior of the system, it is necessary to introduce the relative motion and internal motion coordinates for each partition. There are three partitions:

$$\alpha = P: (P)(NC), \quad (\text{A7a})$$

$$\alpha = N: (N)(PC), \quad (\text{A7b})$$

$$\alpha = D: (NP)(C). \quad (\text{A7c})$$

The relative ( $r_\alpha$ ) and internal ( $\rho_\alpha$ ) coordinates for each partition are

$$r_P = x_P, \quad \rho_P = x_N, \quad (\text{A8a})$$

$$r_N = x_N, \quad \rho_N = x_P, \quad (\text{A8b})$$

and

$$r_D = \frac{M_N x_N + M_P x_P}{M_N + M_P}, \quad \rho_D = x_N - x_P. \quad (\text{A8c})$$

In terms of these coordinates, the kinetic energy operator is

$$T = T_\alpha + \tau_\alpha, \quad (\text{A9a})$$

where

$$T_\alpha = -\frac{\hbar^2}{2m_\alpha} \frac{\partial^2}{\partial r_\alpha^2} \quad (\text{A9b})$$

and

$$\tau_\alpha = -\frac{\hbar^2}{2\mu_\alpha} \frac{\partial^2}{\partial \rho_\alpha^2}. \quad (\text{A9c})$$

Here

$$m_P = M_P, \quad \mu_P = M_N, \quad (\text{A10a})$$

$$m_N = M_N, \quad \mu_N = M_P, \quad (\text{A10b})$$

and

$$m_D = M_N + M_P, \quad \mu_D = \frac{M_N M_P}{M_N + M_P}. \quad (\text{A10c})$$

Next we introduce the partition Hamiltonian  $H_\alpha$ , the partition internal motion Hamiltonian  $\mathcal{H}_\alpha$ , and the partition residual interaction  $V_\alpha$ :

$$H = H_\alpha + V_\alpha \quad (\text{A11})$$

with

$$H_\alpha = T_\alpha + \mathcal{H}_\alpha, \quad (\text{A12})$$

where

$$\mathcal{H}_P = \tau_P + V_{NC}, \quad V_P = V_{PC} + V_{NP}, \quad (\text{A13a})$$

$$\mathcal{H}_N = \tau_N + V_{PC}, \quad V_N = V_{NC} + V_{NP}, \quad (\text{A13b})$$

and

$$\mathcal{H}_D = \tau_D + V_{NP}, \quad V_D = V_{NC} + V_{PC}. \quad (\text{A13c})$$

The asymptotic behavior of the system can be discussed in terms of the channel states  $\chi_{ac}(\rho_\alpha)$ , which are eigenfunctions of the partition internal motion Hamiltonian:

$$(\mathcal{H}_\alpha - \epsilon_{ac}) \chi_{ac}(\rho_\alpha) = 0. \quad (\text{A14})$$

Let  $E$  be the total energy of the system and  $\Psi_k^{(+)}$  ( $k=1, 2, \dots, m$ ), where  $m$  is the number of open channels, be the corresponding scattering wave functions which satisfy the Schrödinger equation

$$(H - E) \Psi_k^{(+)} = 0 \quad (\text{A15})$$

and represent unit incoming flux in channel  $k$  and purely outgoing flux in all other channels. Associated with each partition  $\alpha$  is an asymptotic region of configuration space corresponding to large values of  $r_\alpha$ , where the partition residual interaction vanishes. In this region, a channel-state expansion

$$\Psi_k^{(+)}(\rho_\alpha, r_\alpha) = \sum_{c \in \alpha} \chi_{ac}(\rho_\alpha) \omega_{ac}^{(k)}(r_\alpha) \quad (\text{A16})$$

defines the channel radial wave functions  $\omega_{ac}^{(k)}$ , which are solutions of

$$(T_\alpha - E_{ac}) \omega_{ac}^{(k)}(r_\alpha) = 0, \quad (\text{A17})$$

where

$$E_{ac} = \frac{\hbar^2}{2m_\alpha} k_c^2 = E - \varepsilon_{ac}. \quad (\text{A18})$$

It should be noted that for the purposes of this Appendix, any dependence of the reduced mass  $m_\alpha$  on the excitation energy  $\varepsilon_{ac}$  is neglected. The asymptotic behavior of the system is described in term of the amplitudes of the ingoing and outgoing wave parts of the radial wave functions,  $\omega_{ac}^{(k)}$ , i.e.,

$$\omega_{ac}^{(k)} = \left( \frac{m_\alpha}{\hbar k_c} \right)^{1/2} (e^{-ik_c r_\alpha} \delta_{ck} - e^{ik_c r_\alpha} U_{ck}) \quad (\text{large } r_\alpha), \quad (\text{A19})$$

where  $U$  is the collision matrix.

Figure 56 shows the two-dimensional configuration

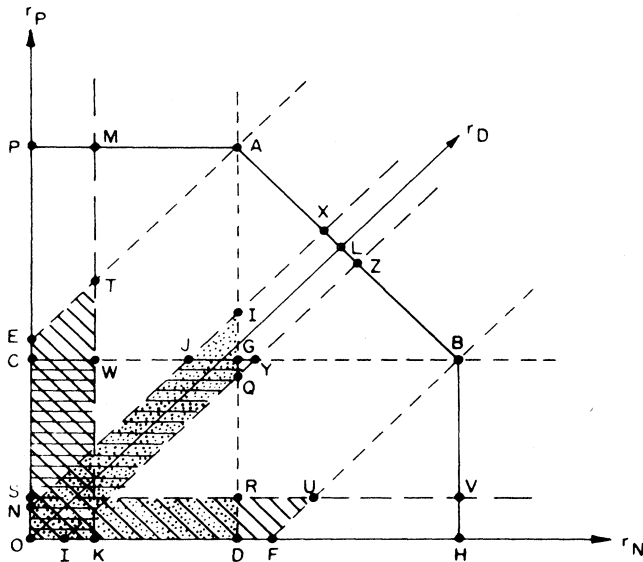


FIG. 56. Configuration space diagram for the one-dimensional three-body system.  $r_N$  and  $r_P$  are the displacements of particles  $N$  and  $P$ , respectively, from the infinite mass, impenetrable particle  $C$ :

$$r_D = (m_N r_N + m_P r_P) / (m_N + m_P)$$

(from Chandler and Tobocman, 1979).

space and the channel entrance surface for the simple system being considered. The channel entrance surface is made up of the segments  $PA$ ,  $AB$ , and  $BH$ , which are the channel entrances for the partitions  $P$ ,  $D$ , and  $N$ , respectively.

The inside region  $\mathcal{R}$  is the interior of the polygon  $OPABH$ . The partition projectors are defined as follows:

$$P_P = \begin{cases} 1, & \text{inside } OPAD \\ 0, & \text{elsewhere,} \end{cases} \quad (\text{A20a})$$

$$P_N = \begin{cases} 1, & \text{inside } OCBH \\ 0, & \text{elsewhere,} \end{cases} \quad (\text{A20b})$$

$$P_D = \begin{cases} 1, & \text{inside } OEABH \\ 0, & \text{elsewhere.} \end{cases} \quad (\text{A20c})$$

The channel radii are

$$R_P = OP, \quad (\text{A21a})$$

$$R_N = OH, \quad (\text{A21b})$$

and

$$R_D = OL. \quad (\text{A21c})$$

In the  $R$ -matrix formalism, the channel states  $\chi_{ac}$  are required to vanish at the channel entrance edges, i.e.,

$$\chi_{Pc} = 0 \text{ for } \rho_P = 0, OD, \quad (\text{A22a})$$

$$\chi_{Nc'} = 0 \text{ for } \rho_N = 0, OC, \quad (\text{A22b})$$

$$\chi_{Dc''} = 0 \text{ for } \rho_D = -LA, LB. \quad (\text{A22c})$$

For this reason, the channel states provide a description of the physical asymptotic states only in the limit as the channel radii  $R_P$ ,  $R_N$ , and  $R_D$  all approach infinity.

The dashed lines in Fig. 56 have been used to delimit the ranges of interaction of the two-body potentials. The potential  $V_{PC}$  is different from zero only between the lines  $SV$  and  $OH$ , the potential  $V_{NC}$  vanishes everywhere except between the lines  $OP$  and  $KM$ , and the potential  $V_{NP}$  is nonzero only between the lines  $NX$  and  $IZ$ . The region where  $P_P V_P$  is nonvanishing is speckled in the diagram, the region where  $P_D V_D$  is nonzero is cross-hatched with sloping lines, and the region where  $P_N V_N$  is nonvanishing is cross-hatched with horizontal lines.

The region  $\mathcal{R}_0$ , where  $P_P = P_N = P_D = 1$ , is the rectangle  $OCGD$ . One sees that only small cross-hatched and speckled areas are excluded from  $\mathcal{R}_0$ . Now consider what happens when the channel radii  $R_P$ ,  $R_N$ , and  $R_D$  get larger, keeping their ratios to each other fixed. Certain dimensions of the diagram increase while others do not. The region  $\mathcal{R}_0$  grows, but the ranges of the potentials  $PM$ ,  $XZ$ , and  $VH$  do not. Consequently, increasing the channel radii causes an increase in the cross-hatched and speckled areas inside  $\mathcal{R}_0$  while the cross-hatched and speckled regions excluded from  $\mathcal{R}_0$  remain fixed in area but are displaced further from the origin  $O$ . Thus in the limit when the channel radii become infinitely large, the region of nonvanishing  $P_\alpha V_\alpha$  excluded from  $\mathcal{R}_0$  loses all significance.

Now let us consider the question of the surface terms  $\bar{G}_\alpha \Delta G$  and  $G \Delta \bar{G}_\beta$  in the generalized resolvent equations. These are in general difficult quantities to evaluate in addition to the fact that an explicit expression for the system Green's function  $G$  is hard to construct. Consequently, we shall use the quantity  $G_N \Delta G_P$  to illustrate the phenomenon we employ to justify the neglect of surface terms.

The partition Green's-function operators for the one-dimensional three-body system are

$$G_\alpha = \sum_{c \in \alpha} |\chi_{ac}\rangle \left[ -\frac{2}{\hbar} \right] f_{ac}(r_<) y_{ac}(r_>) \langle \chi_{ac} |, \quad (\text{A23})$$

$$G_N \Delta G_P = \frac{2}{m_N} \sum_{cc'} |\chi_{Nc}(r_P) f_{Nc}(r_N)\rangle \left\{ y_{Nc}(a_N) \left[ \left[ \frac{\partial}{\partial a_N} \right] - \frac{\partial}{\partial a_N} \right] \chi_{Pc'}(a_N) \right\} \langle \chi_{Pc'}(r_N) L_{Pc',Nc}(r_P) | \\ + \frac{2}{m_P} \sum_{cc'} |\chi_{Nc}(r_P) L_{Nc,Pc'}(r_N)\rangle \left\{ \chi_{Nc}(a_P) \left[ \left[ \frac{\partial}{\partial a_P} \right] - \frac{\partial}{\partial a_P} \right] y_{Pc'}(a_P) \right\} \langle \chi_{Pc'}(r_N) f_{Pc'}(r_P) | \quad (\text{A26})$$

$$L_{Pc',Nc}(r_P) = y_{Pc'}(r_P) \int_0^{r_P} dr \chi_{Nc}(r) f_{Nc}(r) \\ + f_{Pc'}(r_P) \int_{r_P}^{a_P} dr \chi_{Nc}(r) y_{Nc}(r). \quad (\text{A27})$$

The lengths  $a_N$  and  $a_P$  are the dimensions of the region  $\mathcal{R}_0$ :

$$a_N = OD \text{ and } a_P = OC. \quad (\text{A28})$$

The boundary conditions imposed on the channel states imply that

$$\chi_{ac} = \left[ \frac{2}{\pi} \right]^{1/2} \sin[\kappa_c(r_\alpha - a_\alpha)] \text{ for } r_\alpha \approx a_\alpha, \quad (\text{A29})$$

$$G_N \Delta G_P = - \left[ \frac{2}{\pi} \right]^{1/2} \sum_{cc'} |\chi_{Nc}(r_P) f_{Nc}(r_N)\rangle \left[ \frac{2\kappa_{c'}}{m_N} \right] y_{Nc}(a_N) \langle \chi_{Pc'}(r_N) L_{Pc',Nc}(r_P) | \\ + \left[ \frac{2}{\pi} \right]^{1/2} \sum_{cc'} |\chi_{Nc}(r_P) L_{Nc,Pc'}(r_N)\rangle \left[ \frac{2\kappa_c}{m_P} \right] y_{Pc'}(a_P) \langle \chi_{Pc'}(r_N) f_{Pc'}(r_P) |, \quad (\text{A31})$$

where use has been made of Eqs. (A22).

The dependence of this expression on the lengths  $a_N$  and  $a_P$  is quite explicit. It is seen that the quantity  $G_N \Delta G_P$  is a sum of terms having a sinusoidal dependence on  $\kappa_c a_N$  or  $\kappa_c a_P$ . Clearly, for large values of  $a_N$  and  $a_P$ , one will observe a rapid oscillatory dependence of the quantity  $G_N \Delta G_P$  on the total energy  $E$ . Therefore, if an energy over a small finite-energy interval is made, we have

$$\frac{1}{2\delta} \int_{E-\delta}^{E+\delta} dE G_N \Delta G_P \approx 0. \quad (\text{A32})$$

where the asymptotic forms of the radial functions are

$$f_{ac}(r_\alpha) \sim \left[ \frac{m_\alpha}{\hbar \kappa_c} \right]^{1/2} \sin(\kappa_c r_\alpha) \quad (\text{A24})$$

and

$$y_{ac}(r_\alpha) \sim \left[ \frac{m_\alpha}{\hbar \kappa_c} \right]^{1/2} \cos(\kappa_c r_\alpha) - s_c f_{ac}(r_\alpha). \quad (\text{A25})$$

Using Eq. (3.5), we have

where

$$E_{ac} = \frac{\hbar^2 \kappa_c^2}{2\mu_\alpha} \quad (\text{A30})$$

for the breakup channels  $ac$ . The bound-state (two-cluster) channels can be ignored, since for arbitrarily large channel radii the corresponding channel states will be negligible at  $r_\alpha \approx a_\alpha$ . Inserting Eq. (A29) into Eq. (A27) gives

where

## APPENDIX B: POST-PRIOR EQUIVALENCE AND THE LIPPMANN IDENTITY

In this Appendix we shall discuss the Lippmann identity and the post-prior equivalence in the context of the calculable transition operator formalism of Secs. IX and XIV. For these purposes we need only to recognize that the partition Green's-function operators  $\bar{G}_{\gamma_n^\alpha}$  are nonvanishing only in the region projected onto by the operator  $P_\alpha$  and that  $\bar{G}_{\gamma_n^\alpha}$  fulfills the same boundary condition constraint on the partition  $\alpha$  channel entrance as does the

system Green's-function operator  $G$ .

First, let us present a derivation of the Lippmann identity

$$\delta_{\alpha\beta} \Phi_{\gamma_n \tilde{c}_n}^{(+)\alpha} = \bar{G}_{\gamma_n \tilde{c}_n} \bar{G}_{\epsilon_n \tilde{c}_n}^{-1} \Phi_{\epsilon_n \tilde{c}_n}^{(+)\beta} = \bar{G}_{\gamma_n \tilde{c}_n} \Delta \Phi_{\epsilon_n \tilde{c}_n}^{(+)\beta}. \quad (\text{B1})$$

This is the form appropriate to the  $R$ -matrix formulation of scattering theory and differs from the form appropriate to the wave packet formulations used by Lippmann (1956). The Green's-function operators are understood to fulfill outgoing wave boundary condition constraints on the relevant channel entrances. The surface on which the integral is performed is the boundary of the region projected onto by  $P_\alpha P_\beta$ . If  $\alpha \neq \beta$ , this region does not include a channel entrance. In this case, the situation is similar to that described in the discussion of Appendix A justifying the neglect of the  $\Delta$  terms in the resolvent relations. Therefore, we expect that when  $\alpha \neq \beta$ , the right side of Eq. (B1) will be a strongly oscillatory function of the energy whose average over a finite-energy interval will vanish in the limit as the channel radii become very large.

In the case when  $\alpha = \beta$ , the entire contribution to the

surface integral on the right side of Eq. (B1) comes from the channel entrance  $\beta$ . For  $\Phi_{\epsilon_n \tilde{c}_n}^{(+)\beta}$  we can write

$$\Phi_{\epsilon_n \tilde{c}_n}^{(+)\beta} = 2e^{i\delta_{\tilde{c}_n}} \bar{u}_{\beta \tilde{c}_n}(r_\beta) | \beta \epsilon_n \tilde{c}_n \rangle, \quad (\text{B2})$$

where  $\bar{u}_{\beta \tilde{c}_n}$  is defined by Eqs. (9.4) and (9.6). For  $\bar{G}_{\gamma_n \tilde{c}_n}$  we can employ Eqs. (9.1) and (9.2) to write

$$\bar{G}_{\gamma_n \tilde{c}_n} = \sum_{\tilde{c}'_n \in \gamma_n^\beta} | \beta \gamma_n \tilde{c}'_n \rangle \left[ -\frac{2}{\hbar} \right] \bar{u}_{\beta \tilde{c}'_n}(r_<) \bar{v}_{\beta \tilde{c}'_n}(r_>) \langle \beta \gamma_n \tilde{c}'_n |. \quad (\text{B3})$$

Finally, using Eqs. (3.4) and (3.5) we have

$$\Delta = \sum_{\beta} \sum_{c' \in \beta} | c' \rangle \left[ \left[ \frac{\hbar^2}{2m_c a_\beta} \delta(r_\beta - a_\beta) \frac{\partial}{\partial r_\beta} r_\beta \right]^\dagger - \left[ \frac{\hbar^2}{2m_c a_\beta} \delta(r_\beta - a_\beta) \frac{\partial}{\partial r_\beta} r_\beta \right] \right] \langle c' |. \quad (\text{B4})$$

Thus

$$\bar{G}_{\gamma_n \tilde{c}_n} \Delta \Phi_{\epsilon_n \tilde{c}_n}^{(+)\beta} = \sum_{\tilde{c}'_n \in \gamma_n^\beta} \Phi_{\gamma_n \tilde{c}'_n}^{(+)\beta} e^{-i\delta_{\tilde{c}'_n}} \langle \beta \gamma_n \tilde{c}'_n | \beta \epsilon_n \tilde{c}_n \rangle e^{i\delta_{\tilde{c}_n}} \frac{\hbar}{m_{\tilde{c}'_n}} \left\{ a_{\beta \tilde{c}'_n} \bar{v}_{\beta \tilde{c}'_n}(a_\beta) \left[ \frac{\partial}{\partial a_\beta} - \left[ \frac{\partial}{\partial a_\beta} \right] \right] a_{\beta \tilde{c}_n} \bar{u}_{\beta \tilde{c}_n}(a_\beta) \right\}. \quad (\text{B5})$$

The channel state overlap  $\langle \beta \gamma_n \tilde{c}'_n | \beta \epsilon_n \tilde{c}_n \rangle$  vanishes unless the channels  $\tilde{c}'_n$  and  $\tilde{c}_n$  have both the same cluster structure and the same relative asymptotic motion, i.e.,  $\tilde{c}'_n = \tilde{c}_n$ . If  $\tilde{c}'_n = \tilde{c}_n$ , the overlap is unity and the Wronskian factor involving  $\bar{v}_{\beta \tilde{c}'_n}$  and  $\bar{u}_{\beta \tilde{c}_n}$  becomes  $m_{\tilde{c}_n}/\hbar$ , so that

$$\bar{G}_{\gamma_n \tilde{c}_n} \Delta \Phi_{\epsilon_n \tilde{c}_n}^{(+)\beta} = \Phi_{\gamma_n \tilde{c}_n}^{(+)\beta}. \quad (\text{B6})$$

This, of course, is just a special case of Eq. (10.31).

Next let us consider the post-prior identity

$$0 = \langle \Phi_{\gamma_n \tilde{c}_n}^{(-)\alpha} | \bar{V}_{\gamma_n} - \bar{V}_{\delta_m} | \Phi_{\delta_m \tilde{c}'_m}^{(+)\beta} \rangle. \quad (\text{B7})$$

This transforms, using Eq. (14.3), to

$$\begin{aligned} 0 &= \langle \Phi_{\gamma_n \tilde{c}_n}^{(-)\alpha} | H^\dagger - E + E - H | \Phi_{\delta_m \tilde{c}'_m}^{(+)\beta} \rangle \\ &= - \langle \Phi_{\gamma_n \tilde{c}_n}^{(-)\alpha} | \Delta | \Phi_{\delta_m \tilde{c}'_m}^{(+)\beta} \rangle. \end{aligned} \quad (\text{B8})$$

The surface over which this integral is done is the boundary of the region projected onto by  $P_\alpha P_\beta$ . If  $\beta \neq \alpha$ , the surface over which the integration is done does not in-

clude a channel entrance. The surface integral then can be expected to be a highly oscillatory function of the energy in the large channel radii limit, and we can expect that the destructive interference when averaged over a finite-energy interval will be complete, just as in the discussion of Appendix A, justifying the neglect of the  $\Delta$  terms in the resolvent relations.

If  $\beta = \alpha$ , the entire nonvanishing contribution comes from the channel entrance  $\alpha$ . In this case there are two possibilities: the internal energies  $E_{\gamma_n \tilde{c}_n}$  and  $E_{\delta_m \tilde{c}'_m}$  of the channel states  $| \alpha \gamma_n \tilde{c}_n \rangle$  and  $| \alpha \delta_m \tilde{c}'_m \rangle$  are either equal or unequal. If they are equal, the radial wave functions will be identical and the Wronskian of the radial functions will vanish. If they are unequal, the wave numbers of the two radial functions will not be equal and the Wronskian will be an oscillatory function of the energy. These oscillations become more closely spaced as the channel radii are increased and the average over a small finite-energy interval will vanish.

Therefore, if an energy average over a small finite-energy interval is understood, the post-prior equivalence identity will be valid.

Alternatively, in the  $\alpha = \beta$  case we can write

$$\langle \Phi_{\gamma_n \tilde{c}_n}^{(-)\beta} | \Delta | \Phi_{\delta_m \tilde{c}'_m}^{(+)\beta} \rangle = \frac{2\hbar^2}{m_{\tilde{c}'_m}} \langle \beta \gamma_n \tilde{c}_n | \beta \delta_m \tilde{c}'_m \rangle e^{i\delta_{\tilde{c}'_m}} e^{i\delta_{\tilde{c}_n}} \left\{ a_{\beta \tilde{c}'_m} \bar{u}_{\beta \tilde{c}'_m}(a_\beta) \left[ \left[ \frac{\partial}{\partial a_\beta} \right] - \frac{\partial}{\partial a_\beta} \right] a_{\beta \tilde{c}_n} \bar{u}_{\beta \tilde{c}_n}(a_\beta) \right\}. \quad (\text{B9})$$

This quantity is seen to vanish as a consequence of the effective orthonormality of the channel states when  $\tilde{c}_n \neq \tilde{c}'_m$ .

### APPENDIX C: UNITARITY CONSTRAINTS ON THE BKLT FORMALISM

Conservation of flux and time reversal invariance require that the collision matrix be unitary and symmetric. To determine the consequence of this for the transition amplitude, we use Eq. (9.23):

$$\tilde{U}\tilde{U}^\dagger = \mathbb{1} = (\mathbb{1} - 2i\tilde{T})(\mathbb{1} + 2i\tilde{T}^\dagger), \quad (C1)$$

where

$$\tilde{T}_{\tilde{c}\tilde{c}'} \equiv \bar{T}_{\tilde{c}\tilde{c}'} + T_{\tilde{c}\tilde{c}'}. \quad (C2)$$

By virtue of the fact that Eq. (9.23) can be written in the form

$$U_{\tilde{c}\tilde{c}'} = e^{i\delta_{\tilde{c}\tilde{c}'}} (\delta_{\tilde{c}\tilde{c}'} - 2i\tilde{T}_{\tilde{c}\tilde{c}'}) e^{i\delta_{\tilde{c}\tilde{c}'}} \quad (C3)$$

provided that we define

$$\tilde{T}_{\tilde{c}\tilde{c}'} = 2\hbar^{-1} \langle \bar{u}_{\alpha\tilde{c}} | \hat{T}_{\alpha\beta} | \bar{u}_{\beta\tilde{c}'} \rangle, \quad (C4)$$

we see that definition (C4) is also consistent with Eq. (C1). Definition (C4) is used in what follows. Equation (C1) implies that

$$\tilde{T}_{\tilde{c}\tilde{c}'} - \tilde{T}_{\tilde{c}'\tilde{c}}^* = -2i \sum_{\tilde{c}''} \tilde{T}_{\tilde{c}\tilde{c}''} T_{\tilde{c}'\tilde{c}''}^*, \quad (C5)$$

$$\langle \bar{u}_{\alpha\tilde{c}} | \hat{\tau}_{\alpha\beta} | \bar{u}_{\beta\tilde{c}'} \rangle - \langle \bar{u}_{\alpha\tilde{c}'} | \hat{\tau}_{\alpha\beta}^* | \bar{u}_{\beta\tilde{c}} \rangle = \sum_{\gamma} \langle \bar{u}_{\alpha\tilde{c}} | \hat{\tau}_{\alpha\gamma} (\bar{G}_{\gamma} - \bar{G}_{\gamma}^*) \hat{\tau}_{\gamma\beta}^* | \bar{u}_{\beta\tilde{c}'} \rangle, \quad (C12)$$

where  $\tilde{c} \in \alpha$  and  $\tilde{c}' \in \beta$ . For the imaginary part of the Green's-function operators, we can write for sufficiently large channel radii

$$\bar{G}_{\gamma} - \bar{G}_{\gamma}^* = 2i\pi\delta(E - \bar{H}_{\gamma}) = -i4\hbar^{-1} \sum_{\tilde{c}'' \in \gamma} | \bar{u}_{\gamma\tilde{c}''} \rangle \langle \bar{u}_{\gamma\tilde{c}''} |, \quad (C13)$$

where the summation is restricted to open channels. From Eqs. (C4) and (C9) we have

$$\begin{aligned} \tilde{T}_{\tilde{c}\tilde{c}'} &= 2\hbar^{-1} \langle \bar{u}_{\alpha\tilde{c}} | \hat{T}_{\alpha\beta} | \bar{u}_{\beta\tilde{c}'} \rangle \\ &= 2\hbar^{-1} \sum_{\gamma} \langle \bar{u}_{\alpha\tilde{c}} | \hat{\tau}_{\alpha\beta} \bar{G}_{\gamma} \bar{G}_{\beta}^{-1} | \bar{u}_{\beta\tilde{c}'} \rangle \\ &= 2\hbar^{-1} \langle \bar{u}_{\alpha\tilde{c}} | \hat{\tau}_{\alpha\beta} | \bar{u}_{\beta\tilde{c}'} \rangle, \end{aligned} \quad (C14)$$

by virtue of the Lippmann identity (Lippmann, 1956). Substituting Eqs. (C13) and (C14) into Eq. (C12) gives

$$\begin{aligned} \tilde{T}_{\tilde{c}\tilde{c}'} - \tilde{T}_{\tilde{c}'\tilde{c}}^* &= -\frac{8i}{\hbar^2} \sum_{\gamma} \sum_{\tilde{c}'' \in \gamma} \langle \bar{u}_{\alpha\tilde{c}} | \hat{\tau}_{\alpha\gamma} | \bar{u}_{\gamma\tilde{c}''} \rangle \langle \bar{u}_{\alpha\tilde{c}'} | \tau_{\gamma\beta}^* | \bar{u}_{\beta\tilde{c}'} \rangle \\ &= -2i \sum_{\gamma} \sum_{\tilde{c}'' \in \gamma} \tilde{T}_{\tilde{c}\tilde{c}''} \tilde{T}_{\tilde{c}'\tilde{c}''}^*. \end{aligned} \quad (C15)$$

Equation (C15) is equivalent to the unitarity relation [Eq. (C5)], since the transition matrix is symmetric. It should be noted that the sum over channels in Eq. (C15)

and for  $\tilde{c}' = \tilde{c}$

$$\tilde{T}_{\tilde{c}\tilde{c}} - \tilde{T}_{\tilde{c}\tilde{c}}^* = -2i \sum_{\tilde{c}''} | \tilde{T}_{\tilde{c}\tilde{c}''} |^2, \quad (C6)$$

which is the optical theorem.

Now let us see what the BKLT formalism predicts for  $\tilde{T}_{\tilde{c}\tilde{c}'} - \tilde{T}_{\tilde{c}'\tilde{c}}^*$ . A somewhat different analysis from the following has been given by Benoist-Gueutal (1975). For  $s_{\tilde{c}} = -i$ , Eq. (10.4) becomes

$$\hat{T} = \hat{V}\hat{W}\hat{G}\hat{U}\hat{G}^{-1} + \hat{V}\hat{W}\hat{G}\hat{T}. \quad (C7)$$

For convenience, we introduce the operator  $\hat{\tau}$ , which is the solution of the equation

$$\hat{\tau} = \hat{V}\hat{W} + \hat{V}\hat{W}\hat{G}\hat{\tau} = \hat{V}\hat{W} + \hat{\tau}\hat{G}\hat{V}\hat{W} \quad (C8)$$

and is related to the transition matrix operator  $\hat{T}$  by the equation

$$\hat{T} = \hat{\tau}\hat{G}\hat{U}\hat{G}^{-1}. \quad (C9)$$

From Eq. (C8) and its complex conjugate we have

$$\hat{V}\hat{W} = (\mathbb{1} + \hat{\tau}\hat{G})^{-1} \hat{\tau} = \hat{\tau}^* (\mathbb{1} + \hat{G}^* \hat{\tau}^*)^{-1}, \quad (C10)$$

and from this equation it follows that

$$\hat{\tau} - \hat{\tau}^* = \hat{\tau} (\hat{G} - \hat{G}^*) \hat{\tau}^*. \quad (C11)$$

Taking the matrix element with respect to the asymptotic states  $| \bar{u}_{\alpha\tilde{c}} \rangle$  and  $| \bar{u}_{\beta\tilde{c}'} \rangle$ , we see that Eq. (C11) gives

includes all the open channels which are included in the spectral decompositions of the totality of the partition Hamiltonians included in the coupling scheme. Benoist-Gueutal noted that the coupling scheme must include all two-cluster partitions, at least, in order for the sum to be free of omissions. In addition, from the arguments given in Sec. XIV, we note that the coupling scheme should contain no more than the complete set of two-cluster partitions to avoid redundancy in the sum.

### REFERENCES

- Adams, J. L., 1967, Ph.D. thesis (Florida State University, Tallahassee).  
 Adhikari, S. K., and W. Glöckle, 1979, Phys. Rev. C 19, 616.  
 Adhikari, S. K., and W. Glöckle, 1980, Phys. Rev. C 22, 309.  
 Afzal, S. A., A. A. Z. Ahmad, and S. Ali, 1969, Rev. Mod. Phys. 41, 247.

- Ahmad, S. S., 1978, *J. Phys. G* **4**, 1751.
- Ahmad, S. S., 1979, *Nuovo Cimento A* **54**, 129.
- Ahmad, S. S., R. F. Barrett, and B. A. Robson, 1976a, *Nucl. Phys. A* **257**, 378.
- Ahmad, S. S., R. F. Barrett, and B. A. Robson, 1976b, *Nucl. Phys. A* **270**, 1.
- Alt, E. O., P. Grassberger, and W. Sandhas, 1967, *Nucl. Phys. B* **2**, 167.
- Andrick, D., and A. Bitsch, 1975, *J. Phys. B* **8**, 393.
- Baer, M., and D. J. Kouri, 1972, *J. Chem. Phys.* **56**, 4840.
- Baer, M., and D. J. Kouri, 1973, *J. Math. Phys.* **14**, 1637.
- Baldock, R. A., 1980, Ph.D. thesis (Australian National University, Canberra).
- Baldock, R. A., R. F. Barrett, and B. A. Robson, 1979, *Nucl. Phys. A* **321**, 171.
- Baldock, R. A., B. A. Robson, and R. F. Barrett, 1981, *Nucl. Phys. A* **351**, 157.
- Barker, F. C., 1961, *Nucl. Phys.* **28**, 96.
- Barker, F. C., 1972, *Aust. J. Phys.* **25**, 341.
- Barrett, R. F., L. C. Biedenharn, M. Danos, P. P. Delsanto, W. Greiner, and H. G. Wahsweiler, 1973, *Rev. Mod. Phys.* **45**, 44.
- Barrett, R. F., and P. P. Delsanto, 1971, *Nucl. Phys. A* **173**, 641.
- Barrett, R. F., and P. P. Delsanto, 1974, *Phys. Rev. C* **10**, 101.
- Barrett, R. F., and B. A. Robson, 1979, *J. Phys. B* **12**, 105.
- Baye, D., 1976, *Nucl. Phys. A* **272**, 445.
- Baye, D., and P.-H. Heenen, 1974, *Nucl. Phys. A* **233**, 304.
- Baye, D., and P.-H. Heenen, 1977a, *Nucl. Phys. A* **276**, 354.
- Baye, D., and P.-H. Heenen, 1977b, *Nucl. Phys. A* **282**, 176.
- Baye, D., and P.-H. Heenen, 1977c, *Fizika (Zagreb)* **9** Suppl. 3, 1.
- Baye, D., P.-H. Heenen, and M. Libert-Heinemann, 1977, *Nucl. Phys. A* **291**, 230.
- Baye, D., P.-H. Heenen, and M. Libert-Heinemann, 1978, *Nucl. Phys. A* **308**, 229.
- Baye, D., and Y. Salmon, 1979a, *Nucl. Phys. A* **323**, 521.
- Baye, D., and Y. Salmon, 1979b, *Nucl. Phys. A* **331**, 254.
- Beck, R., J. Borysowicz, D. M. Brink, and M. V. Mihailović, 1975a, *Nucl. Phys. A* **244**, 45.
- Beck, R., J. Borysowicz, D. M. Brink, and M. V. Mihailović, 1975b, *Nucl. Phys. A* **244**, 58.
- Bederson, B., and L. J. Kieffer, 1971, *Rev. Mod. Phys.* **43**, 601.
- Bencze, Gy., 1973, *Nucl. Phys. A* **210**, 568.
- Benoist-Gueutal, P., 1975, *Phys. Lett. B* **56**, 413.
- Bevelacqua, J. J., and R. J. Philpott, 1977, *Nucl. Phys. A* **275**, 301.
- Blaauw, H. J., R. W. Wagenaar, D. H. Barends, and F. J. De Heer, 1980, *J. Phys. B* **13**, 359.
- Blatt, J. M., and J. D. Jackson, 1949, *Phys. Rev.* **76**, 18.
- Bloch, C., 1957, *Nucl. Phys.* **4**, 503.
- Bloch, C., and V. Gillet, 1965, *Phys. Lett.* **16**, 62.
- Bohr, N., 1936, *Nature* **137**, 344.
- Breit, G., 1940, *Phys. Rev.* **58**, 1068.
- Breit, G., 1959, "Theory of resonance reactions and allied topics," in *Encyclopedia of Physics*, edited by S. Flügge, Handbuch der Physik (Springer, Berlin), Vol. XLI/1, p. 1.
- Brink, D. M., 1966, "The alpha-particle model of light nuclei," in *Many-Body Description of Nuclear Structure and Reactions*, edited by C. Bloch, Proceedings of the International School of Physics Enrico Fermi, Course XXXVI (Academic, New York), p. 247.
- Brink, D. M., and E. Boeker, 1967, *Nucl. Phys. A* **91**, 1.
- Brode, R. B., 1925, *Phys. Rev.* **25**, 636.
- Brown, G. E., and C. T. de Dominicis, 1958, *Proc. Phys. Soc., London, Sect. A* **72**, 70.
- Brüche, E., D. Lilienthal, and K. Schrödter, 1927, *Ann. Phys. (Leipzig)* **8**, 279.
- Buck, B., 1963, *Phys. Rev.* **130**, 712.
- Buckingham, R. A., and H. S. W. Massey, 1941, *Proc. R. Soc. London, Ser. A* **179**, 123.
- Buckley, B. D., P. G. Burke, and Vo Ky Lan, 1979, *Comput. Phys. Commun.* **17**, 89.
- Burke, P. G., J. W. Cooper, and S. Ormonde, 1969, *Phys. Rev.* **183**, 245.
- Burke, P. G., A. Hibbert, and W. D. Robb, 1971, *J. Phys. B* **4**, 153.
- Burke, P. G., I. Mackey, and I. Shimamura, 1977, *J. Phys. B* **10**, 2497.
- Burke, P. G., and W. D. Robb, 1972, *J. Phys. B* **5**, 44.
- Burke, P. G., and W. D. Robb, 1975, *Adv. At. Mol. Phys.* **11**, 143.
- Buttle, P. J. A., 1967, *Phys. Rev.* **160**, 719.
- Callaway, J., 1978, *Phys. Rep. C* **45**, 89.
- Callaway, J., R. W. LaBahn, R. T. Pu, and W. M. Duxler, 1968, *Phys. Rev.* **168**, 12.
- Canto, L. F., and D. M. Brink, 1977, *Nucl. Phys. A* **279**, 85.
- Carlaw, H. S., 1930, *Introduction to the Theory of Fourier's Series and Integrals*, 3rd ed. (Dover, New York).
- Cattapan, G., and V. Vanzani, 1979, *Phys. Rev. C* **19**, 1168.
- Chandler, C., 1978, *Nucl. Phys. A* **301**, 1.
- Chandler, C., and A. G. Gibson, 1977, *J. Math. Phys.* **18**, 2336.
- Chandler, C., and W. Tobocman, 1979, *Phys. Rev. C* **19**, 1660.
- Charlton, M., T. C. Griffith, G. R. Heyland, and T. R. Twomey, 1980, *J. Phys. B* **13**, L239.
- Crompton, R. W., M. T. Elford, and R. L. Jory, 1967, *Aust. J. Phys.* **20**, 369.
- Crompton, R. W., M. T. Elford, and A. G. Robertson, 1970, *Aust. J. Phys.* **23**, 667.
- Danos, M., and W. Greiner, 1966, *Phys. Rev.* **146**, 708.
- de Takacsy, N. B., 1972, *Phys. Rev. C* **5**, 1883.
- Delsanto, P. P., A. Pompei, and P. Quarati, 1977, *J. Phys. G* **3**, 1133.
- Delsanto, P. P., and P. Quarati, 1976, *J. Phys. G* **2**, L161.
- Delsanto, P. P., and P. Quarati, 1978, *Nuovo Cimento A* **43**, 658.
- Delsanto, P. P., and P. Quarati, 1979, *Lett. Nuovo Cimento* **25**, 117.
- Ekstein, H., 1956, *Phys. Rev.* **101**, 880.
- Faddeev, L. D., 1960, *Zh. Eksp. Teor. Fiz.* **39**, 1459 [Sov. Phys.—JETP **12**, 1014 (1961)].
- Feshbach, H., 1958, *Ann. Phys. (N.Y.)* **5**, 357.
- Feshbach, H., 1962, *Ann. Phys. (N.Y.)* **19**, 287.
- Feshbach, H., and S. I. Rubinow, 1952, *Phys. Rev.* **88**, 484.
- Fiebig, H. R., and W. Timm, 1981, *Nucl. Phys. A* **368**, 164.
- Foldy, L. L., and W. Tobocman, 1957, *Phys. Rev.* **105**, 1099.
- Fonda, L., and R. G. Newton, 1960, *Ann. Phys. (N.Y.)* **10**, 490.
- Ford, W. K., and F. S. Levin, 1982, *Phys. Lett. B* **109**, 155.
- Friedrich, H., H. Hüsken, and A. Weiguny, 1974, *Nucl. Phys. A* **220**, 125.
- Galetti, D., and A. F. R. de Toledo Piza, 1978, *Phys. Rev. C* **17**, 774.
- Garside, L., and W. Tobocman, 1968, *Phys. Rev.* **173**, 1047.
- Garside, L., and W. Tobocman, 1969, *Ann. Phys. (N.Y.)* **53**, 115.
- Giraud, B., and J. LeTourneaux, 1972, *Nucl. Phys. A* **197**, 410.
- Giraud, B., and J. LeTourneaux, 1975, *Nucl. Phys. A* **240**, 365.
- Glöckle, W., 1966, *Z. Phys.* **190**, 391.

- Glöckle, W., J. Hüfner, and H. A. Weidenmüller, 1967, Nucl. Phys. A **90**, 481.
- Golden, D. E., and H. W. Bandel, 1965, Phys. Rev. **138**, 14A.
- Goldflam, R., R. M. Thaler, and W. Tobocman, 1981, Nucl. Phys. A **359**, 122.
- Goldflam, R., and W. Tobocman, 1978, Phys. Rev. C **17**, 1914.
- Goldflam, R., and W. Tobocman, 1979, Phys. Rev. C **20**, 904.
- Greben, J. M., and F. S. Levin, 1977, Phys. Lett. B **71**, 252.
- Greben, J. M., and F. S. Levin, 1979, Nucl. Phys. A **325**, 145.
- Griffin, J. J., and J. A. Wheeler, 1957, Phys. Rev. **108**, 311.
- Haglund, M. E., and D. Robson, 1965, Phys. Lett. **14**, 225.
- Hahn, Y., D. J. Kouri, and F. S. Levin, 1974, Phys. Rev. C **10**, 1615.
- Haxel, O., J. H. D. Jensen, and H. E. Suess, 1949, Phys. Rev. **75**, 1766.
- Heenen, P.-H., 1976, Nucl. Phys. A **272**, 399.
- Hill, D. L., and J. A. Wheeler, 1953, Phys. Rev. **89**, 1102.
- Horiuchi, H., 1970, Prog. Theor. Phys. **43**, 375.
- Horiuchi, H., 1977, Prog. Theor. Phys. Suppl. **62**, 90.
- Hüfner, J., and R. H. Lemmer, 1968, Phys. Rev. **175**, 1394.
- Hulbert, H. M., and J. O. Hirschfelder, 1943, J. Chem. Phys. **11**, 276.
- Hulthén, L., 1944, K. Fysiogr. Sällsk. Lund Förh. **14**, No. 21.
- Hulthén, L., 1948, Ark. Mat. Astron. Fys. A **35**, No. 25.
- Hulthén, L., and S. Shavlem, 1952, Phys. Rev. **87**, 297.
- Joachain, C. J., 1975, *Quantum Collision Theory* (North-Holland, Amsterdam).
- Kamimura, M., 1977, Prog. Theor. Phys. Suppl. **62**, 236.
- Kamimura, M., and T. Matsuse, 1974, Prog. Theor. Phys. **51**, 438.
- Kapur, P. L., and R. E. Peierls, 1938, Proc. R. Soc. London, Ser. A **166**, 277.
- Karlsson, B. R., and E. M. Zeiger, 1975, Phys. Rev. D **11**, 939.
- Kaupilla, W. E., T. S. Stein, G. Jesion, M. S. Dababneh, and W. Pol, 1977, Rev. Sci. Instrum. **48**, 822.
- Kennerly, R. W., and R. A. Bonham, 1978, Phys. Rev. A **17**, 1844.
- Kohn, W., 1948, Phys. Rev. **74**, 1763.
- Kouri, D. J., M. Craigie, and D. Secrest, 1974, J. Chem. Phys. **60**, 1851.
- Kouri, D. J., H. Krüger, and F. S. Levin, 1977, Phys. Rev. D **15**, 1156.
- Kouri, D. J., and F. S. Levin, 1974, Phys. Rev. A **10**, 1616.
- Kouri, D. J., and F. S. Levin, 1975a, Phys. Rev. C **11**, 352.
- Kouri, D. J., and F. S. Levin, 1975b, Nucl. Phys. A **253**, 395.
- Kouri, D. J., F. S. Levin, M. Craigie, and D. Secrest, 1974, J. Chem. Phys. **61**, 17.
- Kowalski, K. L., 1978, Lett. Nuovo Cimento **22**, 531.
- Krüger, H., and F. S. Levin, 1977, Chem. Phys. Lett. **46**, 95.
- Lane, A. M., 1960, Rev. Mod. Phys. **32**, 519.
- Lane, A. M., and D. Robson, 1966, Phys. Rev. **151**, 774.
- Lane, A. M., and D. Robson, 1969a, Phys. Rev. **178**, 1715.
- Lane, A. M., and D. Robson, 1969b, Phys. Rev. **185**, 1403.
- Lane, A. M., and R. G. Thomas, 1958, Rev. Mod. Phys. **30**, 257.
- Lejeune, A., and C. Mahaux, 1970, Nucl. Phys. A **145**, 613.
- Lejeune, A., and M. A. Nagarajan, 1970, Nucl. Phys. A **154**, 602.
- Lejeune, A., and M. A. Nagarajan, 1971, Nucl. Phys. A **164**, 246.
- Levin, F. S., 1978, Int. J. Quantum Chem., Symp. **12**, 109.
- Levin, F. S., 1980, Phys. Rev. C **21**, 2199.
- Levin, F. S., and H. Krüger, 1977a, Phys. Rev. A **15**, 2147.
- Levin, F. S., and H. Krüger, 1977b, Phys. Rev. A **16**, 836.
- Lewanski, A. J., and W. Tobocman, 1978, Phys. Rev. C **17**, 423.
- Lippmann, B. A., 1956, Phys. Rev. **102**, 264.
- Lippmann, B. A., and J. Schwinger, 1950, Phys. Rev. **79**, 469.
- Lovelace, C., 1964, Phys. Rev. **135**, 1225B.
- Lucchese, R. R., and V. McKoy, 1979, J. Phys. B **12**, L421.
- Lumbroso, A., 1974, Phys. Rev. C **10**, 1271.
- Lumbroso, A., 1976, "An application of the generator coordinate formalism:  $\alpha$ - $\alpha$  scattering," in *Nuclear Spectroscopy and Nuclear Reactions with Heavy Ions*, edited by H. Faraggi and R. A. Ricci, Proceedings of the International School of Physics Enrico Fermi, Course LXII (Academic, New York), p. 581.
- MacDonald, W., 1964a, Nucl. Phys. **54**, 393.
- MacDonald, W., 1964b, Nucl. Phys. **56**, 636.
- MacDonald, W., 1964c, Nucl. Phys. **56**, 647.
- Mahaux, C., and H. A. Weidenmüller, 1965, Ann. Phys. (N.Y.) **32**, 259.
- Mahaux, C., and H. A. Weidenmüller, 1967, Nucl. Phys. A **97**, 378.
- Mahaux, C., and H. A. Weidenmüller, 1969, *Shell Model Approach to Nuclear Reactions* (North-Holland, Amsterdam).
- Malik, F. B., 1962, Ann. Phys. (N.Y.) **20**, 464.
- Margenau, H., 1941, Phys. Rev. **59**, 37.
- Mayer, M. G., 1949, Phys. Rev. **75**, 1969.
- Milloy, H. B., and R. W. Crompton, 1977, Phys. Rev. A **15**, 1847.
- Mito, Y., and M. Kamimura, 1976, Prog. Theor. Phys. **56**, 583.
- Mori, A., 1972, Phys. Rev. C **5**, 1795.
- Mori, A., 1973, Prog. Theor. Phys. **49**, 1960.
- Mori, A., and T. Terasawa, 1972, Prog. Theor. Phys. **48**, 826.
- Nagarajan, M. A., S. K. Shah, and W. Tobocman, 1965, Phys. Rev. **140**, 63B.
- Nagata, S., and Y. Yamamoto, 1977, Prog. Theor. Phys. **57**, 1088.
- Nesbet, R. K., 1968, Phys. Rev. **175**, 134.
- Nesbet, R. K., 1977, Adv. At. Mol. Phys. **13**, 15.
- Nesbet, R. K., 1979a, J. Phys. B **12**, L243.
- Nesbet, R. K., 1979b, Phys. Rev. A **20**, 58.
- Nesbet, R. K., 1980, *Variational Methods in Electron-Atom Scattering Theory* (Plenum, New York).
- Nesbet, R. K., and R. S. Oberoi, 1972, Phys. Rev. A **6**, 1855.
- Newton, R. G., 1959, Ann. Phys. (N.Y.) **4**, 29.
- Newton, R. G., 1961, J. Math. Phys. **2**, 188.
- Neynaber, R. H., S. M. Trujillo, L. L. Marino, and E. W. Rothe, 1964, in *Proceedings of the 3rd International Conference on Physics of Electronic and Atomic Collisions* (Wiley, New York), p. 1089.
- Nordholm, S., and G. Bacskay, 1978, J. Phys. B **11**, 193.
- Normand, C. E., 1930, Phys. Rev. **35**, 1217.
- O'Malley, T. F., 1963, Phys. Rev. **130**, 1020.
- O'Malley, T. F., P. G. Burke, and K. A. Berrington, 1979, J. Phys. B **12**, 953.
- Philpott, R. J., 1973, Nucl. Phys. A **208**, 236.
- Philpott, R. J., 1976, Nucl. Phys. A **266**, 109.
- Philpott, R. J., 1977, Nucl. Phys. A **289**, 109.
- Philpott, R. J., and J. George, 1974, Nucl. Phys. A **233**, 164.
- Philpott, R. J., and D. Halderson, 1980, "Theoretical studies of the polarization-analyzing power difference in  ${}^3\text{H}(p, n){}^3\text{He}$  and  ${}^{15}\text{N}(p, n){}^{15}\text{O}$ ," in *The (p, n) Reaction and the Nucleon-Nucleon Force*, edited by Charles D. Goodman, Sam M. Austin, Stewart D. Bloom, J. Rapaport, and G. R. Satchler (Plenum, New York), p. 491.
- Philpott, R. J., D. Mukhopadhyay, and J. E. Purcell, 1978, Nucl. Phys. A **294**, 6.



- Polyzou, W. N., and E. F. Redish, 1979, *Ann. Phys. (N.Y.)* **119**, 1.
- Preston, M. A., 1962, *Physics of the Nucleus* (Addison-Wesley, Reading, Mass.).
- Purcell, J. E., 1969a, Florida State University Tech. Report No. 1.
- Purcell, J. E., 1969b, *Phys. Rev.* **185**, 1279.
- Ramsauer, C., 1921a, *Ann. Phys. (Leipzig)* **64**, 513.
- Ramsauer, C., 1921b, *Ann. Phys. (Leipzig)* **66**, 546.
- Ramsauer, C., and R. Kollath, 1932, *Ann. Phys. (Leipzig)* **12**, 529.
- Raphael, R., P. C. Tandy, and W. Tobocman, 1976, *Phys. Rev. C* **14**, 1355.
- Redish, E. F., 1974, *Nucl. Phys. A* **225**, 16.
- Reynolds, J. T., C. J. Slavik, C. R. Lubitz, and N. C. Francis, 1968, *Phys. Rev.* **176**, 1213.
- Robson, B. A., and D. Robson, 1967, *Phys. Lett. B* **25**, 504.
- Robson, B. A., and W. J. van Meegen, 1972a, *Nucl. Phys. A* **184**, 50.
- Robson, B. A., and W. J. van Meegen, 1972b, *Nucl. Phys. A* **184**, 67.
- Robson, D., 1975, "New approaches in resonance reactions," in *Nuclear Spectroscopy and Reactions*, edited by J. Cerny, Pure and Applied Physics (Academic, New York), Vol. 40-D, p. 179.
- Rouhaninejad, H., and J. Yoccoz, 1966, *Nucl. Phys.* **78**, 353.
- Rubinow, S. I., 1955, *Phys. Rev.* **98**, 183.
- Rudge, M. R. H., 1973, *J. Phys. B* **6**, 1788.
- Saito, S., 1977, *Prog. Theor. Phys. Suppl.* **62**, 11.
- Schmittroth, F., and W. Tobocman, 1971, *Phys. Rev. C* **3**, 1010.
- Schwartz, C., 1961, *Phys. Rev.* **124**, 1468.
- Sinclair, A. L., and R. K. Nesbet, 1972, *Phys. Rev. A* **6**, 2118.
- Sloan, I. H., 1972, *Phys. Rev. C* **6**, 1945.
- Stehn, J. R., M. D. Goldberg, B. A. Magurno, and R. Wiener-Chasman, 1964, *Neutron Cross Sections*, Brookhaven Natl. Lab. Report No. BNL-325, 2nd ed., 2nd Suppl., Vol. I.
- Stein, T. S., W. E. Kauppila, V. Pol, J. H. Smart, and G. Jesion, 1978, *Phys. Rev. A* **17**, 1600.
- Strang, G., and G. J. Fix, 1973, *An Analysis of the Finite Element Method* (Prentice-Hall, Englewood Cliffs, N.J.).
- Sünkel, W., and K. Wildermuth, 1972, *Phys. Lett. B* **41**, 439.
- Takatsuka, K., and V. McKoy, 1980, *Phys. Rev. Lett.* **45**, 1396.
- Takeuchi, K., and P. A. Moldauer, 1970, *Phys. Rev. C* **2**, 925.
- Tamura, T., 1965, *Rev. Mod. Phys.* **37**, 679.
- Tanabe, F., A. Tohsaki, and R. Tamagaki, 1973, *Prog. Theor. Phys.* **50**, 1774.
- Tang, Y. C., 1981, "Microscopic description of the nuclear cluster theory," in *Topics in Nuclear Physics, II*, edited by T. T. S. Kuo and S. S. M. Wong, Lecture Notes in Physics (Springer, Berlin), Vol. 145, p. 571.
- Tang, Y. C., M. LeMere, and D. R. Thompson, 1978, *Phys. Rep. C* **47**, 167.
- Thompson, D. R., and Y. C. Tang, 1975, *Phys. Rev. C* **12**, 1432.
- Thompson, D. R., and Y. C. Tang, 1976, *Phys. Rev. C* **13**, 2597.
- Tobocman, W., 1961, *Theory of Direct Nuclear Reactions* (Oxford University, London).
- Tobocman, W., 1972, *Phys. Rev. C* **6**, 1553.
- Tobocman, W., 1974a, *Phys. Rev. C* **9**, 2466.
- Tobocman, W., 1974b, *Phys. Rev. C* **10**, 60.
- Tobocman, W., 1975a, *Phys. Rev. C* **11**, 43.
- Tobocman, W., 1975b, *Phys. Rev. C* **12**, 1146.
- Tobocman, W., 1981, *Phys. Rev. C* **24**, 2743.
- Tobocman, W., and M. A. Nagarajan, 1965, *Phys. Rev.* **138**, 1351B.
- Tohsaki-Suzuki, A., 1977, *Prog. Theor. Phys. Suppl.* **62**, 191.
- Tohsaki-Suzuki, A., 1978, *Prog. Theor. Phys.* **59**, 1261.
- Vanzani, V., 1976, *Lett. Nuovo Cimento* **16**, 1.
- Vanzani, V., 1978, *Lett. Nuovo Cimento* **23**, 586.
- Vogt, E., 1962, *Rev. Mod. Phys.* **34**, 723.
- Volkov, A. B., 1965, *Nucl. Phys.* **74**, 33.
- Weidenmüller, H. A., 1964, *Ann. Phys. (N.Y.)* **29**, 378.
- Weidenmüller, H. A., 1965, *Nucl. Phys.* **69**, 113.
- Weidenmüller, H. A., 1966, *Nucl. Phys.* **75**, 189.
- Weidenmüller, H. A., and K. Dietrich, 1966, *Nucl. Phys.* **83**, 332.
- Westin, G. D., and J. L. Adams, 1971, *Phys. Rev. C* **4**, 363.
- Westin, G. D., and J. L. Adams, 1973, *Phys. Rev. C* **8**, 1.
- Wheeler, J. A., 1937a, *Phys. Rev.* **52**, 1083.
- Wheeler, J. A., 1937b, *Phys. Rev.* **52**, 1107.
- Wichmann, E., and P. Heiss, 1974, *J. Phys. B* **7**, 1042.
- Wigner, E. P., 1946a, *Phys. Rev.* **70**, 15.
- Wigner, E. P., 1946b, *Phys. Rev.* **70**, 606.
- Wigner, E. P., and L. Eisenbud, 1947, *Phys. Rev.* **72**, 29.
- Wildermuth, K., and T. Kanellopoulos, 1958/59, *Nucl. Phys. A* **9**, 449.
- Wong, C. W., 1975, *Phys. Rep. C* **15**, 283.
- Yakubovskii, O. A., 1967, *Yad. Fiz.* **5**, 1312 [*Sov. J. Nucl. Phys.* **5**, 937 (1967)].
- Zvijac, D. J., E. J. Heller, and J. C. Light, 1975, *J. Phys. B* **8**, 1016.